Progress in Materials Science 154 (2025) 101516

Contents lists available at ScienceDirect

Progress in Materials Science

journal homepage: www.elsevier.com/locate/pmatsci

Developing safe and high-performance lithium-ion batteries: Strategies and approaches

Guanjun Chen [a,1], Rui Tan [b,*,1], Chunlin Zeng [a,1], Yan Li [a], Zexin Zou [c], Hansen Wang [d,**], Chuying Ouyang [d,e,**], Jiayu Wan [f,*], Jinlong Yang [a,*]

[a] Guangdong Provincial Key Laboratory of New Energy Materials Service Safety, College of Materials Science and Engineering, Shenzhen University, Shenzhen 518060, China
[b] Department of Chemical Engineering, Swansea University, Swansea SA1 8EN, UK
[c] Guangdong Testing Institute of Product Quality Supervision, Guangzhou 510670, China
[d] 21C LAB, Contemporary Amperex Technology Co., Limited, Ningde 352000 Fujian, China
[e] Department of Physics, Jiangxi Normal University, Nanchang 330022 Jiangxi, China
[f] Future Battery Research Center, Global Institute of Future Technology, Shanghai Jiao Tong University, Shanghai 200240, China

ARTICLE INFO

Keywords:
Lithium-ion battery
Thermal and safety performance
Material strategy
Battery management
Industrial-scale manufacture
Theoretical simulation

ABSTRACT

Lithium-ion batteries (LIBs) as an effective low carbon technology provide a solution for achieving NetZero emissions, in line with the Sustainable Development Goals set by the United Nations. Research efforts have been devoted to increasing the energy density and efficiency of LIBs. However, large-scale deployment of LIBs is challenged by thermal runaway and safety problems, particularly under abusive conditions. To tackle this challenge, we must gain insight into the safety features of batteries and design durable strategies by fundamentally analyzing battery thermal runaway processes. In this review, we systematically summarize the abusive indicators that may trigger the thermal issues at the macroscopic level from thermal, chemical, and mechanical perspectives, and point out failure mechanisms that correlate with each component, e.g., cathode, anode, separator, electrolyte and current collector. Beyond material innovations, we emphasize the importance of optimizing industrial-scale manufacturing, integrating regulatory frameworks through advanced battery management systems, and enhancing safety engineering from an battery external perspective. Moreover, we systematically evaluate the contributions of theoretical and computational approaches to battery safety, critically comparing physics-based, machine learning, and hybrid models, and proposing targeted improvements. The broader implications of these safety strategies are considered in the context of environmental sustainability and recycling. Finally, we present design principles for safer, high-performance batteries and outline emerging research and industrial directions through a critical synthesis of thermal runaway mechanisms and mitigation strategies.

* Corresponding author.
** Corresponding author at: 21C LAB, Contemporary Amperex Technology Co., Limited, Ningde 352000, Fujian, China (Hansen Wang and Chuying Ouyang).
E-mail addresses: ruitan@swansea.ac.uk (R. Tan), wanghs@catl-21c.com (H. Wang), ouyangcy@catl.com (C. Ouyang), wanjy@sjtu.edu.cn (J. Wan), yangjl18@szu.edu.cn (J. Yang).
[1] These authors contributed equally to this work.

https://doi.org/10.1016/j.pmatsci.2025.101516
Received 22 February 2025; Received in revised form 6 May 2025; Accepted 20 May 2025
Available online 23 May 2025

1. Introduction

• As modern society advances, the global energy landscape is undergoing a fundamental transformation. Conventional fossil fuels such as coal, oil and natural gas are increasingly constrained by resource depletion and associated environmental pollution [1,2]. In response, renewable energy sources such as solar, wind, tidal and geothermal energy have attracted significant attention due to their sustainability and minimal environmental impact. However, their inherent intermittency and variability present major challenges for reliable energy supply [3,4]. Chemical energy storage systems offer a viable solution by storing energy in chemical form and enabling direct conversion to electricity via electrochemical reactions. As such, they are essential to the efficient integration and utilization of renewable energy sources [5,6].

With ongoing advances in science and technology, chemical power sources have evolved from the early Voltaic pile to nickel–hydrogen batteries, nickel–iron batteries, nickel batteries, acid batteries, alkaline zinc batteries, and LIBs. Among various electrochemical energy storage technologies, low-carbon LIBs offer numerous advantages, such as high operating voltage, large energy density and high energy efficiency, dominating the use in energy storage [7–9]. However, the energy density of LIBs, approximately 200 Wh/kg, is far lower than that of fossil fuels (13,000 Wh/kg), making it challenging to meet the demand for a daily range of 500 km for electric vehicles (EVs) [10,11]. Enhancing the battery energy density has inevitably become a focus in ongoing development [12]. The thermal stability of the energy-intensive batteries tends to decrease over operation, along with the risk of thermal runaway issues [12–15]. Therefore, it is crucial to enhance the battery while maintaining safety performance, for which the fundamentals of safety issues involved in LIBs require intensive investigation to provide durable strategies.

Electrochemical chemistries, operating conditions and abusive tolerances dominate the safety performance of a given battery system [16–18]. LIBs typically deliver insufficient safety performance when facing abusive conditions such as ***mechanical abuses*** including dropping, impact, penetration, infiltration and immersion, etc; ***electrical abuses*** including overcharging, over-discharging and short-circuiting, etc; ***thermal abuses*** such as overcooling and overheating [19]. On the one hand, overall battery safety is closely affected by the stability of the anode, electrolyte, separator, cathode and current collector; on the other hand, safety performance is determined by the capability of battery management and control systems. Once these abuses can hardly be tolerated by battery systems, unfavorable reactions will be triggered, such as lithium dendrite formation, electrolyte decomposition, separator melting, cathode material decomposition and current collector cracking, leading to serious safety accidents [20–22]. Furthermore, manufacturing defects during battery production can significantly compromise safety. Therefore, to improve the overall safety and stability of LIBs, a comprehensive study is needed as per the development of safe battery components, strict battery manufacturing, and reliable management systems.

A comprehensive understanding of battery safety and the thermal runaway process is essential for developing durable and effective mitigation strategies. A growing body of review articles has significantly advanced battery safety research, with systematic coverage of electrode materials, electrolyte formulations, next-generation safe battery designs, and fundamental thermal runaway principles. For example, Lyu et al. [13] summarized the thermal behavior of LIBs under varying temperatures and discussed thermal propagation and battery thermal management strategies. Duan et al. [23] reviewed failure mechanisms across LIB components and proposed safety enhancement strategies, alongside real-time monitoring techniques to prevent thermal runaway. In their classic LIB safety review, Liu et al. [24] comprehensively addressed underlying failure mechanisms while showcasing progress in safety-oriented material design. However, in recent years, with the rapid development of new technologies such as high-energy–density systems and solid-state electrolytes, as well as the continuous increase in safety requirements for batteries from electric vehicles and energy storage stations, the scope of research in this field is constantly expanding. In this context, there are still several key directions that require attention in current research. First, the safety issues in large-scale production processes have not yet received sufficient attention, and relevant research is relatively limited. Second, the correlation mechanism between material design and component-level safety performance still needs more comprehensive analysis, especially the systematic impact of auxiliary materials such as current collectors, which remains to be clarified. In addition, although computational models have shown potential in predicting safety, a collaborative verification system with experimental data has not yet been fully established.

To this end, this review innovatively establishes a comprehensive safety evaluation framework spanning from fundamental materials research to engineering applications. By integrating multiphysics (thermal-electrical–mechanical) coupling analysis, multiscale failure mechanisms, and system-level safety design strategies, we comprehensively elucidate the field's critical scientific issues and technical challenges. Specifically, we systematically examine the multidimensional causes of thermal runaway in LIBs, encompassing macroscopic factors such as thermal, electrical and mechanical abuse. We analyze the failure mechanisms of critical internal components—including the cathode, anode, electrolyte, separator and current collector—under extreme conditions from a microscopic perspective. Regarding external battery factors, we focused on analyzing the safety control mechanisms of the battery management system, explored process optimization and safety engineering design strategies in industrial manufacturing, and comprehensively evaluated safety prediction computational technologies based on physical models, machine learning, and hybrid approaches. Through comparative analysis of their respective advantages and limitations, we propose targeted improvement solutions. We also explore the broader implications of safety strategies for environmental sustainability and battery recycling. By critically evaluating current technologies, we highlight key limitations and propose a design framework for next-generation high-safety battery systems, offering a new direction for overcoming thermal runaway challenges in both academic and industrial contexts.

2. Battery safety issues

2.1. Factors to safety concerns

As aforementioned, various types of abuses may cause harsh conditions and thermal runaway over battery operation [25] where the abuse factors are generally classified into macro and micro causes (Fig. 1). At the macro level, safety concern is mainly attributed to external abusive conditions along with inadequate regulation capability of the external management systems while it can be attributed to the limited thermal/electrochemical/chemical stability of the battery components at the micro level. Under harsh conditions, e.g., penetration, these battery components are prone to have unfavorable reactions and in turn generate a large amount of heat and gases. Though categorized from different dimensions, the overall safety performance is still complex, which requires us to gain insight into working and failure mechanisms of each factor. To gain insightful understandings, we first analyse the abusive factors affecting battery performance at the macro level in this chapter, and then comprehensively investigating the stability of the battery components at the micro level in the subsequent chapters.

2.2. Macro causes

2.2.1. Mechanical abuse

Mechanical abuses include drop, impact, penetration and immersion, usually occurring in scenarios of traffic accidents. As shown in Fig. 2**a-b**, penetration leads to case rupture, separator breakdown, and electrolyte leakage inside the battery or battery pack [26–28], undesirably triggering short circuit (Fig. 2**c**). Subsequently, the increased internal temperature eventually caused the fire and

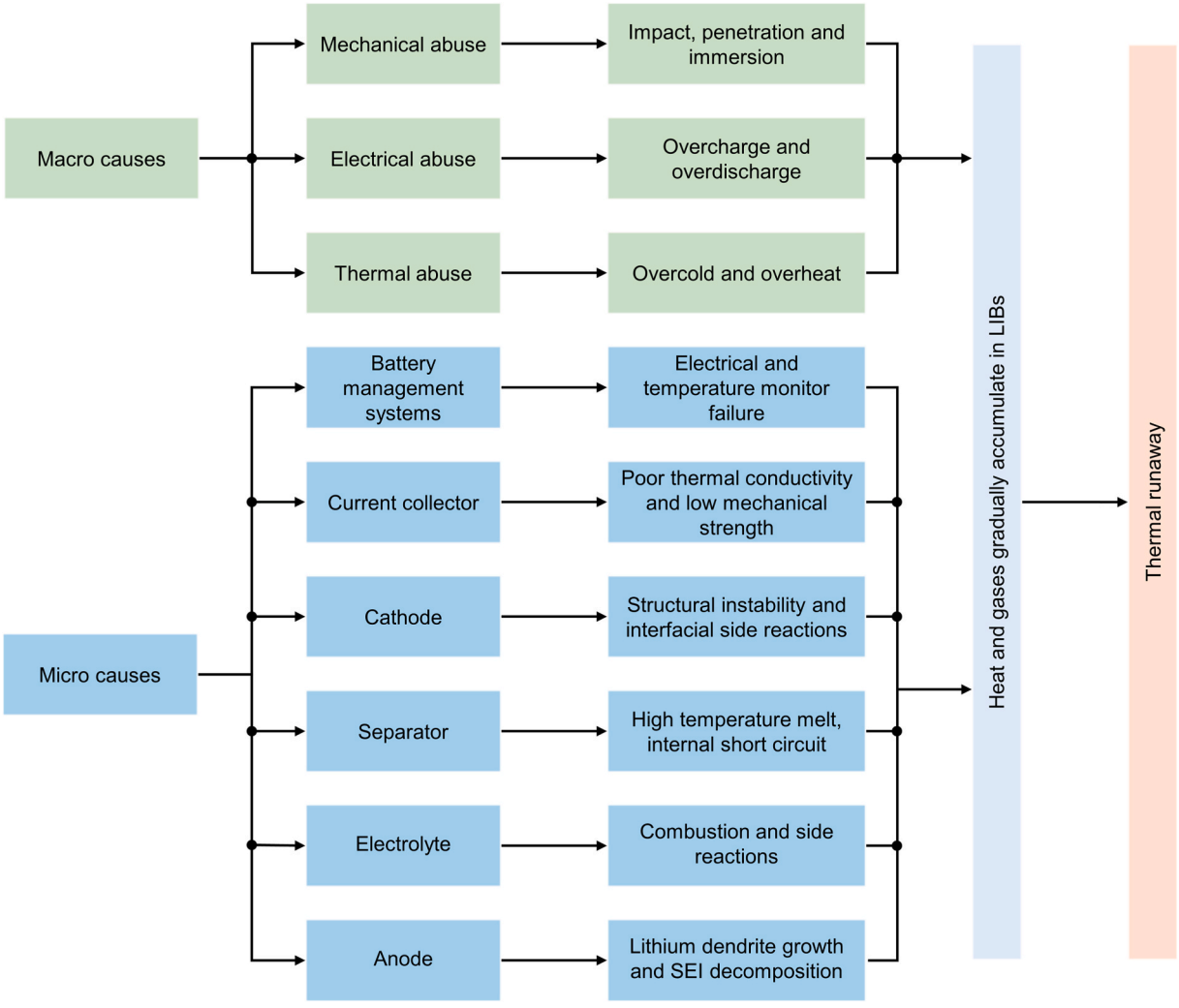

Fig. 1. Schematic diagram of the macro-/micro- causes and different stages of thermal runaway in LIBs.

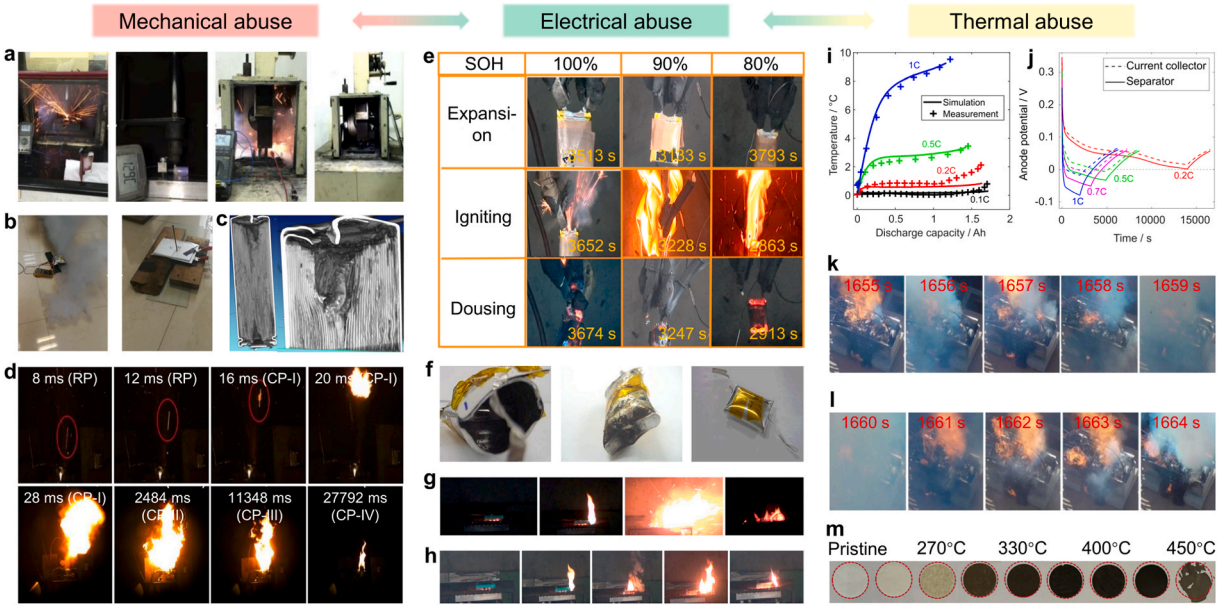

Fig. 2. Various abuse conditions and their corresponding thermal runaway processes. (a) Puncture and crush safety tests for 1.8 Ah type 18,650 cells and (b) puncture safety tests for 12 Ah type pressed cells with original and modified electrodes [31]. Copyright (2021) American Chemical Society. (c) Imaging of a battery after the puncture test [32]. Copyright (2014) Elsevier. (d) Rupture process (RP) and combustion process (CP) of a battery undergoing thermal runaway in air [33]. Copyright (2021) Elsevier. (e) Overcharging process at different states of health (SOH) of the battery [34]. Copyright (2021) Elsevier. (f) Pictures of the battery after overcharging experiments at 2C [35]. Copyright (2004) Elsevier. (g) Thermal runaway due to overcharging and (h) thermal runaway due to over-discharging [36]. Copyright (2018) Royal Society of Chemistry. (i) Changes in the electrical capacity under over-cooling conditions and (j) changes in the anode potential (vs. Li/Li^+) [37]. Copyright (2019) Elsevier. (k) and (l) alternating gas and flame injection during overheating of large-size LIBs [38]. Copyright (2019) MDPI. (m) Shape changes of PET/ceramic nonwoven separators from room temperature (pristine) to 450 °C [39]. Copyright (2018) Cell Press.

explosion of batteries (Fig. 2**d**).

Mechanical abuse is closely linked with the short-circuit issues that can be classified into external short circuits (ESC) and internal short circuits (ISC). ESC usually happens in the situations of case deformation, water immersion and incorrectly connected cables, together with rapidly increased currents [29], dramatically increased temperature (77 ~ 121 °C) [30] and irreversible construction damage. ISCs can also be triggered by external mechanical abuse, e.g., collision, crush, deformation and perforation, and internal factors, such as material impurities during manufacturing process and produced internal lithium dendrites.

2.2.2. *Electrical abuse*

Electrical abuse refers to the incorrect battery operation, such as overcharging, over-discharging and external or ISC. Specifically, ***overcharging*** occurs when a battery exceeds cut-off voltages and keeps charging. During this process, applied electrical field drives excessive Li-ions to deintercalate from the cathode electrode material, irreversibly causing structural changes of cathodes and generating substantial heat, oxygen and secondary gases as byproducts [13]. On the anode electrode side, the excessive Li-ions will deposit on the anode surface and irreversibly react with the organic electrolyte [40,41]. In addition to released heat and gas [40], formed metal dendrites can penetrate the polymeric separators, trigger a short circuit, and further induce thermal runaway (Fig. 2**e-g**) [42–44].

Likewise, ***over-discharging*** occurs when the discharge process extends beyond the designated cut-off voltages. For an over-discharged battery, solid electrolyte interface (SEI) on the anode decomposes, producing heat and gas byproducts, such as carbon dioxide, methane and carbon monoxide [45]. Reformation of stable SEI requires the use of excessive organic electrode and leads to the decrease in capacity and charging efficiency [46]. Meanwhile, current collectors in the anode side can be oxidized to Cu^{2+}, once the anode potential reaches ~ 3.5 V vs. Li/Li^+. Cu^{2+} will dissolve into the electrolyte, migrate across the separators [47,48] and deposit on the cathode in a dendritic format [48]. These metallic dendrites can pierce the separators, potentially causing thermal runaway (Fig. 2**h**) [46]. Unlike overcharging, the thermal issues resulting from over-discharging are less severe but still necessitate strict control.

2.2.3. *Thermal abuse*

Thermal abuse involves operating batteries beyond their recommended temperature range, including overcooling and overheating situations. Though both situations are mainly determined by environmental variables, overheating is closely associated with other abusive factors and limited heat dissipation efficiency of battery materials. Since LIBs are sensitive to operating temperature, deviations beyond 5 °C from the optimal range of 15 °C-35 °C can quickly result in safety incidents [49].

In the case of ***overcooling*** (< 0 °C), the electrolyte conductivity sustains an extremely low value [50] leading to restrained charge kinetics [51–53], the decreased Li-diffusion coefficient and faded battery performance (Fig. 2**i**). Importantly, low Li-diffusion coefficient challenges the insertion of Li-ions into the anode during the charging process and results in a high anodic overpotential (Fig. 2**j**) where Li-ions tend to deposit on the anode surface and produce dendritic metal [54–56]. ***Overheating*** typically destroys the stable structure of polymeric separators SEI and electrodes [13,57]. Fig. 2**k-l** demonstrate the intense combustion of overheated LIBs and the shape variation of polymeric separators against increased temperature. Specifically, the thermal runaway under this situation can be broken down into the following steps.

(a) SEI decomposition starts with a temperature of above 60 °C. At the temperature of about 90 °C, the SEI will completely decompose and emit heat and gases [58]. Decomposition of the SEI allows the anode surface exposed to the organic electrolyte where the Li-ions inserted in the anode will directly react with the organic solvents to produce combustible gases and heat [13].

(b) At about 130 °C, polymeric separators, polyethylene (PE)/polypropylene (PP), will melt and allow the direct contact of cathodes and anodes as well as induce irreversible side reactions [24].

(c) Cathode material will decompose at 180 °C and generate substantial heat and oxygen, leading to micro-cracking of the cathode [59]. Particularly, the nickel-rich layered material will be thermally destroyed at about 100 °C [60].

(d) As the temperature approaches 600 °C, the Al and Cu current collector gradually lose their mechanical strength and structural integrity, and even melt and produce a large number of cracks and pinholes, which aggravates the thermal runaway process of LIBs.

In a short summary, the thermal runaway of LIBs involves a complex interplay of three types of abuse conditions: mechanical, electrical, and thermal. Mechanical abuse can cause ESC, electrical abuse may lead to overheating, and thermal abuse could damage or melt the separator, leading to ISC. Thus, understanding thermal runaway requires a holistic examination of these interconnected factors. To enhance battery safety effectively, we must consider the entire system, including the anode, electrolyte, separator, cathode, current collector, and battery management system, rather than focusing on individual components. This review will outline the failure mechanisms of these components under abusive conditions and the regulatory role of the management system. With a comprehensive understanding of these dynamics, we will explore strategies to boost the safety performance of each element in batteries.

3. Safe anode materials

Based on the Li-embedding/de-lithiation mechanism, we can categorize anode materials into three categories: (1) intercalation anode materials, such as graphite, graphene, carbon nanotubes (CNTs), titanium dioxide, and other materials [61]. (2) conversion-reaction anode materials, including prototype transition metal oxides/sulphides [62]. (3) alloyed anode materials, such as silicon, tin, germanium, and aluminum, etc [63]. However, limited types of anode materials are commercially available, e.g., graphite, silicon-

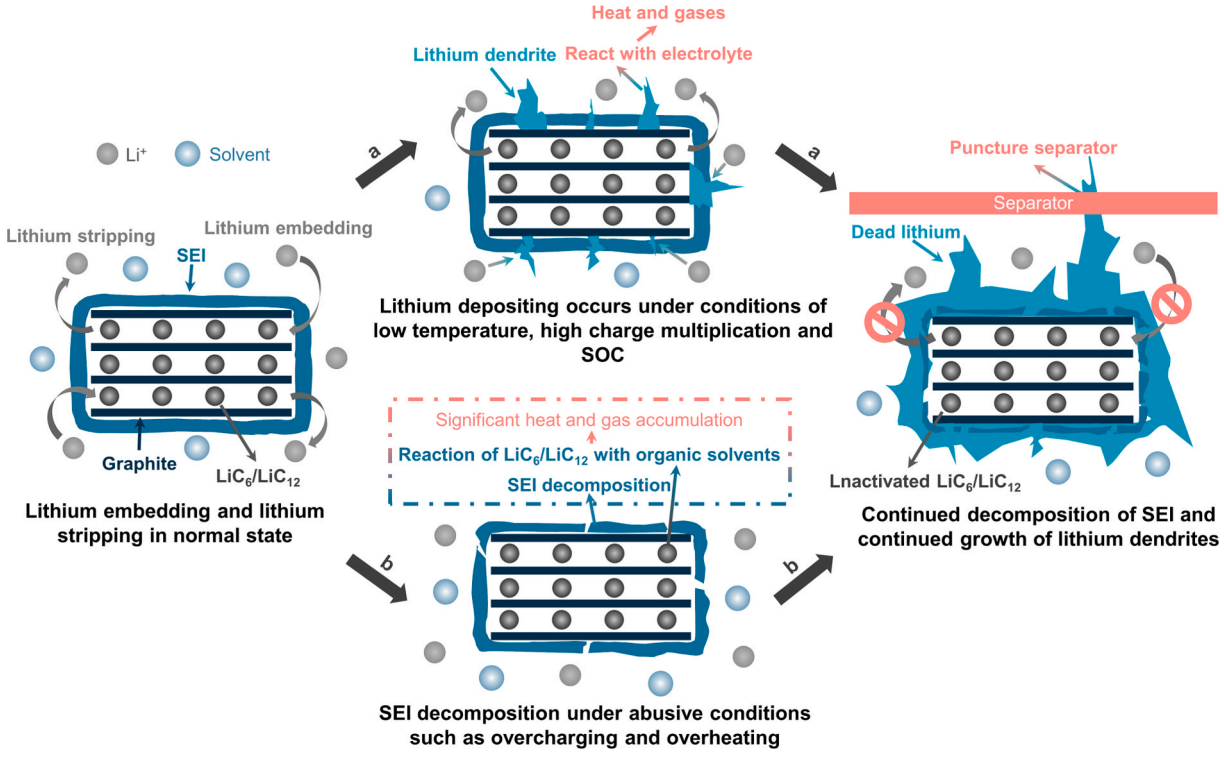

Fig. 3. Failure mechanisms of graphite anode. (a) Illustration of graphite anode failure caused by lithium dendrite growth, and (b) illustration of graphite anode failure due to SEI decomposition.

based and phosphorus-based anodes. Silicon-based and phosphorus-based anodes have high theoretical specific capacity [64–67], yet suffer from poor mechanical integrity and cycling stability due to severe volume expansion (>300 %) [61]. In contrast, with small volume changes (<17 %) during (dis)charging processes and superior electrochemical performance, graphite has thus become a widely used commercial LIB anode [68]. Nonetheless, thermal runaway process often starts with the failure of the anode materials where stable SEI undergoes severe decomposition along with sophisticated side reactions between anodes and organic electrolyte. Therefore, this section focuses on the safety performance and failure mechanism of graphite in LIBs and proposes safety strategies.

3.1. Failure mechanism

Safety issues of graphite anodes closely are associated with the growth of lithium dendrite and the decomposition of stable SEI. **(1) *Formation of Li dendrites.*** During the charging process, Li-ions are de-embedded from the cathode and migrate to the graphite anode through the electrolyte. In anode side, Li-ions embedded in the lamellar structure of the graphite at 0.065–0.2 V versus Li/Li^+ to form graphite intercalation compounds, e.g., LiC_{12} and LiC_6 [69] while partial Li-ions deposit on the surface of the graphite anode at ~ 0 V versus Li/ Li^+ to produce lithium metal [70,71]. Prior to the formation of Li metal, Li-embedding reaction prefers to occur with a positive potential [72],. However, if the polarization effect results in a reduced anodic potential that is lower than that of Li deposition, a metal-formation reaction will take place [72–74]. The polarization effects mainly result from sluggish charge transfer and ion diffusion in electrodes, and limited mass transfer in electrolyte [75], as well as the operation conditions, such as low temperature, high currents and high states of charge [76,77].

Theoretically, the Li metal is redox active and can convert to Li-ions during the discharging process. However, partial Li metal lacks direct electrically contact with the graphite anode and undesirably perform as the redox inactive component, namely “dead lithium”, in the formats of needles and dendrites [78,79]. Over cycling, when the graphite is gradually coated with “dead lithium”, the subsequent Li^+ (de)embedding processes are substantially affected (Fig. 3**a**). The growing lithium dendrites may puncture the separator, resulting in a short circuit and a severe exothermic reaction [80]. Furthermore, the deposited dendrites may react with the electrolyte to produce more heat and accelerate the process of thermal runaway [81].

(2) *Decompostion of stale SEI.* The structural integrity of SEI can be destroyed under the abusive conditions [82,83]. SEI decomposition results in the surface and bulk of the graphite anode being directly exposed to the electrolyte environment (Fig. 3**b**), where chemically active LiC_{12} and LiC_6 will react with the organic electrolyte solvent and produce combustible gases and heat [84,85]. Moreover, as SEI continues to decompose and reorganize during cycling, it tends to develop uneven distribution. This uneven distribution leads to localized variations in surface currents on the graphite anode, subsequently elevating the overpotential for lithium deposition at specific sites. This, in turn, intensifies the formation of lithium dendrites [24,86–90].

In a nutshell, durable strategies for developing safe graphite anode should consider how to design thermally and structurally stable SEI while eliminating the growth of lithium dendrites.

3.2. Design strategies of safe anodes

3.2.1. Optimizing surface overpotentials to inhibit lithium dendrites

Tuning the overpotential of electrodes provides a solution to maintaining the positive redox potential close to the equilibrium value [94]. In this case, redox reaction of electrodes prefers to take place rather than the formation of Li dendrite. On the other hand, increasing the overpotential of forming Li dendrites can possibly increase the activation energy for the growth of Li dendrites. For instance, Tallman et al. [73] reduced the nucleation sites on the graphite surface by direct current (DC) magnetron sputtering of nanoscale Cu and Ni layers (Fig. 4**a and b**), which increased the overpotential for the initial nucleation of Li on the graphite surface, i.e., increased the overpotential for lithium deposition. As shown in Fig. 4**c**, after six hours of plating at −20 mV, a large interconnected dense lithium film (dark part) was observed on the surface of the graphite electrode without the metal layer. Conversely, the graphite electrode coated with nanometer-thick layers of Cu and Ni retains a clear graphite structure, indicating that these Cu and Ni films effectively prevent lithium dendrite formation under voltage conditions conducive to lithium deposition. However, the long-term stability and reproducibility of this method require further validation. In particular, the durability of nanoscale metal layers under repeated charge–discharge cycles remains a critical concern, as delamination or corrosion can significantly degrade battery performance. To address this, optimization of both the fabrication process and material selection is essential to enhance the structural integrity and electrochemical stability of the metal layers over extended cycling.

Surface coating is a facile approach to adjust the overpotential of graphite surface and enhance mechanical stability. Dong et al. [90] fabricated TiO_{2-x} nanoparticles on the graphite surface through an in situ carbothermal reduction process (Fig. 4**d**), in which the oxygen vacancies can reduce the activation energy of Li-ion insertion. The lithiated $Li_\delta TiO_{2-x}$ reduces the adsorption energy of Li^+ on the graphite surface, which favors the lithium migration during the cycling process. Moreover, surface modification with TiO_{2-x} can effectively inhibit undesired side reactions on the graphite surface, as well as maintain the path of lithium migration in the electrodes, which in turn inhibits the formation of lithium dendrites (Fig. 4**e-j**). Despite its promise, this method presents several challenges. The synthesis of TiO_{2-x} nanoparticles often requires high temperatures and complex processing conditions, which can increase production costs and energy consumption. Additionally, ensuring uniform dispersion and long-term stability of nanoparticles is critical, as inhomogeneous coatings may result in performance inconsistencies. These limitations may be mitigated through the development of low-temperature or green synthesis approaches, alongside optimization of processing parameters to improve scalability and reliability.

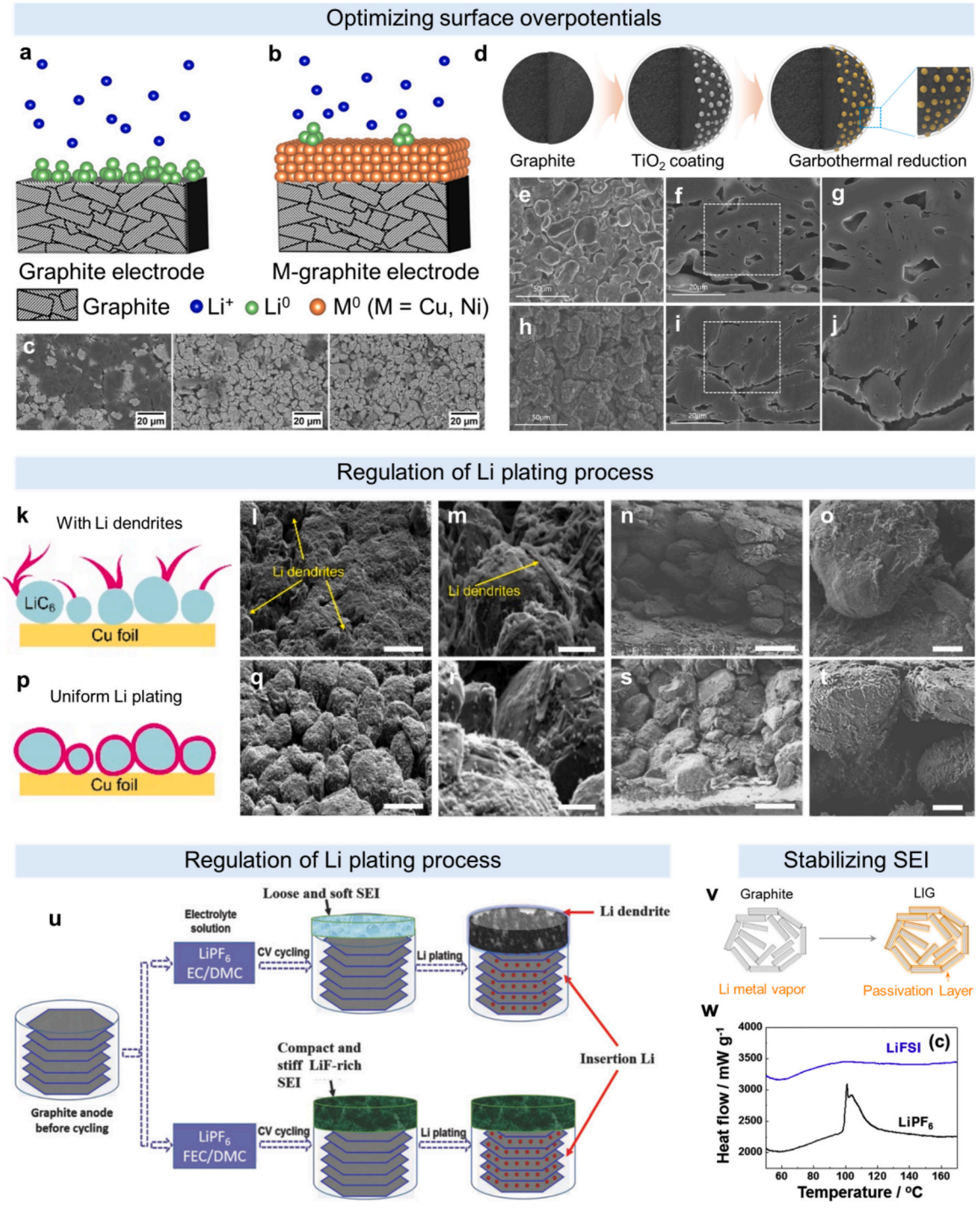

Fig. 4. Safe modification of anodes. (a) Schematic representation of lithium metal nucleation on graphite surface during high current charging, (b) decrease in nucleation due to increase in super-potential for lithium metal deposition provided by Cu or Ni surface coatings with structural mismatch, (c) morphology after lithium plating on graphite electrodes with uncoated metal, Cu, and Ni layers at −20 mV [73]. Copyright (2022) John Wiley and Sons. (d) Schematic representation of the material design and synthesis process of TiO_{2-x} modified graphite anode by in-situ carbothermal reduction process for TiO_{2-x} modified graphite after 100 cycles, (e) top view, (f) cross-section, and (g) magnification of graphite anode, and (h) full view, (i) cross-section, and (j) magnification of TiO_2-x-modified graphite anode in FESEM images [90]. Copyright (2020) Elsevier. (k) Schematic and (l-o) corresponding SEM images of graphite electrodes containing Li dendrites: (l, m) top surface, (n, o) cross-section, (p) Schematic and (g-j) corresponding SEM images of uniformly lithium-coated graphite electrodes with (q, r) top surface, (s, t) cross-section, scale lengths in (l, n, q, s) and (m, o, I, t) 20 nm and 5 nm, respectively [80]. Copyright (2021) John Wiley and Sons. (u) Schematic representation of the

effect of Li dendrite inhibition by 1.0 m $LiPF_6$ in ethylene carbonate (EC)/dimethyl carbonate (DMC) and 1.0 m $LiPF_6$ in FEC/DMC electrolytes [91]. Copyright (2017) Wiley-Blackwell. (v) Graphite particles before and after thermal treatment in lithium metal vapor [92]. Copyright (2018) Elsevier. (w) LiFSI and $LiPF_6$ electrolytes subjected to DSC curves of fully de-lithiated graphite electrodes subjected to three cycles [93]. Copyright (2018) Elsevier.

3.2.2. Regulation of Li plating process

The composition of organic electrolyte is directly linked to the formation of SEI layers, offering a solution to constructing functional SEI layer that can regulate Li transport. For example, Cai et al. employed a localized high-concentration electrolyte to generate a thin yet robust SEI on the surface of the graphite anode [80]. As shown in Fig. 4**k-t**, this optimized SEI allowed the uniform deposition of Li on the surface of graphite anode. The lithium deposition reaction is fully reversible without the formation of "dead lithium" during cycles, enabling enhanced battery performance. Likewise, Shen et al. [91] used a fluorinated ethylene carbonate-based electrolyte to induce the formation of LiF-rich SEIs, which are stiffer and denser than those formed within ethylene carbonate-based electrolytes. Since this SEI has better mechanical properties and more excellent electrical resistance, the reduction of Li^+ and the formation of lithium dendrites can be effectively inhibited. In addition, with high surface energy, LiF can promote the uniform diffusion of Li-ion during lithium deposition, forming a dendrite-free morphology (Fig. 4**u**). However, these electrolyte systems also encounter practical challenges, including high cost, elevated viscosity, and concerns over environmental safety. These issues can be addressed by developing novel electrolyte materials, refining synthesis processes, integrating the strengths of different electrolyte types, and implementing holistic improvement strategies. Such approaches are expected to enhance the stability and functionality of the SEI layer, thereby enabling comprehensive performance optimization of LIBs.

In addition, there are researchers applying new polymer separator materials to the anode surface. Their higher ion transport properties make them effective in improving the uniformity of the lithium plating layer [95]. For example, Baran et al. coated polymers of intrinsic microporosity (PIMs) containing bis(catechol) free volume elements (FVEs) on the anode surface [96]. The results show that this PIM with solid solvation cages for Li^+ promotes uniform plating and stripping of lithium metal, thereby improving the safety and stability of the battery. Similarly, Fu et al. coated the LiF@PIM composite on the anode surface [97]. This coating made the lithium coating denser by limiting the extent of space charge accumulation on the anode surface, effectively inhibiting the formation of dendrites. In addition, due to the unique mechanical strength of the coating, its upper layer can also act as an additional dendrite-blocking layer, further enhancing the safety performance of the battery. Also, there are some new separator designs for flow batteries that can be learnt from [98–104].

3.2.3. Stabilizing SEI

Besides adopting specific organic solvents, prelithiation and addition of functional Li salts also play an important role in stabilizing the SEI and further contribute to the safety performance of batteries. Choi et al. [92] generated prelithiated graphite (LIG) by immersing the graphite into lithium metal vapor followed by exposure to the ambient atmosphere. The lithium metal on the surface of the LIG was oxidized to form a thin and stable passivation layer (Fig. 4**v**). This passivation layer consists of stable and water-insoluble

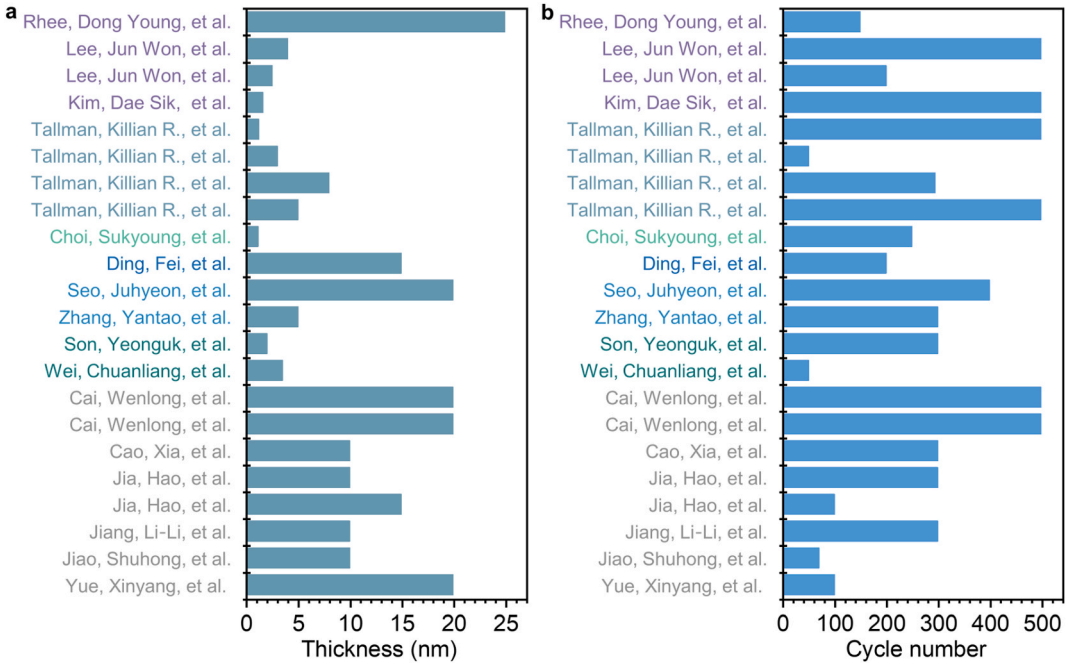

Fig. 5. SEI-related strategies to help suppress lithium dendrites and improve battery stability. a) Thickness of SEI layer, b) Number of cycles.

inorganic compounds (e.g., Li_2CO_3), significantly enhancing the safety performance of graphite anodes even under abusive conditions. Apart from pre-fabricating the passivation layer, the passivation layer can be in situ constructed using functional Li salts. As a typical example, Kang et al. [93] used a lithium bis(fluorosulfonyl) imide (LiFSI)-based electrolyte to form a thin and thermally stable layer of inorganic-rich SEI on the surface of the graphite anode. As shown in Fig. 4**w**, SEI formed by LiFSI possessed a stable and broad thermal window, whereas the SEI layer produced from lithium hexafluorophosphate ($LiPF_6$)-based electrolyte started to decompose at approximately 98 °C.

In addition, we summarize several methods for constructing stable SEI layers, including strategies such as metal oxide coating, Sputtering deposited metals, and pre-lithiation treatment (Fig. 5). Fig. 5**a** illustrates the thickness of the SEI layers prepared using these strategies, while Fig. 5**b** shows the number of cycles of the corresponding cells, as detailed in Table 1. Through these methods, stable SEI layers can be successfully constructed on the surface of graphite anode. Although the thickness of these SEI layers varies, they can all effectively inhibit the growth of lithium dendrites and enhance the cycling stability of the battery. However, these strategies may have different degrees of impact on the capacity of the battery. The challenge is therefore to find the right balance between safety and electrochemical performance, and to achieve the highest safety performance with the least loss of performance.

3.2.4. Other approaches

Additionally, several effective material solutions have been explored to enhance battery safety. For instance, Gribble et al. [120] used the commercial conductive polymer poly (3,4-ethylenedioxythiophene) polystyrene sulfonate (PEDOT: PSS) as a binder, which exhibits greater stability with actively embedded lithium, and significant reduces heat generation during the SEI decomposition; Chang et al. [121] applied a heat-resistant coating to the surface of the graphite anode, which acts as a barrier during thermal runaway—when the separator shrinks or melts, the coating isolates the cathode from the anode, preventing direct contact and short-circuiting. Zhao et al. [122] embedded metal-aluminum nanoparticles into graphite materials via oxidative expansion, leading to a notable improvement in thermal conductivity. Deng et al. [123] introduced positive temperature coefficient thermosensitive polymer microspheres (TSPMs) into graphite anodes, enhancing batteries safety under abusive conditions.

While current strategies have substantially improved the safety of graphite anodes, several critical factors must be carefully considered for practical deployment. For example, the use of artificial membranes to suppress lithium dendrite formation, although promising, requires thorough evaluation of its impact on energy density and lithium-ion diffusion kinetics. As lithium-ion diffusion efficiency governs fast-charging performance, and energy density determines driving range, any modification affecting these parameters demands rigorous experimental validation and process optimization. In parallel, approaches aimed at stabilizing the SEI must account for their influence on the overpotential of lithium intercalation and deposition. Elevated overpotential can reduce Coulombic efficiency and compromise overall energy efficiency. Therefore, an ideal modification strategy should balance improved safety with preserved electrochemical performance. The incorporation of nanoporous materials or composite membrane architectures offers a potential pathway, combining mechanical robustness with enhanced ion transport.

From a full life cycle perspective, environmental considerations are critical and must not be overlooked [124]. The adoption of new materials can introduce additional environmental burdens across three key stages: raw material extraction, energy-intensive manufacturing processes, and challenges in end-of-life disposal [125,126]. Moreover, the increasing complexity of material systems complicates recycling, underscoring the need for advanced, targeted green recovery technologies [127,128]. Modifying graphite anodes thus remains a multifaceted challenge requiring ongoing research to balance safety, energy performance, environmental

Table 1
SEI layer thickness and cycling stability under various modification methods.

Methods	SEI layer thickness (nm)	Cycle number	Capacity retention (%)	Ref
Metal oxide coating	20.0	100	99.8	[105]
	10.0	70	71.4	[106]
	10.0	300	85.6	[106]
	15.0	100	97.2	[107]
Sputtering deposited metals	10.0	300	76.0	[73]
	10.0	300	90.0	[73]
	20.0	500	77.0	[108]
	20.0	500	76.0	[108]
Prelithiated	3.5	50	92.0	[92]
Fluoride coating	2.0	300	92.0	[109]
Polymer coating	5.0	300	84.0	[110]
	20.0	400	50.0	[111]
Non-metallic coating	15.0	200	99.0	[112]
	1.1	250	76.1	[113]
Electrolyte additive	5.0	500	80.2	[114]
	8.0	295	End-of-life	[114]
	3.0	50	99.0	[115]
	1.2	500	95.6	[116]
	1.6	500	75.8	[116]
	2.5	200	85.5	[117]
	4.0	500	80.0	[118]
	25.0	150	84.4	[119]

sustainability and cost. Addressing this challenge demands not only materials innovation but also the integration of insights from environmental engineering and industrial economics. We propose a comprehensive four-dimensional evaluation framework encompassing performance, safety, environmental impact and cost to guide the development of safer and more sustainable graphite anode systems.

4. Safe electrolytes

Electrolyte serves as the charge-carrier medium in batteries, including solid, liquid and hybrid types, and conventional commercial electrolytes are liquid, consisting of two parts: an organic solvent (Table 2) [129] and a lithium salt (Table 3) [130]. Ideal organic solvents for electrolytes should fulfill following requirements: (1) a low vapor pressure, a low melting point, and a high boiling point to afford a wide operating temperature range; (2) high dielectric constant and low viscosity to improve conductivity. However, the trade-off between dielectric constant and viscosity requires the mixture of various solvents to provide sufficient properties. For example, by mixing linear carbonates (e.g., EC, DMC, diethyl carbonate (DEC), and ethyl methyl carbonate (EMC)) with cyclic carbonates, a composite electrolyte with appropriate electrochemical stability and good interfacial properties can be obtained [131]. This is the most common combination within commercial electrolytes. However, its low flash point increases its risk of decomposing into flammable gases that can ignite quickly under abusive conditions, producing significant heat and potentially leading to thermal runaway.

Ideal lithium salts should feature the following traits: (a) strong thermal stability, resistant to decomposition; (b) high ionic conductivity in solution; (c) strong chemical stability, meaning no reaction with solvents or electrode materials. Among the prevalent lithium salts, $LiPF_6$ is commonly chosen for commercial use due to its excellent ionic conductivity and capacity to passivate aluminum collectors. However, its thermal stability is limited. At high temperature, $LiPF_6$ tends to decompose into LiF and PF_5, and PF_5 will react with organic solvents and produce heat and combustible gas [132–135].

Clearly, safety performance is a significant concern even in widely used commercial lithium-ion battery electrolyte systems. As such, there is a pressing need to develop electrolyte systems that offer enhanced safety. Three critical research directions have been focused throughout this field.

(1) The use of functional additives, e.g., flame-retardants and overcharging protectors, to enhance the safety performance of liquid electrolytes.

(2) Nonflammable electrolyte solvents can also be used, such as ionic liquids, deep eutectic solvents, aqueous electrolytes, and low-molecular-weight hydrofluoroethers, etc. However, these solvents are not cost-effective and sacrifice the energy outputs.

(3) Nonflammable solid-state and quasi-solid electrolytes, such as gel polymer electrolytes, solid polymer electrolytes, solid inorganic electrolytes, and composite solid-state electrolytes. Solid-state electrolytes address issues like electrolyte leakage and ISC, yet they also face challenges, including lithium dendrite growth, low ionic conductivity, and limited electrochemical stability.

In summary, while these three approaches to improving electrolytes each have their benefits and drawbacks, the crucial aspect in enhancing the safety of lithium-ion battery electrolytes, regardless of the approach, is to find a balance between electrochemical performance and safety. Given that liquid electrolytes are the predominant choice in current electrolyte technologies, this chapter will concentrate on liquid electrolytes.

4.1. Failure mechanism of liquid electrolyte

Safety concerns with liquid electrolytes stem from two main components: the organic solvent and the lithium salt solute. The organic solvent consists of highly flammable carbonates [136–142]. As shown in Fig. 6 (left), under abusive conditions that lead to excessively high internal battery temperatures, the carbonates will decompose into gaseous flammable vapor (RH). The combustion product of RH and H • radicals, subsequently react with the oxygen released from the anode during thermal runaway, producing HO • radicals and O • radicals. The HO • and O • radicals tend to react with hydrogen from electrolytes and hydrogen from the decomposition of trace residual water, leading to the formation of H • and HO • radicals. This cycle of reactions generates a large number of free radicals that facilitate combustion, thereby accelerating the thermal runaway process, as illustrated in the equation provided (Eq. 1–4) [143]:

$$RH \rightarrow R\bullet + H\bullet \quad (1)$$

Table 2
Basic properties of common organic solvents for battery electrolytes [129]. Copyright (2006) Elsevier.

Attributes	PC	EC	DMC	DEC
Molecular formula	$C_4H_6O_3$	$C_3H_4O_3$	$C_3H_6O_3$	$C_5H_{10}O_3$
Molecular weight (g mol^{-1})	102.09	88.06	90.08	118.13
Density (25 °C) (g cm^{-3})	1.2	1.4	1.06	0.971
Boiling point (°C)	242	238	90	126
Melting point (°C)	−49	37	3	−43
Viscidity (mPa·S)	2.5	1.9(40 °C)	0.59	0.75
Flash point (°C)	132	157	18	33
Permittivity (C V^{-1} m^{-1})	65	96	3.1	2.8

Table 3
Physical and electrochemical properties of common lithium salts and conclusive assessment of their safety [130]. Copyright (2014) American Chemical Society.

Salt properties	$LiPF_6$	LiFAP	$LiBF_4$	$LiAsF_6$	$LiClO_4$	LiTFSI
Ionic conductivity	+	+	**o**	+	+	+
Electrochemical stability	+	**o**	**o**	+	+	+
Thermal stability	−	**o**	**o**	+	−	+
Moisture stability	−	**o**	**o**	**o**	**o**	+
Current collector passivation	+	+	+	+	**o**	−
Toxicity	−	−	−	−	−	−
∑ safety	−	−/**o**	**o**	−	−	+

Note: +, High; **o**, medium; −, low.

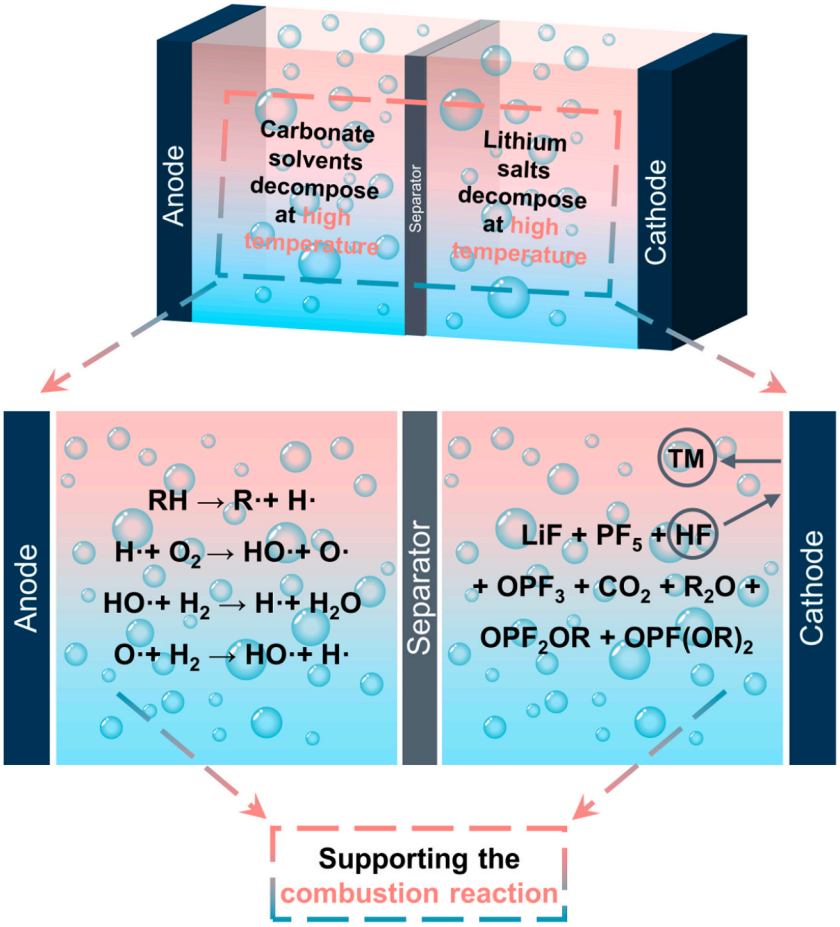

Fig. 6. Schematic showing the failure mechanisms of liquid electrolyte at high temperatures.

$$H\bullet + O_2 \rightarrow HO\bullet + O\bullet \quad (2)$$

$$HO\bullet + H_2 \rightarrow H\bullet + H_2O \quad (3)$$

$$O\bullet + H_2 \rightarrow HO\bullet + H\bullet \quad (4)$$

Given this failure mechanism, two strategies have been employed to enhance safety of organic solvents, one by reducing the flammable free radicals, such as the use of fluoride flame-retardant additives [144] and phosphorus flame-retardant additives [145]; the other by employing overcharge protection additives such as shutdown overcharge additives [140,146] and redox shuttle additives [147–149].

As illustrated in Fig. 6 (right), $LiPF_6$—the most used salt—decomposes instantly at high temperatures to produce LiF and PF_5, a strong Lewis acid that can react with organic solvents in the electrolyte or trace residual water to form oxides of fluorine (OPF_3) and HF. The formed OPF_3 can induce multiple and complex side reactions to produce CO_2, alkyl ethers (R_2O) and fluoro-phosphates

(OPF_2OR and $OPF(OR)_2$) [150]. Moreover, the formed HF also corrodes the surface of the cathode material and enables the dissolution of transition metals, affecting battery performance and causing safety issues. To address this problem, potential alternatives towards $LiPF_6$ are being developed, such as lithium bis(oxalate)borate (LiBOB) [151] and lithium difluoro(oxalate)borate (LiDFOB) [152]. Although these new lithium salts offer certain advantages, their ionic conductivity is lower compared to $LiPF_6$, and they exhibit instability at high potentials of > 4.2 V. Consequently, these novel salts cannot fully replace $LiPF_6$. Instead, they are frequently used as additives, combined with $LiPF_6$, to enhance the safety of liquid electrolytes.

4.2. Liquid electrolytes modification

4.2.1. Flame-retardant additives

Flame retardants can be categorized into physical and chemical flame-retardants according to their working principles. Physical flame retardants typically work by generating flame-retardant vapors that dilute combustible elements and block oxygen, thereby improving their flame-retardant efficacy. However, the main issue with traditional physical flame retardants is their poor compatibility with electrolytes, which can significantly affect the electrochemical performance of batteries when added. Therefore, it is necessary to adjust their molecular structure and design for better integration. For example, Chen et al. [153] developed 2-ethoxy-2,4,4,6,6-pentafluoro-1,3,5,2,4,6-triazatriphosphine (abbreviated as PFTP) and perfluoro-2-methyl-3-pentanone (abbreviated as PMP) through intermolecular interactions to obtain a novel "supramolecular flame-retardant" (defined as "SFR"). As shown in Fig. 7**a** and Fig. 7**b**, the SFR exhibits better flame-retardant properties than conventional carbonate electrolytes. In addition, SFR reduces the self-extinguishing time (SET) of the carbonate-based electrolyte from about 100 s/g to about 0 s/g (Fig. 7**c**) and effectively suppresses

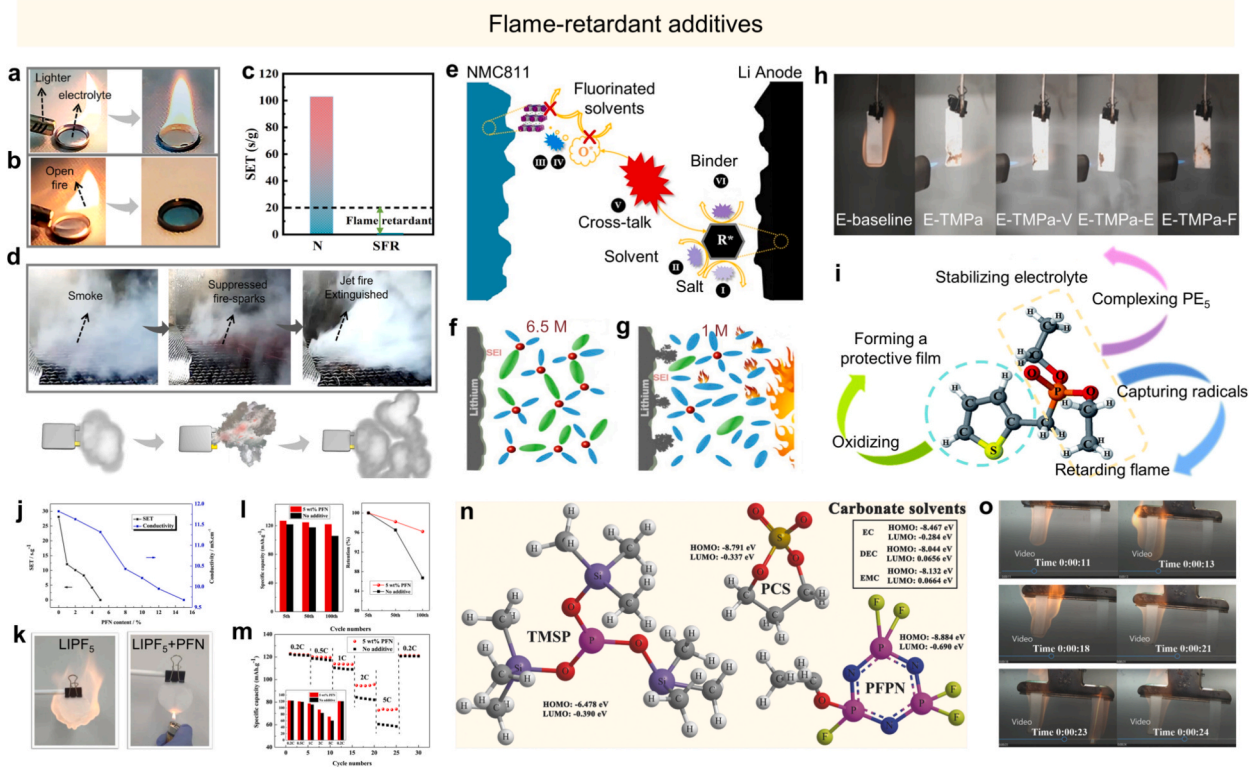

Fig. 7. Flame-retardant additives. (a) Flame-retardant tests of conventional electrolyte and (b) SFR electrolytes, (c) SET values of SFR and conventional electrolytes, (d) Flame-retardant tests of pouch battery with SFR electrolyte and its schematic diagram [153]. Copyright (2022) Elsevier. (e) NCM811|Gr-FEC + D_2 battery during thermal runaway with key exothermic reactions diagram [154]. Copyright (2022) John Wiley and Sons. (f) Schematic diagram of lithium-sulfur battery using 6.5 M lithium bis(trifluoromethanesulfonyl)imide (LiTFSI)/FEC and (g) 1 M LiDFOB/PC [155]. Copyright (2020) Elsevier. (h) Determination of flammability comparing different electrolytes by ignition test [156]. Copyright (2021) John Wiley and Sons. (i) Molecular structure and function of DTYP [157]. Copyright (2018) Royal Society of Chemistry. (j) SET and ionic conductivity of electrolytes containing different concentrations of PFN, (k) Photographs of electrolyte flammability tests: base electrolyte 1 M $LiPF_6$/EC + DEC + DMC (1:1:1, v/v/v) and the same electrolyte containing 5 wt% PFN additive, (l) Capacity retention of $LiNi_{0.5}Mn_{1.5}O_4$ cells with and without PFN additive, (m) Rate performance of $LiNi_{0.5}Mn_{1.5}O_4$ cells with and without PFN additive at different current rates ranging from 0.2C to 5C [158]. Copyright (2018) Elsevier. (n) Chemical structures of TMSP, PCS, PFPN additives and their HOMO and LUMO energy levels, (o) flame-retardant test demonstration: carbonate base electrolyte (BE) (left side of clip) and (right side of clip) BE + ternary functional additives (1 wt% TMSP + 1 wt% PCS + 7 wt% PFPN). BE burned continuously from the first ignition, while BE + ternary functional additive self-extinguished 5 times each after combustion [159]. Copyright (2018) Wiley-VCH.

the "jet fire" (Fig. 7**d**), which improves the thermal safety of commercial pouch LIBs. Nonetheless, the flame-retardant efficacy of physical flame retardants on their own remains limited, making it challenging to use them solely as electrolyte additives.

As a result, current research is concentrating on chemical flame retardants to enhance the thermal stability of liquid electrolytes more efficiently. These chemical flame retardants primarily function by neutralizing various reactive radicals involved in combustion reactions. Based on their specific flame-retardant mechanisms and constituent elements, chemical flame retardants can be broadly classified into three categories: fluoride, phosphorus, and composite flame-retardant additives.

Fluoride-based flame retardants.

Organic solvents containing fluoride flame-retardant additives tend to have higher oxidative stability, lower melting points and higher flash points due to the highest electronegativity and low polarization of their fluorine atoms. More importantly, fluoride flame-retardants can inhibit the propagation of flame-retardant radicals during combustion. For example, allyl tris(2,2,2 trifluoroethyl) carbonate (ATFEC) forms gaseous ATFEC at high temperatures, and the gaseous ATFEC breaks down into small fluoride ion radicals, which interact with H • radicals, thereby interrupting the radical reactions that fuel combustion (Eq. 5–7) [160]:

$$ATFEC_{liquid} \rightarrow ATFEC_{gas} \tag{5}$$

$$ATFEC_{gas} \rightarrow [F]\bullet \tag{6}$$

$$[F]\bullet + H\bullet \rightarrow H[F] \tag{7}$$

By following this principle, Hou et al. [154] used fluoroethylene carbonate (FEC) as a flame-retardant additive in $LiNi_{0.8}Co_{0.1}Mn_{0.1}$ (NCM811)|Gr pouch batteries to improve the thermal stability performance of LIBs. They observed the thermal runaway evolution of this cell using accelerated calorimetry (ARC) and cone calorimetry (Fig. 7**e**). As a result, fluorinated electrolyte effectively inhibited the propagation of oxygen radicals and significantly reduced the heat release during the thermal runaway. Besides, fluoride flame-retardant additives can facilitate the formation of a stable SEI. For example, Yu et al. [155] designed a novel concentrated electrolyte (6.5 M lithium bis(trifluoro methylsulfonyl)imide/fluoroethylene carbonate), which contributes to the formation of the stable LiF-rich solid-state electrolyte interface formed on the lithium metal anode in Li-S batteries (Fig. 7**f** and Fig. 7**g**). The resulting Li-S batteries exhibited a good cycling performance even at 90 °C.

While fluoride flame-retardant additives can notably enhance the thermal stability of liquid electrolytes, challenges such as their high cost, limited compatibility with $LiPF_6$, and the need for high concentrations significantly restrict their practical use. Thus, it is crucial to either find lithium salts that better match fluoride flame-retardant additives or to enhance the compatibility of these additives with $LiPF_6$. For example, developing electrolyte systems based on novel lithium salts such as LiFSI can improve compatibility with fluorinated flame-retardant additives. Alternatively, molecular structure modification of these additives can enhance their dispersion and stability within the electrolyte.

Phosphorus flame retardants.

Phosphorus flame-retardant additives are widely used due to their diversity, cost effectiveness, compatibility with $LiPF_6$ and effective flame-retardant function. The working mechanism of this retardant is like that of fluoride flame retardants. As a typical example, liquid trimethyl phosphate (TMP) evaporates into gaseous TMP at high temperatures and subsequently decomposes to produce phosphorus-containing radicals, which react with H • radicals and inhibit the combustion reaction (Eq. 8–10) [143]:

$$TMP_{liquid} \rightarrow TMP_{gas} \tag{8}$$

$$TMP_{gas} \rightarrow [P]\bullet \tag{9}$$

$$[P]\bullet + H\bullet \rightarrow H[P] \tag{10}$$

By following this mechanism, Jia et al. [156] prepared trimethyl phosphate (TMP_a)-based electrolytes using the high-concentration electrolyte (LHCE) approach. As shown in Fig. 7**h**, the TMP_a-based LHCEs (E-TMP_a, E-TMP_a-V, E-TMP_a-E, and E-TMP_a-F) exhibited remarkable flame-retardant performance. In addition, the structures of phosphorous flame retardant are tunable to afford enhanced performance. For example, Zhu et al. [157] designed a novel phosphorus additive, diethyl(thiophen-2-ylmethyl) phosphonate (DTYP) (Fig. 7**i**). Oxygen atoms in DTYP can eliminate PF_5 by the acid-base interaction, preventing PF_5 from reacting with organic solvents. Moreover, the phosphate group can also inhibit the combustion reaction by preventing the propagation of free radicals during the combustion process. Incorporating a tiny amount of DTYP can significantly enhance the thermal stability of electrolytes.

Although phosphorus flame-retardant additives offer good thermal stability, their effectiveness at low doses is limited, and their high viscosity can affect electrochemical performance. Furthermore, their narrow electrochemical window may lead to adverse reactions on the anode surface, increasing impedance and reducing capacity. Thus, optimizing phosphorus flame-retardant additives to balance their flame-retardant and electrochemical properties is crucial, e.g., use of polymer protecting shell [161] and co-precipitation of phosphorus additives [162].

Composite flame retardants.

Composite strategy can be adopted to combine the advanced features from different additives to afford enhanced flame-retardant function, solubility and electrochemical compatibility. The use of combined flame-retardant elements results in a synergistic effect, enhancing thermal stability with minimal additive quantities without compromising its electrochemical performance [163–165]. For example, Liu et al. [158] demonstrates a novel composite flame-retardant additive, ethoxy-(pentafluoro)-cyclotriphosphazene (PFN)

and paired it with high-voltage lithium nickel manganese oxide (LNMO) materials. PFN combines the structures of the noncombustible cyclotriphosphazene and fluorine to deliver a highly synergistic flame-retardant effect and enhanced electrochemical compatibility (Fig. 7**j** and Fig. 7**k**). Moreover, PFN promoted the formation of a thinner and more uniform cathode electrolyte interface (CEI), enabling excellent cycle stability and multiplication performance (Fig. 7**l** and Fig. 7**m**).

Besides the use of flame retardants, additives with other functions can be also introduced in the composites. Xu et al. [159] designed a composite functional additive where tris(trimethylsilyl) phosphite (TMSP) and 1, 3-propanediolcyclic sulfate (PCS) contributed to the formation of stable SEI (Fig. 7**n**), and (Ethoxy)-penta-fluoro-*cyclo*-triphosphazene (PFPN) as a flame-retardant additive to enhance thermal safety (Fig. 7**o**). This combination can effectively balance flame retardancy and electrochemical performance.

In addition, we analyzed the regularity of the variation of SET and ionic conductivity with additive volume in different systems (Fig. 8**)**. Fig. 8**a** shows that the SET shows a decreasing trend with increasing additive volume (see Table 4 for data details). However, in some cases, SET rebounded when the additive volume was higher, mainly because although additives can improve the flame retardancy of electrolytes, once combustion occurs, such additives will burn for a longer time than the base electrolyte. Meanwhile, Fig. 8**b** shows that ionic conductivity decreases as the additive volume increases, a trend typically attributed to the rising viscosity of the electrolyte. Interestingly, in certain cases, increasing the additive content can initially enhance ionic conductivity, which is a favorable outcome. However, beyond a certain threshold, further increases in additive volume led to a decline in ionic conductivity. In summary, while improving the flame-retardant properties of electrolytes, it is essential to carefully consider their impact on electrochemical performance and strive to achieve an optimal balance.

4.2.2. Overcharging protection additive

Overcharge protection additives fall into two types: shutdown additives, which permanently disable the battery via polymerization, and redox shuttle additives, which reversibly prevent overcharging through redox reactions. Shutdown overcharge additives offer irreversible protection against overcharging by operating through two mechanisms: (1) releasing significant gas at high potentials to trigger a current interrupter, disconnecting the battery from external circuits, and (2) initiating a polymerization reaction at elevated potentials to coat the cathode surface, thereby preventing overcharging. Typical shutdown overcharge additives include xylene [176], cyclohexylbenzene [177] and biphenyl [178], 2,2-diphenylpropane [179] and its derivatives [170], while redox shuttle additives are biphenyl, pyrrole, and thiophene, as well as other substituted aromatic compounds [180,181].

The key feature of shutdown overcharge additives is their ability to provide overcharge protection at high voltages/currents. For example, by modifying the ligands in 1,3-dimethylimidazolidin-2-um-trifluoroborate (NHC-BF_3) and 1,3-dimethylimidazolidin-2-um-tetrafluorotrifluoromethylphosphate (NHC-PF_4CF_3), Janssen et al. [184] synthesized 1,3-dimethylimidazolidin-2-um-pentafluorophosphate (NHC-PF_5) with varying cutoff voltages. The different electron-withdrawing group strengths led to cutoff voltages of 4.5 V for NHC-BF_3, 4.6 V for NHC-PF_5, and 4.7 V for NHC-PF_4CF_3. Importantly, these variations did not impact the cycling performance of batteries operating within the 4.2 V voltage range. Nevertheless, the shutdown overcharge additives with less sustainability are not

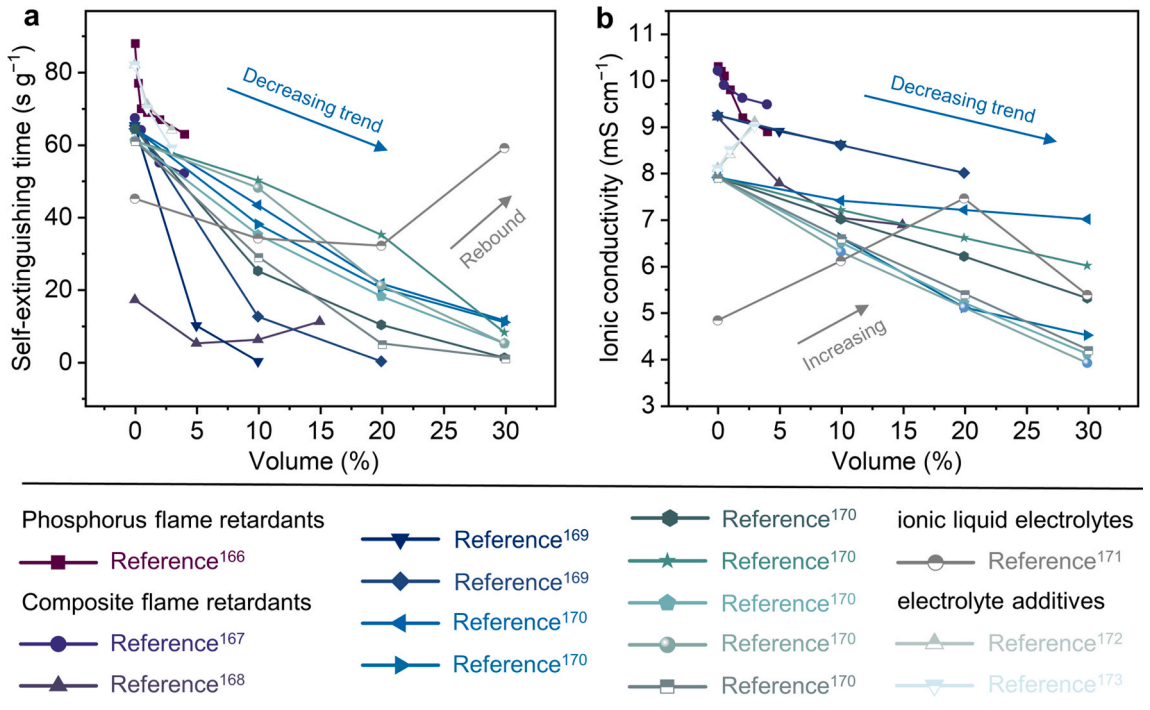

Fig. 8. Variation of self-extinguishing time and ionic conductivity with additives volume. (a) Self-extinguishing time and (b) Ionic conductivity.

Table 4
Variation of set and ionic conductivity with additive volume in different systems.

Methods	Material	SET (s g^{-1})	σ (mS cm^{-1})	Reference
Phosphorus flame retardants	1.0 M $LiPF_6$ in EC/EMC (3:7)	88	10.3	[166]
	0.25 % Diethyl(thiophen-2-ylmethyl)phosphonate-containing electrolytes (DTYP)	77	10.2	[166]
	0.5 % DTYP-containing electrolytes	70	10.1	[166]
	1 % DTYP-containing electrolytes	69	9.8	[166]
	2 % DTYP-containing electrolytes	67	9.2	[166]
	4 % DTYP-containing electrolytes	63	8.9	[166]
Composite flame retardants	1.0 M $LiPF_6$ in EC/DMC/DEC (1:1:1)	67.3	10.21	[167]
	0.5 % Tris (pentafluorophenyl) phosphine (TPFPP)	64	9.9	[167]
	2 % Tris (pentafluorophenyl) phosphine (TPFPP)	55	9.62	[167]
	4 % Tris (pentafluorophenyl) phosphine (TPFPP)	52	9.48	[167]
	1.0 M $LiPF_6$ in EC/DMC (1:1)	17	9.2	[168]
	5 % pentafluoroethoxy cyclotriphosphazene (PFPN)	5	7.78	[168]
	5 % PFPN + 5 % dimethylacetamide (DMAC)	6	7.03	[168]
	5 % PFPN + 10 % DMAC	11	6.88	[168]
	1.0 M $LiPF_6$ in EC/EMC (3:7)	65.2	9.24	[169]
	5 % ethoxy(pentafluoro)cyclotriphosphazene (PFPN)	9.9	8.9	[169]
	10 % PFPN	0	8.62	[169]
	10 % fluoroethylene carbonate (FEC)	66.7	9.2	[169]
	5 % FEC + 5 % FECPFPN	12.4	8.6	[169]
	10 % FEC + 10 %PFPN	0	8	[169]
	1.0 M $LiPF_6$ in EC:DEC (1:1)	64.3	7.9	[170]
	10 % triethyl phosphate (TEP)	43.2	7.4	[170]
	20 % TEP	21.5	7.2	[170]
	30 % TEP	11.3	7	[170]
	10 % tris(2,2-difluoroethyl) phosphate (TFHP)	37.9	6.6	[170]
	20 % TFHP	20.3	5.1	[170]
	30 % TFHP	10.8	4.5	[170]
	10 % tris(2,2,2-trifluoroethyl) phosphate (TFP)	25	7	[170]
	20 % TFP	10.1	6.2	[170]
	30 % TFP	1	5.3	[170]
	1.0 M $LiPF_6$ in EC:DEC (1:1)	61	7.9	[170]
	10 % alkyl phosphate tripropyl phoshphate (TPrP)	50	7.2	[170]
	20 % TPrP	35	6.6	[170]
	30 % TPrP	8	6	[170]
	10 % tris(3,3,3-trifluoropropyl) phosphate (3F-TPrP)	35	6.5	[170]
	20 % 3F-TPrP	18	5.2	[170]
	30 % 3F-TPrP	5	4.1	[170]
	10 % tris(2,2,3,3-tetrafluoropropyl) phosphate (4F-TPrP)	48	6.3	[170]
	20 % 4F-TPtP	21	5.1	[170]
	30 % 4F-TPtP	5	3.9	[170]
	10 % tris(2,2,3,3,3-pentafluoropropyl) phosphate (5F-TPrP)	29	6.6	[170]
	20 % 5F-TPrP	5	5.4	[170]
	30 % 5F-TPrP	1	4.2	[170]
Ionic liquid electrolytes	Commercial carbonate electrolyte	126.8	0.46525	[171]
	20 % 1-butyl-1-methyl pyrrolidinium bis (trifluoromethyl sulfonyl) azanide ionic liquid ([BMP]TFSI)	94.3	0.59284	[171]
	40 % [BMP]TFSI	82.3	0.57957	[171]
	60 % [BMP]TFSI	67.8	0.47258	[171]
	80 % [BMP]TFSI	0	–	[171]
	100 % [BMP]TFSI	0	–	[171]
Electrolyte additives	1.0 M $LiPF_6$ in EC/DMC (1:1)	45	4.82	[172]
	10 % sulfolane (SL)	34	6.1	[172]
	20 % SL	32	7.45	[172]
	30 % SL	59	5.37	[172]
	1.15 M $LiPF_6$ in EC/EMC (3:7)	82	8.1	[173]
	1 % 1-ethyl-3-methylimidazolium hexafluorophosphate (IMI IL)	71	8.4	[173]
	3 % IMI IL	64	9.1	[173]
	1 % 1-butyl-3-methylpyrrolidinium hexafluorophosphate (Pyr IL)	70	8.5	[173]
	3 % Pyr IL	59	9	[173]
Gel polymer electrolytes	1.0 M $LiPF_6$ in EC/DMC (3:7)	48.6	–	[174]
	Liquid DES	23	1.32	[174]
	gel polymer electrolytes-1	4.3	0.64	[174]
	gel polymer electrolytes-2	3.2	–	[174]
	dual-salt gel electrolyte	17	0.034	[175]
	8.97 % triethyl phosphat	0.03	3.1	[175]

cost-effective and challenging the large-scale application.

In contrast, redox shuttle additives demonstrate enhanced reversibility. At normal voltages, these additives remain inactive. Upon overcharging, they are oxidized at the cathode surface, transforming into their oxidized state [O]. Then they diffuse through the electrolyte to the anode, where a reduction reaction converts them back to their initial state [R]. The reduced redox shuttle additives can diffuse back to the cathode, ready to repeat the cycle if overcharging occurs again [185]. This process can be described below (Eq. 11–12).

$$R \rightarrow O + ne^- \tag{11}$$

$$O + ne^- \rightarrow R \tag{12}$$

Redox shuttle additives are designed with an oxidation potential higher than that of electrolytes and a reduction potential lower than that of electrolytes. This setup ensures they can prevent electrolyte decomposition during overcharging by intervening before the electrolyte breaks down. Given this reason, a rigorous molecular structure design is required. For example, Ahn et al. [182] developed a fluorinated redox shuttle additive, 2,4-difluorobiphenyl (FBP) as shown in Fig. 9**a-c**. The lowest occupied molecular orbitals (LUMO) values of BP and FBP are lower than those of EC and EMC (Fig. 9**d**), so they will preferentially undergo a reduction reaction on the cathode surface [186]. Meanwhile, BP and FBP prefer to undergo an oxidation reaction [187] due to their highest occupied molecular orbitals (HOMO), much higher than those of EC and EMC. Therefore, during overcharging, FBP acts in place of EC and EMC in the redox reaction, offering enhanced protection against overcharging. While BP and FBP, with their aromatic hydrocarbon structures, improve overcharge protection, their solubility in carbonate-based electrolytes is limited [188]. According to Fick's Law of Diffusion, lower solubility results in slower diffusion rates. A slower diffusion rate diminishes the cycling efficiency of redox shuttle additives and their ability to manage excess current, thereby compromising overcharge protection. Thus, the solubility of redox shuttle additives in organic electrolytes is crucial for effective overcharge protection, highlighting the need for solubility improvements.

Although redox shuttle additives are theoretically reversible, their cycle life can be affected by side reactions on the active surface

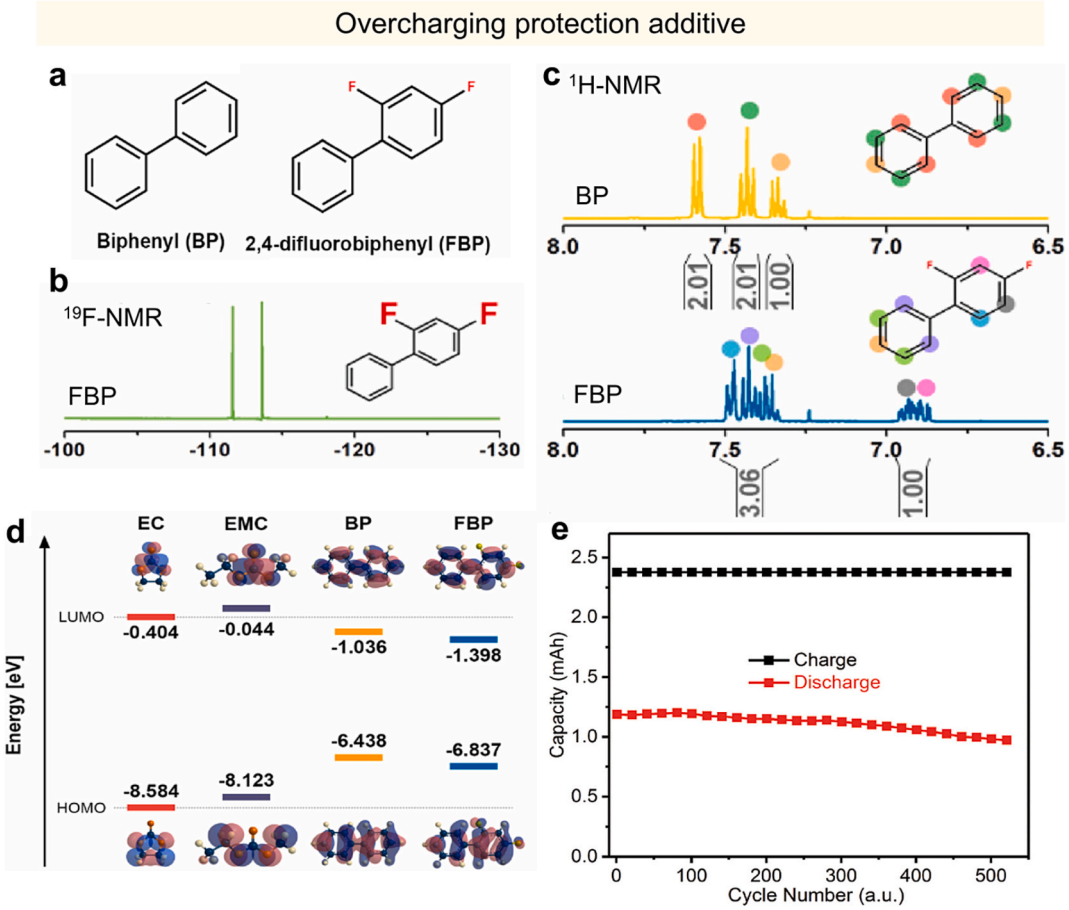

Fig. 9. Overcharging protection additives. (a) Molecular structures of BP and FBP, (b) 19F NMR spectra of FBP, (c) 1H NMR spectra of BP and FBP, and (d) HOMO and LUMO calculated by density-functional theory [182]. Copyright (2021) Elsevier. (e) Capacity curves at C-rate of C/2 and overcharge rate of 100 % [183]. Copyright (2019) Elsevier.

of electrodes [189]. To address this issue, specific modification is required. For instance, Zhang et al. developed highly soluble 1,4-dialkoxybenzene (DMMB) redox shuttle additives, which demonstrate exceptional solubility in carbonate electrolytes [183]. The planar structure of DMMB enhances the stability of its radical cations, significantly extending its overcharge cycle life. As illustrated in Fig. 9**e, a** battery combining a DMMB-containing mesocarbon microbead (MCMB) graphite anode with a $LiFePO_4$ cathode showed robust overcharge protection, maintaining performance across more than 500 cycles at a C-rate of C/2 and a 100 % overcharge rate.

Overcharge protection additives fall into two main categories, each with distinct advantages and limitations. Shutdown additives offer rapid response by irreversibly interrupting the circuit to prevent thermal runaway, but this mechanism compromises battery reusability. In contrast, redox shuttle additives provide reversible protection through charge dissipation, allowing continued operation. However, their performance is hindered by inherent limitations of organic molecules, including low solubility, limited diffusion coefficients and narrow electrochemical windows [190,191]. From a life cycle perspective, both additive types pose environmental concerns. Shutdown additives often rely on transition metal oxides, which generate substantial carbon emissions during smelting and carry risks of heavy metal leaching post-disposal. Redox shuttles, being poorly biodegradable, are inefficiently recovered through conventional physical recycling methods [192,193].

Future advances should prioritize molecular design innovation. Computer-aided strategies can enable the development of organometallic complex additives featuring chelating structures, which retain redox reversibility while enhancing solubility via coordination interactions. Concurrently, green recycling methods based on ionic liquids should be explored to achieve selective additive recovery through targeted dissolution. This multi-objective approach, i.e., integrating high-throughput screening and AI-driven prediction, seeks to maintain overcharge protection while improving environmental compatibility and economic viability, thereby enabling sustainable performance across the full cycle of protection, reuse and recycling.

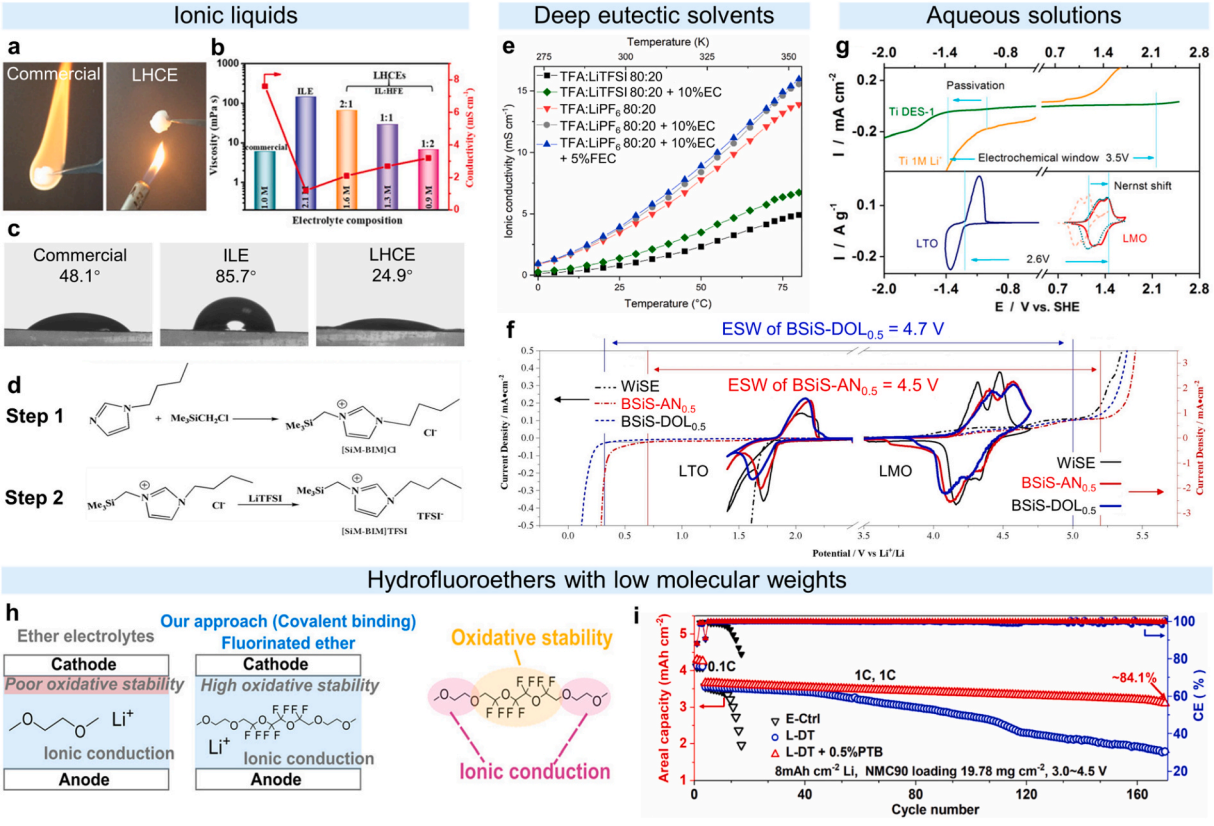

Fig. 10. Optimization of nonflammable liquid electrolytes. (a) Combustion test of commercial electrolyte and LHCE, (b) Viscosity and ionic conductivity of different electrolytes at 25 °C, (c) Wettability of commercial electrolyte, pure ionic liquid electrolyte (ILE) and LHCE [194]. Copyright (2021) Wiley-VCH. (d) Preparation flow of [SiM-BIM]TFSI [195]. Copyright (2019) American Chemical Society. (e) Ionic conductivity of DESs based on different HBAs at eutectic composition [196]. Copyright (2023) Elsevier. (f) Electrochemical stability window (ESW) of the electrolytes measured by linear sweep voltammetry (LSV) and cyclic voltammograms (CV) tests on LMO and $Li_4Ti_5O_{12}$ (LTO) using WiSE, BSiS-$AN_{0.5}$, and BSiS-$DOL_{0.5}$ electrolytes, respectively [197]. Copyright (2022) Elsevier. (g) (Upper) LSV of the collector Ti in DES-1 (MSM: $LiClO_4$:H_2O = 1.8:1:1) electrolyte and a typical aqueous solution of 1 mol L^{-1} $LiClO_4/H_2O$, (Lower) CVs of the LMO and LTO electrodes in DES-1 electrolyte [198]. Copyright (2019) American Chemical Society. (h) Schematic structure of the new fluorinated ether electrolyte with high ionic conductivity and oxidative stability [199]. Copyright (2020) American Chemical Society. (i) Cycling performance of Li||$LiNi_{0.9}Mn_{0.05}Co_{0.05}O_2$ (NCM90) cells using conventional carbonate electrolyte (E-Ctrl), LiFSI + DME/TTE electrolyte (L-DT), and LiFSI + DME/TTE + 0.5 wt% PTB electrolyte (L-DT + 0.5 % PTB), respectively (1C = 200 mA g^{-1}) [200]. Copyright (2022) Elsevier.

4.3. Nonflammable liquid electrolytes

Nonflammable liquid electrolyte systems are being constructed by using nonflammable electrolyte solvents, including ionic liquids, deep eutectic solvents, aqueous solutions, and low-molecular-weight hydrofluoroethers.

4.3.1. Ionic liquids

Ionic liquids, often referred to as low-temperature molten salts, are salts made of anions and cations that are liquid at or near room temperature. These include widely used cations like aliphatic quaternary ammoniums, imidazole, morpholines, pyrrolidines, and piperidines, along with common anions such as halide ions, tetrafluoroborate ions, and hexafluorophosphate ions [201]. In comparison to conventional electrolytes, ionic liquids have the advantages of low volatility, non-flammability, good chemical stability, and a wide temperature window [202–205], and therefore hold a promise for safe electrolytes. However, they suffer from high cost, poor wettability, high viscosity and low ionic conductivity, which hinders their practical application [203,206]. Therefore, strategies are needed to address these issues.

To lower the viscosity and enhance the ionic conductivity of ionic liquids, organic components acting as diluents can be introduced. For example, Wang et al. [194] developed an ionic liquid-based LHCE using LiFSI as the lithium salt, with ionic liquid N-methyl-N-propyl-piperidinium bis(fluoro sulfonyl)imide ([PP_{13}][FSI]), and 1,1,2,2-tetrafluoroethyl-2,2,3,3-tetrafluo-ropropylether (HFE) serving as a diluent. As a result, LHCE showed enhanced nonflammability (Fig. 10**a** and Fig. 10**b**). Moreover, adding HFE significantly reduced the viscosity of the ionic liquid electrolyte while improving its ionic conductivity and wettability (Fig. 10**c**).

Beyond incorporating specific organic solvents, designing the molecular structure is another effective strategy to enhance the electrochemical properties of ionic liquids. For instance, Chen et al. [195] crafted a novel heteroatomic silica-substituted imidazolium-based ionic liquid electrolyte, termed 1-trimethylsilylmethyl-3-butylimidazolebis(trifluoromethylsulfonyl)imide ([SiM-BIM]TFSI), with its preparation process illustrated in Fig. 10**d**. The inclusion of heteroatomic silicon substituents allowed [SiM-BIM]TFSI to achieve a low viscosity of 73.5 cP and an ionic conductivity exceeding 1.5 mS/cm at room temperature.

In conclusion, ionic liquids present promising prospects as a new class of nonflammable liquid electrolytes. However, challenges related to their synthesis process, viscosity, purity, ionic conductivity, and cost complicate their practical application. Further research focused on modifications is necessary to overcome these hurdles. For example, introducing low-viscosity side chains or employing mixed ionic liquid systems can reduce viscosity while preserving non-flammability. Additionally, optimizing the molecular structure of the ionic liquid can enhance ionic conductivity, thereby improving the battery's electrochemical performance.

4.3.2. Deep eutectic solvents

Deep eutectic solvents (DES) are similar to ionic liquids, as both are classified as low-temperature molten salts. DES are typically composed of hydrogen bond donors (HBDs), such as acetamides, urea, carboxylic acids, and polyols; and hydrogen bond acceptors (HBAs) including quaternary ammonium salts like choline chloride and amphoteric ions like betaine [207,208]. Their freezing points are significantly lower than the melting points of the individual components of the pure substance [209,210], due to the formation of hydrogen bonds. The eutectic solvents are also characterized by a low vapor pressure (typically below 100 Pa at 373 K). In contrast to ionic liquids, DES offer lower cost, higher biodegradability and lower toxicity [211]. Nevertheless, DES suffer from high viscosity and low ionic conductivity at room temperature. To address this challenge, Mezzomo et al. [196] developed a novel low eutectic solvent using 2,2,2-trifluoroacetamide (TFA) as HBD and $LiPF_6$ as HBA. The deep eutectic solvent with eutectic compositions of TFA and $LiFP_6$ exhibited higher ionic conductivity than that of the low eutectic solvents (TFA and LiTFSI). The viscosity of TFA/ $LiFP_6$ was reduced by adding a small amount of EC/FEC, enabling improved ionic conductivity (Fig. 10**e**).

DES with N–H bonds, like urea and acetamide, lack strong reduction stability and show peak reduction decomposition at potentials above those for lithium deposition and stripping in cyclic voltammetry (CV) tests [209,212]. Thus, enhancing intermolecular interaction forces and reduction tolerance of DES is crucial for better ion migration and stability. For example, Ogawa et al. [213] demonstrated that deep eutectic solvent consisting of 1,1,3,3-tetramethylurea (TMU) and LiTFSI have enhanced electrochemical stability and ionic conductivity. TMU has higher reduction stability due to the absence of N–H bonds than amides containing N–H bonds. Unfortunately, the lack of N–H bonds in TMU also means weaker intermolecular interaction forces and less thermal stability. Specifically, TMU experiences a 10 % mass loss at 55 °C, indicating poor thermal stability and suggesting that it may not maintain good performance under high-temperature conditions. In addition, the synthesis and purification processes of TMU may be relatively complex, which increases production costs and process complexity.

4.3.3. Aqueous solutions

Aqueous electrolytes offer several benefits over non-aqueous electrolytes, including lower cost, eco-friendliness, safety, high ionic conductivity, and superior high-rate performance [214]. However, their narrow electrochemical stabilization window (around 1.23 V) leads to the rapid onset of hydrogen-extraction reaction (HER) and oxygen-extraction reaction (OER) during electrochemical cycling [215–217], limiting battery energy density and complicating electrode material compatibility [218–220]. Therefore, strategies have been made to expand the electrochemical stabilization window of aqueous electrolytes, including adjusting the electrolyte pH [221], using a concentrated salt [222], and adding additives [223], etc. For example, Ma et al. [197] added 1,3-dioxolane (DOL) in water to obtain a novel "water-in-salt" aqueous electrolyte (BSIS-$DOL_{0.5}$). The presence of DOL reduces the content of free water molecules on the anode and forms a LiF-rich SEI, which inhibits the precipitation of hydrogen. As shown in Fig. 10**f**, the BSiS-$DOL_{0.5}$ has the widest ESW (4.7 V) compared to the common aqueous electrolyte (WISE) and the water/acetonitrile hybrid electrolyte (BSiS-$AN_{0.5}$).

Furthermore, DES can be introduced in aqueous electrolytes to expand the ESW of aqueous electrolytes. For example, Jiang et al.

[198] prepared a novel "salt-in-water" aqueous electrolyte by mixing a DES based on methylsulfonylmethane (MSM) and $LiClO_4$ with water. Upon addition of this DES, Li^+ is coordinated with MSM, ClO_4^- and water molecules to form an ultra-concentrated lithium salt electrolyte. As shown in Fig. 10**g**, the ESW of this aqueous electrolyte expands to about 3.5 V when the molar ratio of water content is 1.0.

However, expanding the ESW of these "water-in-salt" aqueous electrolytes tends to increase the production cost and the electrolyte viscosity, decreasing the wettability of the electrolyte with the electrode and affecting its commercialization [224]. Thus, in expanding the ESW of aqueous electrolytes, it is crucial to also maintain a balance with their other properties. Functional additives (such as organic solvents, polymers, etc.) can be added to improve the overall performance of the electrolyte. For example, organic solvents can reduce the viscosity of aqueous electrolytes, increase ionic conductivity, while maintaining a relatively wide ESW.

4.3.4. Hydrofluoroethers with low molecular weights

Hydrofluoroethers with low molecular weights are another new type of electrolyte, offering the advantages of high flash point, high oxidative stability, high wettability, low melting point, low solidification temperature, etc. These hydrofluoroethers are nonflammable when their fluorine/hydrogen ratio (F/H) is higher [225]. However, lithium salts can hardly be dissolved in low-molecular-weight hydrofluoroethers, enabling the low ionic conductivity [226].

Given the above challenge, the structure of these hydrofluoroethers must be further tuned to afford the ability to dissolve Li salts and deliver enhanced ionic conductivity. For instance, Amanchukwu et al. [199] prepared a novel fluorinated ether composite electrolyte that combines the high oxidative stability of low-molecular-weight hydrofluoroethers and the high ionic conductivity of ether-based electrolytes (Fig. 10***h***). This fluorinated ether electrolyte possessed an ionic conductivity of up to 2.7×10^{-4} S/cm (30 °C) and exhibited good ionic conductivity and electrochemical stability when used with a NCM811 for more than 100 cycles at a of C-rate of C/5.

In addition to structural design, we can also use specific organic solvents to build complex interfacial layers to enhance the electrochemical performance of low-molecular-weight hydrofluoroethers electrolytes. For example, Xia et al. [200] designed a conventional electrolyte consisting of LiFSI, dimethyl ether (DME), hydrofluoroether (TTE), and potassium trifluoride (trifluoromethyl) borate (PTB) additives. The CF_3BF_3 ions in the PTB additives exhibited the better ionic conductivity and showed a better ionic conductivity at a 4.0 mA cm^{-2} charging current showed better cycling stability through the formation of an interfacial layer containing boron and lithium fluoride (Fig. 10**i**).

Non-flammable liquid electrolytes offer promising alternatives to conventional flammable organic solvents, significantly enhancing the safety of LIBs. However, their practical deployment is limited by persistent challenges, including low ionic conductivity, poor interfacial compatibility, limited electrochemical stability and high production costs. For instance, while ionic liquids exhibit flash points above 200 °C and negligible vapor pressure, their high viscosity results in low lithium-ion transference numbers. Deep eutectic solvents offer reduced viscosity but often lack compatibility with high-voltage cathode materials.

From a life cycle assessment perspective, these electrolytes also raise environmental concerns. The synthesis of low-molecular-weight perfluoropolyethers, for example, may involve hazardous precursors, and their end-of-life disposal poses risks of soil and water contamination [227]. Developing efficient recycling strategies is therefore essential. Ionic liquids, in particular, can be recovered through physical or chemical methods to reduce resource consumption and environmental impact, although these technologies remain at an early stage and require further optimization and cost reduction [228].

Addressing these issues calls for a comprehensive research approach that integrates materials science with environmental science and engineering. Such multidisciplinary efforts are vital to enabling the sustainable application of non-flammable electrolytes in next-generation LIBs.

4.4. Solid-state electrolytes

The solid-state electrolyte, a solid ion conductor containing little to no liquid and eliminating the need for a separator, effectively addresses issues of electrolyte leakage and internal short-circuiting [229]. Solid-state electrolytes typically exhibit strong thermal stability, mechanical strength, and impact resistance [230,231], making them highly promising for enhancing the safety of batteries.

Solid electrolytes can be divided into two main categories based on their liquid content: quasi-solid-state electrolytes and all-solid-state electrolytes. Quasi-solid electrolytes, or gel polymer electrolytes, incorporate a liquid component within a solid matrix. All-solid-state electrolytes, which contain no liquid, are further classified into solid polymer electrolytes, solid inorganic electrolytes, and composite solid electrolytes. The subsequent discussion will cover recent research on these types of solid-state electrolytes.

4.4.1. Gel polymer electrolytes

Gel polymer electrolytes generally comprise a polymer matrix (e.g., poly(ethylene oxide) (PEO), poly(vinylidene fluoride) (PVDF), and poly(acrylonitrile) (PAN)), a lithium salt, and a non-aqueous organic solvent as a plasticizer. The polymer forms a three-dimensional mesh structure, while the lithium salt and non-aqueous organic solvent make up the liquid electrolyte. Ion transport within gel polymer electrolytes occurs through the liquid electrolyte contained within this mesh structure [232–235]. Gel polymer electrolytes are midway between liquid and solid electrolytes, combining mechanical properties of solids with the transport capabilities of liquids. However, they are less safe than all-solid electrolytes due to their flammable liquid content.

To tackle safety concerns, one approach involves adding flame-retardant additives to gel polymer electrolytes to enhance their fire resistance. For instance, Long et al. [236] incorporated the phosphorus-based flame retardant, diethyl vinyl phosphonate (DEVP), into a cross-linked poly(ethylene glycol) diacrylate matrix. This resulted in a flame-retardant gel polymer electrolyte through in-situ

crosslinking polymerization, with the process depicted in Fig. 11**a**. The phosphorus content of DEVP is notably high at 18.9 wt%. During thermal runaway, DEVP releases phosphorus-containing radicals that inhibit combustion, thereby boosting the safety of the gel polymer electrolyte.

A second approach is to use nonflammable liquid electrolytes instead of flammable ones. Commonly, ionic liquids are employed to create ionic gel polymer electrolytes, significantly enhancing safety. However, as noted in ***section 4.3.1***, ionic liquids tend to have higher viscosity and lower ionic conductivity, necessitating enhancements in their ionic transport capabilities for safer ionic gel polymer electrolytes [237,238]. Other strategies involve adding inorganic additives with specific functionalities to the gel polymer electrolyte to boost electrochemical performance and ionic migration. For instance, Kim et al. [239] developed ionic gel polymer electrolytes with amine-functionalized boron nitride nanosheets (AFBNNS) through thermal polymerization. The amine groups on AFBNNS strongly interacted with TFSI- in LiTFSI, reducing TFSI- mobility and thus enhancing lithium-ion mobility and ionic conductivity, as illustrated in Fig. 10**b**.

4.4.2. Solid polymer electrolytes

Solid-state polymer electrolytes (SPEs) are primarily composed of a polymer matrix and lithium salts, lacking the plasticizer found in gel polymer electrolytes [240]. Despite this single difference, they exhibit distinct variations in diffusion mechanisms, performance, and other areas. Li-ion transport in solid polymer electrolytes does not rely on liquid electrolytes but occurs through a complexation-decomplexation process involving ion migration and interaction with the polar groups of polymers under an electric field. Additionally, the absence of flammable liquids in solid polymer electrolytes usually results in higher thermal stability compared to their gel

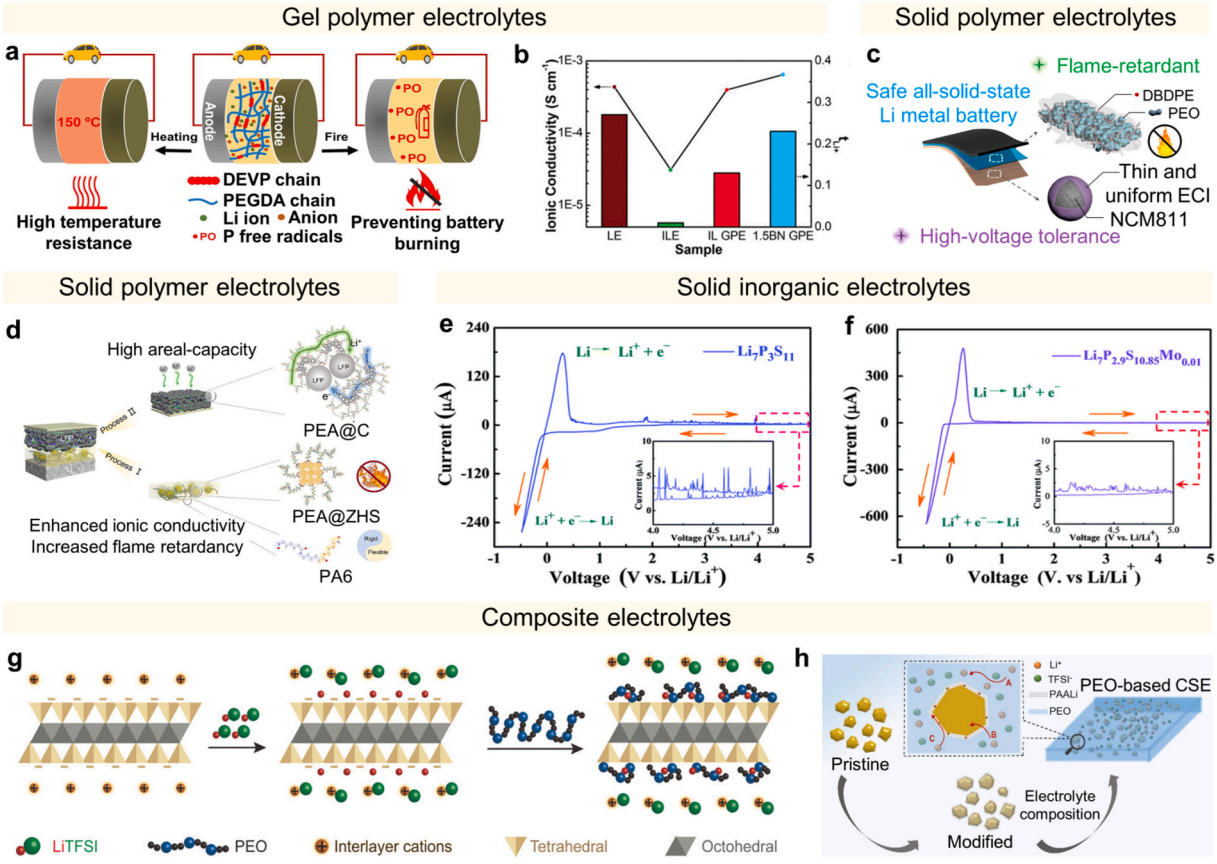

Fig. 11. Solid-state electrolytes. (a) Schematic diagram of LIB modified with GPE [236]. Copyright (2022) Elsevier. (b) Lithium-ion mobility (t_{Li+}) and ionic conductivity of organic liquid electrolyte (LE), ionic liquid electrolyte (ILE), ionic gel polymer electrolyte (IL GPE), and ionic gel polymer electrolyte (1.5BN GPE) with 1.5 wt% AFBNNS at 25 °C [239]. Copyright (2020) Wiley-VCH. (c) Design principles of flame-retardant and high-voltage solid-state electrolytes for safe all-solid-state lithium batteries [248]. Copyright (2022) American Chemical Society (d) Schematic representation of solid-state electrolyte modification: Introducing polyether amine modified zinc hydroxystannate (PEA@ZHS) nanoparticles and polyamide 6 (PA6) chain segments into the PEO matrix improves ionic conductivity, flame-retardant, and dendrimer inhibition strength [249]. Copyright (2022) Elsevier. (e) CV curves of $Li_7P_3S_{11}$ and (f) $Li_7P_{2.9}S_{10.85}Mo_{0.01}$ in the potential range of 0.5 V to 5 V vs. Li/Li^+ at a scanning rate of 1 mV s^{-1} at a temperature of 298 K. The inset shows the CV enlargement curves between 4 and 5 V [250]. Copyright (2017) Royal Society of Chemistry. (g) Photographs of VS composite SPE (left) and SPE before and after thermal treatment at different temperatures for 30 min; the schematic shows the mechanism by which VS enhances ionic conductivity in SPE [251]. Copyright (2018) John Wiley and Sons. (h) Schematic of the modification of ceramic particles and interfacial phases in the composite solid state electrolyte [252]. Copyright (2022) Elsevier.

counterparts. Solid polymer electrolytes also offer benefits like being lightweight, easily processable, cost-effective, compatible with lithium salts, and showing better electrochemical stability with lithium metal, making them a more promising option for solid-state applications [241,242].

However, the polymer matrix in SPEs is flammable, and under thermal abuse, it can ignite, producing toxic gases [243]. Furthermore, the electrochemical stability of SPEs, including those based on PEO and PVDF, is relatively poor, limiting their use in high-voltage batteries [244,245]. SPEs also exhibit lower ionic conductivity compared to liquid and gel polymer electrolytes [246]. Additionally, the inherent softness of solid polymer electrolytes does not prevent dendrite growth, making them susceptible to being pierced by dendrites, which can lead to battery short-circuiting [247].

Research efforts have been devoted to addressing the challenges associated with SPEs [253,254]. For instance, Zhou et al. [248] developed a novel flame-retardant and high-voltage resistant solid polymer electrolyte using PEO, LiTFSI, and decabromodiphenyl ethane (DBDPE), with the design principle illustrated in Fig. 11**c**. DBDPE aids in forming LiBr nanoparticles at the cathode/solid-state electrolyte interface, fostering a homogeneous and organic-rich high-voltage resistant CEI passivation layer (up to 4.5 V). Additionally, DBDPE releases Br radicals at high temperatures, capturing H • and HO • radicals and effectively halting combustion reactions. Furthermore, Zhang et al. [249] enhanced solid-state polymer electrolytes by incorporating PEA-modified zinc hydroxy stannate (PEA@ZHS) and PA6 into PEO-based electrolytes, with the modification principles depicted in Fig. 11**d**. PEA@ZHS serves as a non-toxic flame retardant, significantly improving thermal safety (reducing the heat release rate by 22 %). Meanwhile, PA6 increases mechanical stiffness, optimizing the Young's modulus of the electrolytes (3.41 GPa) to effectively prevent dendrite growth. The polymerization of PEA@ZHS and PA6 also enhances ionic conductivity (4.29×10^{-4} S cm^{-1} at 55 °C), demonstrating a multifaceted approach to improving the performance of PEO-based solid polymer electrolytes.

4.4.3. Solid inorganic electrolytes

Solid inorganic electrolytes (SIEs) are composed of distinct inorganic ions and charges with lithium-ion transport largely dependent on defect types [255,256]. Unlike gel polymer electrolytes and solid-state polymer electrolytes, solid-state inorganic electrolytes lack flammable liquids and polymer matrices, making them inherently nonflammable. They also offer greater mechanical strength, which helps prevent dendrite growth more effectively [257]. Additionally, their wider electrochemical window is compatible with high-voltage cathode materials [258].

SIEs can be divided into two types: oxide and sulfide, including $Li_7La_3Zr_2O_{12}$ (LLZO), $Li_{3x}La_{2/3x}TiO_3$ (LLTO), $Li_{1.3}Al_{0.3}Ti_{1.7}(PO_4)_3$ (LATP), $Li_{1.5}Al_{0.5}Ge_{1.5}(PO_4)_3$ (LAGP), $Li_7P_3S_{11}$ (LPS), Li_6PS_5Cl (LPSCl), and $Li_{10}GeP_2S_{12}$ (LGPS) [259]. Oxide-based SIEs usually have good thermal and electrochemical stability, but they generally have low ionic conductivity and poor inter-particle contact [260,261]. In contrast, sulfide-based SIEs have higher ionic conductivity with better inter-particle contact but have lower chemical stability with lithium metal. They are susceptible to side reactions with lithium, leading to the production of gases (oxygen and toxic hydrogen sulfide gas) and thermal runaway [259,262].

To enhance the particle contact in oxide solid inorganic electrolytes, specialized preparation methods can be utilized. For example, Nagata et al. [263] developed a highly deformed oxide solid inorganic electrolyte, $50Li_2SO_4$-$50Li_2CO_3$ (LSCO), using a high-energy mechanical milling process. A subsequent cold-pressing treatment improved the contact between the oxide solid inorganic electrolyte particles and the electrode, allowing LSCO to achieve high ionic conductivity (6.3×10^{-7} S cm^{-1}) at room temperature. For sulfide solid inorganic electrolytes, elemental doping is crucial for enhancing chemical stability with lithium metal. Xu et al. [250] prepared MoS_2-doped Li_2S-P_2S_5 sulfide solid inorganic electrolytes ($Li_7P_{2.9}S_{10.85}Mo_{0.01}$) through a straightforward high-energy ball milling and annealing method. The cyclic voltammetry (CV) curves of both the $Li_7P_3S_{11}$ electrolyte and the modified $Li_7P_{2.9}S_{10.85}Mo_{0.01}$ electrolyte, as shown in Fig. 11**e** and Fig. 11**f**, reveal that the Mo-doped $Li_7P_{2.9}S_{10.85}Mo_{0.01}$ electrolyte displays a stable and broad electrochemical window up to 5 V vs. Li/Li$^+$ at room temperature, significantly enhancing its electrochemical compatibility with lithium metal.

4.4.4. Composite electrolytes

Currently, no single solid-state electrolyte—polymer or inorganic—meets all the needs for solid-state lithium batteries [264]. Combining different electrolytes can afford functional composite electrolytes [265–267]. These composites blend the processing ease and flexibility of polymer electrolytes with the high mechanical strength and extensive electrochemical window of inorganic electrolytes [268–271].

The lithium-ion diffusion in composite electrolytes varies with the type of inorganic filler used. With inert fillers e.g., SiO_2, Al_2O_3, and ZrO_2, diffusion mirrors that in SPEs, where fillers cannot directly facilitate Li$^+$ transfer but help by reducing polymer crystallinity and aiding lithium salt dissociation, thus boosting ionic conductivity [272]. Tang et al. [251] developed PEO-based composite electrolytes with 2D vermiculite clay flakes (VS) additive, significantly enhancing properties such as ionic conductivity, thermal and electrochemical stability, flame resistance, interfacial resistance, and mechanical modulus. The increased ionic conductivity is linked to LiTFSI dissociation facilitated by electronegative silicates on VS surfaces (Fig. 11**g**), which also adsorb Li$^+$, creating more free conducting Li$^+$.

When active fillers, e.g., LLZO, LLTO, and LATP, are introduced, the ionic transport mechanism in composite solid-state electrolytes becomes highly complex and is still under study. Generally, enhancements in ionic conductivity are attributed to the creation of additional Li$^+$ pathways within the composite structure [272]. Tong et al. [252] explored incorporating $Li_{6.4}La_3Zr_{1.4}Ta_{0.6}O_{12}$ (LLZTO) and $LiTa_2PO_8$ (LTPO) into PEO-based solid-state polymer electrolytes using two distinct methods, resulting in composites with improved ionic conductivity, electrochemical window, and resistance to lithium dendrite formation. LLZTO and LTPO contributed to forming a novel polymer lithium salt phase on the surface of lithium polyacrylate (PAALi), improving compatibility and uniformity

between the polymer and inorganic fillers. This also created extra paths for lithium-ion movement, boosting the ionic conductivity of the composites (Fig. 11***h***). Composite solid-state electrolytes, created by merging solid-state inorganic and polymer electrolytes, are viewed as the most promising candidates as solid-state electrolytes. Yet, when compared to traditional liquid electrolytes, they exhibit noticeable shortcomings in ionic conductivity, interfacial compatibility and manufacturing costs. Furthermore, the mechanisms of Li-ion conduction through various inorganic fillers and polymer matrices remain unclear. Consequently, comprehensive research on composite solid-state electrolytes is essential to overcome these challenges in future developments.

Solid-state electrolytes are emerging as a critical component of next-generation LIBs, widely recognized for their superior safety compared to conventional liquid electrolytes. Whether in the form of gel polymers, solid polymers, inorganic solids or composite systems, solid-state electrolytes exhibit reduced flammability, eliminate leakage risks and offer enhanced protection against overcharge and overdischarge, key attributes for improving battery safety.

Despite these advantages, several barriers impede their commercialization. Low ionic conductivity, limited electrochemical stability and high production costs remain significant challenges. Inorganic electrolytes such as oxides and sulfides offer high ionic conductivity but often require elevated operating temperatures, which limits their use in portable electronics. Polymer based electrolytes, while more compatible with room temperature operation, generally exhibit lower conductivity than liquid counterparts. To address these limitations, hybrid and nanocomposite electrolyte systems are being explored to enhance ion transport while preserving safety. Structural optimization and process refinement can further improve conductivity and charge and discharge performance. Cost reduction strategies including continuous production processes and the use of efficient catalysts are also essential to enabling economic viability.

From a full life cycle perspective, solid state electrolytes present complex environmental tradeoffs. Although they eliminate risks associated with organic solvent leakage, their production often involves energy intensive sintering and controlled atmospheres, resulting in higher carbon emissions [273,274]. Moreover, recycling poses new challenges, as the separation and recovery of inorganic components from spent batteries can be both costly and environmentally burdensome [275,276].

To achieve commercial breakthroughs, a multidimensional evaluation framework must be established, incorporating ionic transport, interface stability and thermodynamic compatibility. Machine learning assisted with material discovery and comprehensive performance databases will be critical in accelerating electrolyte development. With optimization of continuous manufacturing and domestic sourcing of raw materials, it is projected that costs could fall to $150–200/kWh within five years, and potentially below

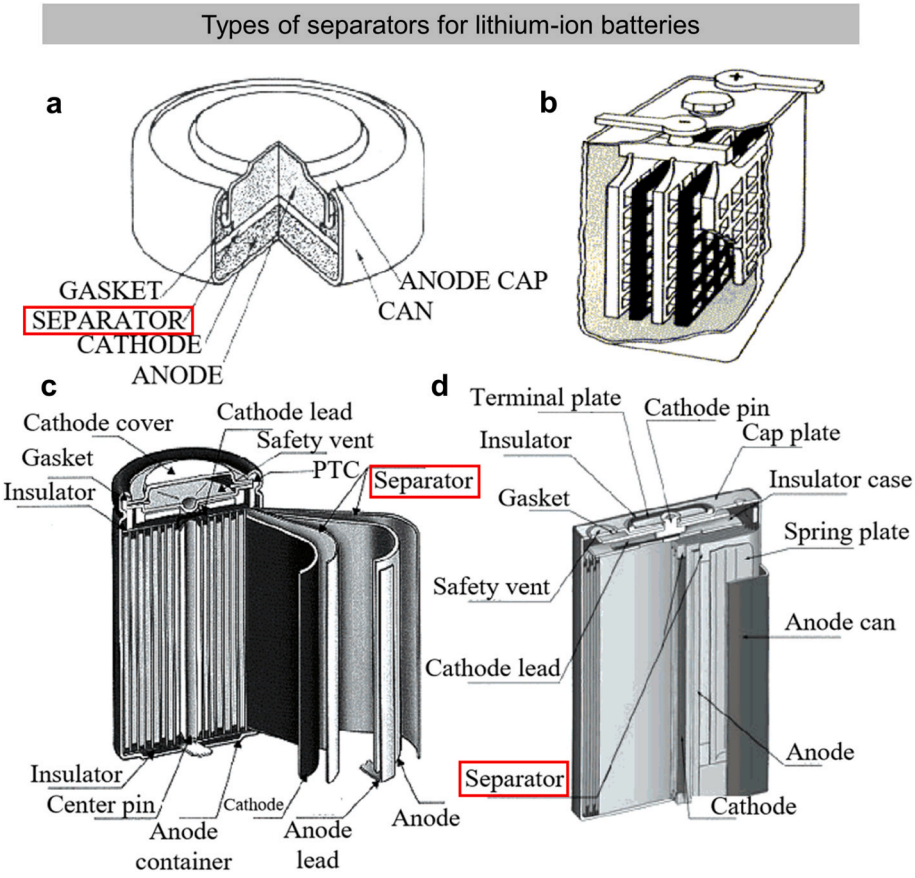

Fig. 12. Types of separators for LIBs. (a-d) different lithium-ion battery types.

$100/kWh thereafter. Realizing this vision will require close collaboration across materials science, engineering and policy to drive the transition toward intrinsically safe battery technologies.

5. Safe separators

As an indispensable part of LIBs, separators have been widely used in a variety of LIBs, such as button batteries (Fig. 12**a**), box batteries (Fig. 12**b**), cylindrical batteries (Fig. 12**c**), sheet batteries (Fig. 12**d**). Separators, such as polyolefin separators, are expected to possess an exemplary insulating nature, adequate Li conductivity, electrolyte compatibility and superior mechanical performance. Currently, common separator materials include multilayer composite separators composed of polypropylene (PP) and polythene (PE), inorganic coated separators, organic coated separators, and organic/inorganic composite separators, such as fiberglass [277], ceramic separators [278,279], aramid [280], and polyimide [281,282]. Among them, multilayer composite separators are divided into PP/PE two-layer composite separators and PP/PE/PE three-layer composite separators, which are widely commercially applied separator materials. However, the PP and PE membranes are less thermally stable due to their lower melt collapse temperatures (135 ~ 165 °C) [283,284]. By contrast, inorganic coated separators have the combined properties of inorganic and organic materials, possessing a high degree of flexibility, effectively preventing lithium dendrites from puncturing the separator. The organic materials in organic-coated separators mainly include PDA, PVDF, PAN, ANF, and PMMA [285].

However, these separators pose safety concerns during battery thermal runaway [286]. When the temperature surpasses a specific threshold, the separator may melt and collapse, causing a short circuit. As previously discussed in ***section 3.1***, a major factor in thermal runaway is separator failure, which results in a sudden surge in current due to battery short-circuit and a swift increase in temperature, potentially causing combustion or explosion. Particularly, PE- and PP-based multilayer composite separators (Fig. 13**a**), the most

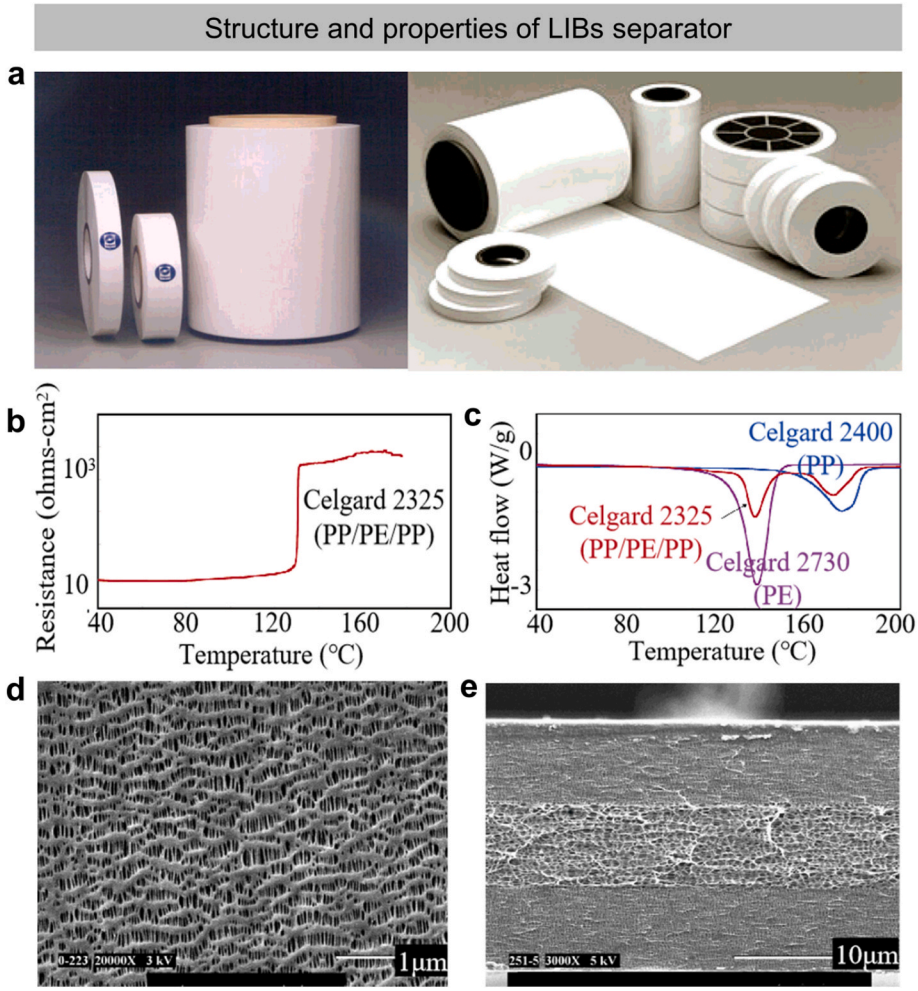

Fig. 13. Structure and properties of LIBs separator. (a) lithium-ion battery separators; (b-c) thermo-mechanical properties of polyethene (PE) and polypropylene (PP) separators; (d-e) surface and cross-section SEM images of the three-layer separators [286]. Copyright (2004) American Chemical Society.

common in commercial use, face limitations due to their inadequate thermal stability and mechanical strength, which hampers the advancement of lithium-ion battery separator materials (Fig. 13**b-e**) [287]. To facilitate large-scale production and practical application of LIBs [288], it is crucial to enhance the thermal stability and mechanical strength of separators without compromising its ionic conductivity, chemical stability, and electrolyte wettability. This improvement is essential to prevent thermal runaway in LIBs [289].

5.1. Failure mechanism

Polymeric separators are prone to causing safety incidents [24,290], where failures typically occur due to mechanical integrity and thermal issues.

(1) **Failure of the mechanical integrity**. The mechanical integrity of a separator reflects its resistance to external forces, determined by its puncture and stretching resistance. The limited mechanical strength of separators can result in failure under abusive conditions like overcharging or overcooling, where anode-generated lithium dendrites may pierce the separator, causing a short circuit [291]. Furthermore, mechanical stress from impacts, extrusion, or bending can damage the separator through scratches, tears, or perforations, also leading to short circuits.
(2) **Thermal issues**. Separators require robust chemical stability to avoid reactions with the electrolyte and electrode materials, as well as high temperature resistance. However, widely used commercial separators, such as PE and PP, suffer from poor heat resistance, melting at 135 °C and 165 °C, respectively. If a lithium-ion battery internal temperature reaches these melting points under abusive conditions, the separator can lose its structure, thermally shrink, or melt, causing an ISC. This can lead to a rapid increase in temperature inside the battery, potentially resulting in combustion and explosion (Fig. 14) [292].

Therefore, it is crucial to improve the safety and stability of lithium-ion battery separator materials by enhancing their mechanical and thermal resilience. Such advancements will accelerate the commercialization of LIBs.

5.2. Material design strategies

Conventional design approaches include optimizing production and preparation processes and selecting materials with better mechanical and thermal stability. (1) ***Grafting modification*** [293,294]. By chemical initiators and UV irradiation methods, functional chemical groups can be grafted onto the polymer surface, improving separator wettability and compatibility. (2) ***Composite modification*** [295]. To improve the overall performance, composite modifications can be adopted, including using a substrate with strong mechanical properties, coating the film surface with another substance, or applying composite treatments with various materials. These improvements can boost the separator liquid absorption, extend the battery cycle life, and strengthen the separator mechanical durability. (3) ***Blending modification*** [296]. By integrating the properties of various materials, the performance of the composite separator can be enhanced. (4) ***Filling modification*** [297]. Inorganic nanoparticles, such as SiO_2, TiO_2, Al_2O_3, and Fe_3O_4, can be added to the polymer materials to deliver multifunctions. (5) ***Others*** [298]. Thermal treatments, reticulation organization and increase of crystallinity in the separators can be used to improve the mechanical properties of separators [299].

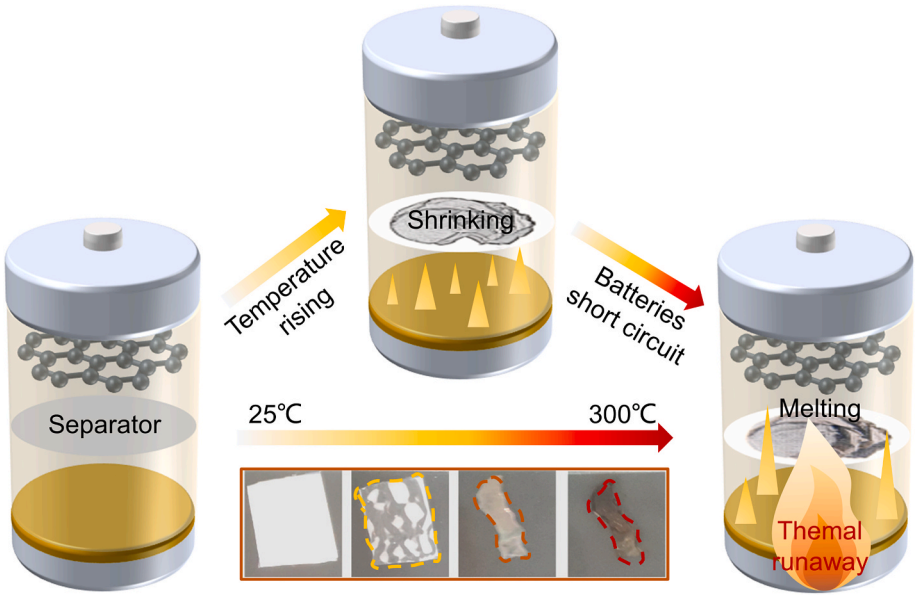

Fig. 14. Failure mechanism of LIB separators.

Building on the mentioned enhancement strategies, we summarize three effective methods to boost separator safety: incorporating flame retardants, integrating inert ceramics, and optimizing structural design. We will delve into these three approaches in further detail next.

5.2.1. Addition of flame-retardant additives

The incorporation of flame retardants or fiber-like substances within the separators serves as a simple yet efficient method for enhancing battery safety [301,302]. This method is low-cost and effective, and largely enhances safety by simply dipping flame retardants on the separator surface or encapsulating flame retardants in the separator fibers. For example, Han et al. [290] coated a highly efficient flame retardant (melamine pyrophosphate, MPP) on a polyethene (vinylidene fluoride-co-hexafluoropropylene) (PVDF-HFP) separator to obtain a new flame retardant separator, successfully used in a ternary cell (Fig. 15**a**). The flame-retardant separator has negligible shrinkage above 200 °C, and it takes only 0.54 s to extinguish the flame in the ignition test, much better than that of commercial separators. The performance of PVDF-HFP/MPP separators is also demonstrated in pouch cells (Fig. 15**b-c**). Likewise, Fu et al. [300] developed a thermal stable PP/DBDPE separator with a thickness of 15 μm by dispersing the flame retardant DBDPE and PVDF in N-methyl-2-pyrrolidone (NMP) at a mass ratio of 9:1 and casted it onto a PP substrate (Fig. 15**d**). However, an overly thick separator may affect ion mobility, leading to an increase in the internal resistance of the battery. To address this, atomic layer deposition technology can be employed to achieve uniform nanoscale coating, thereby reducing the resistance to ion transport. Additionally, Chou et al. [303] applied a coating of flame retardant on the separator, which is resistant to dissolution in the electrolyte (Fig. 16**a**). DBDPE combined with antimony oxide created a 4 μm thick flame-retardant separator coating, expanding flame resistance compared to standard separators (Fig. 16**b**). This method enhances safety with minimal impact on battery performance, offering a new solution for LIB safety issues (Fig. 16**c-d**).

5.2.2. Addition of inert ceramics

Inert ceramic-coated separators improve lithium-ion battery safety by minimizing thermal deformation and enhancing mechanical strength. These separators consist of a polyolefin base, a polymer binder for stability and compatibility with electrolytes, and ceramic material for high-temperature resistance and improved ion migration. The polymer binder ensures structural integrity at high temperatures and compatibility with the battery interface, while water-soluble binders like CMC/SBR reduce costs and environmental impact. Ceramic components add benefits like hydrophilicity and SEI growth inhibition. The effectiveness of ceramic separators depends on the ceramic particle size, morphology, and chemistry, with materials like Al_2O_3, SiO_2, and innovative nanomaterials being used to further enhance thermal stability and ion transport.

The aluminum oxide coating and substrate exhibit strong compatibility, enabling the potential for applying additional inorganic material coatings on the separator to further enhance the safety of LIBs. For example, Yang et al. [304] compared conventional alumina ceramic-coated PE separators with boehmite-coated separators where the boehmite coating can reduce the coating thickness while ensuring the excellent thermal stability. Meanwhile, the modified PE film has good wettability, favorable for Li-ion transport (Fig. 17**a**). Zeng et al. [305] combined molybdenum trioxide and aluminum-doped $Li_{6.75}La_3Zr_{1.75}Ta_{0.25}O_{12}$ (LLZTO) to develop the double-layer flame-resistant separators. Simulations show that within the bilayer separator, abundant hydrogen bonds with van der Waals forces can inhibit the combustion of molybdenum trioxide and LLZTO with poly(vinylidene fluoride)hexafluoropropylene. The formation of molybdenum fluoride (MoFx) and lanthanum fluoride (LaFx) was induced during the combustion process, which reduced

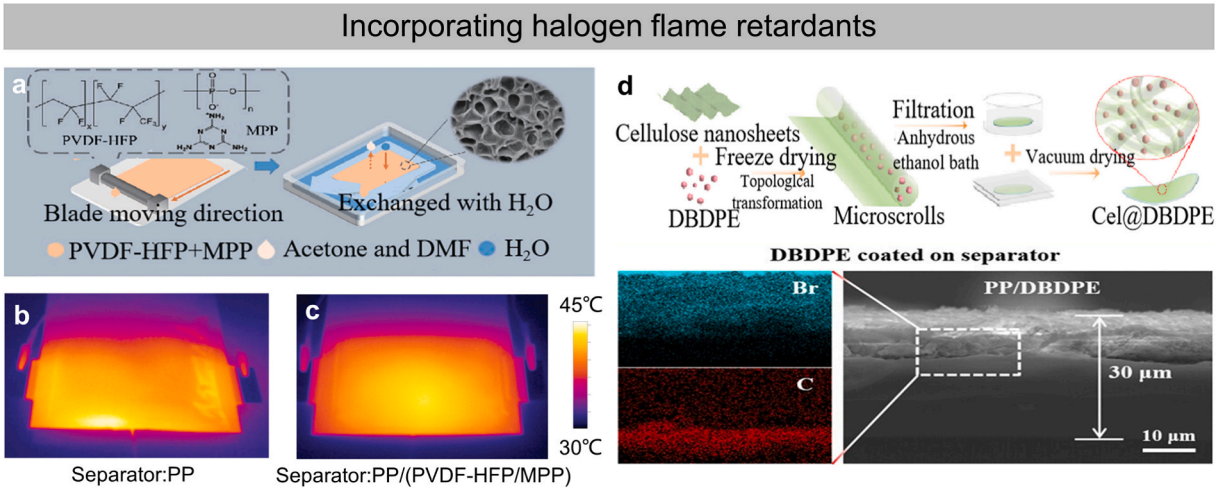

Fig. 15. Addition of flame-retardant additives to optimize separator safety. (a) Schematic diagram of the preparation for PVDF-HFP/MPP flame-retardant separators, (b, c) Thermal distribution images of the whole cell assembled with PP separator and PP/PVDF-HFP/MPP separator tested by FLIR analysis during overcharging[222]. Copyright (2019) Springer Nature. (d) Schematic diagram of the preparation of the Cel@DBDPE separator and characterization of the surface structure [300]. Copyright (2023) John Wiley and Sons.

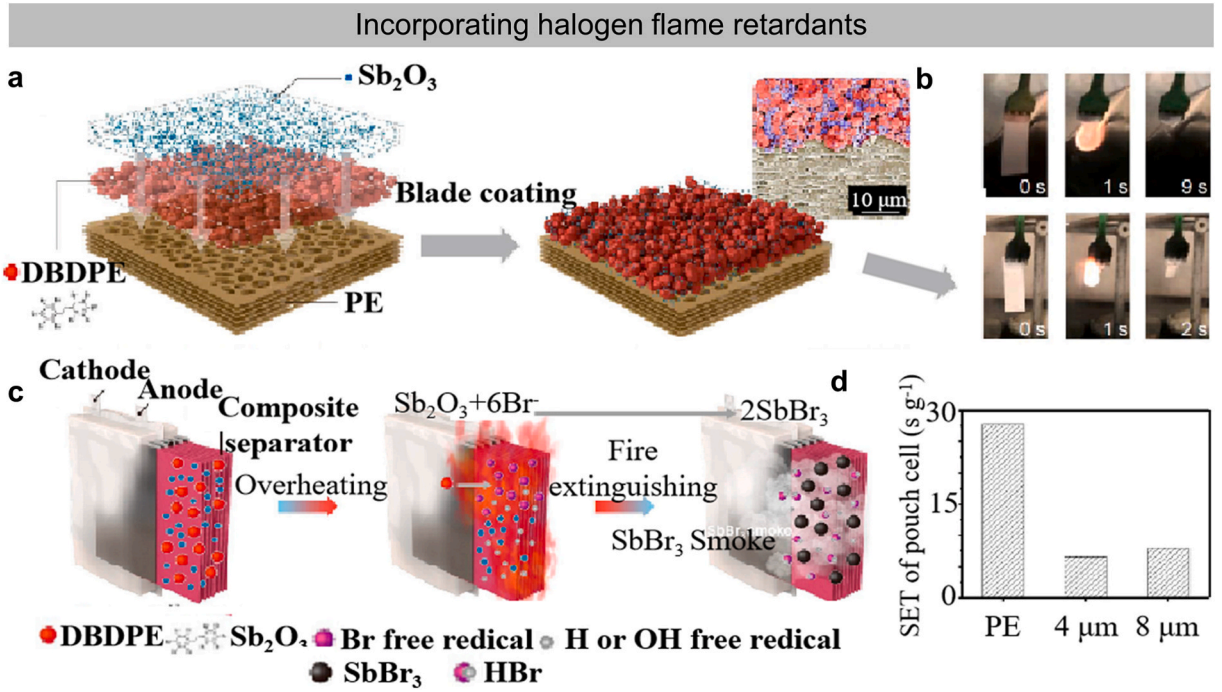

Fig. 16. Incorporating halogen flame retardants (a) Flame-retardant composite separator preparation schematic. (b) Vertical ignition experiment of flame-retardant composite separator. (c) Flame retardant mechanism of flame-retardant composite separator. (d) Comparison of SET values of flame retardant composite separator [303]. Copyright (2021) American Chemical Society.

heat accumulation. These bilayer separators enabled durable battery cycling (Fig. 17**b**). However, while coating technology can reduce the dissolution of flame retardants, these retardants may still gradually leach out after long-term cycling, thereby compromising safety. Strategies such as chemical bonding and microencapsulation technologies could be considered to enhance the stability of flame retardants under high temperatures or during prolonged use, ensuring their reliability in practical applications.

In fact, relevant research work also follows this fundamental principle. For example, Huang et al. [306] developed a functional separator using phosphonate-modified silica-ceramic nanoparticles to enhance the safety of silica-ceramic separators. They attached the flame retardant dimethylphosphonate (DMVP) to silica via anhydrous polymerization, coating this modified silica (m-SiO_2) onto a polyethylene separator. This modified ceramic separator showed excellent thermal stability by leveraging the combined benefits of ceramics and phosphonates, remaining stable without significant shrinkage up to 200 °C, thus greatly enhancing LIB safety (Fig. 17**c**). Liu et al. [307] created a thermally responsive composite separator by coating ceramic-silica microcapsules onto a commercial polyolefin separator, encapsulating a phase change material (PCM) and a flame retardant (Fig. 17**d**). The PCM acts as a "smart gatekeeper", absorbing heat to slow temperature increase and controlling the release of the flame retardant to prevent thermal runaway, thereby improving LIB safety.

5.2.3. Structural optimization

Creating separators with three-dimensional structures and polymer materials can offer improved mechanical strength and thermal stability, thereby boosting battery safety. Enhancing the thermal response structure and fine-tuning the temperature sensitivity of battery separator materials provide an effective way to swiftly address thermal runaway. Liu et al. [161] developed an innovative electrospun core–shell microfiber separator with heat-activated flame retardant capabilities. This separator features microfibers created through electrostatic spinning, forming a core–shell structure. The core is loaded with the flame retardant triphenyl phosphate (TPP), while the shell consists of polyvinylidene fluoride-hexafluoropropylene (PVDF-HFP). In thermal runaway, the PVDF-HFP shell melts as temperatures rise, releasing the TPP flame retardant into the electrolyte and effectively preventing electrolyte combustion (Fig. 18**a**).

Inorganic ion-conductive materials have also been investigated as functional separators. However, conventional inorganic ion-conducting materials are brittle and have difficulty accommodating the volume changes that occur during the battery's charge and discharge processes. Fu et al. [298] created flame retardant 3D garnet-based polymer composite (FRPC) separators by immersing a garnet-type $Li_{6.4}La_3Zr_2Al_{0.2}O_{12}$ nanofiber three-dimensional ceramic network in a LiTFSI-PEO polymer solution to fill the network (Fig. 18**b**), which also improved the flexibility of the three-dimensional ceramic network. This innovation enhances the electrochemical performance and safety of all-solid-state batteries. Despite this, the filled PEO is prone to oxidation at high potentials (>4 V), which limits its application in high-voltage batteries. To address this issue, alternative polymers can be considered, such as replacing PEO with polyacrylonitrile (PAN) to enhance oxidation resistance. Duan et al. [308] formulated a lithium-ion battery separator using

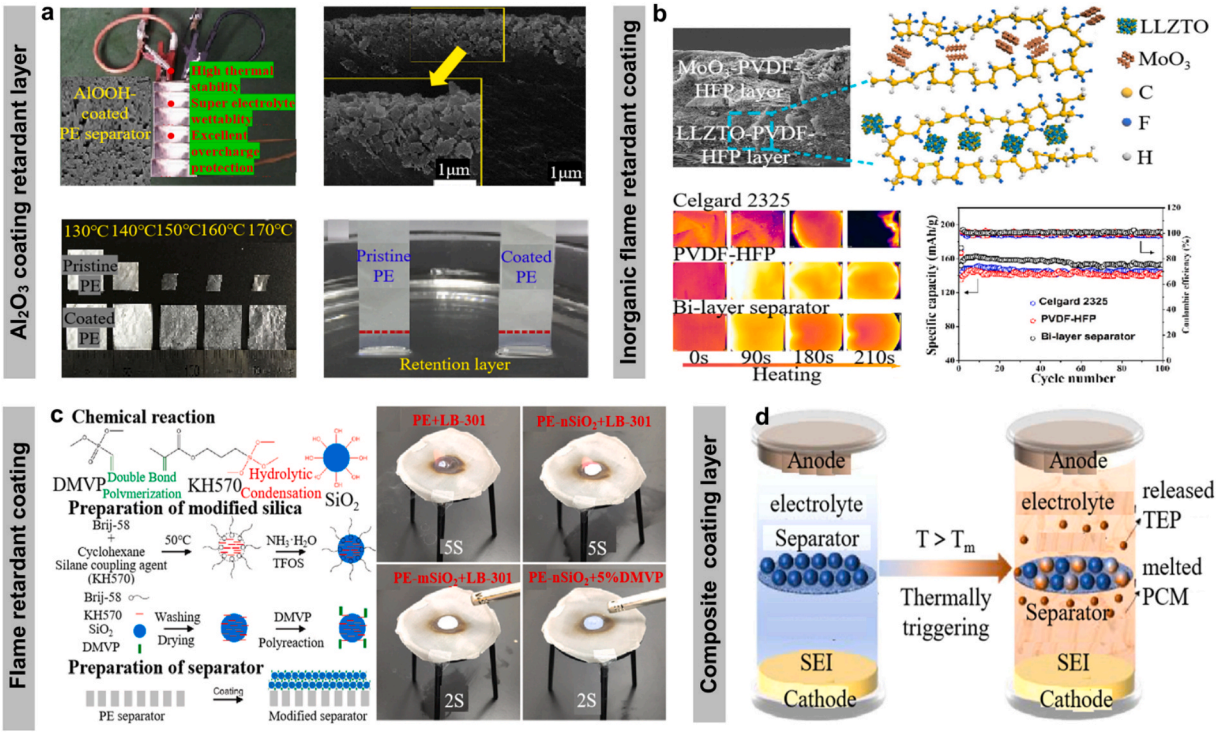

Fig. 17. Adding inert ceramics to optimize separator safety. (a) Thermal stability and characterization of AlOOH-coated PE separators for electrolyte wetting tests [304]. Copyright (2017) Elsevier. (b) Structural characterization and thermodynamic performance tests of LLZTO and MoO_3 [305]. Copyright (2019) American Chemical Society. (c) Preparation process, structural characterization, and ignition experiments of modified silica particles and modified separators [306]. Copyright (2021) Elsevier. (d) Thermal response mechanism and preparation of PCM-TEP@SiO_x separator process, electrochemical characterization, and vertical ignition experiments [307]. Copyright (2022) Elsevier.

57.5 % GDIL, 16.5 % lithium bis(trifluoromethylsulfonyl)imide salt (LiTFSI), and 26 % poly(vinylidene fluoride) hexafluoropropylene (PVDF-HFP) (Fig. 19**a**), optimizing the performance of lithium metal anodes. This battery, with LFP and a lithium metal anode, remained fire-free throughout pinning experiments, enhancing lithium metal anode safety. However, the high concentration of GDIL and LiTFSI may increase the internal resistance of the separator, thereby affecting the charge and discharge performance of the battery. To address this, a porous structure design can be employed, such as preparing gradient-porous PVDF-HFP membranes via electrospinning, to balance ionic transport with mechanical strength. Stalin et al. [309] developed a polymer conductive network separator through a chemical cross-linking reaction of sulfonate and phosphate (Fig. 19**b**). This separator, featuring various active functional groups, improves electrolyte safety in LIBs, reducing thermal runaway risk without compromising electrochemical performance. Nevertheless, this chemical cross-linking process is complex and difficult to scale up for mass production. UV curing technology can be employed to simplify the cross-linking steps and reduce costs.

In summary, the separator, as a critical component of the battery, directly influences key performance indicators such as cycle life, safety, and energy and power density. Mainstream polyolefin separators, typically based on polyethylene or polypropylene, exhibit excellent mechanical strength and chemical stability, but suffer from limited thermal stability. Under high temperature conditions, they are prone to shrinkage or melting, which can result in ISC and thermal runaway.

To improve safety, various strategies have been pursued, including the incorporation of flame retardants and inorganic fillers, or the use of inherently nonflammable materials such as glass fibers and polyimides. These approaches, however, present limitations. For instance, the integration of flame retardants and inorganic materials can compromise separator flexibility and increase internal resistance, negatively affecting power output and charge and discharge efficiency. Although materials like glass fibers and polyimides offer superior thermal stability, they are often expensive and challenging to process, limiting their scalability.To address these challenges, material formulations and processing methods should be optimized to preserve flexibility and conductivity while enhancing thermal stability. In parallel, the development of advanced separator materials or composite structures that combine complementary properties offers a promising route to achieving a balance among cost, safety and performance.

From a full life cycle perspective, separator materials pose significant environmental challenges. Conventional polyolefin separators are derived from petrochemical feedstocks and exhibit poor degradability at the end of life. In contrast, newer ceramic separators involve energy intensive production processes and present difficulties in recycling [310,311]. To address these issues, a tiered treatment approach is recommended. For polyolefin separators, efforts should focus on developing efficient physical recycling methods, while for ceramic separators, breakthroughs in scalable chemical recycling technologies are urgently needed [312,313]. Achieving sustainable development in battery technology requires an integrated innovation framework encompassing material design,

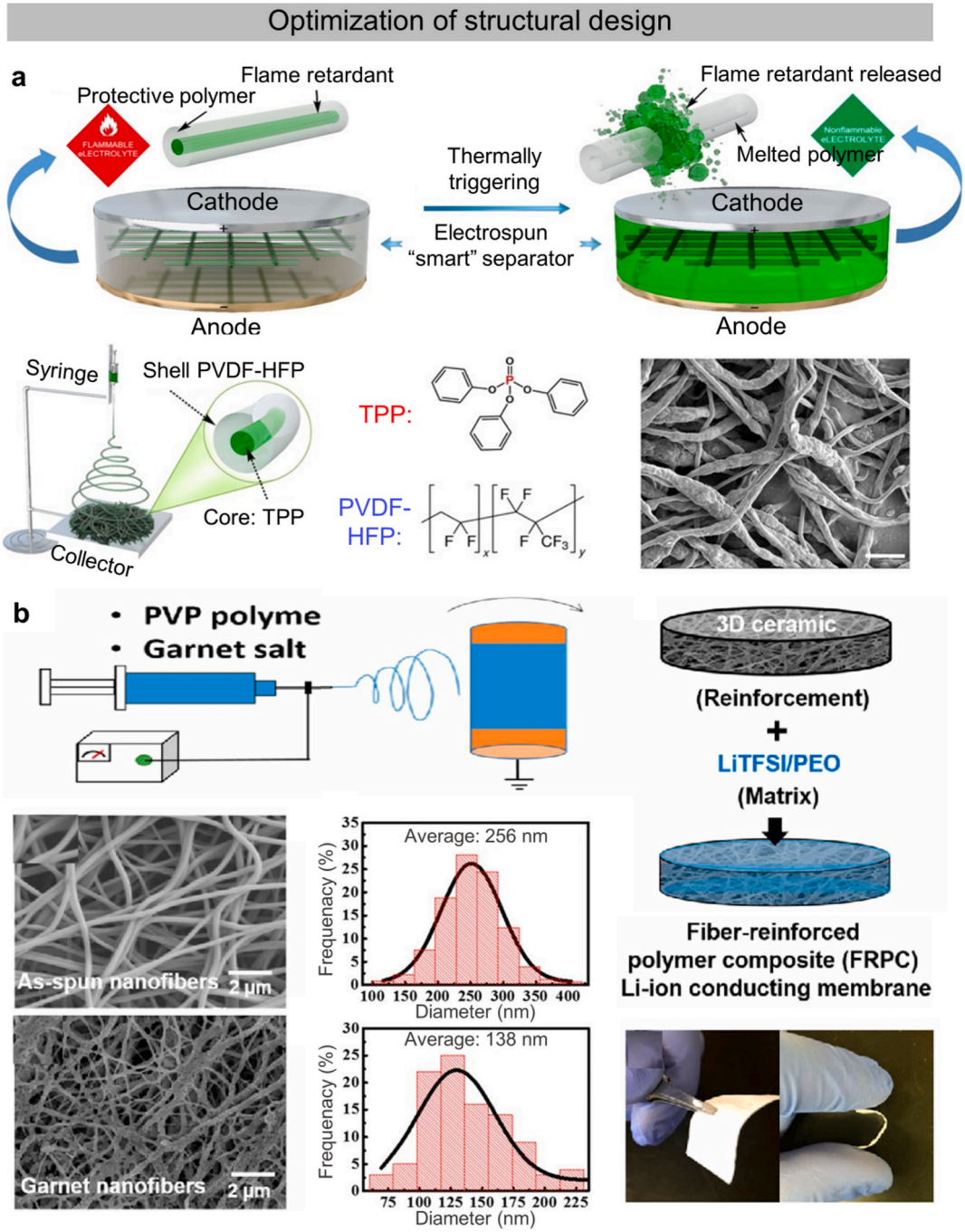

Fig. 18. Optimization of structural design for separators. (a) Thermally responsive separator preparation process, structural characterization and electrochemical test [161]. Copyright (2017) American Association for the Advancement of Science. (b) Ionic flame-retardant separator operation mechanism, structural characterization, electrochemical characterization and full-cell pinning experiments [298]. Copyright (2016) National Academy of Sciences.

processing, system integration and recycling. Coordinated progress across these domains is necessary to balance performance, safety and environmental impact. This calls for collaboration among academia, industry and research institutions to collectively advance the sustainability of battery technologies.

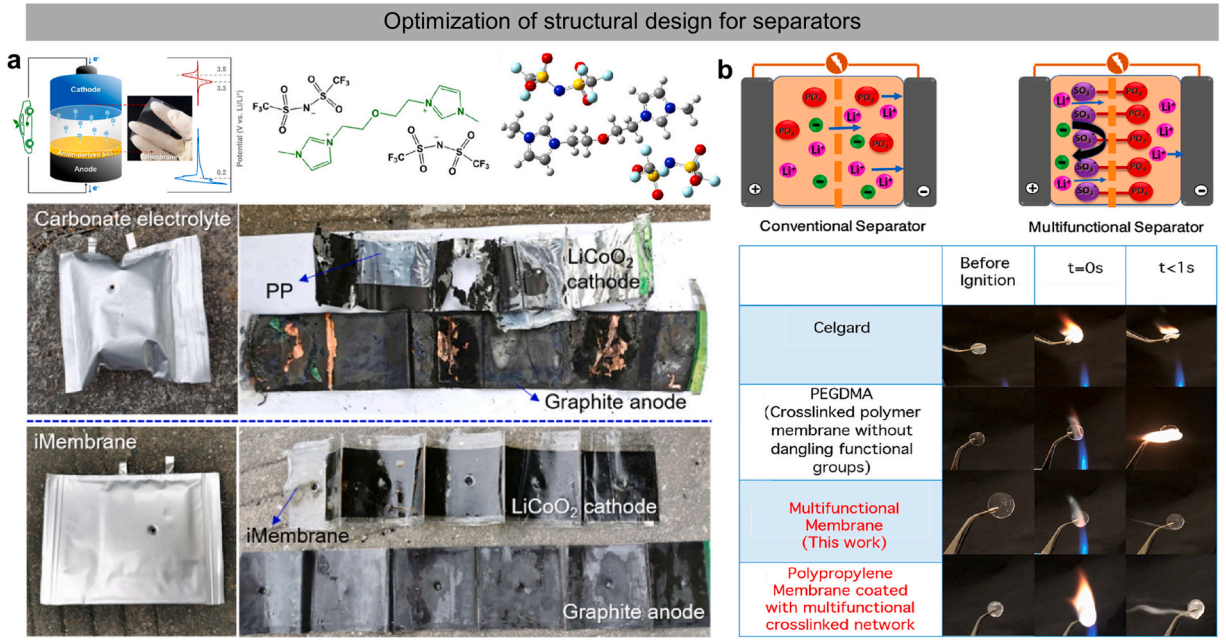

Fig. 19. (a) Schematic structure of 3D garnet-type polymer composite (FRPC) separator [308]. Copyright (2021) American Chemical Society. (b) Crosslinked polymer separator mechanism of action, surface structural characterization, and comparison of the separator ignition experiments [309]. Copyright (2018) American Chemical Society.

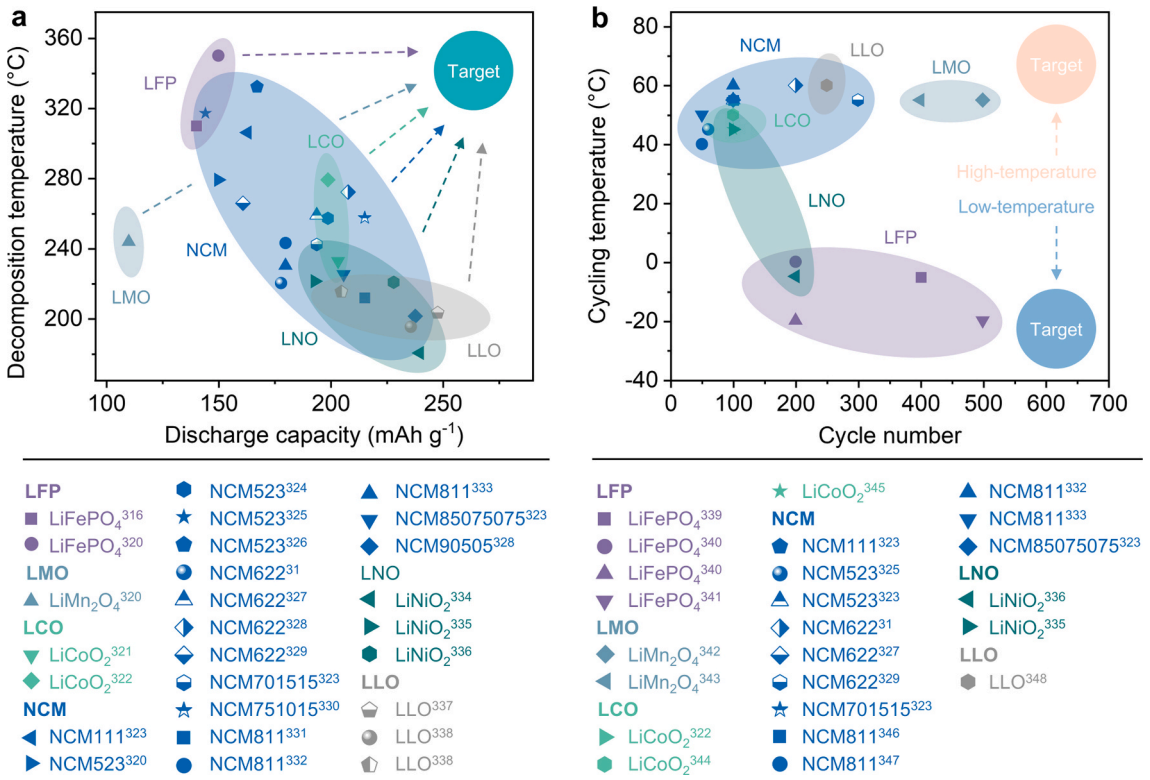

Fig. 20. Thermal stability of various common cathode materials. (a) Thermal decomposition temperature and specific discharge capacity are key measures of safety and electrochemical performance, where the circular area in the upper right corner of the chart represents the ideal performance target for the cathode material; (b) Cycling stability at both low and high temperatures is equally critical, and the circular areas in the upper and lower right corners of the chart indicate the ideal performance target for cathode materials operating at extreme temperatures.

6. Safe cathode materials

The common cathode materials for LIBs are $LiFePO_4$ (LFP), $LiMn2O_4$ (LMO), $LiCoO_2$ (LCO), $Li(Ni_xCo_yMn_z)O_2$ (NCM), $LiNiO_2$ (LNO) and, $xLi_2MnO_3{\cdot}(1\text{-}x)LiMO_2$ (LLO, M=Ni, Co, Mn) [314,315], their thermal stability is summarised in Fig. 20. Fig. 20**a** shows their thermal decomposition temperatures and discharge specific capacities (see Table 5 for detailed data). Among them, the best thermally stable cathode material is LFP, which can remain stable at 350 °C [316]. This is attributed to its strong P=O covalent bonding [317]. Moreover, as can be seen from Fig. 20**b**, LFP also exhibits better cycling stability at low temperatures (Table 6 for detailed data). However, the stacking and compaction densities of LFP are low, and the cost per watthour is relatively high [314]. LMO has lower cost and toxicity compared to LFP. However, LMO exhibits lower energy density and cycling stability because it is prone to Mn dissolution at higher temperatures. LCO, on the other hand, has a high specific capacity and excellent cycling performance advantages and is currently the most used cathode material for commercial LIBs. However, its thermal stability is insufficient, and it will thermally decompose at about 250 °C to release oxygen [318].

Compared to the above types of cathode materials, NCM exhibits a high specific capacity, and its specific capacity further improves with an increase in the Ni ratio. Therefore, it is also considered the most promising cathode material to replace LFP and LCO [319]. However, due to the substantial oxidizing property of Ni^{4+}, NCM will thermally decompose at around 200 °C, especially for the nickel-rich cathode materials with a high Ni ratio, which show inferior thermal stability and capacity retention. Given this challenge, research efforts have been focused on improving the thermal stability of NCM. This chapter will also focus on strategies to achieve safe NCM cathodes.

Note: —, not mentioned.

6.1. Failure mechanism

The failure mechanisms of cathode materials vary, but generally, they involve structural phase changes under abusive conditions like overcharging and overheating, alongside side reactions with the electrolyte. We will detail the failure process of cathode materials in LIBs using a representative nickel-rich cathode material as an example.

In nickel-rich cathode materials, high oxidation states like Ni^{4+} react with lattice oxygen at elevated temperatures, releasing significant heat and oxygen [351]. This reaction leads to Ni^{2+} migrating into Li^+ layers, causing cationic mixing [352] and transforming the original layered structure into spinel and NiO-like phases [353–355]. This transformation increases mechanical stress, leading to microcracks [356], especially in materials with higher nickel content [349]. As nickel content rises, thermal stability and

Table 5
Thermal decomposition temperature and electrochemical properties of common lithium-ion battery cathode materials.

Cathode	C-rate	Discharge capacity (mAh g^{-1})	Cycle number	Capacity retention (%)	Decomposition temperature (°C)	Ref
$LiFePO_4$	–	140.00	–	–	310.00	[316]
$LiFePO_4$	–	150.00	–	–	350.00	[320]
$LiMn_2O_4$	–	110.00	–	–	243.60	[320]
$LiCoO_2$	0.50	203.50	150	79.56	232.50	[321]
$LiCoO_2$	1.00	199.00	200	90.30	279.00	[322]
$Li(Ni_{1/3}Co_{1/3}Mn_{1/3})O_2$	0.50	163.00	100	92.40	306.00	[323]
$Li(Ni_{0.5}Co_{0.2}Mn_{0.3})O_2$	–	150.00	–	–	279.00	[320]
$Li(Ni_{0.5}Co_{0.2}Mn_{0.3})O_2$	1.00	199.00	200	80.00	257.00	[324]
$Li(Ni_{0.5}Co_{0.2}Mn_{0.3})O_2$	1.00	144.25	100	71.14	317.00	[325]
$Li(Ni_{0.5}Co_{0.2}Mn_{0.3})O_2$	1.00	167.30	100	90.30	332.13	[326]
$Li(Ni_{0.5}Co_{0.2}Mn_{0.3})O_2$	1.00	178.00	100	86.70	220.00	[31]
$Li(Ni_{0.6}Co_{0.2}Mn_{0.2})O_2$	1.00	194.00	100	91.34	258.80	[327]
$Li(Ni_{0.6}Co_{0.2}Mn_{0.2})O_2$	0.50	208.00	100	96.00	272.00	[328]
$Li(Ni_{0.6}Co_{0.2}Mn_{0.2})O_2$	1.00	161.00	300	94.00	265.60	[329]
$Li(Ni_{0.7}Co_{0.15}Mn_{0.15})O_2$	0.50	194.00	100	78.50	242.00	[323]
$Li(Ni_{0.75}Co_{0.10}Mn_{0.15})O_2$	0.20	215.40	1000	90.00	257.30	[330]
$Li(Ni_{0.8}Co_{0.1}Mn_{0.1})O_2$	–	215.00	–	–	212.00	[331]
$Li(Ni_{0.8}Co_{0.1}Mn_{0.1})O_2$	0.50	180.00	100	97.22	242.90	[332]
$Li(Ni_{0.8}Co_{0.1}Mn_{0.1})O_2$	0.33	180.00	250	98.00	230.00	[333]
$Li(Ni_{0.85}Co_{0.075}Mn_{0.075})O_2$	0.50	206.00	100	55.60	225.00	[323]
$Li(Ni_{0.90}Co_{0.05}Mn_{0.05})O_2$	0.50	238.00	100	97.00	201.00	[328]
$LiNO_2$	–	240.00	–	–	180.00	[334]
$LiNO_2$	1.00	193.10	100	93.10	221.00	[335]
$LiNO_2$	0.10	228.30	300	84.30	220.40	[336]
$0.18Li_2MnO_3{\cdot}0.82Li(Ni_{0.31}Co_{0.31}Mn_{0.38})O_2$	0.20	248.00	100	65.00	203.00	[337]
$0.125Li_2MnO_3{\cdot}0.875Li(Ni_{0.2}Co_{0.2}Mn_{0.4253})O_2$	0.10	236.00	100	92.00	195.00	[338]
$0.125Li_2MnO_3{\cdot}0.875Li(Ni_{0.2}Co_{0.2}Mn_{0.4253})O_2$	0.10	205.00	50	83.00	215.00	[338]

Note: —, not mentioned.

Table 6
Cycling stability at extreme temperatures of common lithium-ion battery cathode materials.

Material	Temperature(°C)	C-rate	Discharge capacity (mAh g^{-1})	Cycle number	Capacity retention (%)	Ref
$LiFePO_4$	−5.00	0.50	123.00	400	75.61	[339]
$LiFePO_4$	0.00	1.00	135.50	200	99.30	[340]
$LiFePO_4$	−20.00	1.00	105.00	200	96.20	[340]
$LiFePO_4$	−20.00	1.00	100.30	500	99.90	[341]
$LiMn_2O_4$	55.00	10.00	92.20	500	48.81	[342]
$LiMn_2O_4$	55.00	1.00	100.00	400	81.90	[343]
$LiCoO_2$	45.00	1.00	225.00	100	71.11	[322]
$LiCoO_2$	50.00	1.00	180.00	100	79.30	[344]
$LiCoO_2$	45.00	1.00	211.00	100	93.20	[345]
$Li(Ni_{1/3}Co_{1/3}Mn_{1/3})O_2$	55.00	0.50	163.00	100	92.40	[323]
$Li(Ni_{0.5}Co_{0.2}Mn_{0.3})O_2$	45.00	1.00	168.45	60	71.81	[325]
$Li(Ni_{0.5}Co_{0.2}Mn_{0.3})O_2$	55.00	0.50	175.00	100	90.00	[323]
$Li(Ni_{0.6}Co_{0.2}Mn_{0.2})O_2$	60.00	1.00	173.00	200	93.80	[31]
$Li(Ni_{0.6}Co_{0.2}Mn_{0.2})O_2$	55.00	1.00	194.00	100	91.34	[327]
$Li(Ni_{0.6}Co_{0.2}Mn_{0.2})O_2$	55.00	1.00	172.00	300	85.00	[329]
$Li(Ni_{0.7}Co_{0.15}Mn_{0.15})O_2$	55.00	0.50	194.00	100	78.50	[323]
$Li(Ni_{0.8}Co_{0.1}Mn_{0.1})O_2$	55.00	1.00	188.50	100	80.50	[346]
$Li(Ni_{0.8}Co_{0.1}Mn_{0.1})O_2$	40.00	1.00	176.80	50	91.40	[347]
$Li(Ni_{0.8}Co_{0.1}Mn_{0.1})O_2$	60.00	0.50	180.00	100	97.22	[332]
$Li(Ni_{0.8}Co_{0.1}Mn_{0.1})O_2$	50.00	0.50	210.00	50	96.60	[333]
$Li(Ni_{0.85}Co_{0.075}Mn_{0.075})O_2$	55.00	0.50	206.00	100	55.60	[323]
$LiNO_2$	−5.00	1.00	150.70	200	81.20	[336]
$LiNO_2$	45.00	1.00	207.30	100	92.80	[335]
$0.4Li_2MnO_3{\cdot}0.6LiNi_{1/3}Co_{1/3}Mn_{1/3}O_2$	60.00	1.00	250.00	250	72.60	[348]

Note: −, not mentioned.

capacity retention decrease (Fig. 21**a-b**), while oxygen release increases, and phase transition temperature lowers significantly (Fig. 21**c-d**). Microcracks allow electrolyte penetration, exacerbating side reactions between the cathode material and electrolyte [58]. HF from side reactions further dissolves transition metals, enlarging microcracks or causing particle rupture [357] (Fig. 22**a-c**). Excessive heat and gas from these reactions can result in battery combustion or explosion, posing severe safety risks.

The failure of nickel-rich cathode materials is mainly due to microcracking caused by structural phase transitions and exacerbated interfacial side reactions with the electrolyte, a common issue across many LIB cathode materials. To address these problems, modify the cathode surface to prevent side reactions with the electrolyte and stabilizing the crystal structure through elemental doping are prominent methods [31,319,358–360]. Additionally, the development of single-crystal cathode materials aims to fundamentally eliminate microcrack formation [361,362]. Beyond these approaches, extensive research explores further safety enhancements for cathode materials, which we will review in more detail.

6.2. Design strategies

6.2.1. Surface coating

To improve the safety of cathode materials, the most effective approach is coating electrochemically active/inactive coating materials, such as oxide materials, polymer materials, phosphate materials, and lithium-containing composites, on the surface of the cathode, which improves the structural stability. Working principles can be attributed to three aspects: (1) acting as a physical barrier to prevent direct contact between the cathode material and the electrolyte as well as the precipitation of gases [31]; (2) scavenging HF and inhibiting the dissolution of transition metal ions of cathodes [358]; and (3) reducing the redox activity of the oxygen of the surface lattice, which inhibits the phase change of the surface structure of the material [359]. Four types of coating chemistries are introduced below.

- Oxide coating materials include Nb_2O_5 [365], TiO_2 [366] and $Ce_{0.8}Dy_{0.2}O_{1.9}$ [367], etc, which can reduce interfacial side reactions and prevent the O_2 release. For example, Wang et al. [367] coated $Ce_{0.8}Dy_{0.2}O_{1.9}$ solid electrolyte on the surface of NCM811 cathode material. The $Ce_{0.8}Dy_{0.2}O_{1.9}$ coating is rich in oxygen vacancies, which can effectively store unstable oxygen-containing species (e.g., O^{2-}, O^{-}, and O_2^{2-}) generated during the charging process, thus reducing the release of O_2 and improving the structural stability and safety of the material (Fig. 23**a**).
- Polymer coating materials include branched oligomers [31], oligomer additives [368] and polyvinylidene fluoride (PVDF) [369], etc. The polymer coating on the surface of cathode materials can improve the electrical conductivity of cathodes, reduce the Li accumulation on the surface of cathodes, and stabilize the crystal structure [319]. For instance, Yeh et al. [31] synthesized branched zwitterions from uracil and NMP and developed a new solid electrolyte layer on the surface of $LiNi_{0.6}Co_{0.2}Mn_{0.2}O_2$ (NCM622) surface as shown in Fig. 23**b**. The coating ensured the stability of Ni^{4+} formed in the lattice of NCM622 in the 100 % charge state at high temperature (660 K), preventing the formation of rock salt phase and excessive reduction of Ni^{4+} to Ni^{2+}. Although high temperatures do not solve the cation mixing problem, it reduces the degree of disorder, stabilizes the lattice structure NCM622 during high-temperature charging, and improves the battery performance. In addition, this new solid electrolyte layer

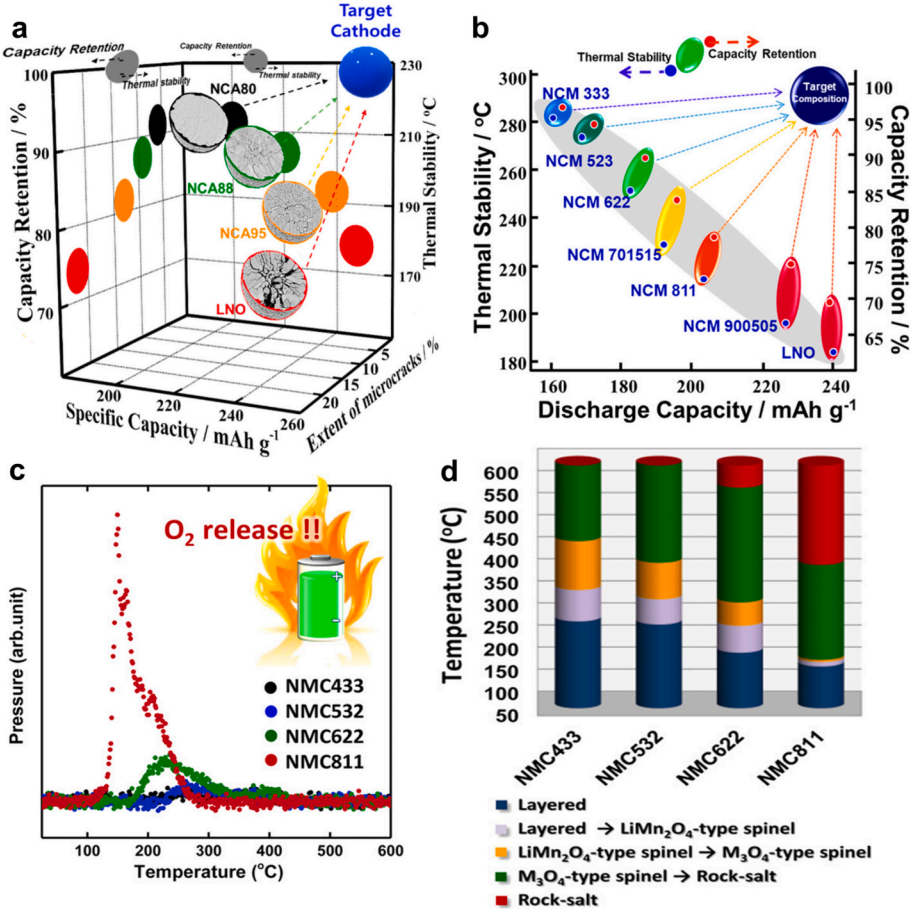

Fig. 21. The failure mechanism of nickel-rich cathodes. (a) Overview of the relationship between the specific capacity, capacity retention, microcracking degree and thermal stability of nickel-rich NCA and LNO cathodes [349]. Copyright (2019) American Chemical Society. (b) Effect of changes in the composition of nickel-rich cathode materials on their thermal stability and capacity retention [323]. Copyright (2013) Elsevier. (c) Effect of changes in the cost of nickel-rich cathode materials on the amount of oxygen released and (d) the phase transition temperature [350]. Copyright (2014) American Chemical Society.

absorbs the heat released from the cathode and prevents thermal runaway from occurring when short circuit or overcharge happens to the battery.

- Phosphate coating materials include $FePO_4$, $AlPO_4$ [35], $Co_3(PO_4)_2$, and $NaTi_2(PO_4)_3$ [370], etc. The PO_4^{3-} group in phosphate materials can form strong covalent bonds with transition metal ions, which can significantly improve the safety stability of the materials after coating on the surface of cathode materials [371]. For example, Liang et al. [370] used the wet-coating method to coat $NaTi_2(PO_4)_3$(NTP) coated on the surface of $LiNi_{0.5}Co_{0.2}Mn_{0.3}O_2$ (NCM523) to form a novel core–shell layer NTP@NCM cathode material, as shown in Fig. 23**c**. The results showed that the NTP coating not only protected the cathode material's laminated structure from the electrolyte's corrosive damage and provided a fast channel for Li^+ transport by the unique inter-diffusion tunneling between its NCM523 core and NTP shell. As a result, the NTP@NCM cathode material exhibits excellent cycling stability and C- rate capacity.
- Li-containing composites include $LiNbO_3$ [332], $LiCoO_2$ [372], Li_3VO_4 [347], $LiFePO_4$ [327], and $LiNbO_3$ [373], etc. Li-containing composites can improve the safety performance of cathode materials while improving the electrochemical performance of cathode materials due to fast Li-ion channels compared to others. For instance, Kim et al. [332] coated $LiNbO_3$ on the surface of a NCM811 material by a simple wet-coating method, as shown in Fig. 23**d**. High-nickel cathode materials with a layered structure usually suffer from structural instability caused by highly active nickel components, whereas the highly crystalline $LiNbO_3$ coated on the surface of NCM811 effectively suppresses the structural changes of the cathode material by promoting the strain relaxation induced by the repeated embedding and de-embedding of Li^+ into and out of the host structure. In addition, its mechanical and thermal stability was greatly improved at high temperatures above 60 °C.

In a short summary, surface coating significantly enhances the safety of cathode materials, yet challenges remain. Achieving a uniform coating often requires complex processing techniques, increasing production costs [371]. Moreover, to effectively prevent

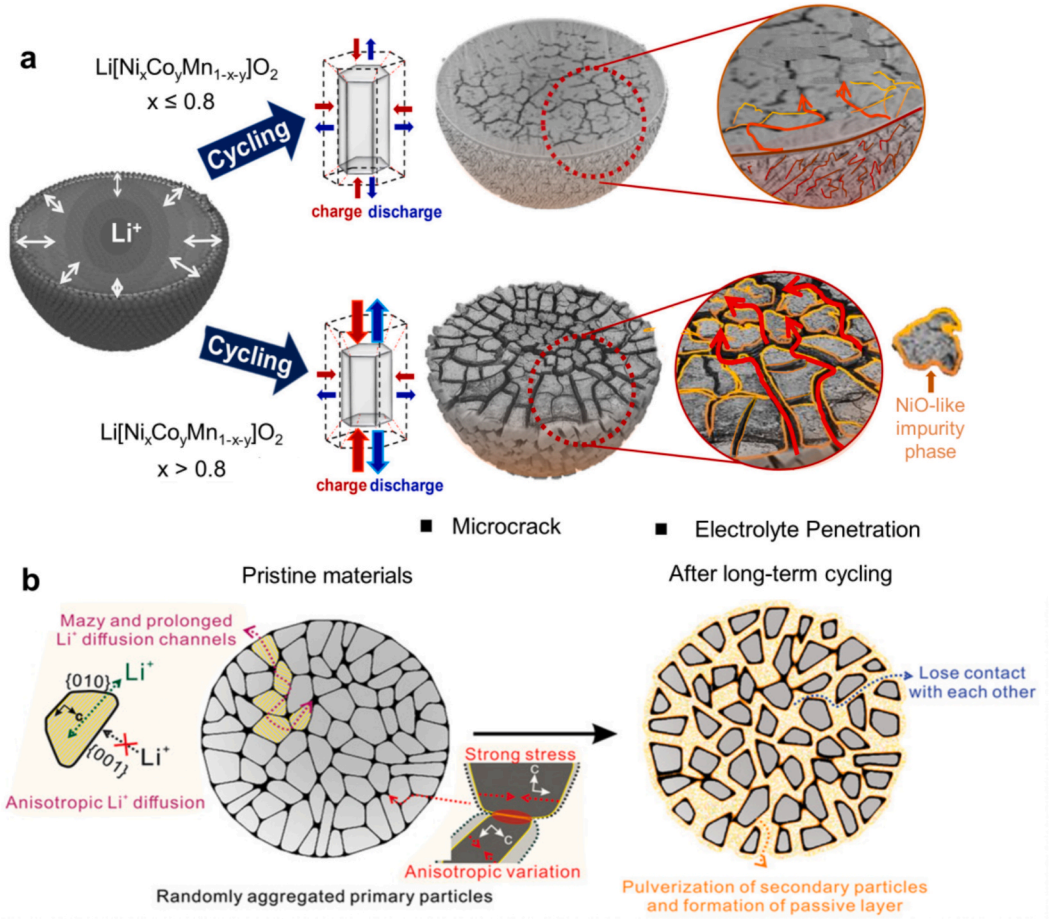

Fig. 22. (a) Capacity decay scheme of nickel-rich cathode materials [363]. Copyright (2018) American Chemical Society. (b) Schematic structure and properties of commercial NCM materials before and after cycling [364]. Copyright (2019) Wiley–VCH (c) Microstructure and composition of the surface of nickel-rich cathode materials after reaction with electrolyte [352]. Copyright (2015) John Wiley and Sons.

thermal runaway, coatings thicker than 20 nm are needed [35], but such thickness can hinder ion and electron transport [371]. Therefore, a systematic study on the surface coating of LIB anode materials is crucial. To achieve this, we need to approach from multiple angles. For example, we can develop roll-to-roll ALD to enhance mass production efficiency, or use nanoparticle suspension spraying to reduce cracking and improve uniformity.

6.2.2. Doping

Doping cations or anions into the cathode bulk is a common method to stabilize its internal structure. This approach enhances cathode safety in three ways: (a) The doped element creates a strong Coulomb force towards transition metal ions, inhibiting their migration and reducing cation mixing to stabilize the structure and enhance thermal stability [360]; (b) It strengthens oxide bonds with transition metal ions, preventing oxygen release and structural changes, thereby boosting material safety [319]; (c) Doping weakens Li-O interactions, enhancing the Li^+ diffusion coefficient and electronic conductivity of the cathode material, reducing heat generation and improving thermal safety [374–376].

Doping cathode materials with cations or anions can significantly enhance their safety. However, several factors must be considered when doping cathode materials. One critical aspect is the impact of doping on the lattice constant and cell volume. If the dopant particle size is smaller than that of the ions of base materials, the lattice constant and cell volume decrease; conversely, if larger, they increase [377]. Excessive changes can alter the cathode structure, making crystals more prone to cracking during Li^+ de-embedding, thus increasing microcrack formation. Additionally, the doping site affects safety performance differently: doping at the Ni site in Ni-rich materials boosts cycling stability [378]; at the Co site, it enhances phase stability [379]; and at the Mn site, it helps mitigate cation mixing and oxygen release [379,380]. These comprehensive factors must be carefully considered to improve cathode stability effectively. The recent studies on cation and anion doping for cathode material safety enhancements are reviewed below.

First, the typical doping cations are Al^{3+}, Ce^{4+}, Mg^{2+}, Ti^{4+}, etc. They can improve structural safety by inhibiting transition ion migration and reducing lattice distortion. For example, Li et al. [336] developed Mg^{2+} doped $LiNi_{0.9}Co_{0.07}Mg_{0.03}O_2$ using a two-step method of co-precipitation and roasting, which could withstand a high voltage charging of 4.7 V with small lattice changes (<1%)

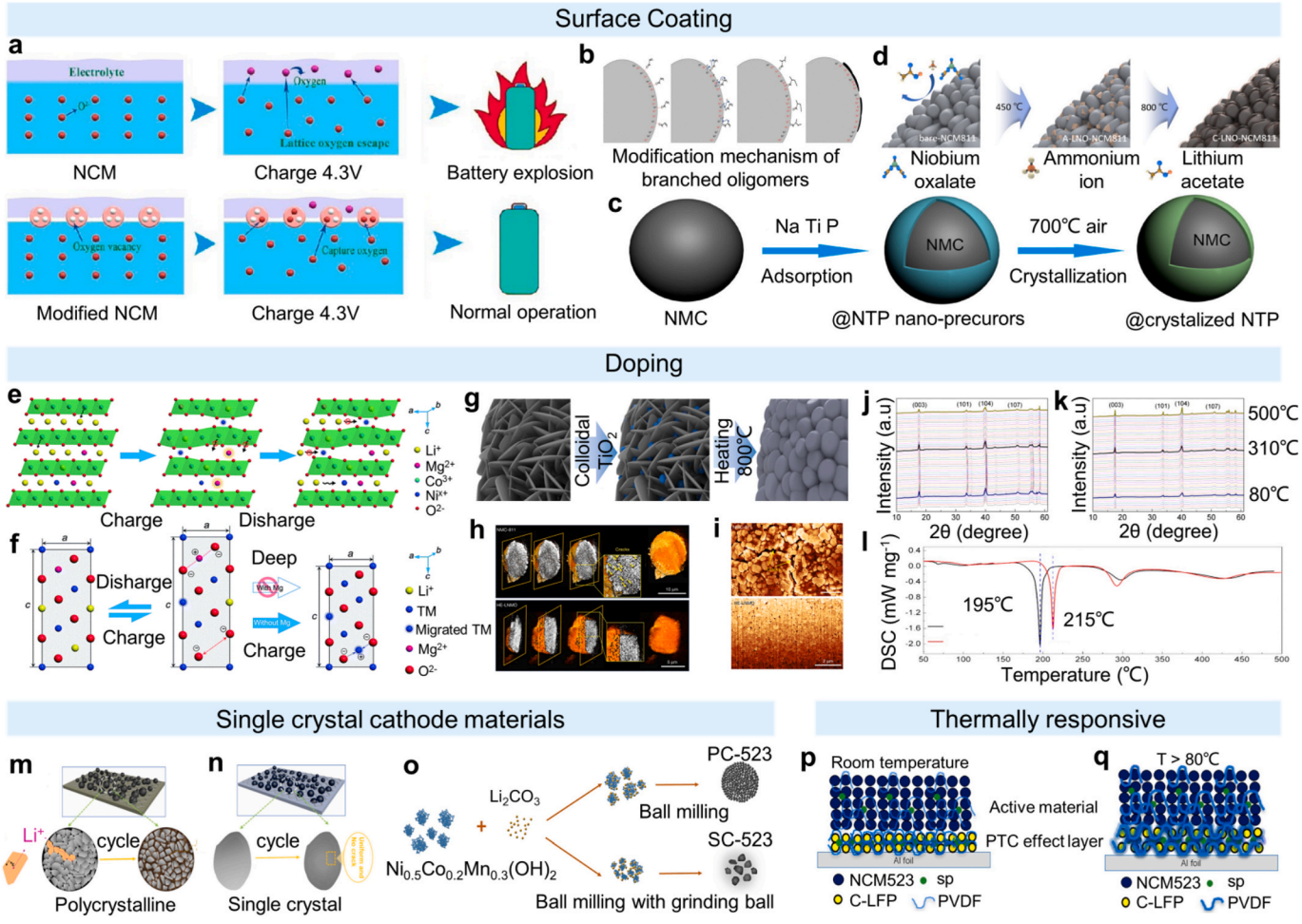

Fig. 23. Strateiges for safe cathodes. (a) Schematic representation of the structural stability of Ni-rich materials enhanced by oxygen vacancies in $Ce_{0.8}Dy_{0.2}O_{1.9}$ [367]. Copyright (2019) American Chemical Society. (b) Schematic representation of a solid electrolyte formation by branched oligomers on the surface of NCM622 [31]. Copyright (2021) American Chemical Society. (c) Schematic representation of a nucleus-shell layer of NTP@NCM cathode material [370]. Copyright (2018) American Chemical Society. (d) Schematic representation of the NCM811 cathode material surface by a simple wet-coating of $LiNbO_3$ [332]. Copyright (2020) American Chemical Society. (e) and (f) Schematic diagram of the column effect of Mg doping [336]. Copyright (2017) Royal Society of Chemistry. (g) Schematic diagram of the synthesis process of T-NCM811 cathode material [381]. Copyright (2020) American Chemical Society. (h) A large number of microcracks (indicated by arrows) appeared in NCM-811 (upper panel) after 100 cycles, whereas no apparent microcracks were observed in HE-LNMO (lower panel); (i) SEM cross-sections of secondary particles of NCM-811 (top panel) and HE-LNMO (bottom panel) [333]. Copyright (2022) Springer Nature. (j) In situ X-ray diffraction spectra of undoped F- and (k) F-doped LMR during heating from room temperature to 500 °C, and (l) DSC curves of undoped F- and F-doped LMR in the fully charged state [338]. Copyright (2018) American Chemical Society. (m) Schematic diagrams of PC material schematic and (n) SC material schematic [382]. Copyright (2022) Elsevier. (o) Schematic of the preparation process of polycrystalline NCM523 (PC-523) and single-crystalline NCM523 (SC-523) [383]. Copyright (2019) Springer Nature. (p) and (q) Schematic of the cathode of the PTC layer safety design [384]. Copyright (2021) American Chemical Society.

without forming an unstable H3 phase and exhibited excellent cycling performance and thermal stability. The strong Coulombic interaction between Mg^{2+} and Ni^{2+} is responsible for these excellent properties, which inhibits the migration of Ni^{2+} to the Li^{+} layer and stabilizes the laminar structure (Fig. 23**e** and Fig. 23**f**). Although this doping method performs excellently in improving battery performance, its two-step co-precipitation and calcination method requires precise control of reaction conditions and temperature, which increases production costs and process complexity. In addition, Dopant elements may also be essential in suppressing intergranular microcracking. For example, Kim et al. [381] prepared Ti^{4+} doped NCM811 cathode materials using a co-precipitation method as shown in Fig. 23**g**. Ti^{4+} doping suppressed unwanted grain boundary corrosion through the formation of strong Ti-O bonds in a given structure and effectively improved the NCM811 particle structural integrity and improved thermal stability. Furthermore, under the influence of Ti doping, the intergranular microcracking due to the repeated embedding and de-embedding of Li^{+} during the cycling process was successfully suppressed, which further improved the cycling stability of the NCM811 cathode material.

Multiple elements can be also doped into the material together. Due to the high entropy effect, they may enhance a better solution for battery safety performance improvement. For example, Zhang et al. [333] concurrently doped Ti^{4+}, Mg^{2+}, Mo^{6+}, and Nb^{5+} into the NCM811 cathode material, drawing inspiration from the traditional high-entropy strategy, and the fabricated $LiNi_{0.8}Mn_{0.13}Ti_{0.02}Mg_{0.02}$ $Nb_{0.01}Mo_{0.02}O_2$ high-entropy material (HE-LNMO) exhibiting remarkable low volumetric strain (less than 0.3 %). As shown in Fig. 23**h** and Fig. 23**i**, the HE-LNMO effectively suppressed the mechanical cracking and the lattice defects during long-term cycling and exhibited excellent structural and thermal stability due to the pinning effect of the dopant. Additionally, this high-entropy doping strategy generally applies to zero-cobalt cathode materials with different nickel contents. The use of multi element doping demands precise control of stoichiometric ratios, as deviations can easily lead to the formation of impurity phases. Although this approach offers a systematic pathway for material enhancement, it is experimentally costly and often requires repeated optimization of element combinations. To overcome these challenges, computational simulations can be employed to predict optimal doping strategies, thereby reducing reliance on trial and error and significantly improving experimental efficiency.

As for anion doping, the most common strategy is to replace O^{2-} in the cathode material with F^{-}, Cl^{-}, S^{2-}, and so on. Among them, since F^{-} is the most electronegative element and has the most potent Coulombic force between it and the transition metal ions in the cathode material, it can effectively prevent cation mixing, oxygen release, and structural degradation, etc., so it has the best effect of safety optimization [385]. For example, Wang et al. [338] used the polyacrylamide-assisted carbonate co-precipitation method to prepare F^{-} doped aspherical $Li[Li_{0.133}Mn_{0.467}Ni_{0.2}Co_{0.2}]O_{1.95}F_{0.05}$ cathode materials. Through in situ X-ray diffraction and differential scanning calorimetry experiments, they characterized the structural stability of F^{-} and F^{-}undoped lithium manganese-rich cathode materials (LMRs) during the heating process from room temperature to 500 °C. As can be seen from Fig. 23**j**, the undoped F^{-} LMR showed some new peaks during the heating process, whereas the X-ray diffractogram of the F^{-} doped LMR did not change during the heating process (Fig. 23**k**). In addition, the fully charged state (Fig. 23**l**), the temperature at which the F^{-} doped LMR appeared to be structurally decomposed (215 °C) was higher than the temperature at which the undoped LMR appeared to be structurally decomposed (195 °C). These results indicate that F^{-} doping can improve the thermal stability of LMR, especially in the charged state.

The primary challenge in elemental doping lies in enhancing safety performance with minimal doping quantities to prevent adverse effects on the electrochemical performance of cathode materials [58]. A more feasible approach is to use multi-element co-doping to enhance the synergistic effects and reduce the amount of doping required. However, considering the complexity of multi-element doping, it is best to combine it with computational simulation predictions to more quickly obtain the optimal combination. Additionally, optimizing the doping process to lower preparation costs is crucial. To address this, we can employ an efficient, uniform, and controllable fluidized bed doping method as an alternative to traditional doping techniques such as solid-state methods or sol–gel processes, in order to improve efficiency and reduce costs. Further research is also needed to understand the specific mechanisms by which doping elements improve battery safety and stability.

6.2.3. Single-crystal cathodes

Ordinary polycrystalline cathode materials are composed of secondary particles, and along-crystal microcracks may occur during the cycling process [386]. These microcracks will cause liquid electrolytes to penetrate the material and induce the side reactions between the cathode material and the electrolyte, which in turn will cause the dissolution of transition metal ions, the precipitation of gases, and the phase transition, and thus affect the cycling and thermal stability of polycrystalline cathode materials. At the same time, due to microcracks along the crystal, polycrystalline cathode materials have lower Li^{+} diffusion coefficients and higher lithium ion transport impedance, which will generate higher heat than single-crystal cathode materials [382]. In contrast, single-crystal cathode materials are composed of individual intact crystal particles of micrometer size and thus do not have along crystal microcracks or side reactions caused by along crystal microcracks. Moreover, since the specific surface area of a single-crystal cathode is much smaller than that of polycrystalline cathode materials, the single-crystal cathode has fewer side reactions with the electrolyte [361,362]. Therefore, using single-crystal cathode materials significantly improves the cycling and thermal stability of LIBs.

Eliminating intergranular microcracks will lead to a more uniform delithiation within the material, which exhibits better structural and thermal stability. For example, Kong et al. [382] investigated the thermal safety performance of two typical high-nickel cathode materials, NCM811 and NCM622, in single-crystal as well as polycrystalline forms. The results show that the thermal safety performance of single-crystal high-Ni materials (SC-NCM) is significantly better than that of polycrystalline high-Ni materials (PC-NCM). As shown in Fig. 23**m**, due to the presence of intergranular microcracks, the ion transport resistance of PC-NCM is more excellent, and its heat production at a high C-rate is higher than that of SC-NCM. Microcracks in PC-NCM also lead to inhomogeneous de-lithiation within the material, which results in more severe structural degradation of the excessively de-lithiated portion, which releases oxygen and heat in advance and reduces the thermal stability of PC-NCM. SC-NCM, on the other hand, has uniform de-lithiation and better

thermal stability (Fig. 23**n**). In addition, the thermal decomposition temperature of single-crystal cathode materials is also much higher than that of polycrystalline cathode materials, showing excellent thermal stability. For example, Zhong et al. [383] successfully synthesized large particles of single-crystal NCM523 (SC-523) through a controlled roasting process, and the preparation process flow is shown in Fig. 23**o**. Compared with polycrystalline NCM523 (PC-523), SC-523 gives superior cycling and thermal stability with its robust and intact single-crystal particles. In the voltage range of 3 V ~ 4.5 V, the capacity retention of SC-523 is 90.3 %, while that of PC-523 is 78.4 %. In addition, the thermal decomposition temperature of SC-523 (332.13 °C) is much higher than that of PC-523 (14.61 °C).

Single-crystal cathode materials face challenges like lower ion diffusion coefficients at room temperature, increased cation mixing and exclusion after high-temperature calcination, and potential microcracks under high-temperature or pressure conditions [386]. Additionally, controlling their morphology and size is difficult, and synthesis costs are high [329,387]. Thus, further exploration is needed to address these issues and enable the industrial production of single-crystal cathode materials promptly. For example, cation/anion co-doping and surface gradient modification can be employed to enhance the diffusion rate of Li^+; or the manufacturing process can be optimized to control the single-crystal grain size to less than 3.5 μm, in order to reduce stress concentration and prevent the propagation of microcracks; additionally, microwave sintering technology can be used as an alternative to solid-state sintering, thereby shortening the sintering time and improving energy efficiency.

6.2.4. Thermally responsive switching cathodes

Positive temperature coefficient (PTC) resistors outside batteries are being used to prevent thermal runaway during overcharging or overheating. If the internal temperature rises too high, the PTC melts quickly, significantly increasing battery resistance and swiftly deactivating the battery to halt thermal runaway [388]. However, external PTCs may respond slowly, risking delayed thermal runaway detection [389].

To address this, PTCs are also placed internally, within components like the cathode, separator, and electrolyte. Since the cathode generates about 80 % of the heat during thermal runaway, placing PTCs at the cathode is more effective, known as thermally responsive switching cathode material. Two main design strategies are direct mixing of PTC material with the cathode material [390] or inserting a PTC layer between the collector and cathode material [384]. For instance, Jin et al. [384] developed thermally responsive switching cathode materials by placing a PTC layer, composed of carbon-coated $LiFePO_4$ (C-LFP), polyvinylidene fluoride (PVDF), and Super P (SP) between an aluminum collector and NCM523. C-LFP and SP provide conductivity, while PVDF acts as a thermal switch, expanding with temperature rise to break the conductive path and increase resistance. As shown in Fig. 23**p** and Fig. 23**q**, the PTC effect of PVDF activates at temperatures above 80 °C, effectively halting electron flow and sharply increasing cathode resistance to prevent thermal runaway.

While thermally responsive switching cathode materials effectively prevent thermal runaway, their incorporation into batteries reduces energy density due to their non-electrochemical activity. This reduction is contrary to the trend in EVs and large-scale energy storage systems, which aim for higher capacity and energy density [289]. Hence, there is a need to identify more efficient PTC materials that can deliver the necessary safety performance with minimal usage, thereby minimizing their impact on the battery performance. Alternatively, materials that combine both PTC effects and electrochemical functionality, such as self-passivating cathodes, can be developed to reduce reliance on external PTC components. In summary, a fundamental trade-off remains between the safety benefits provided by current PTC materials and the associated reduction in energy density. Nevertheless, by pursuing multifunctional material design, localized structural optimization and system level synergistic strategies, it is possible to move closer to the objective of minimal performance loss with maximum safety protection.

In summary, surface coating, elemental doping, single crystal preparation and thermally responsive switchable cathode materials are all effective strategies for enhancing the safety and stability of LIB cathodes. While these modifications can improve thermal and structural resilience, it is essential to evaluate their effects on electrochemical performance to achieve an optimal balance between safety and functionality. For instance, although surface coatings and doping can enhance thermal stability, they may reduce specific capacity or shorten cycle life. Thus, careful optimization of coating materials and doping elements in terms of type and quantity is critical. Furthermore, the synergistic effects between different modification methods, e.g., combining surface coatings with elemental doping, warrant further investigation through both experimental and theoretical approaches.

To support large scale commercialization, simplification of processing techniques and cost reduction are also necessary. The high complexity and expense associated with producing single crystal cathodes currently limit their industrial viability. Advancing more efficient crystal growth technologies or identifying low-cost alternatives will be essential. Similarly, the production of thermally responsive switchable cathodes must be optimized to reduce material costs and processing challenges without compromising performance.

From an environmental perspective, the safety benefits of these modification strategies must be weighed against their potential ecological impacts. Certain coating materials and dopants may introduce toxic elements such as heavy metals, raising concerns about pollution during both production and post use disposal [391,392]. Additionally, the fabrication of single crystal materials is energy intensive, which conflicts with the principles of sustainable development [393]. Recycling presents further challenges. Modified cathode materials with surface layers and dopants can complicate separation and purification, reducing the recovery efficiency and economic feasibility of conventional recycling processes [394,395]. Thermally responsive materials, due to their structural complexity, present similar difficulties. Addressing these issues requires the development of compatible recycling technologies. For example, novel chemical methods using selective solvents or reagents could remove surface layers and isolate dopants more effectively. In the case of single crystal materials, targeted physical or chemical strategies must be explored to process their robust crystal frameworks and recover valuable metals. Moreover, the energy demands and environmental impact of these recycling methods must

be carefully assessed to ensure sustainability throughout the entire battery life cycle [396,397].

7. Safe current collectors

Current collectors (CCs) are a key and indispensable component of LIBs, serving primarily to support the active materials, collect electrons generated by electrochemical reactions and transfer them to the external circuits [398,399]. Ideal CCs should have high conductivity, good chemical and electrochemical stability, high mechanical strength, good compatibility and combination with electrode actives, low cost, and light weight [400–405]. Common materials for CCs include the metal conductor materials such as copper, aluminum, nickel and stainless steel, as well as carbon and composite materials [406]. Among them, Cu CCs are often used for anodes due to their high conductivity, good ductility and good stability at low potentials, whereas Al CCs are often used for cathodes due to their light weight, low cost and high oxidation potentials.

However, these conventional CCs materials have inherent safety limitations. For example, during thermal abuse, the internal temperature of the battery can rise sharply, potentially causing the CCs to reach their melting point, which may result in short circuits and exacerbate thermal runaway. In addition, under mechanical abuse, CCs can be punctured, leading to short-circuiting and increasing the risk of safety incidents. Even in widely used commercial LIBs, the safety performance of CCs materials presents certain problems that need to be addressed.

7.1. Failure mechanism

In our previous work, we investigated the failure mechanisms of Al||Cu CCs battery during thermal runaway, as illustrated in Fig. 24 [407]. As various exothermic reactions take place within the battery, the thermal runaway process of the battery intensifies, leading to a progressive temperature rise. Once the temperature reaches the melting point of Al (659 °C), numerous cracks and pinholes form on the Al CCs. At this point, Al also causes an aluminothermic reaction with the active material (Eq. (13), in the case of NCM811), releasing a significant amount of heat and a strong flame, which further accelerates the thermal runaway process [408–411]:

$$4Al + 3MO_2\ (M = Ni/Co/Mn) \rightarrow 3M + 2Al_2O_3 \tag{13}$$

In addition, Cu CCs also gradually lose their structural integrity and mechanical strength at elevated temperatures, resulting in the formation of cracks and further deterioration of the battery. Thus, CCs play a critical role in inducing and accelerating the thermal runaway process. To enhance the safety and stability of CCs, key strategies include improving the heat dissipation performance and adding flame retardant components of CCs. Additionally, increasing the mechanical properties of CCs can mitigate the damage from the mechanical abuse, thereby improving the safety of LIBs. Numerous studies have also explored different types of safety modification methods for CCs, and we will review this in more detail.

7.2. Safe design strategies

7.2.1. Heat dissipation

Thermal runaway is a complex process, typically characterized by a rapid increase in temperature, often progressing from localized

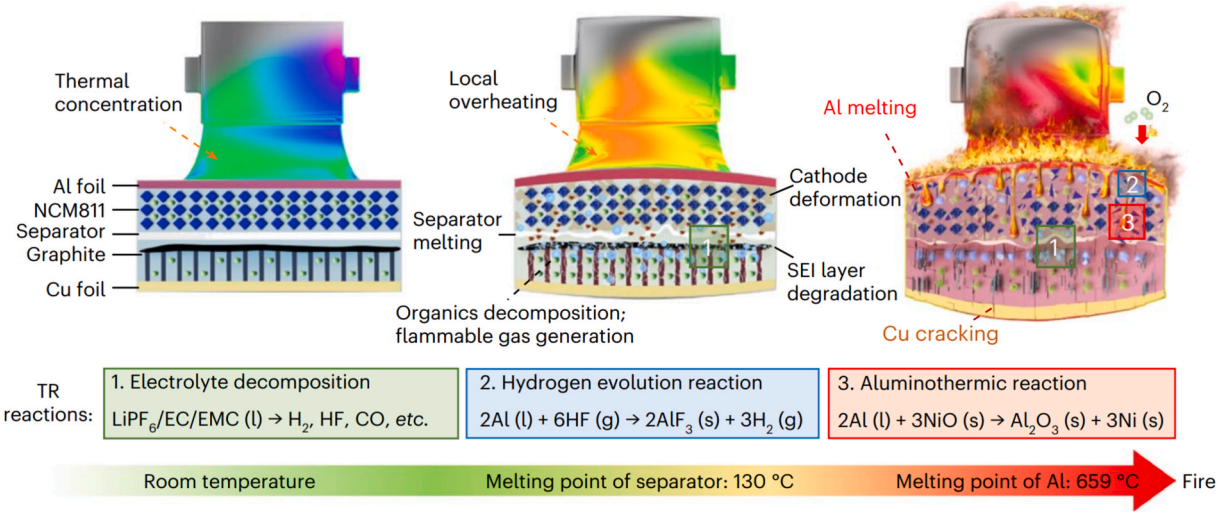

Fig. 24. Failure mechanism of Al||Cu CCs. Incendiary explosion reaction mechanism of Al||Cu battery during thermal runaway (TR) [407]. Copyright (2024) Springer Nature.

hotspots to an overall rise in temperature. Reducing localized temperature accumulation can significantly delay or even avoid thermal runaway [412–414]. As the carrier of electrode materials, CCs absorb a large amount of heat; however, the traditional Al and Cu CCs have poor thermal conductivity that can barely dissipate the accumulated heat [415]. Therefore, improving the heat dissipation performance of CCs is crucial for enhancing the safety and stability of LIBs.

Common modification strategies are structural design and material optimization of CCs. For example, in our previous work [407], we manufactured Gr foils with high heat dissipation properties using a continuous hot pressing process. This Gr foil exhibited a high thermal conductivity of 400.8 W m^{-1} K^{-1}, which is an order of magnitude higher than those of Al and Cu foils. Batteries using this Gr foil dissipate heat faster than conventional Al||Cu batteries, not only eliminating localized heat concentration, but also avoiding violent aluminothermic and hydrogen precipitation reactions (Fig. 25**a**). Moreover, compared to other NCM811 cathode-based work, this work has the lowest peak temperature when thermal runaway occurs (Fig. 25**b**). Conventional safe modification of CCs increases the proportion of non-electrochemically active materials, negatively affecting the energy density. However, the Gr CCs from this method are lighter in weight, thus improving both the energy and power density of LIBs.

7.2.2. Flame-retardant

Thermal stability of CCs can be improved by incorporating PTCs materials or adding flame retardant additives, which improve the safety performance. Of note, CCs are usually not electrochemically active, so modifications aimed at improving safety must carefully consider the potential adverse effects on key parameters such as weight and conductivity. For example, Ye et al. [416] obtained an ultralight self-extinguishing CCs by embedding triphenyl phosphate (TPP) flame retardant into a lightweight PI film, then coating two ultrathin metal layers on both sides (Fig. 25**c**). In the fire exposure test (Fig. 25**d**), conventional Cu||Al batteries are rapidly ignited and burn intensely, whereas the modified PI-TPP-Cu||PI-TPP-Al batteries exhibit weak flames and rapid self-extinguishing. In addition, these composite CCs not only can extinguish the fire quickly under thermal runaway conditions, but also has a density that is a quarter lower than conventional commercial CCs, leading to higher specific energy.

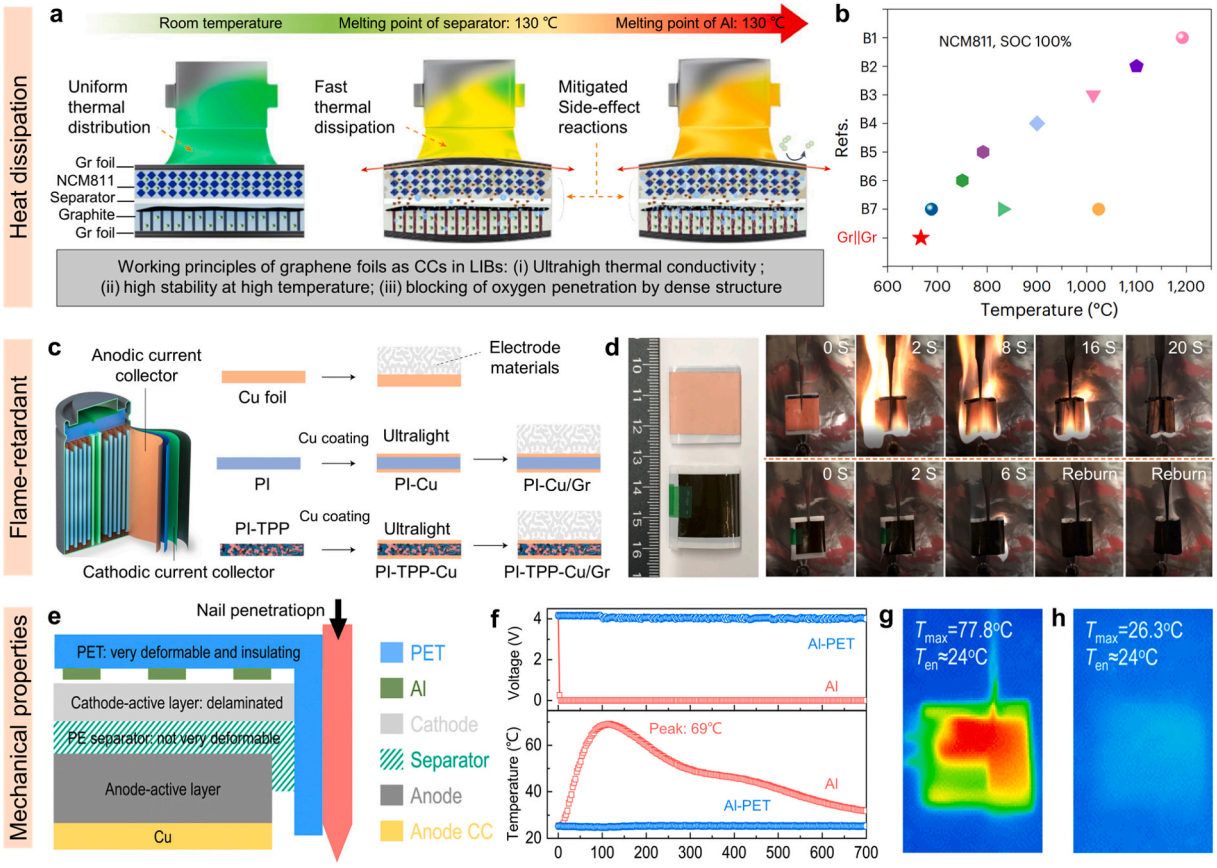

Fig. 25. Safety CCs strategy. (a) Safety enhancement mechanism of Gr||Gr batteries, (b) Comparison of peak temperature under thermal runaway between this work and other literature based on NCM811 cathode [407]. Copyright (2024) Springer Nature. (c) Conventional CCs and design ideas for this work, (d) Fire exposure test of an assembled pouch full batteries using Al||Cu (bottom) and PI-TPP-Al||PI-TPP-Cu (top), Cu||Al pouch batteries immediately ignite [416]. Copyright (2020) Springer Nature. (e) Schematic diagram of the Al-PET CCs nail penetration tests. (f) Voltage and temperature variations of Al||Al-PET pouch full batteries during the nail penetration test, (g) and (h) are the temperature distributions near the peak temperature point in (f) [417]. Copyright (2022) Royal Society of Chemistry.

7.2.3. Mechanical properties

In addition to optimising heat dissipation and adding flame retardant components, enhancing the mechanical properties of CCs can help mitigate thermal runaway resulting from mechanical abuse, thus improving the safety of LIBs [418]. For instance, Liu et al. [417] prepared Al-coated polyethylene terephthalate (Al–PET) CCs via a high-speed roll-to-roll process. These composite CCs can wrap around broken edges and block ISC caused by punctures (Fig. 25**e**). In the nail penetration test, the battery using Al-PET CCs maintained stable voltage and showed no significant temperature rise, while the conventional Al CCs battery experienced rapid short-circuit and a sharp temperature rise (Fig. 25**f**). Moreover, the background environmental temperature test revealed that the battery using Al-PET CCs exhibits a uniform temperature of up to 26.3 °C, whereas the Al CCs battery exhibits a localized temperature of up to 77.8 °C centered on the puncture point (Fig. 25**g**). In addition to improve the safety during severe mechanical penetration accidents, the CCs' low thickness and weight also increase the energy density. The combination of enhanced safety and electrochemical performance highlights an effective safety strategy for LIBs.

7.2.4. Other approaches

In addition to the previously mentioned methods, surface treatment and structural design strategies have also been explored. Through surface treatment of CCs, the stability and safety performance of batteries have been enhanced by improving their binding energy with active materials and their corrosion resistance to electrolyte. Wen et al. [419] coated the conducting polymers (poly(3,4-ethylenedioxythiophene) (PEDOT) and polyaniline (PANi)) on the surface of Cu CCs, which improved the chemical and electrochemical corrosion resistance of the CCs in lithium-ion electrolytes, and also improved the bonding strength of the CCs to the electrode materials. In addition, Cao et al. [420] formed a honeycomb-like alumina film on the surface of Al CCs by sulfuric acid and phosphoric acid treatment, which improved the adhesion between the active material and CCs and the corrosion resistance of CCs in the electrolyte. In addition, structural design of CCs can also enhance the abuse resistance of the battery. For instance, Wang et al. [421] designed a CCs with dense surface notches, which can effectively improve the safety performance of batteries under mechanical abuse. To be specific, when the battery is subjected to external impact, this notch-designed CCs can completely isolate the damaged area of the electrodes from the undamaged area, which effectively reduces the heat generated by the ISCs, and thus inhibits the process of thermal runaway.

In conclusion, the safety improvement of CCs is a multifaceted process, which needs to be based on ensuring the electrochemical performance of the battery, and achieving the best balance between electrochemical performance and safety performance through material innovation and process optimisation. With the continuous development and maturity of related technologies, it is expected that more CCs with high safety, high conductivity and light weight will be available in the future.

To enhance the safety and stability of CCs, key strategies include improving heat dissipation, incorporating flame retardants and strengthening mechanical properties. While these approaches contribute significantly to battery safety, each presents specific limitations that must be addressed. Improving heat dissipation effectively lowers the operating temperature of the battery, thereby reducing the risk of thermal runaway. However, this strategy may increase system complexity and cost. Moreover, implementing effective thermal management within the limited space of battery packs can create design and integration challenges. These limitations can be mitigated by employing advanced cooling materials such as high thermal conductivity nanocomposites, or by optimizing the geometry of cooling channels to improve heat transfer efficiency without significantly increasing battery volume or cost.

The addition of flame retardants significantly reduces fire risk but may adversely affect electrochemical performance, including reductions in capacity and cycle life. Furthermore, certain flame retardants contain halogens or other harmful substances, which can lead to environmental pollution during production and disposal [422]. To overcome these challenges, environmentally friendly flame retardants should be developed that maintain effective fire resistance without compromising electrochemical properties. Inorganic or bio-based flame retardants, for example, offer promising pathways toward improved environmental compatibility.

Enhancing the mechanical properties of CCs can reduce damage caused by mechanical abuse, thereby increasing battery safety. However, materials used to improve mechanical strength often contribute to increased weight and cost, which negatively impacts energy density and economic viability. This tradeoff can be addressed by using lightweight high strength materials such as aluminum alloys or carbon fiber composites. Additionally, refining the microstructure and processing techniques of these materials can further enhance performance without raising production costs.

From an environmental perspective, these safety strategies introduce new challenges. The use of halogen containing flame retardants poses a risk of environmental contamination, while the production of high strength materials typically requires substantial energy and resources, resulting in increased carbon emissions [423]. Green chemistry approaches can reduce these impacts by lowering energy consumption and minimizing harmful byproducts during material synthesis.

Recycling improved CCs also presents technical and economic challenges. For example, the presence of flame retardants may necessitate specialized removal processes, while recycling high strength materials often demands additional energy and resource input. To improve recycling efficiency and cost effectiveness, innovative methods such as chemical reduction and mechanical separation should be explored [424]. These processes can facilitate the removal of flame retardants and allow for more efficient material recovery. Moreover, optimizing recycling workflows by incorporating efficient separation and purification technologies can enhance metal recovery rates and reduce overall costs.

In conclusion, improving the safety of CCs requires an integrated approach that balances electrochemical performance, safety, environmental sustainability and recyclability. Material innovation and process optimization are essential to achieving this balance. Although challenges remain, continued advances in technology are expected to yield safer, more conductive and lightweight CCs. Their development and deployment must be guided by sustainability principles to ensure environmental responsibility and economic feasibility throughout the full life cycle.

8. Controlled manufacturing: Key to safe batteries

In modern industries and EVs, the safety and performance of LIBs are critical. Component failures within a battery can lead to heat accumulation and gas release, triggering thermal runaway. While the previously discussed modifications enhance the thermal stability, chemical stability, and mechanical strength of LIBs (Fig. 26), manufacturing defects—arising from production flaws or impurities in raw materials—remain a significant cause of battery failures during cycling, particularly in industrial production settings [425]. Strict control over every step of battery manufacturing, along with the effective identification and sorting of defective batteries, is essential to ensuring the safety of battery packs. Additionally, the selection and design of insulating materials play a critical role in enhancing the safety performance when assembling individual batteries into battery packs.

8.1. Manufacturing consistency

The manufacturing process of LIBs is intricate, involving multiple steps, and varies slightly among manufacturers due to differences in battery designs. However, the overall manufacturing processes remain largely consistent. Fig. 27 outlines the most commonly used processes, which can be broadly categorized into three main stages: electrode preparation, battery assembly, and electrochemical activation [426].

8.1.1. Electrode preparation

The electrode preparation process is a critical phase in LIBs manufacturing and typically includes steps such as mixing, coating, drying, solvent recovery, calendaring, slitting, and vacuum drying. These steps are fundamental for achieving consistent battery performance, as any irregularities can lead to significant variations in capacity and cycle life within the same batch [425]. For example, uneven mixing or coating can result in capacity disparities and reduced longevity, outcomes that manufacturers strive to avoid [427].

More critically, manufacturing defects such as particle agglomeration or contamination with metal foreign matter during electrode preparation can pose severe safety risks, including ISC and overheating [428,429]. Mechanical stress during slitting may also induce defects like edge burrs or warping, generating dust particles and cutting debris [430]. Yao et al. [431] investigated the burr phenomenon during electrode formation, revealing that even minor burrs can penetrate the separator, potentially causing safety issues over time. Thus, precise control of the electrode preparation process is paramount for ensuring both the electrochemical performance

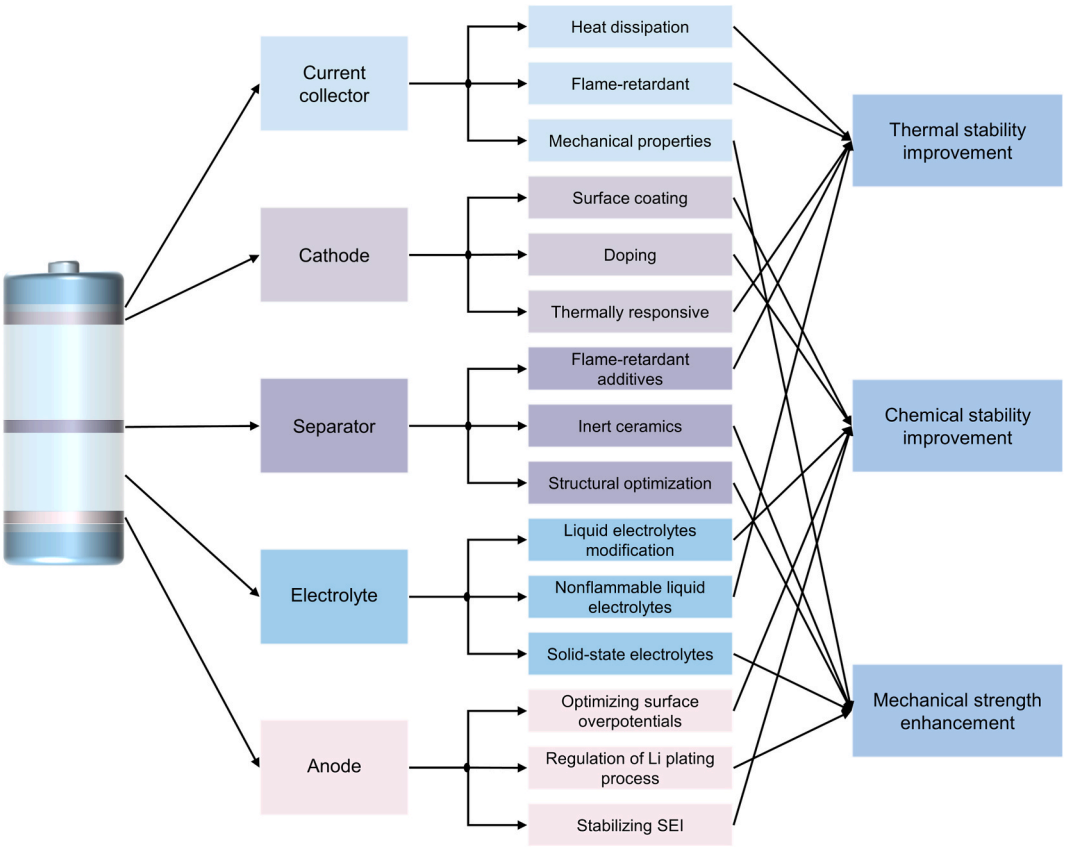

Fig. 26. Summary of modification measures for internal components of LIBs.

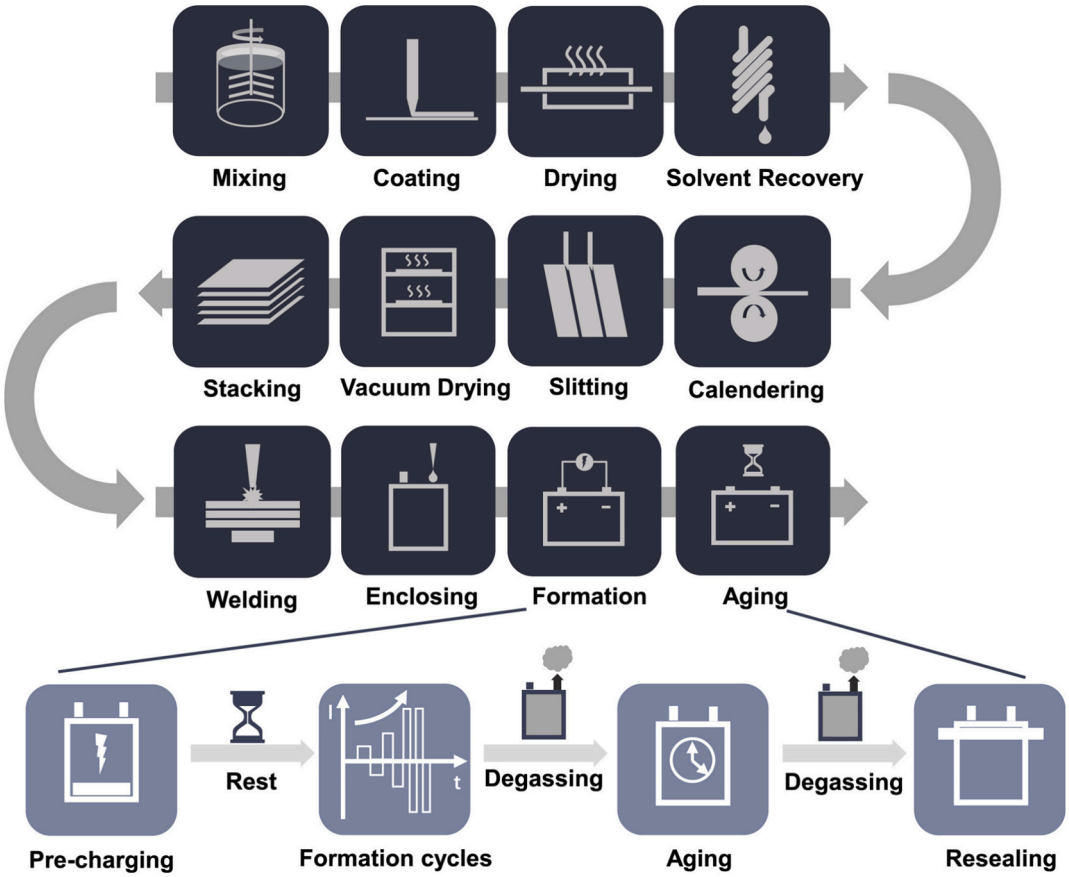

Fig. 27. Schematic of LIB manufacturing processes [426]. Copyright (2021) Elsevier.

and safety of LIBs.

8.1.2. Battery assembly

The battery assembly process primarily involves stacking, welding, and enclosing, each of which plays a critical role in determining the performance and safety of LIBs. For instance, improper handling during stacking can result in defects such as wrinkles in the separator or electrode sheets and misalignment of electrode layers [432]. These issues can compromise the uniformity and stability of the battery.

Despite advancements in welding technology, challenges remain in connecting battery tabs [433]. Misaligned tabs or incorrect welding parameters can lead to welding defects, such as tab tearing. Pan et al. [425] found that tearing of the negative tab can cause severe consequences, including significant lithium release and capacity degradation. Moreover, in LIBs used for vehicle power, high-temperature operation (up to 80 °C) exacerbates the risks. Poor tab welding quality can increase connection resistance and temperature fluctuations, leading to thermal expansion or thermal fatigue, which can damage tab connections [434,435]. Such damage not only reduces battery performance but, in severe cases, may trigger thermal runaway [436]. Therefore, meticulous control over every aspect of the battery assembly process is essential for ensuring the safety and reliability of LIBs.

8.1.3. Electrochemical activation

Before batteries are delivered to the final product manufacturer, they undergo an electrochemical activation process to ensure operational stability. This process primarily involves formation and aging, which include steps such as pre-charging, resting, formation cycles, degassing, aging, and resealing.

Graphite is the most widely used anode material for commercial LIBs due to its low intercalation potential (0–0.25 V vs. Li^+/Li), which is below the reduction potential of commercial electrolytes (approximately 1 V vs. Li^+/Li) [437]. During charge–discharge cycles, the electrolyte decomposes on the anode surface, forming a SEI layer. The formation and aging processes aim to stabilize this SEI layer; otherwise, ongoing electrolyte decomposition would deplete the electrolyte and lithium from the cathode, resulting in capacity decline. If the current or temperature during formation is too high, a dense SEI layer may fail to develop [438]. Typically, batteries are charged and discharged at low rates during formation to facilitate controlled electrolyte decomposition and SEI formation, followed by stabilization at gradually increasing rates. To ensure complete electrolyte wetting and SEI stability, batteries are

often left to rest for several days to weeks—a step that significantly impacts production efficiency and costs.While increasing current can reduce processing time, it risks forming uneven SEI layers [438] or even lithium dendrites on the graphite surface, which can lead to ISC and severe safety hazards [439,440]. Consequently, there is a need for optimized formation and aging protocols to enhance production efficiency without compromising safety or performance.

As a reference, in our previous study [441], we developed a stable CEI layer in situ through a brief external short-circuit connection. This method significantly improved the cycling reliability of the battery, offering potential insights into improving formation and aging processes for anodes.

8.2. Identification and sorting of defective batteries

Despite strict control over the battery manufacturing process, due to the inherent complexity of the process, manufacturing defects may still occur in actual production for various reasons. These defects can lead to inconsistencies in capacity, internal resistance, and other parameters among batteries of the same model [442]. When a battery pack includes these inconsistent individual cells, the differences between the cells within the pack will gradually amplify as the number of cycles increases, thereby accelerating the aging process of the entire battery pack. More seriously, the performance differences between individual cells can lead to instability in current and voltage. This instability increases the risk of thermal runaway in the battery pack and may trigger serious safety accidents such as fires or explosions [443]. Therefore, it is essential to identify these abnormal cells and perform precise sorting to ensure the consistency of the battery pack after assembly [444]. Doing so not only enhances the battery pack's service life and energy density but, more importantly, increases its safety [445].

The specific sorting process is as follows: First, the individual cells to be sorted are transported to the sorting station via a conveyor line or manual handling. Next, the cells are sorted based on one or more parameter criteria, and high-precision measurement technologies and intelligent big data equivalent models are used to improve the accuracy of the sorting. Qualified cells are then sent to the next process for assembly, while cells that do not meet the standards or exhibit abnormal performance are discarded or subjected to special treatment. In terms of battery sorting methods, they can be divided into static sorting methods (including single-factor and multi-factor methods) and dynamic sorting methods, depending on the category of the selected parameters [446,447].

8.2.1. Static sorting method

Traditionally, the static sorting method has been widely applied in the battery industry. This method primarily relies on the static parameters of the battery, which are the parameters measured when the battery is not receiving or delivering energy, i.e., at a specific point in time, rather than during operation [448]. These parameters typically include the battery's capacity, open-circuit voltage, and internal resistance, among others [449].

The static sorting method can be further divided into single-factor sorting and multi-factor sorting. Single-factor sorting refers to the selection of only one parameter as the sole criterion for sorting. Common choices include the battery's ohmic internal resistance, polarization internal resistance, charging cut-off voltage, and capacity. Multi-factor sorting, on the other hand, is based on multiple representative parameters. Similar to single-factor sorting, it usually considers two or more parameters. For example, taking into account multiple conditions such as capacity, internal resistance, voltage, and self-discharge rate can more accurately sort out battery packs with better consistency. However, this method requires high accuracy in single-parameter sorting and is time-consuming [450].

For a long period, static sorting has been the mainstream sorting method in the lithium battery industry. However, static sorting cannot reflect the parameter changes of the battery during operation. Electrochemical reactions are complex dynamic processes, and relying solely on a few static parameters makes it difficult to fully and accurately predict the future performance of the battery.

8.2.2. Dynamic sorting method

Dynamic sorting is based on data collected from individual cells during the charging and discharging process, and the parameters used are called dynamic parameters, such as charge–discharge curves, temperature, and electrochemical impedance. Compared to static sorting, dynamic sorting pays more attention to the rate of change of battery parameters over their service life. It addresses the issue that static parameter sorting does not involve the battery's energy input and output conditions, and thus better reflects the actual use of the battery. In particular, this method significantly extends the service life of battery packs, which is welcomed by battery manufacturers and is gradually replacing static sorting [449]. However, the implementation of dynamic sorting is relatively complex, usually requiring more advanced testing equipment and longer testing times [451]. For example, Du et al. [452] used the charge–discharge voltage curve as a consistency sorting parameter, establishing a similarity function based on points on the voltage curve, which resulted in good sorting effects but involved large computational loads and slower efficiency. Moreover, in actual batch operations, it is difficult to quantify the similarity of curves, and the precision errors of equipment also limit the accuracy of sorting.

8.2.3. Others

In practical applications, to improve efficiency and accuracy, techniques such as machine vision inspection, X-ray detection, and equivalent model calculations are often employed [453,454]. For instance, Christiane et al. [455] studied the internal void structure of batteries and identified material morphology using X-ray and CT scanning, thereby establishing a model for analyzing battery defect morphology. Chen et al. [456] combined visual inspection hardware with battery defect algorithms, enabling efficient and accurate identification of battery defects, thus effectively avoiding potential risks.

In actual production, manufacturers often combine two or more methods to achieve better battery consistency [457]. For example, Yun et al. [458] used clustering analysis with a self-organizing map (SOM) neural network, employing collected parameters such as

temperature and capacity to sort batteries, resulting in battery packs that exhibited excellent electrochemical performance. However, the operation of such integrated methods is more complex, and the execution time is relatively longer.

The ideal classification method should minimize operational complexity while maintaining high accuracy. To achieve this objective, several strategies can be adopted. First, more efficient data acquisition and processing techniques should be developed to reduce measurement errors and enhance processing speed. For example, the use of high precision sensors in combination with real time data processing systems can improve both data accuracy and timeliness. Second, optimizing the architecture and algorithms of neural networks can reduce computational demands and shorten execution time. This can be accomplished by simplifying network structures or employing more efficient optimization algorithms, thereby improving operational efficiency without compromising accuracy. Finally, integrating the strengths of traditional and advanced approaches can lead to a more robust classification method. Such a hybrid strategy can reduce system complexity and operational cost while maintaining performance, making it more suitable for large scale industrial applications.

8.3. Selection and design of insulating materials

Battery insulation refers to the use of insulating materials and techniques to isolate the cathode and anode of a battery, preventing unnecessary current leakage and short circuits between cells, while also protecting the electrical isolation between the battery casing and other components, ensuring the electrical safety and stable performance of the battery [459]. Specifically, battery insulation includes the following aspects: (1) Preventing short circuits. Insulating materials can effectively isolate the cathode and anode of the battery, preventing current from flowing through unintended paths, thereby preventing short circuits [460]. (2) Enhancing safety. Good insulation performance can reduce the risk of safety accidents such as overheating and fires in batteries, ensuring the safe operation of the battery system. For example, placing an insulating layer between cells and modules can prevent the failure of a single cell from spreading to other cells, thereby reducing the impact of cell failures on the entire battery system and improving system safety [461,462]. (3) Extending service life. By preventing current leakage and thermal runaway, insulation helps to improve the energy efficiency of the battery, reduce energy loss, and thus extend the service life of the battery [463].

8.3.1. Selection of insulating materials

When selecting insulating materials for batteries, manufacturers typically consider various factors such as the material's electrical insulation performance, mechanical strength, heat resistance, and chemical resistance [464]. Below are several common types of battery insulating materials: (1) Polymer materials, such as polyethylene (PE), polypropylene (PP), and polyvinyl chloride (PVC), which are often used for battery casings and internal separators. They possess good insulation properties and are cost-effective. (2) Ceramic materials, such as alumina (Al_2O_3) and silicon nitride (Si_3N_4), which have excellent electrical insulation and high-temperature resistance, making them suitable for high-power batteries and special applications. (3) Composite materials, which combine polymers with ceramic particles, metal oxides, and other materials, can further enhance insulation performance and thermal stability [465].

8.3.2. Design of insulating materials

When designing battery insulation, it is necessary to consider multiple factors comprehensively to ensure its performance and safety, which mainly include the following points: (1) Electrical safety. The insulation layer must effectively prevent current leakage and short circuits, as well as the risk of fires, under various operating conditions [460]. (2) Thermal management. A significant amount of heat is generated during battery charging and discharging; a well-designed insulation can effectively isolate this heat, preventing premature battery life reduction or safety accidents due to overheating [461,462]. (3) Mechanical strength. Batteries are subjected to vibrations and impacts during use; selecting insulating materials with high mechanical strength can reduce the risk of accidents [466]. (4) Chemical resistance. The battery working environment may come into contact with various chemical substances; the insulating material must have good corrosion resistance to ensure long-term stability [463]. (5) Environmental adaptability. With the expansion of electric vehicle application scenarios, insulating materials must be able to adapt to changes in temperature, humidity, and pressure [467].

With the continuous advancement of battery technology, insulating materials and processing methods are also constantly innovating to meet the demands for higher performance and safety. For instance, new UV-coated insulating materials, due to their excellent performance and environmental friendliness, are gradually replacing traditional PET blue films [468]. The widespread application of ultraviolet coating materials presents several potential challenges. For instance, the production of UV coatings often requires higher technical standards and specialized equipment, which may limit adoption among smaller manufacturers. Additionally, the relatively high cost of UV coating materials can increase the overall cost of battery production, particularly in large scale manufacturing contexts [469]. Furthermore, during the recycling process, the presence of UV coatings may necessitate specific chemical treatments for effective removal, thereby increasing the complexity and cost of recycling operations. Additionally, materials such as aerogels, with their superior insulation and fireproof properties, have become breakthroughs in the field of electric vehicle battery insulation [470]. Furthermore, aerogels possess relatively low mechanical strength, which necessitates additional protective measures to prevent structural damage during battery assembly and operation. From an environmental standpoint, the production of aerogels is highly energy intensive, contributing to an increased carbon footprint [471]. In addition, their complex porous structure and low density present challenges for separation and purification during recycling, potentially reducing the efficiency and economic viability of recovery processes.

In summary, the insulation treatment of batteries is a key link in ensuring their safe operation. Rational insulation design and material selection can effectively prevent short circuits between cells, thereby enhancing the safety and reliability of the battery

system. Optimizing insulating materials requires balancing performance, cost, environmental impact and recyclability. A comprehensive approach can lead to the development of safe, efficient and sustainable solutions that support the advancement of battery technology.

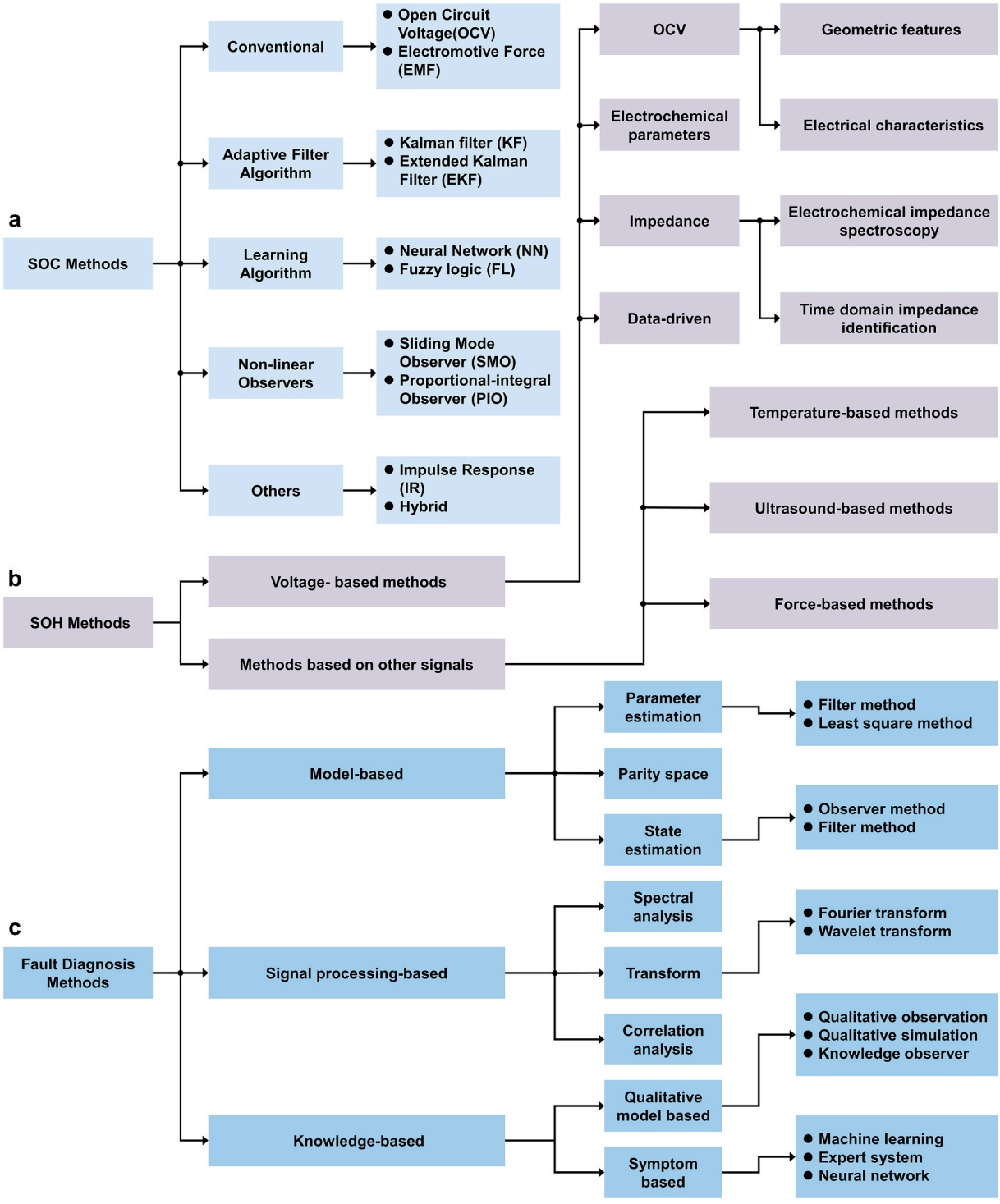

Fig. 28. Framework diagram for categorization of (a) state of charge, (b) state of health and (c) troubleshooting methods.

9. Safe management system

After ensuring strict control over the manufacturing process, safer battery packs can be achieved. However, even after assembly, battery modules cannot be deployed immediately; they must first be integrated with a Battery Management Systems (BMS). This integration is crucial because combining individual cells into a battery pack introduces more complex safety challenges. In industrial applications, the BMS plays a vital role in preventing performance degradation and safety incidents by continuously monitoring key battery parameters in real time. It enables the timely detection and management of abnormal conditions [472], significantly enhancing the safety and reliability of the battery pack.

However, BMS rely on sensitive sensors to detect changes in parameters such as current, voltage, and temperature. When the accuracy of the sensors is insufficient, the management system cannot accurately monitor, control the state of the battery and prevent abnormal operations, e.g., overheating, overcharging and over-discharging. Furthermore, an excellent BMS should not only be able to capture all abnormal signals from the batteries but also avoid overreacting to non-critical issues. Otherwise, frequent false alarms from the BMS could lead to unnecessary vehicle stops, causing inconvenience for customers. Conversely, missed alarms could result in undetected safety issues. Both scenarios are highly undesirable. Therefore, a multifaceted approach is essential to improving the accuracy and efficiency of the BMS, ensuring it reliably enhances the safety and performance of the battery.

The BMS usually consists of sensors, actuators, and microcontrollers for data acquisition, condition monitoring, battery fault diagnosis, and thermal and electrical balance management. Battery safety strategies are divided into internal passive and external active strategies. The internal passive strategies mainly involve the optimization of the internal materials of the battery, as mentioned before. External active strategies include battery condition monitoring, fault diagnosis, and thermal and electrical balance management systems [473,474]. During the operation of battery cells and packs, issues such as abuse may arise. Hence, we need to take a comprehensive approach considering aspects like battery state estimation, fault diagnostics, thermal and electrical balance management, and protective casing. By exploring future improvement directions in these areas, the BMS will not only enhance the performance and safety of batteries but also provide more reliable and efficient energy management solutions for EVs and other industrial

Table 7
Advantages and disadvantages of SOC methods.

Method	Advantages	Disadvantages	Ref
OCV	• Easy to implement• High precision	• Long rest time to reach an equilibrium condition• Only applicable when the vehicles are not moving	[481]
EMF	• Simple, low cost	• Current interruption to model OCV relaxation process need time	[482]
CC	• Easy to implement•Less power consumption	• Inaccurate results due to uncertain disturbances• Difficulties in determining the initial value of SOC	[483]
Resistance	• Simple and easy	• High accuracy only during the end of discharging• Resistance is difficult to observe within the full SOC.	[484]
EIS	• Online, low cost	• Results have an impact on aging and temperature	[485]
Model-based	• Online• High precision	• Highly depend on model accuracy• Electrochemical reactions are unclear.	[486]
KF	• Accurately estimate states affected by external disturbances	• Cannot predict nonlinear system•Require highly complex mathematical calculations	[179]
EKF	• Predict a non-linear dynamic state with good precision	• Limited robustness• Linearization error happens to nonlinear system.	[487]
UKF	• Exclude Jacobian matrix and Gaussian noise• Accurately predict non-linear system	• Suffer from poor robustness due to uncertainty in modeling and disturbances in the system	[488]
SPKF	•Without considering Jacobian matrices•High accuracy and robustness	• Complicated• Heavy calculations	[489]
PF	• Less computation time and high accuracy	• Need a complex mathematical tool	[181]
H∞ Filter	• Satisfactory performance in accuracy, computational cost and time efficiency	• Aging, hysteresis and temperature effects could deviate the accuracy of the model	[490]
RLS	• High accuracy• Eliminate noise in the measured voltage	• Heavy computation• Unstable operation with the improper forgetting value	[189]
NN	• Work in battery non-linear conditions	• Need large memory storage to store the trained data	[491]
FL	• Perform well in non-linear dynamic system• Consider charging state, aging, temperature	• Require large memory unit and complex computation.• Needs costly processing unit	[203]
SVM	• Well in non-linear, high dimension models• Predict the SOC quickly	• High complex computation• Trial and error process is needed to adjust the parameters of model	[492]
GA	• High accuracy• Robust against noisy function	• Heavy computation and delay in optimization response time• Fine tuning of parameters is required to get effective results	[493]
SMO	• High stability and robustness	• Difficult to adjust switching gain to control sliding regime	[494]
PIO	• High accuracy with less computation time• High Robustness	• Inaccurate results if the controller is not properly designed	[495]
NLO	• Improved performance in accuracy convergent speed and computation cost• Enhanced robustness against disturbances	• Difficult to find a proper gain matrix to reduce the error	[496]
BI	• Provide stability in performance• High accuracy	• Formation of 3D SOC look-up is a challenging task	[497]
IR	• Estimated value demonstrates best fit to the real value of SOC	• Inaccuracy if the width of the narrow current pulse is insufficiently smaller than the shortest time constant.	[498]
Hybrid	• The lower cost of the system, the more effective and reliable estimation results	• Combining two or three methods is a laborious task• High complex computation	[499]

applications.

9.1. Battery state estimation and fault diagnosis

The battery state estimation includes state of charge (SOC) and depth of discharge (DOD) as well as state of health (SOH). By monitoring SOC and SOH, battery life can be effectively extended. In LIBs, there are several state estimations and troubleshooting methods. The BMS utilizes the collected data to estimate the state of charge (SOC) and state of health (SOH) of the battery for the next stage. DOD is the percentage of power removed from a battery about its rated capacity. We recommend not exceeding a depth of discharge of 25 % for shallow-cycle batteries, while deep-cycle batteries can safely release up to 80 % of their charge. LIBs are typically discharged to depths between 80 % and 90 %, meaning they can deliver more power in a single use, but this also leads to faster capacity degradation and shorter cycle life. In order to maintain battery performance and life at deeper discharge depths, it is essential to coordinate the relationship between the cycle depth and capacity of the battery in the system design. With the help of appropriate algorithms, the battery capacity estimation module controls the maximum charge/discharge current. The result of this module is transmitted to the battery equalizer to limit the overcharge/over-discharge anomalies of the battery. SOC and SOH are the key metrics to reflect the performance of batteries and predict their behavior. We can derive appropriate fault diagnoses from them and provide optimal energy storage performance management. However, current state estimation methods lack explicit sensitivity assessment, and researchers have yet to characterize the development of a complete state estimation model exhaustively.

9.1.1. State of charge

The state of charge (SOC) estimation is the basis for other status monitoring in the battery management system of an electric vehicle. On the one hand, it shows how much energy is left in the battery and tells the user when it needs to be charged. On the other hand, accurate SOC estimation prevents overcharging and over-discharging of the battery, improves discharge efficiency and extends cycle life [475].

However, the complex electrochemical properties of a given battery result in a high degree of nonlinearity during use. The SOC variables of the battery cannot be directly measured and can only be estimated using externally measurable parameters such as battery terminal voltages, charging and discharging currents, and more. Moreover, the estimation process is susceptible to various factors like temperature, cycle time, discharge rate, voltage, noise, etc., making it difficult to achieve accurate real-time estimation of the battery SOC [476]. Hannan et al. [477] have researched the literature and elaborated several types of estimation methods for SOC, as shown in the Fig. 28**a**, and the advantages and disadvantages of the corresponding methods as listed in the Table 7, which synthesize that the learning algorithm performs well in modelling nonlinear dynamic systems that take into account aging, temperature, and noise. This approach is computationally complex, requires larger storage units to store the training data, and the model may produce inaccurate results if the controller is not designed correctly. Challenges faced in implementing various SOC methods and possible solutions are also discussed.

Recent advances in battery state estimation have led to significant improvements in SOC estimation algorithms through the integration of sophisticated mathematical models and optimization techniques. These developments have substantially enhanced both the accuracy and robustness of SOC determination. Notable contributions include Wang et al.'s radial basis correction-differential support vector machine (RBC-DSVM) approach [478], which combines limited memory recursive least squares for parameter identification with SVM-based error correction. This hybrid method achieves remarkable precision, with maximum errors below 0.037 % in hybrid pulse power characterization tests, effectively balancing accuracy and stability. Further innovations include square root unscented Kalman filtering with full-parameter online identification [479], offering improved numerical stability and computational efficiency-crucial advantages for real-time battery management applications. Additionally, Wang et al. [480] developed an enhanced particle swarm optimization-adaptive square root cubature Kalman filter (PSO-ASRCKF) that maintains high estimation accuracy across diverse operating conditions, including varying temperatures and initial SOC states. The enhanced accuracy and robustness of these methods make state awareness more precise, which is crucial for implementing advanced battery control strategies.

In summary, we need to build an efficient management system that enhances the robustness of the nonlinear system and predictive analytical modeling by designing appropriate controllers to improve the accuracy of SOC estimation and ensure the safety, durability and dynamics of the management systems.

9.1.2. State of health

SOH is an indicator for evaluating the aging level of batteries, the health status of batteries is usually defined from the perspective of capacity loss and impedance increase. Accurately evaluating battery SOH can remind users to replace aging batteries and help predict catastrophic failures that may lead to fires or explosions [15].

In applications such as EVs, battery packs consist of multiple cells connected in series or parallel at each module or system level. Therefore, Berecibar et al. [500] mentioned that the algorithms or methods developed should fulfil the need to cover the cell level. Similarly, cell balancing is necessary because cell imbalance can impact performance. However, even with cell balancing methods, controlling the heterogeneity of cell aging remains challenging.

According to the literature reviewed by Tian et al [474] (Fig. 28**b**), these methods can be categorized into two main types according to HIS: based on end voltage and based on other signals. Most HIS methods are extracted from end voltages, including open circuit voltage (OCV)-based methods, impedance-based methods, electrochemical parameter-based methods and data-based methods. In addition, OCV-based methods can be further categorized into geometric feature-based and electrical property-based methods. Impedance is directly calculated through the relationship between current and voltage responses, and impedance-based SOH

evaluation is of great significance in applications that focus on battery power capacity [501,502].

Therefore, to monitor battery aging more comprehensively, we should explore the mechanism from different perspectives based on the OCV method and combine it with impedance and electrochemical parameters. Meanwhile, we should also consider the effects of temperature, ultrasound and force on the battery management system and propose corresponding state health estimation methods.

9.1.3. Battery fault diagnosis

The primary functions of fault diagnosis include the detection and alarm of short circuits, thermal runaway, overcharge/over-discharge, sensor/actuator faults, etc. The system is designed to detect and alert the battery management system of any faults. The hundreds or thousands of individual cells connected in series and parallel are often used to form the system due to the limited capacity and voltage of a single cell. However, due to the inconsistencies between individual cells in capacity, voltage, and internal resistance, as well as their coupling effects with aging, BMS are often challenged with failures, which places tremendous demands on the safe and reliable operation of BMS. To ensure the safety and performance of BMS, fault diagnosis is essential. A typical fault diagnosis method is illustrated in Fig. 28**c**.

Xiong et al. [503] discussed the research progress of battery management system faults and diagnosis, and analyzed the causes and effects of sensor, actuator, internal/external short-circuit, overcharging/over-discharging, connection faults, inconsistencies, insulation faults, and thermal management system faults. Finally, the future challenges and potential research directions of battery management system fault diagnosis driven by new technologies such as big data are further discussed. Yu et al. [504] comprehensively reviewed and compared failure modes, fault data and fault diagnosis methods in different scenarios such as laboratory, electric vehicle, energy storage system and simulation. Fault diagnosis methods in laboratory scenarios are more advanced than real-world applications. However, there are still challenges in applying these methods to real-world scenarios. The researchers discuss the prospects and challenges of fault diagnosis methods between laboratory and real-world applications in terms of a unified framework for fault diagnosis methods, cloud big data fusion, and the application of laboratory measurement techniques. More significant work in advanced laboratory research is needed for more accurate fault diagnosis.

Overcharge/over-discharge faults can be detected by comparing the signal collected by the voltage sensor to the upper cutoff voltage or threshold of the battery. This method is simple and easy to use, and therefore more research needs to be done on diagnosing overcharge and over-discharge faults. However, minor overcharge/over-discharge faults may still occur in some cells in a battery management system due to the inconsistency of the battery system. If overcharge or over-discharge faults occur continuously, it will lead to rapid degradation of the system and a safety hazard.

Overall, battery fault types in energy storage systems vary, and faults occur randomly during actual operation. Current fault diagnosis studies rely on data collected by sensors to characterize the external response of the battery management system. The differences in external parameters between faults could be more precise, making accurate isolation of specific responsibilities difficult. Furthermore, setting fault thresholds involves a trade-off between the ability to detect glitches and false alarms. Battery aging also affects the accuracy of the thresholds, so the thresholds need to be adjusted to the aging stage of the battery rather than using fixed thresholds. Although adaptive thresholds can address the shortcomings of fixed thresholds, their application in battery management system fault diagnosis requires further research.

9.2. Battery thermal management systems

Battery thermal management systems (BTMs) are used to control and manage battery temperatures to improve battery thermal stability and safety [505]. BTMs protect batteries and prevent thermal runaway through a series of regulatory mechanisms that maintain the temperature of LIBs in a safe and adequate temperature range of 15–35 °C [506]. Their essential functions include battery heating and heat dissipation. Moreover, prevent thermal abuse such as overcooling, overheating, and thermal shock. BTMs have the following critical requirements for vehicle applications: adaptable, inexpensive, lightweight, reliable, small, and easy to maintain.

9.2.1. Regulatory mechanisms of BTMs

The fast self-heating rate of the thermal runaway process leads to a very high heat generated by the thermal runaway process. When the temperature reaches a certain level, it may trigger the combustion and explosion of EVs. Heat generation can be categorized into reversible and irreversible heat. Reversible heat is the structural reorganization of the electrode active material due to the insertion and detachment of lithium ions. Irreversible heat includes polarization heat and ohmic heat. Polarization heat is mainly generated due to polarization resistance, and ohmic heat is primarily due to lithium-ion diffusion and electron conduction resistance [507]. Although the heat generation of the battery can be reduced by lowering the internal resistance of the battery, the heat generated inside the battery by electrochemical reactions cannot be avoided. Therefore, thermal management systems are needed to prevent the generation, accumulation, and propagation of heat within the battery pack and to accelerate the heat dissipation of the battery pack. Thermal issues such as thermal runaway, low-temperature battery performance and battery heat generation are key factors affecting the application of LIBs.

9.2.2. Low temperature heating strategy

As described in ***section 2.2.3***, lithium plating and dendrites are easily triggered at low temperatures, which can lead to ISC in LIBs [508]. The BTM external heating methods are mainly categorized as liquid or gas heating [509,510], heating plates or tubes [511], Peltier heating [512] and so on. Although external heating strategies are easy to implement, the energy loss is high, the heating generation rate is slow, and the battery temperature increase is not uniform.

Alternating current (AC) and direct current (DC) are crucial internal heating strategies to prevent low-temperature thermal runaway. As shown in Fig. 29**a-b**, Wang et al. [513] inserted a metallic nickel foil into the cell to generate internal heating from low temperatures and provide rapid heat transfer to the electrodes and electrolyte. The self-heating function is activated by closing the switch between the activation and negative terminals. When the switch is off during battery activation for self-heating, electrons flow through the nickel foil, generating a large amount of ohmic heat and rapid warming. Dai et al. [52] analyzed the effects of current frequency, amplitude, and waveform in AC heating on the behavior of lithium plating. The results show that low-frequency high currents cause complex side reactions that trigger lithium plating on the graphite anode surface, whereas high frequencies do not trigger lithium plating; higher amplitudes are favorable for heat accumulation, and AC heating does not exacerbate the degradation of LIBs even in the lower frequency range. As shown in Fig. 29**c**, Jiang et al. [514] used a low-temperature internal heating strategy of AC + DC to determine the allowable AC and DC to avoid lithium ion deposition. They designed a simple low-loss soft-switching circuit for heating the battery pack. The heating process resulted in a uniform temperature distribution inside the battery pack, and they observed that the lifetime of the battery pack was not shortened even after conducting 600 repetitions of the heating experiment. Xiong et al. [515] used the Butler-Volmer equation based on the AC heating strategy, and the optimal ladder preheating strategy was obtained by calculating the available heating current based on the electro-thermal coupling model. The battery cell can be heated from −20.3 °C to 10.02 °C in 13.7 min with an average temperature increase rate of 2.21 °C/min. The battery pack can be heated from −20.84 °C to

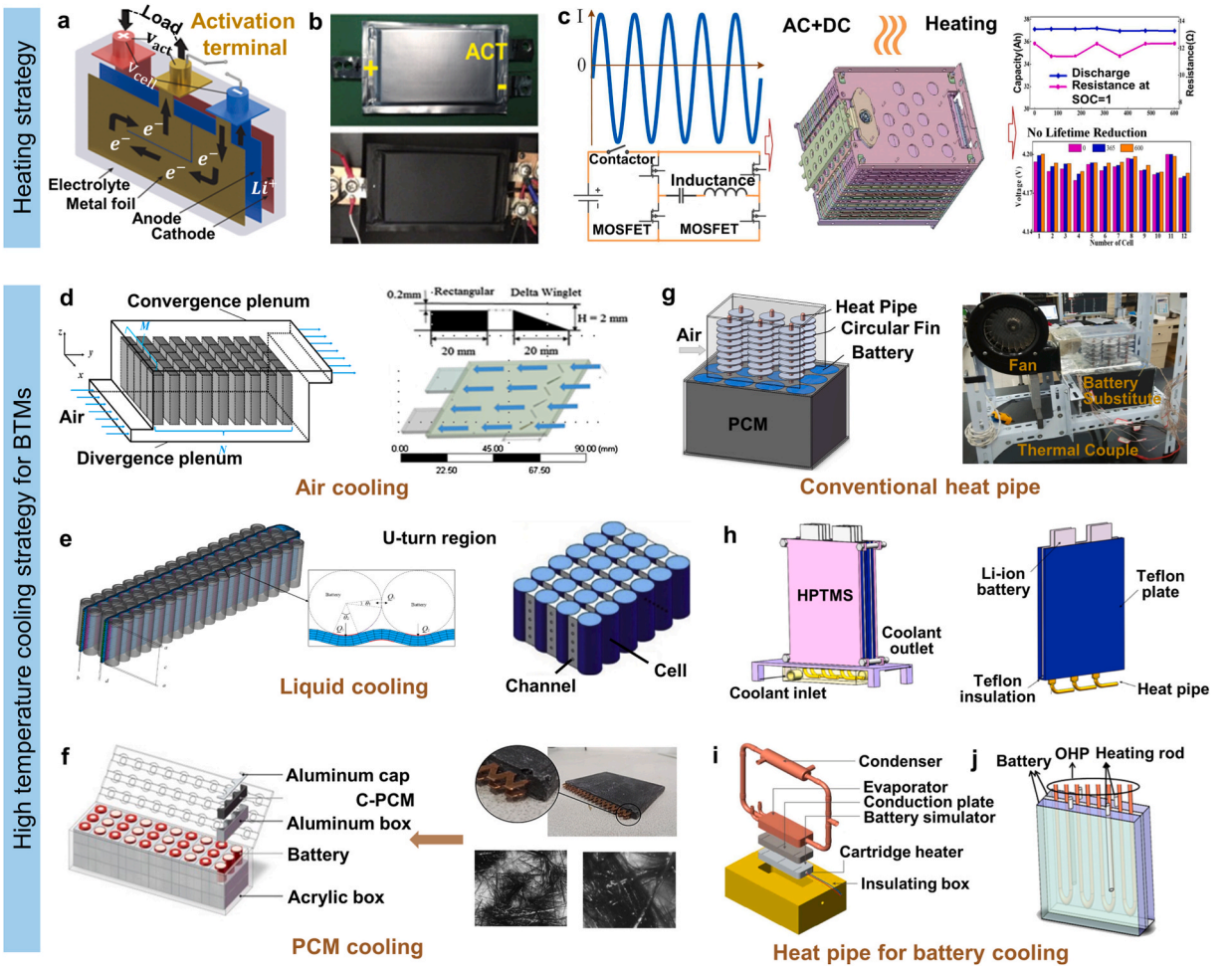

Fig. 29. Low-temperature heating strategy and high-temperature cooling strategy. (a) (b) Self-heating strategy for battery insertion of metallic nickel foil [513]. Copyright (2016) Springer Nature. (c) Low-temperature internal heating strategy for battery pack AC + DC [514]. Copyright (2018) Elsevier. (d) Schematic diagram of air-cooled battery thermal management system with parallel cavity ports [516], Copyright (2017) MDPI, vortex generator for enhanced air-cooling performance [517].Copyright (2019) Elsevier. (e) U-tube channel for enhanced liquid cooling [506], Copyright (2019) Elsevier; microchannel for aluminum cooling block with variable contact surfaces and straight and small channels [518]. Copyright (2017) Elsevier. (f) Passive battery thermal management system using PCM [519]: PCM plate [520] and carbon fiber with high thermal conductivity added to the PCM [521]. Copyright (2018) Elsevier. (g) Conventional heat pipe BTM coupled with PCM [522]. Copyright (2017) Elsevier. (h) Battery heat pipe with high thermal conductivity [198]. Copyright (2018) American Chemical Society. (i)Cyclic closed-loop-type heat pipe for battery thermal management system [523]. Copyright (2016) Elsevier. (j) OHP-based oscillating heat pipe cooling system [524]. Copyright (2016) Elsevier.

10 °C in 12.4 min with an average temperature increase rate of 2.47 °C/min. This strategy does not harm the battery health and balances the heat generation rate and lifetime degradation.

Low temperature heating strategies must consider factors such as battery type, operating conditions, energy consumption, and system complexity. A reasonable low-temperature heating strategy can improve the performance and reliability of the battery in a low-temperature environment. However, it also needs to ensure the safety and energy efficiency of the heating system. Therefore, in practical applications, comprehensive evaluation and optimized design are needed according to specific conditions.

9.2.3. High temperature cooling strategy

High temperature cooling strategies for BTMs include air cooling, liquid cooling, PCM cooling, heat pipe cooling, and hybrid cooling.

Air cooling is achieved by expanding the surface area or increasing the flow of air over the object to be cooled. Air cooling can be categorized as either natural convection or forced convection. The main advantages of air cooling over other cooling strategies are its simplicity and electrical safety [13]. However, the natural method has limitations in more demanding environmental conditions, and large thermal gradients may occur between battery blocks. Forced air systems are therefore necessary, and although they require additional power, their effectiveness in reducing maximum temperatures has been extensively studied. Forced air systems can be provided in two ways: one is air from the vehicle cockpit, and the other is air from the environment via a separate micro air conditioning unit. As shown in Fig. 29**d**, Chen [516]and Xie [517] et al. performed a series of optimization works on the system parameters of the battery pack BTMs, including the width of the arrangement inlet and outlet, airflow rate, angle of static pressure, and cell spacing. These optimization efforts significantly reduced the maximum temperature and maximum temperature difference of the battery pack. This work is important for the further development of smarter air-cooling strategies.

Liquid cooling is a method of utilizing liquids to reduce the temperature of a battery pack. Commonly used liquids include water, glycol, mineral oil, and acetone. Liquid cooling can come into direct or indirect contact with the battery pack to achieve a cooling effect [525]. Liquid cooling uses different liquids with good specific heat and thermal conductivity properties and can solve the problem of heat dissipation from battery packs under extreme conditions. As shown in Fig. 29**e**, conventional liquid cooling is achieved by flowing a working fluid through a heat-absorbing plate, or called a cooling plate, in contact with a heat source [506]. Currently, researchers are mainly focusing on optimizing the flow structure inside the cooling plate and are trying to improve the thermal conductivity of the fluid by employing nanofluids. Nanofluids are liquids containing nanoparticles (NPs) made of metals, nonmetals, or metal oxides and have higher thermal conductivity than conventional coolants. The main NPs commonly used to improve thermal conductivity are Al_2O_3, CuO, CNT, MWCNT, Ag, Cu, SiO_2, etc. Rana et al. [526] showed a 14 % increase in the heat transfer coefficient of the NPs with 3 % CuO as a nanofluid at a velocity of 0.01 m/s.

PCM cooling utilizes the heat-absorption effect released during a phase change of a substance, e.g., melting, evaporation, sublimation, to achieve the cooling of a battery pack to maintain its overall temperature uniformity. In order to improve the heat transfer performance of PCM-based BTM systems, researchers are working to improve the thermal conductivity of PCMs, which has become a hot issue in current research [527]. Many researchers have attempted to design composite porous materials or highly thermally conductive particles with PCM, as shown in Fig. 29**f**. They have used conventional PCMs as the base material and added highly thermally conductive additives to improve the overall thermal conductivity of the composite phase change material (CPCM). Researchers typically use two types of additives to achieve high thermal conductivity; one is to add highly thermally conductive carbon-based materials to the PCM, such as expanded graphite (EG), graphene, carbon fibers, multi-walled carbon nanotubes (MWCNTs); the other is to add metal-based materials to the PCM [528], such as copper foams, nickel foams, and copper mesh copper fibers. Most researchers use expanded graphite (EG) and graphene, which have stable properties, to improve the thermal conductivity of PCMs for better thermal management performance.

Heat pipe cooling is accomplished by filling a closed pipe with a volatile liquid and rapidly transferring the heat from the hot end to the cold end. The operation principle of a traditional heat pipe is shown in Fig. 29**g**, which adopts a core-closed shell structure inside. When the heat pipe is heated, the internal liquid evaporates in the evaporation section, condenses in the condensation section, and then returns to the evaporator through the core structure after condensation, through which a large amount of heat can be transferred. As an efficient heat transfer device, the heat pipe has the advantages of high thermal conductivity, flexible structure, and low cost, as shown in Fig. 29**h**. Researchers have conducted relevant studies on the thermal management of single cells, battery packs, and BMS. The single-cell heat pipe cooling method can realize core cooling, but it will lead to a decrease in battery energy density and an increase in battery weight [529]. The micro-channels can effectively stop the thermal runaway propagation between two neighboring cells in the battery pack, as shown in Fig. 29**i-j** for the circulating heat pipe and the OHP-based oscillating heat pipe, respectively. In the BTM, the wet-cooling heat pipe is considered the best cooling strategy. It can control the maximum temperature below 21.5 °C at 3C rate and the maximum temperature difference below 0.5 °C [505].

In summary, high-temperature operation of the battery pack and uneven temperatures between battery cells will accelerate battery aging and lead to thermal runaway. The built-in cooling system is an important part of the safety management system, which can accelerate the heat dissipation of the battery during high-temperature operation. Air and liquid cooling are widely used methods in commercial EVs. Compared to conventional liquid cooling systems, heat pipe-based BTMs can provide better cell/module temperature uniformity, simpler design, and a safer system. Nano-additive-enhanced liquid cooling technology is one of the hot areas of research in BTMs. However, BTMs with nanofluids are still developing due to some challenges in setup cost, application complexity, power consumption, and system pressure drop [530]. More in-depth research is needed before they can be used for commercial applications. To further investigate the thermal problems and thermal safety performance of Li-ion batteries, it is necessary to establish a battery thermal model and combine it with thermal management strategies.

9.3. Electrical management systems

Typically, the thermal behavior of a battery pack is caused by electrical behavior, so by performing electrical detection of the battery and the battery pack, it is possible to warn the battery of possible thermal problems. When a battery is overcharged or over-discharged or when an ESC occurs, electrical abuse may occur and trigger a series of undesirable electrochemical reactions. Cell balancing is part of the BMS function and is designed to maximize the performance of a battery management system consisting of cells connected in parallel and series.

9.3.1. Regulatory mechanisms of electrical abuse by BMS

Electrical abuse mainly includes overcharging (OC), over-discharging (OD), ESC, and ISC. In the previous ***section 2.3***, we introduced some factors that trigger overcharging, over-discharging, external short-circuiting, and internal short-circuiting of batteries. There are many reasons for electrical abuse, and one of the main reasons is the inconsistency of the batteries. When using a series-connected battery pack, smaller capacity monobloc batteries will reach full charge first, which leads to the risk of overcharging and gassing. On the other hand, larger monobloc batteries may be undercharged, resulting in reduced electrolyte activity and performance degradation. If the management system cannot effectively monitor the voltage of each cell, there is a risk of overcharging. Overcharging can lead to too much energy storage in the battery, which is very dangerous. The following are some equalization strategies for battery electrical management systems that we summarize and discuss.

9.3.2. Equalization strategies for battery electrical management systems

The battery equalization strategy is divided into active and passive strategies, where the voltage, capacity, or SOC of all batteries is measured and compared after each charging cycle [160]. Active equalization involves using various circuit topologies and control strategies to transfer energy between different cells and modules without dissipation, thereby equalizing the system (Fig. 30 **a**). Passive equalization strategies, on the other hand, use capacitive, inductive, and transformer-basedmethods [531]. These methods typically adjust variables during equalization, including actual voltage and battery capacity SOC. Concretely, active equalization is to monitor the voltage, SOC, and other state parameters of all the cells in the battery pack through the equalization control circuit during the battery charging process (Fig. 30**b**). By controlling the switch, resistance is applied to make the high-power cell discharge, it consumes

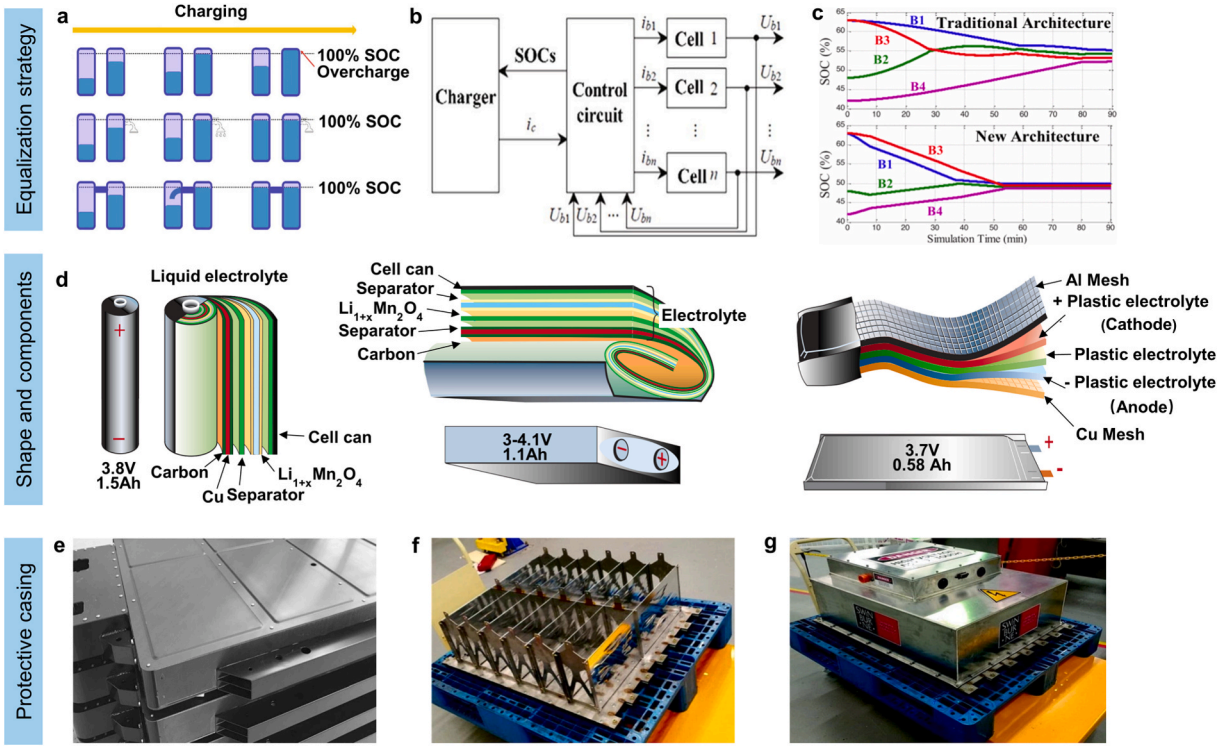

Fig. 30. Electrical management system equalization strategy. (a) Schematic diagram of passive and active equalization, (b) block diagram of equalizing charge control system [14]. Copyright (2021) Elsevier. (c) Comparison of the results of battery equalization under conventional and new architectures for four battery packs [532]. Copyright (2011) IEEE. (d) Schematic diagrams of lithium-ion battery configurations in shape and components: cylindrical cell, prismatic cell, pouch cell [533]. Copyright (2001) Springer Nature. (e) Battery casing made of CFRP [534]. Copyright (2019) Springer Nature. (f) Battery base plate and frame structure made of SS304 (g) Mountable complete battery pack [535]. Copyright (2018) Springer Nature.

energy. In contrast, the switch is disconnected for the low-power cell, which does not consume discharge energy, and finally, equalization is achieved. As charging proceeds, the voltage difference decreases and reaches a good equilibrium in the late-charging stage, thus improving the performance and cycle life of the battery pack.

Passive equalization typically reduces inconsistencies between cells by using energy-dissipating components to convert excess power in individual cells into heat for consumption (e.g., Fig. 30**c**). The primary type of passive equalization is a switching resistor, which is connected to a balancing resistor in the circuit to consume some of the energy from the cells by generating heat. Passive equalization can release the electrical energy of overcharged high-capacity cells in the battery pack but cannot replenish the energy of low-capacity cells. Active balancing is superior to passive balancing from the perspective of energy utilization and balancing efficiency. However, since the application of active equalization is currently limited by the difficulty of developing small systems that are easy to integrate, inexpensive, fast and reliable, passive equalization technology is now widely used.

Through experimental studies on the charge/discharge characteristics of single batteries and literature analysis, we found that factors such as the type of battery, manufacturing process, and production batch affect the performance consistency of batteries. Moreover, when these batteries are combined into a battery pack, the effect of inconsistency is further amplified, which increases the management difficulty of the BMS. Therefore, to assess the consistency of batteries and understand their performance, selecting appropriate cells for charge/discharge characterization is necessary.

9.4. Battery protective casing

The battery protective casing effectively protects against mechanical abuse, such as crushing, dropping, and vibration, as well as thermal abuse, such as thermal shock and fire [536]. Through a suitable protective casing, the battery can provide additional physical protection against damage and destruction by external forces. In addition, the protective enclosure effectively isolates the heat inside the battery when subjected to thermal abuse. It prevents the heat from spreading to the surrounding environment, thus reducing the risk of thermal shock and providing more time for emergency response and fire control. Ideal for protecting batteries from external loads and fire, battery protective enclosures should have several essential features, including dust and water resistance, high rigidity, corrosion resistance, high-temperature resistance, thermal management, insulation protection, and more. Therefore, designing battery protective casing with these features is urgently needed today.

9.4.1. Mechanisms of modulation of mechanical abuse

During mechanical abuse of the load, the battery monobloc undergoes four distinct phases: mechanical deformation, internal short-circuiting of the battery, thermal runaway and explosion/fire. The deformation causes internal stresses; in some cases, the increase in stresses will trigger an ISC. Battery casing must withstand mechanical forces without rupture and maintain the integrity of the internal structure under certain deformation conditions [537]. Therefore, it must be considered when designing and selecting case materials and battery combinations.

9.4.2. Optimization strategies for battery protective casing

Steel, aluminum alloy, and aluminum laminate polyethylene film are the most common battery casing materials. Of these three materials, steel has the most vital mechanical properties. However, it is more likely to cause an explosion, aluminum casing is lightweight and has good heat dissipation properties, and aluminum laminate polyethylene film is prone to fracture [538].The researchers investigated different materials such as carbon fiber sheet molding composite (CF-SMC), carbon fiber reinforced polymer (CFRP), cold sprayed aluminum, glass reinforced thermoplastic (GMT), and carbon fiber composites to fabricate the battery casing. As shown in Fig. 30**e**, the battery casing is made of carbon fiber-reinforced plastic (CFRP), which provides better performance compared to conventional aluminum and stainless-steel casings, and to some extent, improves the safety of the battery, achieves lightweight, and is cost-effective. Experimental simulations have concluded that CF-SMC is expected to replace aluminum and steel. CF-SMC material provides structural integrity, thermal management and crack protection as a battery protective shell. The weight of the battery protective case made from CF-SMC material was reduced by 46 % compared to aluminum, and CF-SMC is a potential material for preformed battery shells [539].

Overall, the battery casing maintains the integrity of the battery pack and the stability of the electrochemical environment while withstanding mechanical and thermal loads. The outer shell provides the first thermal and mechanical protection of a battery. There is a need to develop battery casing materials that surpass current options in terms of weight, cost, corrosion and fire resistance, as well as rigidity and integrity. Additionally, optimizing the arrangement and uniformity of battery cells is crucial for enhancing battery safety against mechanical and thermal abuse.

9.5. Power battery pack external other optimized design

In this section, we will introduce the factors of battery shape and structure, layout design, lightweight design, and insulation design. to maximize the performance of battery packs and optimize the cost. A reasonable battery layout design will add reliability to the battery pack. LIBs have three main shapes and structures, cylindrical cells, square cells, and soft pack batteries, as shown in Fig. 30**d**. The small size and low energy storage of cylindrical batteries and the gaps between individual cells give cylindrical battery packs better heat dissipation performance, facilitate various combinations, and are suitable for the comprehensive layout of electric vehicle space design [540,541].

When cylindrical batteries undergo thermal runaway, flames and particulate matter are typically vented in a controlled direction

through a vent valve, reducing the impact of heat and high-temperature materials on adjacent cells [542]. However, cylindrical batteries, often made of steel or aluminium, are relatively heavy, have a small volume, and exhibit low specific energy. Their wound structure also poorly accommodates high-expansion chemical systems associated with high energy density, potentially leading to reliability issues in such systems [543].

Square (prismatic) batteries, constructed with aluminium alloy, stainless steel, or similar materials, use either a winding or stacking process. Like cylindrical batteries, they feature controllable venting to mitigate heat propagation [544]. However, their larger capacities can reduce the effectiveness of heat suppression compared to cylindrical cells [545]. Additionally, their larger size and higher internal temperatures necessitate more stringent cooling system requirements.

Pouch batteries, on the other hand, use multi-layer packaging materials: an outer barrier layer (typically nylon BOPA or PET), a middle barrier layer (aluminium foil), and an inner multifunctional high-barrier layer. They are lighter and offer higher energy density compared to cylindrical and prismatic batteries in the same system [546,547]. However, their structural strength is relatively weak, requiring additional support structures when grouped, which decreases grouping efficiency. Furthermore, the complex grouping structures of pouch batteries pose significant challenges for effective thermal management design [548]. Factors such as the connection of the battery modules, heat dissipation design, and the arrangement of the battery cells are considered to ensure heat dissipation and thermal management of the battery pack.

Lightweight design and limiting battery movement is also an effective strategy. As shown in Fig. 30**f**, metal plates on the inner side of the battery pack hold each row of cells in place and prevent them from moving around. Forces such as mechanical vibration, shock energy, and ambient temperature fluctuations interact with the battery pack through various interfaces, which are controlled to ensure the safe and efficient operation of the battery pack. Also, more miniature individual battery packs increase user safety, which has advantages when prototyping and testing battery packs [535]. As shown in Fig. 30**g, a** complete battery pack is shown without fitment, considering the constraints of the battery connecting rods and the space for the depressurization vents within the battery. Using lightweight materials and structural design reduces the weight of the battery pack and increases the energy efficiency and range of the vehicle.

To target the deficiencies of the power battery pack, we propose the above strategy, which still requires the use of advanced design tools and simulation and analysis methods to carry out a comprehensive optimization of the design to ensure that the battery pack layout meets the requirements of performance, safety and reliability, and to achieve good integration with the vehicle system.

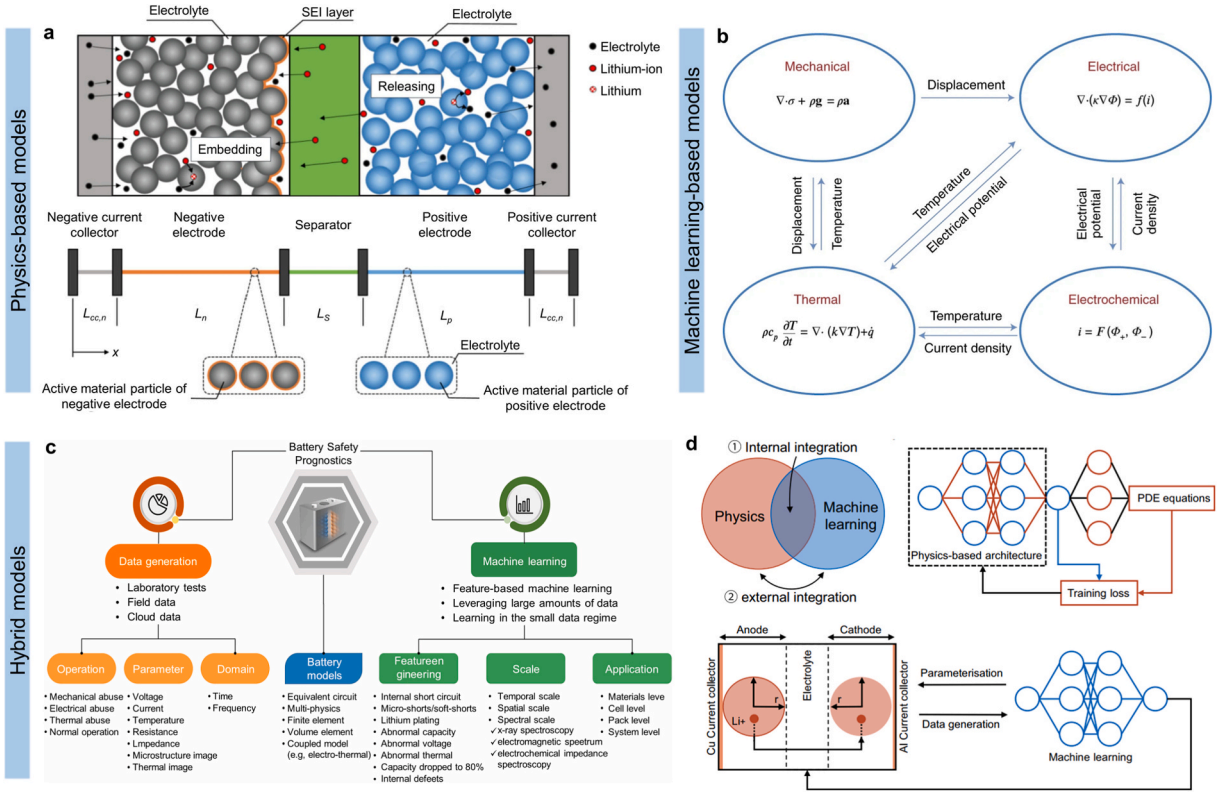

Fig. 31. An Overview of Lithium-Ion Battery Safety Modeling Methods: From Physics-Based Models to Hybrid Models. (a) Schematic of the Doyle-Fuller-Newman model [560]. Copyright (2022) Elsevier. (b) Summary of the coupling scheme in the multi-physics model [568]. Copyright (2018) Springer Nature. (c) A multi-dimensional machine learning-based framework for battery prognostics [591]. Copyright (2024) Elsevier. (d) General Integrated Framework (upper left); Representative Examples of Internal Integration (upper right); Typical Examples of External Integration (bottom) [557]. Copyright (2024) Springer Nature.

10. Safety calculation and modeling of LIBs

Since the introduction of LIBs, thermal runaway has been studied across multiple levels, from components to systems. Traditional experimental methods, such as post mortem analysis and abuse testing, have been foundational in assessing battery safety [460,549,550 551]. However, these approaches face limitations due to the complexity of internal processes, their destructive nature, high cost and limited feasibility during early development stages [552,553].

In contrast, computational modeling and its corresponding theoretical calculations, due to their advantages of being economical, safe, and rapid, have gradually become an important means in the thermal safety research of LIBs [554]. Through theoretical calculations and modeling, it is not only possible to gain a deep understanding of the physicochemical processes within the battery (such as ion transport, thermal effects, mechanical stress, and electrochemical reactions), and to predict potential safety risks, but also to provide theoretical guidance for experimental design and process improvement. This offers the opportunity to quickly evaluate a wide range of design concepts and explore different operating scenarios, thereby accelerating the progress of battery research [555,556].

This chapter will provide a detailed introduction to various methods of safety calculation and modeling for LIBs, including physics-based models, machine-learning-based models, and hybrid models, and will explore their specific roles in the study of lithium-ion battery safety performance.

10.1. Physics-based models

Physics-based models describe the internal physicochemical processes of LIBs through precise physical laws and mathematical equations. These models are commonly referred to as "white-box models" because they can provide clear physical explanations, helping researchers gain a deep understanding of the working principles and potential safety issues of batteries [557]. The transparency of these models not only aids in revealing the intrinsic mechanisms of battery performance and safety but also provides a theoretical foundation for further optimization and improvement.

10.1.1. Single-field modeling

From the 1990 s to the early 21st century, the physical safety modeling of LIBs primarily focused on single-field modeling. Research during this period mainly concentrated on a specific physical process within the battery, such as electrochemical reactions, heat transfer, or mechanical stress, with less consideration of the interactions between these physical processes. This category can be further divided into electrochemical models, heat transfer models, and mechanical stress models [558].

- **Electrochemical Models:** Early electrochemical models were primarily based on the Doyle-Fuller-Newman (DFN) model, whose geometric configuration is shown in Fig. 31**a** [559,560]. This model describes the diffusion and transport processes of lithium ions in the battery electrodes using partial differential equations (PDEs) and can accurately predict the battery's charge and discharge behavior [561]. However, the DFN model mainly focuses on the electrochemical reaction process and pays less attention to other physical processes such as thermal and mechanical effects in the battery.
- **Heat Transfer Models:** During this period, heat transfer models mainly focused on the heat generation and transfer processes within the battery [562,563]. These models typically relied on Fourier's law of heat conduction and predicted the temperature distribution inside the battery by solving the heat conduction equation [564]. However, these models often assumed that the heat sources within the battery were known and did not consider the impact of the electrochemical reaction process on the heat sources.
- **Mechanical Stress Models:** Early mechanical stress models mainly focused on the mechanical stress generated by volume changes during the battery's charge and discharge processes [565,566]. These models usually relied on the theory of elasticity and predicted the stress distribution inside the battery by solving the elasticity equations. However, these models often ignored the influence of the electrochemical reactions and thermal effects inside the battery on the mechanical stress.

10.1.2. Multi-scale and multi-physics coupled modeling

As research into the safety performance of LIBs deepened, researchers gradually realized that the physical processes within the battery are intercoupled, and single-field modeling cannot fully reflect the complex behavior of the battery. Therefore, starting from the 2010 s, multi-scale and multi-physics coupled modeling has become the main development direction for the physical safety modeling of LIBs [567,568].

- **Multi-scale Modeling:** The physical processes within LIBs have significant impacts across different scales, ranging from the microscopic scale of electrode material particles to the macroscopic scale of the entire battery [569]. Multi-scale modeling, by establishing models at different scales and coupling these models with each other, can provide a more comprehensive description of the battery's physical behavior [554]. For example, at the microscopic scale, electrochemical models at the particle level can be developed to investigate reaction processes that are difficult to observe experimentally. For instance, Li et al. [570] used density functional theory (DFT) to evaluate the Gibbs free energy changes (ΔG) of reactions between lithium metal and several metal oxides (including Co_3O_4, SnO_2, and CuO). They found that the low ΔG values imply that doping graphite with these metal oxides can significantly affect the deposition behavior of lithium on the electrode surface, thereby helping to suppress the formation of lithium dendrites. At the macroscopic scale, overall thermal and mechanical models of the battery can be developed to describe heat generation and transfer, as well as the distribution of mechanical stress within the battery. For example, Wu et al. [571] constructed a thermal abuse model for LIBs to study the impact of one-sided high-temperature conditions on the internal

temperature distribution of the battery. This research provided important insights into the heat generation and transfer characteristics of LIBs under extreme high-temperature conditions, contributing to a better understanding of their thermal behavior in such environments.

- **Multi-physics Coupled Modeling:** The physical processes within LIBs, such as electrochemical reactions, heat transfer, and mechanical stress, are intercoupled [568]. For example, electrochemical reactions generate heat, and the heat generation, in turn, affects the rate of electrochemical reactions; changes in mechanical stress can influence the structure and properties of electrode materials, thereby affecting the progress of electrochemical reactions. Multi-physics coupled modeling, by integrating these physical processes, can provide a more comprehensive description of the battery's complex behavior (Fig. 31**b**). For instance, an electro-thermal coupled model can be established to consider both the electrochemical reaction and heat transfer processes simultaneously. By solving the coupled system of partial differential equations, the model can predict the temperature distribution and the rate of electrochemical reactions within the battery. Xie et al. [572] developed an electro-thermal coupled model to predict the temperature changes and distribution within a lithium-ion battery cell during operation. The results showed that the model's mean static absolute error (MSAE) in predicting the cathode temperature could be controlled within 2.65 K, while the MSAE for predicting the anode temperature could be maintained within 0.83 K. This demonstrates the model's high precision and reliability in temperature prediction. Additionally, a thermo-mechanical coupled model can be established to consider both the heat transfer and mechanical stress processes. By solving the coupled system of equations, the model can predict the temperature and mechanical stress distributions within the battery [573]. In summary, through multi-physics coupled modeling, it is possible to more accurately predict the performance and safety risks of batteries under different operating conditions, thereby providing stronger support for the safe design and optimization of batteries.

During this period, with the rapid development of computational technology, numerical calculation methods have been widely applied in the field of multi-scale and multi-physics coupled modeling. For example, numerical calculation techniques such as the finite element method (FEM) and finite volume method (FVM) have become important tools for supporting multi-scale and multi-physics modeling due to their ability to efficiently solve complex coupled systems of partial differential equations.

However, physics-based models also have some limitations, such as high computational costs, time-consuming processes, limited modeling capabilities for complex battery systems, and the need for a large amount of experimental data to validate model parameters [553,555]. Despite these limitations, physics-based models still play an irreplaceable and important role in the study of lithium-ion battery safety performance, especially in predicting the risk of thermal runaway in batteries and optimizing battery design.

10.2. Machine-learning-based models

Machine Learning (ML) is a data-driven approach that enables computers to automatically learn patterns and regularities from data, and it has been widely applied across various technological fields [574–578]. However, its application in the battery domain has only gained significant attention in the past decade. Machine learning models are capable of rapidly and accurately predicting battery safety performance indicators, such as lifespan, internal resistance changes, and the probability of thermal runaway (Fig. 31**c**). These models possess strong data processing and generalization capabilities, allowing them to handle large volumes of complex data in a short period and provide robust support for battery safety assessment and optimization [579,580]. Unlike physics-based models, machine learning models do not rely on physical laws but instead learn the relationship between battery performance and safety status directly from experimental data through a data-driven approach. This method has significant advantages in dealing with complex, nonlinear relationships and is particularly suitable for complex systems like LIBs, which involve multi-physics coupling [581].

10.2.1. Supervised learning

Supervised learning is the most common type of machine learning, where models learn from labeled training data and then make predictions on unlabeled data. In the safety modeling of LIBs, supervised learning is used to predict the battery's state of health, remaining useful life (RUL), and potential safety risks [582–584].

Linear Regression: Linear regression models make predictions by establishing a linear relationship between input features and the target variable. In lithium-ion battery modeling, linear regression can be used to predict indicators with strong linear relationships, such as capacity fade and internal resistance changes in batteries.

Support Vector Machine (SVM): Support Vector Machine is a supervised learning model used for classification and regression. By mapping data into high-dimensional space, SVM can handle nonlinear relationships and has shown excellent performance in battery fault detection and state-of-health classification.

Deep Learning: Deep learning is a subfield of machine learning that constructs multi-layer neural networks to learn complex patterns in data. In lithium-ion battery modeling, deep learning models can process large-scale datasets and automatically extract features, which are used to predict the battery's state of health and remaining useful life.

Convolutional Neural Networks (CNNs): CNNs extract local features through convolutional and pooling layers, making them suitable for processing image data. In lithium-ion battery modeling, CNNs can be used to analyze internal scanning images of batteries to detect internal defects and structural changes.

Recurrent Neural Networks (RNNs): RNNs are capable of processing sequential data and are well-suited for handling time-series data such as battery charge–discharge curves. By learning patterns in time-series data, RNNs can predict the battery's state of health and remaining useful life.

Long Short-Term Memory (LSTM): LSTM is an improved version of RNNs that can effectively handle long-term dependencies. In

lithium-ion battery modeling, LSTM can be used to predict long-term changes in battery health, providing more accurate estimates of remaining useful life.

10.2.2. Unsupervised learning

Unsupervised learning models analyze unlabeled data to automatically discover structures and patterns within the data. In the safety modeling of LIBs, unsupervised learning is used for clustering analysis and anomaly detection of battery data [585–587].

Clustering Algorithms: Clustering algorithms divide data into different clusters to uncover the inherent structure within the data. In lithium-ion battery modeling, clustering algorithms can be used to categorize batteries into different health grades, aiding in the identification of potential safety risks.

K-Means: K-Means is a distance-based clustering algorithm that forms clusters by assigning data points to the nearest cluster center. In lithium-ion battery modeling, K-Means can be used to classify the health status of batteries.

Hierarchical Clustering: Hierarchical clustering constructs a tree-like clustering structure, progressively merging data points into larger clusters. In lithium-ion battery modeling, hierarchical clustering can be used to analyze the hierarchical relationships of battery performance and uncover potential patterns.

Principal Component Analysis (PCA): PCA is a dimensionality reduction technique that reduces data dimensions by extracting the principal components of the data. In lithium-ion battery modeling, PCA can be used to extract the main features of battery data, simplify model inputs, and improve computational efficiency.

10.2.3. Reinforcement learning

Reinforcement learning is a method where an agent learns through trial and error in an environment to obtain an optimal behavioral strategy. In the safety modeling of LIBs, reinforcement learning is used to optimize battery charging strategies and health management systems [588–590].

Q-Learning: Q-Learning is a value-based reinforcement learning algorithm that selects optimal actions by learning the value of state-action pairs. In lithium-ion battery modeling, Q-Learning can be used to optimize battery charging strategies by finding the optimal charging path through trial-and-error learning.

Deep Reinforcement Learning: Deep reinforcement learning combines the strengths of deep learning and reinforcement learning, using deep neural networks to approximate value functions or policy functions. In lithium-ion battery modeling, deep reinforcement learning can be used to optimize battery charging strategies and health management systems by learning optimal policies through interactions between the agent and the environment.

Deep Q-Network (DQN): DQN is a deep reinforcement learning algorithm that approximates the Q-value function using a deep neural network. In lithium-ion battery modeling, DQN can be used to optimize battery charging strategies by learning the optimal charging path to enhance battery lifespan and safety.

However, machine learning models, operating as black-box models, typically lack physically meaningful information and have relatively weak interpretability. They also have high requirements for data quality and quantity. Moreover, machine learning models usually lack physical constraints, which may lead to prediction results that exceed the practically feasible range in some cases [581]. Therefore, in practical applications, it is necessary to combine the strengths of physical models and machine learning models to achieve more accurate predictions and a deeper understanding.

10.3. Hybrid models

To overcome the limitations of single-model approaches, hybrid models have emerged. Hybrid models combine the strengths of physics-based models and machine learning-based models, leveraging the interpretability and precision of physical models while utilizing the data-driven and generalization capabilities of machine learning models. For example, in predicting battery thermal runaway, a hybrid approach can integrate a physics-based thermodynamic model with a machine learning model. The physics-based model provides initial thermodynamic parameters and fundamental heat transfer processes, while the machine learning model fits and optimizes experimental data to more accurately predict the risk of thermal runaway under various operating conditions. Additionally, hybrid models can use machine learning algorithms to optimize the parameters of physical models, thereby enhancing the prediction accuracy of the physical models. Hybrid models hold broad application prospects in the study of lithium-ion battery safety performance, offering more comprehensive and reliable solutions for battery safety design, assessment, and optimization [592–594].

10.3.1. The integration methods of hybrid models

The integration of physics and machine learning is divided into two distinct categories: internal integration and external integration, as shown in Fig. 31**d** [557].

Internal Integration: Internal integration refers to embedding the structure and constraints of physical models directly into machine learning models. This approach incorporates physical laws into the architecture and loss function of machine learning models, enabling the models to satisfy physical principles while learning from data. Physics-Informed Neural Networks (PINNs) are a prime example of internal integration [595]. PINNs embed physical equations (such as electrochemical equations and heat conduction equations) into the loss function of neural networks, ensuring that the network not only learns from the data but also adheres to physical laws during training. When applied to the electrochemical and thermodynamic modeling of batteries, PINNs can more accurately predict battery charge–discharge behavior and temperature distribution [596–598]. In addition to PINNs, common internal integration methods also include physics-constrained deep learning models. By introducing physical constraints into deep learning

models—such as through regularization terms or custom loss functions—the model's output is ensured to comply with physical principles. This can be used for predicting the state of health and estimating the remaining useful life of batteries, thereby enhancing the reliability and interpretability of the model [599].

External Integration: External integration refers to combining physical models and machine learning models as independent modules through data interaction and result fusion [600–602]. This method is typically implemented in the following ways: First, data generation and augmentation, using physical models to generate synthetic data for training machine learning models to reduce the reliance on experimental data and enhance the model's generalization capability, which is applied to battery health status diagnosis and fault prediction, especially in data-scarce situations. Second, parameterization and calibration, using machine learning models to optimize and calibrate the parameters of physical models to improve the prediction accuracy of the physical models, which is applied to the estimation of electrochemical parameters and the calibration of thermodynamic parameters in batteries to enhance the accuracy and reliability of the models. Finally, result fusion, combining the prediction results from physical models and machine learning models through methods such as weighted averaging or voting mechanisms to improve the precision and reliability of the final prediction results, which is applied to the comprehensive safety assessment and health management of batteries to provide more comprehensive decision support.

10.3.2. Applications of hybrid models

The application of hybrid models in the safety modeling of LIBs primarily involves integrating physical mechanisms with data-driven approaches to balance model accuracy and computational efficiency. Typical applications include:

Material Failure Mechanism Research. In the study of material failure mechanisms, the application of hybrid models is crucial for enhancing the safety and lifespan of LIBs. By combining physical and machine learning models, a deeper understanding of material failure processes during use can be achieved. The physical model provides theoretical analysis of the material failure process, while the machine learning model learns the influencing factors and patterns of material failure from experimental data. This approach can be used to investigate the failure mechanisms of new materials over long-term use, such as capacity fade, structural degradation, and interfacial stability, thereby providing theoretical support for material optimization and improvement. For example, Bansal et al. [603] developed a physics-informed machine learning technique to study the capacity degradation of silicon anodes in LIBs. They established a three-dimensional finite element (FE) model to analyze cracking and delamination caused by volumetric stress, as well as capacity loss due to SEI layer growth. The outputs of these models were used to train a Gaussian process regression (GPR) surrogate model, which can quickly and accurately predict battery capacity degradation, aiding in the design of LIBs that meet high energy storage, fast charging, or optimal lifespan requirements.

Safety Material Screening. Hybrid models can be used to predict the performance of new LIB materials, thereby accelerating the material screening process. By integrating physical and machine learning models, a more comprehensive consideration of the physicochemical properties of materials and their impact on LIB performance can be achieved. Specifically, the physical model describes the basic physicochemical properties of the material, while the machine learning model learns the complex relationship between material performance and these properties from a large amount of experimental data. This approach can be used to predict the electrochemical performance of new electrode and electrolyte materials, such as capacity, rate capability, and cycle stability, helping researchers quickly identify promising materials and reduce the number of experiments and costs. For example, Shen et al. [604] used machine learning and first-principles calculations to screen over 20,000 lithium-containing compounds, ultimately identifying 21 ideal materials for solid electrodes in just a few minutes, significantly improving screening efficiency (a million-fold increase in speed).

Battery Health State Diagnosis. The application of hybrid models in battery health state diagnosis primarily focuses on improving the accuracy and reliability of diagnosis by integrating physical and machine learning models. Specific methods include generating synthetic data using physical models and combining it with experimental data to train machine learning models, thereby enhancing the model's ability to recognize different health states. This is particularly important for early fault detection and health state classification in batteries. For example, Weddle et al. [605] innovatively developed the P2D model to generate synthetic data suitable for machine learning and validated the reliability of this method using experimental data. Additionally, incorporating physical constraints into deep learning models can ensure that model outputs comply with the physical characteristics of batteries, thereby improving the interpretability and reliability of health state prediction and fault diagnosis. For instance, Cao et al. [599] developed a deep learning-based online fault diagnosis network for LIBs under unpredictable conditions. The network, which incorporates battery model constraints and uses a framework for managing the evolution of stochastic systems, enables real-time fault diagnosis. Evaluated with 18.2 million data points from 515 vehicles, the results showed that the algorithm increased the true positive rate by more than 46.5 % at a false positive rate of 0 to 0.2, outperforming other methods. Moreover, the algorithm's adjustable output threshold can meet different requirements such as early warning and high recall rate.

Battery Remaining Useful Life Prediction. In the prediction of battery remaining useful life (RUL), the application of hybrid models also centers on enhancing the accuracy and generalization ability of predictions. Physics-Informed Neural Networks (PINNs) embed physical equations into the loss function of neural networks, ensuring that the network adheres to physical laws during training, thereby more accurately predicting the battery's life degradation process. At the same time, optimizing and calibrating the parameters of physical models using machine learning models can also improve the prediction accuracy of physical models, providing more accurate results for RUL prediction. Najera-Flores et al. [606] proposed a Bayesian physics-constrained neural network for RUL prediction, addressing the limitations of existing methods. This method learns the neural differential operator from the first 100 cycles of data, with the operator modeled by a Bayesian neural network architecture that separates fixed historical dependence from time dependence to quantify epistemic uncertainty. Experimental results showed that this physics-constrained neural network provides more accurate RUL estimates compared to other methods under the same training data and is capable of making predictions in the

early stages of battery life.

Battery Safety Risk Assessment. In battery safety risk assessment, the application of hybrid models focuses on improving the identification and prediction capabilities for potential safety risks such as thermal runaway, short circuits, and leakage. By fusing the prediction results from physical models and machine learning models, the precision and reliability of the final prediction results can be enhanced, which is particularly critical in thermal runaway risk assessment and safety early warning for batteries. Additionally, generating synthetic data using physical models and combining it with experimental data to train machine learning models can also improve the model's ability to identify different safety risks, thereby more accurately recognizing potential safety risks. Pang et al. [595] proposed a machine learning-based heat generation rate estimation method that incorporates additional features based on physical models, effectively estimating the heat generation rate of batteries under various driving conditions and significantly improving estimation accuracy.

In summary, hybrid models, by integrating the dual strengths of physical mechanisms and data-driven approaches, have demonstrated unique value in the safety modeling of LIBs: they not only significantly enhance the prediction accuracy and generalization ability of models across different operating conditions but also strengthen engineering applicability through interpretable physical frameworks. This modeling paradigm not only optimizes the real-time decision-making capabilities of BMS but also provides an efficient tool for the safety assessment of new electrode materials.

However, the widespread application of hybrid models still faces several key challenges: their development requires a vast amount of high-quality data, including precise physical parameters (such as the intrinsic properties of electrode materials) and extensive operating condition data (such as temperature field distributions at different charge–discharge rates), which poses extremely high demands on experimental design and data acquisition. At the same time, model construction involves complex multi-physics coupling calculations and deep learning algorithm optimization, necessitating high-performance computing equipment and interdisciplinary expertise, leading to high research and development costs. More importantly, although hybrid models perform excellently under normal operating conditions, their prediction reliability under extreme conditions (such as ultra-low temperatures or the critical state of thermal runaway) still needs to be confirmed through a more rigorous validation system.

To break through these limitations, future research should focus on building standardized battery big data platforms to integrate multi-source heterogeneous data from different laboratories and enterprises, establishing databases that cover the entire life cycle and full range of operating conditions. At the same time, adaptive modeling frameworks should be developed to achieve rapid model optimization under small sample conditions through transfer learning techniques. In terms of technological approaches, interdisciplinary innovation teams comprising electrochemical experts, computational scientists, and engineers are needed to jointly tackle the interface issues in multi-scale modeling.

With the development of emerging technologies such as edge computing and quantum computing, the real-time performance and accuracy of hybrid models are expected to achieve breakthrough improvements. At that time, they will be able to more accurately predict battery safety boundaries, provide stronger decision support for intelligent BMS systems, and ultimately drive lithium-ion battery technology towards safer and more efficient directions.

11. Conclusion and Outlook

With the continuous transformation of the energy structure, the significance of batteries in the energy storage sector is increasing. However, the practical application of LIBs is hindered by certain safety risks due to their poor thermal stability under abusive conditions. Furthermore, as the energy density of LIBs rises, the severity of thermal runaway issues becomes more pronounced. To facilitate the commercialization of LIBs, it is essential to conduct in-depth research on their safety performance to enhance their thermal stability.

This review first investigates the causes of thermal runaway in LIBs from macroscopic thermal, chemical, and mechanical perspectives, including factors such as thermal, electrical, and mechanical abuse, as well as the limited regulatory capability of external BMS. The failure mechanisms of key internal components—cathode, anode, electrolyte, separator, and current collector—under these abusive conditions are then analysed at the micro level. Additionally, we also summarized the mechanisms by which the external BMS regulates the battery in such conditions from a battery external perspective. Moreover, we explore system-level solutions including manufacturing process optimization and advanced safety engineering approaches. Afterward, we further evaluate computational modeling techniques for safety prediction, examining the applicability and limitations of physics-based, machine learning, and hybrid models while suggesting methodological improvements. Finally, we consider the broader implications of these safety strategies, particularly their effects on environmental sustainability and battery recyclability. Based on these insights, corresponding solution measures are reviewed.

While these measures have improved LIB safety performance to some extent, the frequent incidents of LIB explosions and combustion in recent years indicate that further research is required to address these safety concerns effectively. Based on this, we propose following recommendations:

- The safety issues of traditional graphite anodes primarily stem from lithium dendrite growth and the decomposition of the SEI. Improvements can be achieved by modifying overpotential, promoting uniform lithium plating, and stabilizing the SEI. However, these methods may introduce new challenges, such as affecting lithium-ion diffusion rate or altering overpotential for lithium deposition. Therefore, safety modifications to graphite anodes should be pursued with careful consideration of cost, process complexity, and overall battery performance. A multi-scale collaborative strategy is key to addressing this challenge. By tuning

material properties and interfaces across atomic, mesoscopic and macroscopic levels, it balances lithium deposition, interfacial stability and ion transport, offering a path toward safer, high performance anode materials.

- Safety issues vary significantly with electrolyte type. For liquid electrolytes, risks originate from the flammability of organic solvents and lithium salts. Adding flame-retardant or overcharge protection additives, or using non-flammable alternatives like ionic liquids, deep eutectic solvents, aqueous electrolytes, or low molecular weight hydrofluoroethers, can enhance safety. For solid electrolytes, challenges include flammability, poor electrochemical and chemical stability, and susceptibility to dendrite formation. Solutions include incorporating flame-retardant additives, forming stable CEI layers, using mechanical rigidity enhancers, and employing advanced processing techniques like high-energy cold pressing. For any electrolyte system, it is essential to establish a multi-parameter evaluation framework to balance flame retardancy, electrochemical stability, mechanical strength and cost. Integrating artificial intelligence can further accelerate material screening and formulation design. Future efforts should focus on developing intelligent electrolytes with self-healing functions that adapt to internal battery conditions, enabling dynamic control of both safety and performance.
- Conventional separators often suffer from poor thermal stability and mechanical strength, with high-temperature melting leading to short circuits and thermal runaway. Safety improvements include integrating flame-retardant and inorganic materials or replacing polyolefin separators with non-flammable alternatives such as glass fibers or polyimide. Additionally, high-strength materials can inhibit lithium dendrite growth. It is essential that any improvement strategy systematically considers key performance indicators such as ionic conductivity, electrolyte wettability and chemical stability, to avoid compromising fundamental battery functions in pursuit of safety. A promising direction involves the development of intelligent separators with temperature responsive behavior. For example, incorporating phase change materials into the separator can enable automatic pore closure and ion transport shutdown when the temperature exceeds a critical threshold. This form of active protection offers clear advantages over conventional passive methods. Future advancements in separator technology will depend on the design of novel composite materials and the refinement of precision manufacturing techniques, enabling the coordinated enhancement of safety and electrochemical performance through multi scale structural engineering.
- The safety of cathode materials is often linked to structural phase changes and side reactions with the electrolyte during overcharging or overheating. Strategies to address these issues include surface coating, elemental doping, and the preparation of single-crystal materials. Additionally, incorporating PTC materials can act as thermal switches to prevent thermal runaway. While these technologies have significantly enhanced battery safety, each presents inherent limitations. Surface coatings effectively prevent direct contact between cathode materials and the electrolyte but can increase internal resistance. Elemental doping improves thermal and structural stability, yet different dopants exhibit varied effects, and excessive doping may introduce crystal defects. Single crystal materials address grain boundary weaknesses in polycrystalline cathodes, but require strict control of sintering conditions and prolonged annealing, leading to higher production costs and challenges in grain size control. More importantly, complex interactions exist among these strategies. For instance, thick coatings may hinder the benefits of doping, while the low surface area of single crystal materials can compromise coating uniformity. Therefore, a multi scale collaborative optimization approach is necessary. By developing a parametric design framework that integrates doping, coating and morphology, it is possible to minimize electrochemical performance losses while maintaining safety standards. Future research should focus on intelligent adaptive coatings and machine learning based systems for efficient dopant selection, aiming to achieve a more precise balance between safety and overall battery performance.
- Safety concerns for CCs typically involve high-temperature melting, rupture, or failure under mechanical stress. Enhancements such as improved heat dissipation, flame retardancy, ductility, and surface treatments for better bonding and corrosion resistance can address these issues. These measures should avoid increasing internal resistance or reducing energy density. It is particularly important to emphasize that all improvement measures must be implemented with strict control of process parameters to avoid significant increases in current collector thickness or surface roughness, which could adversely affect energy density and power performance. Future advances in current collector technology will likely focus on the integrated design of multifunctional systems, combining material innovation with precision manufacturing to achieve coordinated improvements in both safety and electrochemical performance.
- Safety issues in battery manufacturing often stem from defects and impurities in raw materials, which can lead to battery failures during cycling. Enhancing safety requires strict control of every step in the manufacturing process, along with effective identification and classification of defective batteries. Additionally, the careful selection and design of insulating materials are essential to prevent current leakage and heat accumulation, thereby improving the safety performance of battery packs. Future advancements in battery manufacturing should focus on achieving an optimal balance between safety, precision, and production efficiency. This includes the development of advanced instruments and technologies capable of detecting internal battery characteristics with greater accuracy. Moreover, integrating manufacturing processes with emerging technologies such as big data and machine learning can significantly enhance the precision and efficiency of production, paving the way for safer and more reliable battery systems.
- The safety challenges of BMS stem from the increasing precision required to monitor current, voltage, and temperature parameters. Insufficient monitoring precision can result in ineffective prevention of thermal runaway, overcharging, or overdischarging. Advanced solutions include integrating high-precision sensors, fault diagnosis algorithms, thermal management systems, over-temperature protection devices, and strict charging/discharging controls. Future BMS designs should feature higher integration, adaptive technologies, and intelligent monitoring to enhance fault detection and prevention. For example, developing low-cost, high-precision sensors, optimizing fault diagnosis algorithms, improving the design of thermal management systems, and adopting comprehensive improvement strategies can overcome these key issues, thereby achieving a comprehensive enhancement of the

safety and performance of BMS. Additionally, the design of battery protective casings should improve resistance to thermal runaway, explosions, and mechanical shocks while ensuring consistency across cells.

- Modeling and theoretical calculations are essential tools in LIB safety research. They help reveal interfacial reaction mechanisms, predict risks such as thermal runaway, and guide experimental and manufacturing optimization. Each modeling approach has distinct strengths and limitations. Physics based models offer strong interpretability but are computationally intensive and difficult to scale. Machine learning models can uncover complex patterns from large datasets but often lack transparency. Hybrid models that combine both approaches improve prediction accuracy and interpretability, but face challenges related to model complexity, data quality, computational demand and limited adaptability to production environments. To address these barriers, four strategies are recommended: simplify model architecture using techniques like attention mechanisms; apply advanced optimization algorithms to speed up parameter calibration; establish a national battery database with real world data supported by edge computing; and build joint validation centers with industry partners to enhance model robustness in practical settings. Together, these efforts will strengthen the role of modeling in battery safety prediction and accelerate its real-world application.
- Developing real-time in-situ characterization and monitoring technologies is critical for understanding the physical and chemical changes inside batteries during thermal runaway processes. These technologies enable early detection of potential issues and guide the design, material selection, and process optimization, ultimately enhancing LIB safety.
- Optimizing battery safety must be accompanied by a full life cycle assessment of environmental impact and recyclability. While current safety enhancement technologies have improved battery reliability, they also introduce new environmental challenges. Some flame retardants and stabilizers contain halogenated compounds or heavy metals that can cause long-term pollution if not properly treated. In addition, the presence of complex organic electrolytes and added safety materials complicates recycling. Functional coatings hinder metal recovery, reducing the extraction efficiency of valuable elements like cobalt and nickel. Built-in safety components such as positive temperature coefficient elements also raise disassembly energy consumption, increasing overall recycling costs. To address these issues, a full-chain strategy encompassing green design, clean production and intelligent recycling is essential. Promising solutions include bio-based non-toxic flame retardants, supercritical fluid methods for selective electrode coating removal, and modular battery structures that enable automated disassembly. Realizing this vision requires close collaboration across the supply chain (linking material developers, battery manufacturers and recyclers) under a unified standard system and shared technology platform. This integrated approach will enable the simultaneous advancement of both safety and environmental performance in battery technologies.

In conclusion, the safety performance of LIBs is a complex, multidisciplinary challenge encompassing thermology, chemistry, and mechanics. Achieving safe battery operation requires a comprehensive approach that includes a deep understanding of battery malfunctions, failure mechanisms, and thermal runaway processes, coupled with risk mitigation strategies such as material innovation, battery structure optimization, strict battery manufacturing, and advancements in BMS. Enhancing the safety of LIBs also demands a balanced effort across theoretical research, material development, and advanced characterization techniques. While prioritizing safety improvements, it is essential to evaluate their impact on overall battery performance, stability, compatibility, and cost, striving to achieve a balance between safety and electrochemical performance (Fig. 32). Looking ahead, continuous advancements in LIB safety will significantly enhance their commercial viability, providing a reliable and secure energy storage solution to support the sustainable

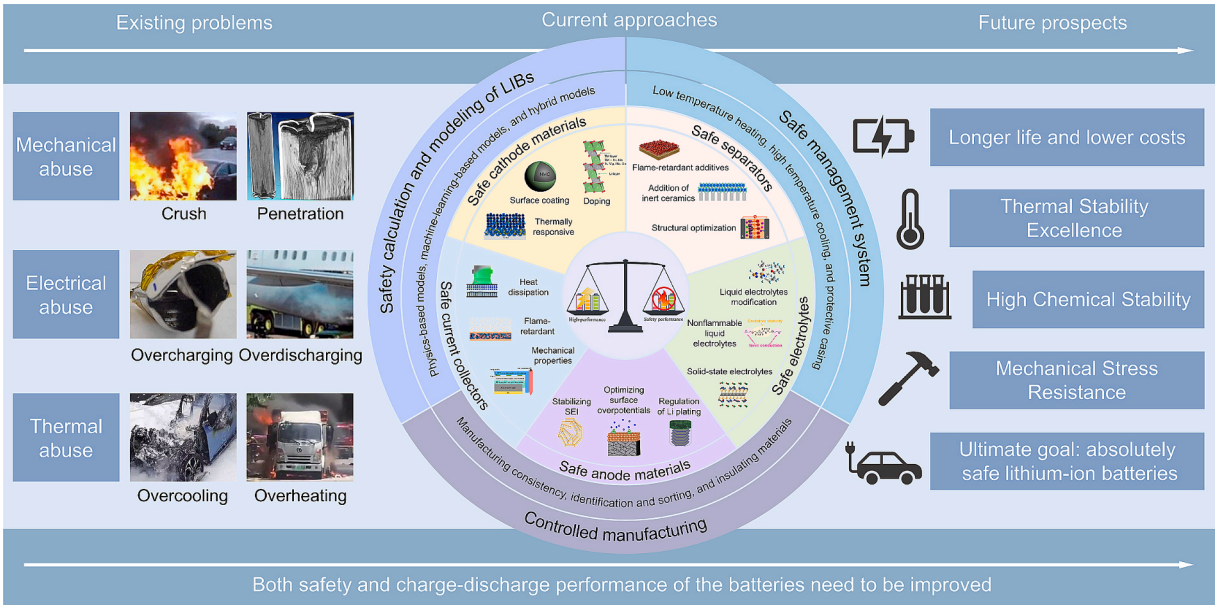

Fig. 32. Development strategies for safe and high-performance LIBs.

energy transition and the development of an electrified society.

CRediT authorship contribution statement

Guanjun Chen: Writing – original draft. **Rui Tan:** Writing – review & editing, Writing – original draft. **Chunlin Zeng:** Writing – original draft. **Yan Li:** Writing – original draft. **Zexin Zou:** Data curation. **Hansen Wang:** Writing – review & editing. **Chuying Ouyang:** Writing – review & editing. **Jiayu Wan:** Writing – review & editing. **Jinlong Yang:** Writing – review & editing.

Declaration of competing interest

The authors declare that they have no known competing financial interests or personal relationships that could have appeared to influence the work reported in this paper.

Acknowledgements

This work was financially supported by the National Key Research and Development Program of China (2023YFB3809300), National Natural Science Foundation of China (52172217), Guangdong Basic and Applied Basic Research Foundation (2024B1515020031), Shenzhen Science and Technology Program (20231122113443001 and ZDSYS20220527171401003), and Guangdong Testing Institute of Product Quality Supervision internal project (2023GQI09). R.T. acknowledges the support from Royal Society Chemistry (RSC), RSC Researcher Collaboration Grant (C23-8220221815) and Royce Industrial Collaboration Grant (RICP-R4-100029).

Data availability

Data will be made available on request.

References

[1] Bildirici ME, Gökmenoğlu SM. Environmental pollution, hydropower energy consumption and economic growth: Evidence from G7 countries. Renew Sust Energ Rev 2017;75:68–85.
[2] Dusastre V, Martiradonna L. Materials for sustainable energy. Nat Mater 2016;16:15.
[3] Chu S, Cui Y, Liu N. The path towards sustainable energy. Nat Mater 2016;16:16–22.
[4] Grey CP, Tarascon JM. Sustainability and in situ monitoring in battery development. Nat Mater 2016;16:45–56.
[5] Armand M, Tarascon JM. Building better batteries. Nature 2008;451:652–7.
[6] Cheng F, Liang J, Tao Z, Chen J. Functional materials for rechargeable batteries. Adv Mater 2011;23:1695–715.
[7] Goodenough JB. Evolution of strategies for modern rechargeable batteries. Acc Chem Res 2013;46:1053–61.
[8] Melot BC, Tarascon JM. Design and preparation of materials for advanced electrochemical storage. Acc Chem Res 2013;46:1226–38.
[9] Xie Y, Huang Y, Chen H, Lin W, Wu T, Wang Y, et al. Dual-Protective Role of PM475: Bolstering Anode and Cathode Stability in Lithium Metal Batteries. Adv Funct Mater 2024;34:2310867.
[10] Andre D, Kim S-J, Lamp P, Lux SF, Maglia F, Paschos O, et al. Future generations of cathode materials: an automotive industry perspective. J Mater Chem A 2015;3:6709–32.
[11] Myung S-T, Maglia F, Park K-J, Yoon CS, Lamp P, Kim S-J, et al. Nickel-Rich Layered Cathode Materials for Automotive Lithium-Ion Batteries: Achievements and Perspectives. ACS Energy Lett 2016;2:196–223.
[12] Zhu J, Wierzbicki T, Li W. A review of safety-focused mechanical modeling of commercial lithium-ion batteries. J Power Sources 2018;378:153–68.
[13] Lyu P, Liu X, Qu J, Zhao J, Huo Y, Qu Z, et al. Recent advances of thermal safety of lithium ion battery for energy storage. Energy Storage Mater 2020;31:195–220.
[14] Chen Y, Kang Y, Zhao Y, Wang L, Liu J, Li Y, et al. A review of lithium-ion battery safety concerns: The issues, strategies, and testing standards. J Energy Chem 2021;59:83–99.
[15] Feng X, Ouyang M, Liu X, Lu L, Xia Y, He X. Thermal runaway mechanism of lithium ion battery for electric vehicles: A review. Energy Storage Mater 2018;10:246–67.
[16] Wang L, Yin S, Yu Z, Wang Y, Yu TX, Zhao J, et al. Unlocking the significant role of shell material for lithium-ion battery safety. Mater Des 2018;160:601–10.
[17] Zhao Q, Guo Z, Wu Y, Wang L, Han Z, Ma X, et al. Hierarchical flower-like spinel manganese-based oxide nanosheets for high-performance lithium ion battery. Sci China-Mater 2019;62:1385–92.
[18] Cai Y, Ku L, Wang L, Ma Y, Zheng H, Xu W, et al. Engineering oxygen vacancies in hierarchically Li-rich layered oxide porous microspheres for high-rate lithium ion battery cathode. Sci China-Mater 2019;62:1374–84.
[19] Rana S, Kumar R, Bharj RS. Current trends, challenges, and prospects in material advances for improving the overall safety of lithium-ion battery pack. Chem. Eng J 2023;463.
[20] Larsson F, Bertilsson S, Furlani M, Albinsson I, Mellander B-E. Gas explosions and thermal runaways during external heating abuse of commercial lithium-ion graphite-$LiCoO_2$ cells at different levels of ageing. J Power Sources 2018;373:220–31.
[21] Koch S, Fill A, Birke KP. Comprehensive gas analysis on large scale automotive lithium-ion cells in thermal runaway. J Power Sources 2018;398:106–12.
[22] Wang H, Zhu Y, Kim SC, Pei A, Li Y, Boyle DT, et al. Underpotential lithium plating on graphite anodes caused by temperature heterogeneity. PNAS 2020;117:29453–61.
[23] Duan J, Tang X, Dai H, Yang Y, Wu W, Wei X, et al. Building safe lithium-ion batteries for electric vehicles: a review. Electrochem Energy Rev 2020;3:1–42.
[24] Liu K, Liu Y, Lin D, Pei A, Cui Y. Materials for lithium-ion battery safety. Sci Adv 2018;4:eaas9820.
[25] Wang Q, Ping P, Zhao X, Chu G, Sun J, Chen C. Thermal runaway caused fire and explosion of lithium ion battery. J Power Sources 2012;208:210–24.
[26] Feng X, He X, Ouyang M, Wang L, Lu L, Ren D, et al. A Coupled Electrochemical-Thermal Failure Model for Predicting the Thermal Runaway Behavior of Lithium-Ion Batteries. J Electrochem Soc 2018;165:A3748–65.
[27] Ren F, Cox T, Wang H. Thermal runaway risk evaluation of Li-ion cells using a pinch–torsion test. J Power Sources 2014;249:156–62.
[28] Sheikh M, Elmarakbi A, Elkady M. Thermal runaway detection of cylindrical 18650 lithium-ion battery under quasi-static loading conditions. J Power Sources 2017;370:61–70.

[29] Kupper C, Spitznagel S, Döring H, Danzer MA, Gutierrez C, Kvasha A, et al. Combined modeling and experimental study of the high-temperature behavior of a lithium-ion cell: Differential scanning calorimetry, accelerating rate calorimetry and external short circuit. Electrochim Acta 2019;306:209–19.
[30] Abaza A, Ferrari S, Wong HK, Lyness C, Moore A, Weaving J, et al. Experimental study of internal and external short circuits of commercial automotive pouch lithium-ion cells. J Energy Storage 2018;16:211–7.
[31] Yeh NH, Wang FM, Khotimah C, Wang XC, Lin YW, Chang SC, et al. Controlling Ni^{2+} from the Surface to the Bulk by a New Cathode Electrolyte Interphase Formation on a Ni-Rich Layered Cathode in High-Safe and High-Energy-Density Lithium-Ion Batteries. ACS Appl Mater Interfaces 2021;13:7355–69.
[32] Lamb J, Orendorff CJ. Evaluation of mechanical abuse techniques in lithium ion batteries. J Power Sources 2014;247:189–96.
[33] Zhu Y-l, Wang C-j, Gao F, Shan M-x, Zhao P-l, Meng Q-f, et al. Rupture and combustion characteristics of lithium-ion battery under overcharge. J Energy Storage. 2021;38.
[34] Feng L, Jiang L, Liu J, Wang Z, Wei Z, Wang Q. Dynamic overcharge investigations of lithium ion batteries with different state of health. J Power Sources 2021;507.
[35] Cho J. Dependence of $AlPO_4$ coating thickness on overcharge behaviour of $LiCoO_2$ cathode material at 1 and 2 C rates. J Power Sources 2004;126:186–9.
[36] Ouyang D, Chen M, Liu J, Wei R, Weng J, Wang J. Investigation of a commercial lithium-ion battery under overcharge/over-discharge failure conditions. RSC Adv 2018;8:33414–24.
[37] von Lüders C, Keil J, Webersberger M, Jossen A. Modeling of lithium plating and lithium stripping in lithium-ion batteries. J Power Sources 2019;414:41–7.
[38] Cheng Li, Ruan W. Thermal Runaway Characteristics of a Large Format Lithium-Ion Battery Module. Energies 2019;12.
[39] Liu X, Ren D, Hsu H, Feng X, Xu G-L, Zhuang M, et al. Thermal Runaway of Lithium-Ion Batteries without Internal Short Circuit. Joule 2018;2:2047–64.
[40] Ouyang M, Ren D, Lu L, Li J, Feng X, Han X, et al. Overcharge-induced capacity fading analysis for large format lithium-ion batteries with $Li_yNi_{1/3}Co_{1/3}Mn_{1/3}O_2 + Li_yMn_2O_4$ composite cathode. J Power Sources 2015;279:626–35.
[41] Sharma N, Peterson VK. Overcharging a lithium-ion battery: Effect on the Li_xC_6 negative electrode determined by in situ neutron diffraction. J Power Sources 2013;244:695–701.
[42] Abraham DP, Roth EP, Kostecki R, McCarthy K, MacLaren S, Doughty DH. Diagnostic examination of thermally abused high-power lithium-ion cells. J Power Sources 2006;161:648–57.
[43] Li Z, Huang J, Yann Liaw B, Metzler V, Zhang J. A review of lithium deposition in lithium-ion and lithium metal secondary batteries. J Power Sources 2014;254:168–82.
[44] Zinth V, von Lüders C, Hofmann M, Hattendorff J, Buchberger I, Erhard S, et al. Lithium plating in lithium-ion batteries at sub-ambient temperatures investigated by in situ neutron diffraction. J Power Sources 2014;271:152–9.
[45] Li H-F, Gao J-K, Zhang S-L. Effect of Overdischarge on Swelling and Recharge Performance of Lithium Ion Cells. Chin J Chem 2008;26:1585–8.
[46] Zhang L, Ma Y, Cheng X, Du C, Guan T, Cui Y, et al. Capacity fading mechanism during long-term cycling of over-discharged $LiCoO_2$/mesocarbon microbeads battery. J Power Sources 2015;293:1006–15.
[47] Guo R, Lu L, Ouyang M, Feng X. Mechanism of the entire overdischarge process and overdischarge-induced internal short circuit in lithium-ion batteries. Sci Rep 2016;6:30248.
[48] Zhao M, Kariuki S, Dewald HD, Lemke FR, Staniewicz RJ, Plichta EJ, et al. Electrochemical Stability of Copper in Lithium-ion Battery Electrolytes. J Electrochem Soc 2000;147.
[49] Thakur AK, Prabakaran R, Elkadeem MR, Sharshir SW, Arıcı M, Wang C, et al. A state of art review and future viewpoint on advance cooling techniques for Lithium–ion battery system of electric vehicles. J Energy Storage 2020;32.
[50] Zhang SS, Xu K, Jow TR. Electrochemical impedance study on the low temperature of Li-ion batteries. Electrochim Acta 2004;49:1057–61.
[51] Herreyre S, Huchet O, Barusseau S, Perton F, Bodet JM, Biensan P. New Li-ion electrolytes for low temperature applications. J Power Sources 2001;97–98:576–80.
[52] Zhu J, Sun Z, Wei X, Dai H. An alternating current heating method for lithium-ion batteries from subzero temperatures. Int J Energy Res 2016;40:1869–83.
[53] Lv C, Lin C, Zhao XS. Enhancing low-temperature electrochemical kinetics and high-temperature cycling stability by decreasing ionic packing factor. eScience 2023;3:100179.
[54] Orsini F, Du Pasquier A, Beaudoin B, Tarascon JM, Trentin M, Langenhuizen N, et al. In situ Scanning Electron Microscopy (SEM) observation of interfaces within plastic lithium batteries. J Power Sources 1998;76:19–29.
[55] Yang Y, Yang W, Yang H, Zhou HJE. Electrolyte design principles for low-temperature lithium-ion batteries. eScience 2023;3:100170.
[56] Zhu J, Sun Z, Wei X, Dai H, Gu W. Experimental investigations of an AC pulse heating method for vehicular high power lithium-ion batteries at subzero temperatures. J Power Sources 2017;367:145–57.
[57] Chen J, Zhang Y, Lu H, Ding J, Wang X, Huang Y, et al. Electrolyte solvation chemistry to construct an anion-tuned interphase for stable high-temperature lithium metal batteries. eScience 2023;3:100135.
[58] Duan J, Tang X, Dai H, Yang Y, Wu W, Wei X, et al. Building Safe Lithium-Ion Batteries for Electric Vehicles: A Review. Electrochem Energy Rev 2019;3:1–42.
[59] Zheng S, Wang L, Feng X, He X. Probing the heat sources during thermal runaway process by thermal analysis of different battery chemistries. J Power Sources 2018;378:527–36.
[60] Hwang S, Kim SM, Bak S-M, Kim SY, Cho B-W, Chung KY, et al. Using Real-Time Electron Microscopy To Explore the Effects of Transition-Metal Composition on the Local Thermal Stability in Charged $Li_xNi_yMn_zCo_{1-y-z}O_2$ Cathode Materials. Chem Mater 2015;27:3927–35.
[61] Rajkamal A, Thapa R. Carbon Allotropes as Anode Material for Lithium-ion Batteries. Adv. Mater Technol 2019;4.
[62] Wang S, Yang Y, Dong Y, Zhang Z, Tang Z. Recent progress in Ti-based nanocomposite anodes for lithium ion batteries. J Adv Ceram 2019;8:1–18.
[63] Hu L, Luo L, Tang L, Lin C, Li R, Chen Y. $Ti_2Nb_{2x}O_{4+5x}$ anode materials for lithium-ion batteries: a comprehensive review. J Mater Chem A 2018;6:9799–815.
[64] Wu J, Ma F, Liu X, Fan X, Shen L, Wu Z, et al. Recent Progress in Advanced Characterization Methods for Silicon-Based Lithium-ion Batteries. Small Methods 2019;3.
[65] Guo J, Dong D, Wang J, Liu D, Yu X, Zheng Y, et al. Silicon-Based Lithium Ion Battery Systems: State-of-the-Art from Half and Full Cell Viewpoint. Adv Funct Mater 2021;31.
[66] Fu Y, Wei Q, Zhang G. Sun S. Advanced Phosphorus-Based Materials for Lithium/Sodium-Ion Batteries: Recent Developments and Future Perspectives. Adv Energy Mater; 2018. p. 8.
[67] Liu W, Zhi H, Yu X. Recent progress in phosphorus based anode materials for lithium/sodium ion batteries. Energy Storage Mater 2019;16:290–322.
[68] Salah M, Murphy P, Hall C, Francis C, Kerr R, Fabretto M. Pure silicon thin-film anodes for lithium-ion batteries: A review. J Power Sources 2019;414:48–67.
[69] Xiong Y, Liu Y, Chen L, Zhang S, Zhu X, Shen T, et al. New Insight on Graphite Anode Degradation Induced by Li-Plating. Energy Environ Mater 2022;5:872–6.
[70] Yang Y, Xu L, Yang S-J, Yan C, Huang J-Q. Electrolyte inhomogeneity induced lithium plating in fast charging lithium-ion batteries. J Energy Chem 2022;73:394–9.
[71] Wang H, Yu Z, Kong X, Kim SC, Boyle DT, Qin J, et al. Liquid electrolyte: The nexus of practical lithium metal batteries. Joule 2022;6:588–616.
[72] Legrand N, Knosp B, Desprez P, Lapicque F, Raël S. Physical characterization of the charging process of a Li-ion battery and prediction of Li plating by electrochemical modelling. J Power Sources 2014;245:208–16.
[73] Tallman KR, Zhang B, Wang L, Yan S, Thompson K, Tong X, et al. Anode Overpotential Control via Interfacial Modification: Inhibition of Lithium Plating on Graphite Anodes. ACS Appl Mater Interfaces 2019;11:46864–74.
[74] Wang X, Luo K, Xiong L, Xiong T, Li Z, Sun J, et al. Li^+ Solvation Mediated Interfacial Kinetic of Alloying Matrix for Stable Li Anodes. Energy Environmental Materials 2023;6:e12317.
[75] Chandrasekaran R. Quantification of bottlenecks to fast charging of lithium-ion-insertion cells for electric vehicles. J Power Sources 2014;271:622–32.
[76] Zhang SS, Xu K, Jow TR. Study of the charging process of a $LiCoO_2$-based Li-ion battery. J Power Sources 2006;160:1349–54.
[77] Liu Q, Du C, Shen B, Zuo P, Cheng X, Ma Y, et al. Understanding undesirable anode lithium plating issues in lithium-ion batteries. RSC Adv 2016;6:88683–700.
[78] Cheng XB, Zhang R, Zhao CZ, Zhang Q. Toward Safe Lithium Metal Anode in Rechargeable Batteries: A Review. Chem Rev 2017;117:10403–73.

[79] Cheng XB, Zhang R, Zhao CZ, Wei F, Zhang JG, Zhang Q. A Review of Solid Electrolyte Interphases on Lithium Metal Anode. Adv Sci 2016;3:1500213.
[80] Cai W, Yan C, Yao YX, Xu L, Chen XR, Huang JQ, et al. The Boundary of Lithium Plating in Graphite Electrode for Safe Lithium-Ion Batteries. Angew Chem Int Ed 2021;60:13007–12.
[81] Waldmann T, Hogg B-I, Wohlfahrt-Mehrens M. Li plating as unwanted side reaction in commercial Li-ion cells – A review. J Power Sources 2018;384:107–24.
[82] Wang Q, Sun J, Yao X, Chen C. Thermal Behavior of Lithiated Graphite with Electrolyte in Lithium-Ion Batteries. J Electrochem Soc 2006;153.
[83] Aurbach D, Zaban A, Ein-Eli Y, Weissman I, Chusid O, Markovsky B, et al. Recent studies on the correlation between surface chemistry, morphology, three-dimensional structures and performance of Li and Li-C intercalation anodes in several important electrolyte systems. J Power Sources 1997;68:91–8.
[84] Maleki H, Deng G, Anani A, Howard J. Thermal Stability Studies of Li-ion Cells and Components. J Electrochem Soc 2019;146:3224–9.
[85] Spotnitz R, Franklin J. Abuse behavior of high-power, lithium-ion cells. J Power Sources 2003;113:81–100.
[86] Yamaki J. Thermal stability of graphite anode with electrolyte in lithium-ion cells. Solid State Ion 2002;148:241–5.
[87] Agubra V, Fergus J. Lithium Ion Battery Anode Aging Mechanisms. Materials 2013;6:1310–25.
[88] Ouyang D, Chen M, Huang Q, Weng J, Wang Z, Wang J. A Review on the Thermal Hazards of the Lithium-Ion Battery and the Corresponding Countermeasures. Appl Sci 2019;9.
[89] Harris SJ, Lu P. Effects of Inhomogeneities—Nanoscale to Mesoscale—on the Durability of Li-ion Batteries. J Phys Chem C 2013;117:6481–92.
[90] Rhee DY, Kim J, Moon J, Park M-S. Off-stoichiometric TiO_{2-x}-decorated graphite anode for high-power lithium-ion batteries. J Alloys Compd 2020;843.
[91] Shen C, Hu G, Cheong LZ, Huang S, Zhang JG, Wang D. Direct Observation of the Growth of Lithium Dendrites on Graphite Anodes by Operando EC-AFM. Small Methods 2017;2.
[92] Choi S, Jung G, Kim JE, Kim T, Suh KS. Lithium intercalated graphite with preformed passivation layer as superior anode for Lithium ion batteries. Appl Surf Sci 2018;455:367–72.
[93] Kang S-J, Park K, Park S-H, Lee H. Unraveling the role of LiFSI electrolyte in the superior performance of graphite anodes for Li-ion batteries. Electrochim Acta 2018;259:949–54.
[94] Lai J, Tan R, Jiang H, Huang X, Tian Z, Hong B, et al. Development of an in situ polymerized artificial layer for dendrite-free and stable lithium metal batteries. Battery Energy 2024;20230070.
[95] Zhang M, Tan R, Wang M, Zhang Z, John Low C, Lai Y. Hypercrosslinked porous and coordination polymer materials for electrolyte membranes in lithium-metal batteries. Battery Energy 2024;3:20230050.
[96] Baran MJ, Carrington ME, Sahu S, Baskin A, Song J, Baird MA, et al. Diversity-oriented synthesis of polymer membranes with ion solvation cages. Nature 2021;592:225–31.
[97] Fu C, Venturi V, Kim J, Ahmad Z, Ells AW, Viswanathan V, et al. Universal chemomechanical design rules for solid-ion conductors to prevent dendrite formation in lithium metal batteries. Nat Mater 2020;19:758–66.
[98] Tan R, Wang A, Malpass-Evans R, Williams R, Zhao EW, Liu T, et al. Hydrophilic microporous membranes for selective ion separation and flow-battery energy storage. Nat Mater 2020;19:195–202.
[99] Zuo P, Li Y, Wang A, Tan R, Liu Y, Liang X, et al. Sulfonated microporous polymer membranes with fast and selective ion transport for electrochemical energy conversion and storage. Angew Chem Int Ed 2020;59:9564–73.
[100] Ye C, Wang A, Breakwell C, Tan R, Grazia Bezzu C, Hunter-Sellars E, et al. Development of efficient aqueous organic redox flow batteries using ion-sieving sulfonated polymer membranes. Nat Commun 2022;13:3184.
[101] Wang A, Tan R, Liu D, Lu J, Wei X, Alvarez-Fernandez A, et al. Ion-Selective Microporous Polymer Membranes with Hydrogen-Bond and Salt-Bridge Networks for Aqueous Organic Redox Flow Batteries. Adv Mater 2023;35:2210098.
[102] Tan R, He H, Wang A, Wong T, Yang Y, Iguodala S, et al. Interfacial Engineering of Polymer Membranes with Intrinsic Microporosity for Dendrite-free Zinc Metal Batteries. Angew Chem.e202409322.
[103] Tan R, Wang A, Ye C, Li J, Liu D, Darwich BP, et al. Thin film composite membranes with regulated crossover and water migration for long-life aqueous redox flow batteries. Adv Sci 2023;10:2206888.
[104] Ye C, Tan R, Wang A, Chen J, Comesaña Gándara B, Breakwell C, et al. Long-life aqueous organic redox flow batteries enabled by amidoxime-functionalized ion-selective polymer membranes. Angew Chem 2022;134:e202207580.
[105] Rhee DY, Kim J, Moon J, Park M-S. Off-stoichiometric TiO_{2-x}-decorated graphite anode for high-power lithium-ion batteries. J Alloys Compd 2020;843:156042.
[106] Lee JW, Kim SY, Rhee DY, Park S, Jung JY, Park M-S. Tailoring the surface of natural graphite with functional metal oxides via facile crystallization for lithium-ion batteries. ACS Appl Mater Interfaces 2022;14:29797–805.
[107] Kim DS, Kim YE, Kim H. Improved fast charging capability of graphite anodes via amorphous Al_2O_3 coating for high power lithium ion batteries. J Power Sources 2019;422:18–24.
[108] Tallman KR, Yan S, Quilty CD, Abraham A, McCarthy AH, Marschilok AC, et al. Improved capacity retention of lithium ion batteries under fast charge via metal-coated graphite electrodes. J Electrochem Soc 2020;167:160503.
[109] Ding F, Xu W, Choi D, Wang W, Li X, Engelhard MH, et al. Enhanced performance of graphite anode materials by AlF 3 coating for lithium-ion batteries. J Mater Chem 2012;22:12745–51.
[110] Seo J, Hyun S, Moon J, Lee JY, Kim C. High performance of a polydopamine-coated graphite anode with a stable SEI layer. ACS Appl Energ Mater 2022;5:5610–6.
[111] Zhang Y, Yang Z, Dou Y, Wang W, Zhang Y, Wang A, et al. Hollow spherical organic polymer artificial layer enabled stable Li metal anode. Chem Eng J 2022;442:136155.
[112] Son Y, Lee T, Wen B, Ma J, Jo C, Cho Y-G, et al. High energy density anodes using hybrid Li intercalation and plating mechanisms on natural graphite. Energy Environ Sci 2020;13:3723–31.
[113] Wei C, Xi B, Wang P, Liang Y, Wang Z, Tian K, et al. In situ anchoring ultrafine ZnS nanodots on 2D MXene nanosheets for accelerating polysulfide redox and regulating Li plating. Adv Mater 2023;35:2303780.
[114] Cai W, Yan C, Yao YX, Xu L, Chen XR, Huang JQ, et al. The boundary of lithium plating in graphite electrode for safe lithium-ion batteries. Angew Chem Int Ed 2021;60:13007–12.
[115] Cao X, Xu Y, Zhang L, Engelhard MH, Zhong L, Ren X, et al. Nonflammable electrolytes for lithium ion batteries enabled by ultraconformal passivation interphases. ACS Energy Lett 2019;4:2529–34.
[116] Jia H, Xu Y, Burton SD, Gao P, Zhang X, Matthews BE, et al. Enabling ether-based electrolytes for long cycle life of lithium-ion batteries at high charge voltage. ACS Appl Mater Interfaces 2020;12:54893–903.
[117] Jiang LL, Yan C, Yao YX, Cai W, Huang JQ, Zhang Q. Inhibiting solvent co-intercalation in a graphite anode by a localized high-concentration electrolyte in fast-charging batteries. Angew Chem Int Ed 2021;60:3402–6.
[118] Jiao S, Ren X, Cao R, Engelhard MH, Liu Y, Hu D, et al. Stable cycling of high-voltage lithium metal batteries in ether electrolytes. Nat Energy 2018;3:739–46.
[119] Yue X, Zhang J, Dong Y, Chen Y, Shi Z, Xu X, et al. Reversible Li Plating on Graphite Anodes through Electrolyte Engineering for Fast-Charging Batteries. Angew Chem 2023;135:e202302285.
[120] Gribble DA, McCulfor E, Li Z, Parekh M, Pol VG. Enhanced capacity and thermal safety of lithium-ion battery graphite anodes with conductive binder. J Power Sources 2023;553.
[121] Chang C-M. Effects of Negative Electrodes Coated by ZnO with Different Morphologies on Electrochemical Performances and Safety of Lithium Ion Batteries. Int J Electrochem Sci 2019;14:1197–207.
[122] Zhao T, She S, Ji X, Guo X, Jin W, Zhu R, et al. Expanded graphite embedded with aluminum nanoparticles as superior thermal conductivity anodes for high-performance lithium-ion batteries. Sci Rep 2016;6:33833.

[123] Deng Y, Wang Z, Ma Z, Nan J. Positive-Temperature-Coefficient Graphite Anode as a Thermal Runaway Firewall to Improve the Safety of $LiCoO_2$/Graphite Batteries under Abusive Conditions. Energy Technol 2019;8.
[124] Engels P, Cerdas F, Dettmer T, Frey C, Hentschel J, Herrmann C, et al. Life cycle assessment of natural graphite production for lithium-ion battery anodes based on industrial primary data. J Clean Prod 2022;336:130474.
[125] Rey I, Vallejo C, Santiago G, Iturrondobeitia M, Lizundia E. Environmental impacts of graphite recycling from spent lithium-ion batteries based on life cycle assessment. ACS Sustainable Chem Eng 2021;9:14488–501.
[126] Zhang Z, Xiao J, Chen Y, Su F, Xu F, Zhong Q. Potential environmental and human health menace of spent graphite in lithium-ion batteries. Environ Res 2024;244:117967.
[127] Abdollahifar M, Doose S, Cavers H, Kwade A. Graphite recycling from end-of-life lithium-ion batteries: processes and applications. Adv Mater Technol 2023;8:2200368.
[128] Niu B, Xiao J, Xu Z. Advances and challenges in anode graphite recycling from spent lithium-ion batteries. J Hazard Mater 2022;439:129678.
[129] Wang Q, Sun J, Yao X, Chen C. Micro calorimeter study on the thermal stability of lithium-ion battery electrolytes. J Loss Prev Process Ind 2006;19:561–9.
[130] Kalhoff J, Eshetu GG, Bresser D, Passerini S. Safer Electrolytes for Lithium-Ion Batteries: State of the Art and Perspectives. ChemSusChem 2015;8:2154–75.
[131] Xu K. Electrolytes and interphases in Li-ion batteries and beyond. Chem Rev 2014;114:11503–618.
[132] Sloop SE, Pugh JK, Wang S, Kerr JB, Kinoshita K. Chemical Reactivity of PF_5 and $LiPF_6$ in Ethylene Carbonate/Dimethyl Carbonate Solutions. Electrochem Solid-State Lett 2001;4.
[133] Kawamura T, Okada S, Yamaki J-i. Decomposition reaction of $LiPF_6$-based electrolytes for lithium ion cells. J Power Sources 2006;156:547–54.
[134] Ping P, Wang Q, Sun J, Xiang H, Chen C. Thermal Stabilities of Some Lithium Salts and Their Electrolyte Solutions With and Without Contact to a $LiFeP_4$ Electrode. J Electrochem Soc 2010;157.
[135] Kawamura T, Kimura A, Egashira M, Okada S, Yamaki J-I. Thermal stability of alkyl carbonate mixed-solvent electrolytes for lithium ion cells. J Power Sources 2002;104:260–4.
[136] Chawla N, Bharti N, Singh S. Recent Advances in Non-Flammable Electrolytes for Safer Lithium-Ion Batteries. Batteries-Basel 2019;5.
[137] Chen W, Lei T, Wu C, Deng M, Gong C, Hu K, et al. Designing Safe Electrolyte Systems for a High-Stability Lithium-Sulfur Battery. Adv Energy Mater 2018;8.
[138] Chen Z, Ren Y, Jansen AN, Lin CK, Weng W, Amine K. New class of nonaqueous electrolytes for long-life and safe lithium-ion batteries. Nat Commun 2013;4:1513.
[139] Kumai K, Miyashiro H, Kobayashi Y, Takei K, Ishikawa R. Gas generation mechanism due to electrolyte decomposition in commercial lithium-ion cell. J Power Sources 1999;81–82:715–9.
[140] Noelle DJ, Shi Y, Wang M, Le AV, Qiao Y. Aggressive electrolyte poisons and multifunctional fluids comprised of diols and diamines for emergency shutdown of lithium-ion batteries. J Power Sources 2018;384:93–7.
[141] Wang Q, Jiang L, Yu Y, Sun J. Progress of enhancing the safety of lithium ion battery from the electrolyte aspect. Nano Energy 2019;55:93–114.
[142] Xu K. Nonaqueous Liquid Electrolytes for Lithium-Based Rechargeable Batteries. Chem Rev 2004;104:4303–418.
[143] Wang X, Yasukawa E. Kasuya S. Nonflammable Trimethyl Phosphate Solvent-Containing Electrolytes for Lithium-Ion Batteries: I. Fundamental Properties. J Electrochem Soc; 2001. p. 148.
[144] Qin Y, Ren Z, Wang Q, Li Y, Liu J, Liu Y, et al. Simplifying the Electrolyte Systems with the Functional Cosolvent. ACS Appl Mater Interfaces 2019;11:27854–61.
[145] Wang W, Liao C, Liu L, Cai W, Yuan Y, Hou Y, et al. Comparable investigation of tervalent and pentavalent phosphorus based flame retardants on improving the safety and capacity of lithium-ion batteries. J Power Sources 2019;420:143–51.
[146] Shi Y, Zhang Q, Zhang Y, Jia L, Xu X. Promising and Reversible Electrolyte with Thermal Switching Behavior for Safer Electrochemical Storage Devices. ACS Appl Mater Interfaces 2018;10:7171–9.
[147] Zhang J, Shkrob IA, Assary RS, Zhang S, Hu B, Liao C, et al. Dual overcharge protection and solid electrolyte interphase-improving action in Li-ion cells containing a bis-annulated dialkoxyarene electrolyte additive. J Power Sources 2018;378:264–7.
[148] Gélinas B, Bibienne T, Dollé M, Rochefort D. Electroactive ionic liquids based on 2,5-ditert-butyl-1,4-dimethoxybenzene and triflimide anion as redox shuttle for $Li_4Ti_5O_{12}$/$LiFePO_4$ lithium-ion batteries. J Power Sources 2017;372:212–20.
[149] Gu Q, Wang M, Liu Y, Deng Y, Wang L, Gao J. Electrolyte Additives for Improving the High-Temperature Storage Performance of Li-Ion Battery NCM523 parallelGraphite with Overcharge Protection. ACS Appl Mater Interfaces 2022;14:4759–66.
[150] Dziembaj R, Molenda M. Stabilization of the spinel structure in $Li_{1+\delta}Mn_{2-\delta}O_4$ obtained by sol–gel method. J Power Sources 2003;119–121:121–4.
[151] Larush-Asraf L, Biton M, Teller H, Zinigrad E, Aurbach D. On the electrochemical and thermal behavior of lithium bis(oxalato)borate (LiBOB) solutions. J Power Sources 2007;174:400–7.
[152] Xu M, Zhou L, Hao L, Xing L, Li W, Lucht BL. Investigation and application of lithium difluoro(oxalate)borate (LiDFOB) as additive to improve the thermal stability of electrolyte for lithium-ion batteries. J Power Sources 2011;196:6794–801.
[153] Chen X, Yan S, Tan T, Zhou P, Hou J, Feng X, et al. Supramolecular "flame-retardant" electrolyte enables safe and stable cycling of lithium-ion batteries. Energy Storage Mater 2022;45:182–90.
[154] Hou J, Wang L, Feng X, Terada J, Lu L, Yamazaki S, et al. Thermal Runaway of Lithium-ion Batteries Employing Flame-Retardant Fluorinated Electrolytes. Energy Environ Mater 2022;6:e12297.
[155] Yu Z, Zhang J, Wang C, Hu R, Du X, Tang B, et al. Flame-retardant concentrated electrolyte enabling a LiF-rich solid electrolyte interface to improve cycle performance of wide-temperature lithium–sulfur batteries. J Energy Chem 2020;51:154–60.
[156] Jia H, Xu Y, Zhang X, Burton SD, Gao P, Matthews BE, et al. Advanced Low-Flammable Electrolytes for Stable Operation of High-Voltage Lithium-Ion Batteries. Angew Chem Int Ed 2021;60:12999–3006.
[157] Zhu Y, Luo X, Zhi H, Liao Y, Xing L, Xu M, et al. Diethyl(thiophen-2-ylmethyl)phosphonate: a novel multifunctional electrolyte additive for high voltage batteries. J Mater Chem A 2018;6:10990–1004.
[158] Liu J, Song X, Zhou L, Wang S, Song W, Liu W, et al. Fluorinated phosphazene derivative – A promising electrolyte additive for high voltage lithium ion batteries: From electrochemical performance to corrosion mechanism. Nano Energy 2018;46:404–14.
[159] Xu G, Pang C, Chen B, Ma J, Wang X, Chai J, et al. Prescribing Functional Additives for Treating the Poor Performances of High-Voltage (5 V-class) $LiNi_{0.5}Mn_{1.5}O_4$/MCMB Li-Ion Batteries. Adv Energy Mater 2018;8:1701398.
[160] Chen S, Wang Z, Zhao H, Qiao H, Luan H, Chen L. A novel flame retardant and film-forming electrolyte additive for lithium ion batteries. J Power Sources 2009;187:229–32.
[161] Liu K, Liu W, Qiu Y, Kong B, Sun Y, Chen Z, et al. Electrospun core-shell microfiber separator with thermal-triggered flame-retardant properties for lithium-ion batteries. Sci Adv 2017;3:e1601978.
[162] Pires J, Castets A, Timperman L, Santos-Peña J, Dumont E, Levasseur S, et al. Tris(2,2,2-trifluoroethyl) phosphite as an electrolyte additive for high-voltage lithium-ion batteries using lithium-rich layered oxide cathode. J Power Sources 2015;296:413–25.
[163] Gu Y, Fang S, Yang L, Hirano S-i. A non-flammable electrolyte for long-life lithium ion batteries operating over a wide-temperature range. J Mater Chem A 2021;9:15363–72.
[164] Li X, Li W, Chen L, Lu Y, Su Y, Bao L, et al. Ethoxy (pentafluoro) cyclotriphosphazene (PFPN) as a multi-functional flame retardant electrolyte additive for lithium-ion batteries. J Power Sources 2018;378:707–16.
[165] Yusuf A, Sai Avvaru V, De la Vega J, Zhang M, Garcia Molleja J, Wang D-Y. Unveiling the structure, chemistry, and formation mechanism of an in-situ phosphazene flame retardant-derived interphase layer in $LiFePO_4$ cathode. Chem. Eng J 2023;455.
[166] Zhu Y, Luo X, Zhi H, Liao Y, Xing L, Xu M, et al. Diethyl (thiophen-2-ylmethyl) phosphonate: a novel multifunctional electrolyte additive for high voltage batteries. J Mater Chem A 2018;6:10990–1004.

[167] Xu M, Liang Y, Li B, Xing L, Wang Y, Li W. Tris (pentafluorophenyl) phosphine: A dual functionality additive for flame-retarding and sacrificial oxidation on $LiMn_2O_4$ for lithium ion battery. Mater Chem Phys 2014;143:1048–54.
[168] Wu Z-H, Wu Y, Tang Y, Jiang J-C, Huang A-C. Evaluation of composite flame-retardant electrolyte additives improvement on the safety performance of lithium-ion batteries. Process Saf Environ Prot 2023;169:285–92.
[169] Liu S, Becker M, Huang-Joos Y, Lai H, Homann G, Grissa R, et al. Multifunctional Additive Ethoxy (pentafluoro) cyclotriphosphazene Enables Safe Carbonate Electrolyte for SiOx-Graphite/NMC811 Batteries. Batteries Supercaps 2023;6:e202300220.
[170] Murmann P, Mönnighoff X, von Aspern N, Janssen P, Kalinovich N, Shevchuk M, et al. Influence of the fluorination degree of organophosphates on flammability and electrochemical performance in lithium ion batteries: Studies on fluorinated compounds deriving from triethyl phosphate. J Electrochem Soc 2016;163:A751.
[171] Chen Z, Shen H, Zhu Y, Hua M, Pan X, Liu Y, et al. Advanced low-flammable pyrrole ionic liquid electrolytes for high safety lithium-ion batteries. J Energy Storage 2023;72:108289.
[172] Luu PH, Tran PH, Van Nguyen H, Phan ALB, Nguyen OH, Van Tran M, et al. Sulfolane as a co-solvent for carbonate-electrolytes in lithium-ion batteries using a $LiMn_2O_4$ cathode. VJSTE 2022;64:9–13.
[173] Subburaj T, Jo YN, Lee CW. Effect of monocationic ionic liquids as electrolyte additives on the electrochemical and thermal properties of Li-ion batteries. Curr Appl Phys 2014;14:1022–7.
[174] Logan MW, Langevin S, Tan B, Freeman AW, Hoffman C, Trigg DB, et al. UV-cured eutectic gel polymer electrolytes for safe and robust Li-ion batteries. J Mater Chem A 2020;8:8485–95.
[175] Tang G, Shen S-P, Li H-J, Zhang L, Zheng J-C, Luo Y, et al. Flame-retardant gel electrolyte toward high-safety lithium metal batteries with high-mass-loading cathodes. J Phys Chem C 2023;127:9463–70.
[176] Moshurchak LM, Lamanna WM, Bulinski M, Wang RL, Garsuch RR, Jiang J, et al. High-Potential Redox Shuttle for Use in Lithium-Ion Batteries. J Electrochem Soc 2009;156.
[177] Wen J-W, Zhang D-W, Chen C-H, Ding C-X, Yu Y, Maier J. Cathodes with intrinsic redox overcharge protection: A new strategy towards safer Li-ion batteries. J Power Sources 2014;264:155–60.
[178] Chen Y. Recent advances of overcharge investigation of lithium-ion batteries. Ionics 2021;28:495–514.
[179] Li Q, Chen J, Fan L, Kong X, Lu Y. Progress in electrolytes for rechargeable Li-based batteries and beyond. Green Energy Environ 2016;1:18–42.
[180] Walker W, Giordani V, Uddin J, Bryantsev VS, Chase GV, Addison D. A rechargeable Li-O_2 battery using a lithium nitrate/N. N-dimethylacetamide electrolyte J Am Chem Soc 2013;135:2076–9.
[181] Feng XM, Ai XP, Yang HX. Possible use of methylbenzenes as electrolyte additives for improving the overcharge tolerances of Li-ion batteries. J Appl Electrochem 2004;34:1199–203.
[182] Ahn J, Im J, Seo H, Yoon S, Cho KY. Enhancing the cycling stability of Ni-rich $LiNi_{0.83}Co_{0.11}Mn_{0.06}O_2$ cathode at 4.5 V via 2,4-difluorobiphenyl additive. J Power Sources 2021;512.
[183] Zhang J, Shkrob IA, Assary RS, Clark RJ, Wilson RE, Jiang S, et al. An extremely durable redox shuttle additive for overcharge protection of lithium-ion batteries. Mater Today Energy 2019;13:308–11.
[184] Janssen P, Streipert B, Krafft R, Murmann P, Wagner R, Lewis-Alleyne L, et al. Shutdown potential adjustment of modified carbene adducts as additives for lithium ion battery electrolytes. J Power Sources 2017;367:72–9.
[185] Chombo PV, Laoonual Y. A review of safety strategies of a Li-ion battery. J Power Sources 2020;478.
[186] Park EJ, Kwon Y-G, Yoon S, Cho KY. Synergistic high-voltage lithium ion battery performance by dual anode and cathode stabilizer additives. J Power Sources 2019;441.
[187] Zheng X, Huang T, Pan Y, Wang W, Fang G, Ding K, et al. Enhancing the High-Voltage Cycling Performance of $LiNi_{1/3}Co_{1/3}Mn_{1/3}O_2$/Graphite Batteries Using Alkyl 3,3,3-Trifluoropropanoate as an Electrolyte Additive. ACS Appl Mater Interfaces 2017;9:18758–65.
[188] Cekic-Laskovic I, von Aspern N, Imholt L, Kaymaksiz S, Oldiges K, Rad BR, et al. Synergistic Effect of Blended Components in Nonaqueous Electrolytes for Lithium Ion Batteries. Top Curr Chem 2017;375:37.
[189] Ji W, Huang H, Huang X, Zhang X, Zheng D, Ding T, et al. A redox-active organic cation for safer high energy density Li-ion batteries. J Mater Chem A 2020;8:17156–62.
[190] Chen Y. Recent advances of overcharge investigation of lithium-ion batteries. Ionics 2022;28:495–514.
[191] Haregewoin AM, Wotango AS, Hwang B-J. Electrolyte additives for lithium ion battery electrodes: progress and perspectives. Energy Environ Sci 2016;9:1955–88.
[192] Lisbona D, Snee T. A review of hazards associated with primary lithium and lithium-ion batteries. Process Saf Environ Prot 2011;89:434–42.
[193] van Ree T. Electrolyte additives for improved lithium-ion battery performance and overcharge protection. Curr Opin Electrochem 2020;21:22–30.
[194] Wang Z, Zhang F, Sun Y, Zheng L, Shen Y, Fu D, et al. Intrinsically Nonflammable Ionic Liquid-Based Localized Highly Concentrated Electrolytes Enable High-Performance Li-Metal Batteries. Adv Energy Mater 2021;11.
[195] Chen N, Guan Y, Shen J, Guo C, Qu W, Li Y, et al. Heteroatom Si Substituent Imidazolium-Based Ionic Liquid Electrolyte Boosts the Performance of Dendrite-Free Lithium Batteries. ACS Appl Mater Interfaces 2019;11:12154–60.
[196] Mezzomo L, Pianta N, Ostroman I, Aloni N, Golodnitsky D, Peled E, et al. Deep eutectic solvent electrolytes based on trifluoroacetamide and $LiPF_6$ for Li-metal batteries. J Power Sources 2023;561.
[197] Ma Z, Chen J, Vatamanu J, Borodin O, Bedrov D, Zhou X, et al. Expanding the low-temperature and high-voltage limits of aqueous lithium-ion battery. Energy Storage Mater 2022;45:903–10.
[198] Jiang P, Chen L, Shao H, Huang S, Wang Q, Su Y, et al. Methylsulfonylmethane-Based Deep Eutectic Solvent as a New Type of Green Electrolyte for a High-Energy-Density Aqueous Lithium-Ion Battery. ACS Energy Lett 2019;4:1419–26.
[199] Amanchukwu CV, Yu Z, Kong X, Qin J, Cui Y, Bao Z. A New Class of Ionically Conducting Fluorinated Ether Electrolytes with High Electrochemical Stability. J Am Chem Soc 2020;142:7393–403.
[200] Xia M, Jiao T, Liu G, Chen Y, Gao J, Cheng Y, et al. Rational design of electrolyte solvation structure for stable cycling and fast charging lithium metal batteries. J Power Sources 2022;548.
[201] Navarra MA, Fujimura K, Sgambetterra M, Tsurumaki A, Panero S, Nakamura N, et al. New Ether-functionalized Morpholinium- and Piperidinium-based Ionic Liquids as Electrolyte Components in Lithium and Lithium-Ion Batteries. ChemSusChem 2017;10:2496–504.
[202] Francis CFJ, Kyratzis IL, Best AS. Lithium-Ion Battery Separators for Ionic-Liquid Electrolytes: A Review. Adv Mater 2020;32:e1904205.
[203] Qi H, Ren Y, Guo S, Wang Y, Li S, Hu Y, et al. High-Voltage Resistant Ionic Liquids for Lithium-Ion Batteries. ACS Appl Mater Interfaces 2020;12:591–600.
[204] Tang X, Lv S, Jiang K, Zhou G, Liu X. Recent development of ionic liquid-based electrolytes in lithium-ion batteries. J Power Sources 2022;542:231792.
[205] Brutti S, Simonetti E, De Francesco M, Sarra A, Paolone A, Palumbo O, et al. Ionic liquid electrolytes for high-voltage, lithium-ion batteries. J Power Sources 2020;479:228791.
[206] Balducci A. Ionic Liquids in Lithium-Ion Batteries. Top Curr Chem 2017;375:20.
[207] Kaur S, Kumari M, Kashyap HK. Microstructure of Deep Eutectic Solvents: Current Understanding and Challenges. J Phys Chem B 2020;124:10601–16.
[208] El Achkar T, Greige-Gerges H, Fourmentin S. Basics and properties of deep eutectic solvents: a review. Environ Chem Lett 2021;19:3397–408.
[209] Ogawa H, Sato Y, Mori H. Tetramethylurea dimer/lithium salt-based deep eutectics as a novel class of eutectic electrolytes. Mater Chem Front 2021;5:8078–85.
[210] Chen Y, Lu Y, Liu Z, Zhou L, Li Z, Jiang J, et al. Efficient Dissolution of Lithium-Ion Batteries Cathode $LiCoO_2$ by Polyethylene Glycol-Based Deep Eutectic Solvents at Mild Temperature. ACS Sustainable Chem Eng 2020;8:11713–20.
[211] Hansen BB, Spittle S, Chen B, Poe D, Zhang Y, Klein JM, et al. Deep Eutectic Solvents: A Review of Fundamentals and Applications. Chem Rev 2021;121:1232–85.

[212] Wu J, Liang Q, Yu X, Lü QF, Ma L, Qin X, et al. Deep Eutectic Solvents for Boosting Electrochemical Energy Storage and Conversion: A Review and Perspective. Adv Funct Mater 2021;31.
[213] Ogawa H, Mori H. Lithium salt/amide-based deep eutectic electrolytes for lithium-ion batteries: electrochemical, thermal and computational study. Phys Chem Chem Phys 2020;22:8853–63.
[214] Zheng J, Tan G, Shan P, Liu T, Hu J, Feng Y, et al. Understanding Thermodynamic and Kinetic Contributions in Expanding the Stability Window of Aqueous Electrolytes. Chem 2018;4:2872–82.
[215] Chao D, Zhou W, Xie F, Ye C, Li H, Jaroniec M, et al. Roadmap for advanced aqueous batteries: From design of materials to applications. Sci Adv 2020;6:eaba4098.
[216] Zhao Y, Chen Z, Mo F, Wang D, Guo Y, Liu Z, et al. Aqueous Rechargeable Metal-Ion Batteries Working at Subzero Temperatures. Adv Sci 2020;8:2002590.
[217] Liang T, Hou R, Dou Q, Zhang H, Yan X. The Applications of Water-in-Salt Electrolytes in Electrochemical Energy Storage Devices. Adv Funct Mater 2020;31.
[218] Wang F, Borodin O, Ding MS, Gobet M, Vatamanu J, Fan X, et al. Hybrid Aqueous/Non-aqueous Electrolyte for Safe and High-Energy Li-Ion Batteries. Joule 2018;2:927–37.
[219] Coustan L, Zaghib K, Bélanger D. New insight in the electrochemical behaviour of stainless steel electrode in water-in-salt electrolyte. J Power Sources 2018;399:299–303.
[220] Eftekhari A. High-Energy Aqueous Lithium Batteries. Adv Energy Mater 2018;8.
[221] Wang F, Suo L, Liang Y, Yang C, Han F, Gao T, et al. Spinel $LiNi_{0.5}Mn_{1.5}O_4$ Cathode for High-Energy Aqueous Lithium-ion Batteries. Adv Energy Mater 2016;7.
[222] Shen Y, Liu B, Liu X, Liu J, Ding J, Zhong C, et al. Water-in-salt electrolyte for safe and high-energy aqueous battery. Energy Storage Mater 2021;34:461–74.
[223] Yang C, Chen J, Qing T, Fan X, Sun W, von Cresce A, et al. 4.0 V Aqueous Li-Ion Batteries. Joule 2017;1:122–32.
[224] Droguet L, Grimaud A, Fontaine O. Tarascon JM. Water-in-Salt Electrolyte (WiSE) for Aqueous Batteries: A Long Way to Practicality. Adv Energy Mater; 2020. p. 10.
[225] Shi P, Fang S, Huang J, Luo D, Yang L, Hirano S-i. A novel mixture of lithium bis(oxalato)borate, gamma-butyrolactone and non-flammable hydrofluoroether as a safe electrolyte for advanced lithium ion batteries. J Mater Chem A 2017;5:19982–90.
[226] Chen L, Fan X, Hu E, Ji X, Chen J, Hou S, et al. Achieving High Energy Density through Increasing the Output Voltage: A Highly Reversible 5.3 V Battery. Chem 2019;5:896–912.
[227] Zhu X, Xiao J, Mao Q, Zhang Z, You Z, Tang L, et al. A promising regeneration of waste carbon residue from spent Lithium-ion batteries via low-temperature fluorination roasting and water leaching. Chem Eng J 2022;430:132703.
[228] Shi H, Luo Y, Yin C, Ou L. Review of the application of ionic liquid systems in achieving green and sustainable recycling of spent lithium-ion batteries. Green Chem 2024;26:8100–22.
[229] Kim A, Jung H, Song J, Kim HJ, Jeong G, Kim H. Lithium-Ion Intercalation into Graphite in SO_2-Based Inorganic Electrolyte toward High-Rate-Capable and Safe Lithium-Ion Batteries. ACS Appl Mater Interfaces 2019;11:9054–61.
[230] Nagao K, Nagata Y, Sakuda A, Hayashi A, Deguchi M, Hotehama C, et al. A reversible oxygen redox reaction in bulk-type all-solid-state batteries. Sci Adv 2020;6:eaax7236.
[231] Wang Z, Tan R, Wang H, Yang L, Hu J, Chen H, et al. A Metal–organic-framework-based electrolyte with nanowetted interfaces for high-energy-density solid-state lithium battery. Adv Mater 2018;30:1704436.
[232] Tang S, Guo W, Fu Y. Advances in Composite Polymer Electrolytes for Lithium Batteries and Beyond. Adv Energy Mater 2020;11.
[233] Zhou D, Shanmukaraj D, Tkacheva A, Armand M, Wang G. Polymer Electrolytes for Lithium-Based Batteries: Advances and Prospects. Chem 2019;5:2326–52.
[234] Zhu M, Wu J, Wang Y, Song M, Long L, Siyal SH, et al. Recent advances in gel polymer electrolyte for high-performance lithium batteries. J Energy Chem 2019;37:126–42.
[235] Chen J, Wu J, Wang X, Aa Z, Yang Z. Research progress and application prospect of solid-state electrolytes in commercial lithium-ion power batteries. Energy Storage Mater 2021;35:70–87.
[236] Long M-C, Wang T, Duan P-H, Gao Y, Wang X-L, Wu G, et al. Thermotolerant and fireproof gel polymer electrolyte toward high-performance and safe lithium-ion battery. J Energy Chem 2022;65:9–18.
[237] Hyun WJ, de Moraes ACM, Lim JM, Downing JR, Park KY, Tan MTZ, et al. High-Modulus Hexagonal Boron Nitride Nanoplatelet Gel Electrolytes for Solid-State Rechargeable Lithium-Ion Batteries. ACS Nano 2019;13:9664–72.
[238] Hyun WJ, Thomas CM, Luu NS, Hersam MC. Layered Heterostructure Ionogel Electrolytes for High-Performance Solid-State Lithium-Ion Batteries. Adv Mater 2021;33:e2007864.
[239] Kim D, Liu X, Yu B, Mateti S, O'Dell LA, Rong Q, et al. Amine-Functionalized Boron Nitride Nanosheets: A New Functional Additive for Robust, Flexible Ion Gel Electrolyte with High Lithium-ion Transference Number. Adv Funct Mater 2020;30.
[240] Mindemark J, Lacey MJ, Bowden T, Brandell D. Beyond PEO—Alternative host materials for Li^+-conducting solid polymer electrolytes. Prog Polym Sci 2018;81:114–43.
[241] Fang R, Xu B, Grundish NS, Xia Y, Li Y, Lu C, et al. Li_2S_6-Integrated PEO-Based Polymer Electrolytes for All-Solid-State Lithium-Metal Batteries. Angew Chem Int Ed 2021;60:17701–6.
[242] Ma Y, Wan J, Yang Y, Ye Y, Xiao X, Boyle DT, et al. Scalable, ultrathin, and high-temperature-resistant solid polymer electrolytes for energy-dense lithium metal batteries. Adv Energy Mater 2022;12:2103720.
[243] Cui Y, Wan J, Ye Y, Liu K, Chou LY, Cui Y. A Fireproof, Lightweight, Polymer-Polymer Solid-State Electrolyte for Safe Lithium Batteries. Nano Lett 2020;20:1686–92.
[244] Nie K, Wang X, Qiu J, Wang Y, Yang Q, Xu J, et al. Increasing Poly(ethylene oxide) Stability to 4.5 V by Surface Coating of the Cathode. ACS Energy Lett 2020;5:826–32.
[245] Yang X, Jiang M, Gao X, Bao D, Sun Q, Holmes N, et al. Determining the limiting factor of the electrochemical stability window for PEO-based solid polymer electrolytes: main chain or terminal –OH group? Energy Environ Sci 2020;13:1318–25.
[246] Mi J, Ma J, Chen L, Lai C, Yang K, Biao J, et al. Topology crafting of polyvinylidene difluoride electrolyte creates ultra-long cycling high-voltage lithium metal solid-state batteries. Energy Storage Mater 2022;48:375–83.
[247] Bai L, Ghiassinejad S, Brassinne J, Fu Y, Wang J, Yang H, et al. High Salt-Content Plasticized Flame-Retardant Polymer Electrolytes. ACS Appl Mater Interfaces 2021;13:44844–59.
[248] Zhou HY, Yan SS, Li J, Dong H, Zhou P, Wan L, et al. Lithium Bromide-Induced Organic-Rich Cathode/Electrolyte Interphase for High-Voltage and Flame-Retardant All-Solid-State Lithium Batteries. ACS Appl Mater Interfaces 2022;14:24469–79.
[249] Zhang M, Zhou K, Ma D, Wang H, Tang X, Bai M, et al. Constructing the high-areal-capacity, solid-state Li polymer battery via the multiscale ion transport pathway design. Mater Today 2022;56:53–65.
[250] J Mater Chem A 2017;5:2829–34.
[251] Tang W, Tang S, Zhang C, Ma Q, Xiang Q, Yang YW, et al. Simultaneously Enhancing the Thermal Stability, Mechanical Modulus, and Electrochemical Performance of Solid Polymer Electrolytes by Incorporating 2D Sheets. Adv Energy Mater 2018;8.
[252] Tong R-A, Luo H, Chen L, Zhang J, Shao G, Wang H, et al. Constructing the lithium polymeric salt interfacial phase in composite solid-state electrolytes for enhancing cycle performance of lithium metal batteries. Chem. Eng J 2022;442.
[253] Wan J, Xie J, Kong X, Liu Z, Liu K, Shi F, et al. Ultrathin, flexible, solid polymer composite electrolyte enabled with aligned nanoporous host for lithium batteries. Nat Nanotechnol 2019;14:705–11.
[254] Yang L, Mu Y, Zou L, Li C, Feng Y, Chu Y, et al. In Situ Formation of Stable Dual-Layer Solid Electrolyte Interphase for Enhanced Stability and Cycle Life in All-Solid-State Lithium Metal Batteries. Nano Lett 2024.
[255] Gao Z, Sun H, Fu L, Ye F, Zhang Y, Luo W, et al. Promises, Challenges, and Recent Progress of Inorganic Solid-State Electrolytes for All-Solid-State Lithium Batteries. Adv Mater 2018;30:e1705702.

[256] Zhang B, Tan R, Yang L, Zheng J, Zhang K, Mo S, et al. Mechanisms and properties of ion-transport in inorganic solid electrolytes. Energy Storage Mater 2018; 10:139–59.
[257] Xu R, Liu F, Ye Y, Chen H, Yang RR, Ma Y, et al. A morphologically stable Li/electrolyte interface for all-solid-state batteries enabled by 3D-micropatterned garnet. Adv Mater 2021;33:2104009.
[258] Famprikis T, Canepa P, Dawson JA, Islam MS, Masquelier C. Fundamentals of inorganic solid-state electrolytes for batteries. Nat Mater 2019;18:1278–91.
[259] Banerjee A, Wang X, Fang C, Wu EA, Meng YS. Interfaces and Interphases in All-Solid-State Batteries with Inorganic Solid Electrolytes. Chem Rev 2020;120: 6878–933.
[260] Krauskopf T, Mogwitz B, Hartmann H, Singh DK, Zeier WG, Janek J. The Fast Charge Transfer Kinetics of the Lithium Metal Anode on the Garnet-Type Solid Electrolyte $Li_{6.25}Al_{0.25}La_3Zr_2O_{12}$. Adv Energy Mater 2020;10.
[261] Zhan X, Li M, Zhao X, Wang Y, Li S, Wang W, et al. Self-assembled hydrated copper coordination compounds as ionic conductors for room temperature solid-state batteries. Nat Commun 2024;15:1056.
[262] Mishra AK, Chaliyawala HA, Patel R, Paneliya S, Vanpariya A, Patel P, et al. Review—Inorganic Solid State Electrolytes: Insights on Current and Future Scope. J Electrochem Soc. 2021;168.
[263] Nagata H, Akimoto J. All-oxide solid-state lithium-ion battery employing $50Li_2SO_4$–$50Li_2CO_3$ glass electrolyte. J Power Sources 2021;491.
[264] Zheng Y, Yao Y, Ou J, Li M, Luo D, Dou H, et al. A review of composite solid-state electrolytes for lithium batteries: fundamentals, key materials and advanced structures. Chem Soc Rev 2020;49:8790–839.
[265] Wan J, Xie J, Mackanic DG, Burke W, Bao Z, Cui Y. Status, promises, and challenges of nanocomposite solid-state electrolytes for safe and high performance lithium batteries. Mater Today Nano 2018;4:1–16.
[266] Tan R, Gao R, Zhao Y, Zhang M, Xu J, Yang J, et al. Novel organic–inorganic hybrid electrolyte to enable $LiFePO_4$ quasi-solid-state Li-ion batteries performed highly around room temperature. ACS Appl Mater Interfaces 2016;8:31273–80.
[267] Yang L, Wang Z, Feng Y, Tan R, Zuo Y, Gao R, et al. Flexible composite solid electrolyte facilitating highly stable “soft contacting” Li–electrolyte interface for solid state lithium-ion batteries. Adv Energy Mater 2017;7:1701437.
[268] Liu W, Meng L, Liu X, Gao L, Wang X, Kang J, et al. 3D spiny AlF_3/Mullite heterostructure nanofiber as solid-state polymer electrolyte fillers with enhanced ionic conductivity and improved interfacial compatibility. J Energy Chem 2023;76:503–15.
[269] Zhang X, Sun Y, Ma C, Guo N, Fan H, Liu J, et al. $Li_{6.4}La_3Zr_{1.4}Ta_{0.6}O_{12}$ Reinforced Polystyrene-Poly(ethylene oxide)-Poly(propylene oxide)-Poly(ethylene oxide)-Polystyrene pentablock copolymer-based composite solid electrolytes for solid-state lithium metal batteries. J Power Sources 2022;542.
[270] Yu X, Manthiram A. A review of composite polymer-ceramic electrolytes for lithium batteries. Energy Storage Mater 2021;34:282–300.
[271] Fan P, Liu H, Marosz V, Samuels NT, Suib SL, Sun L, et al. High Performance Composite Polymer Electrolytes for Lithium-ion Batteries. Adv Funct Mater 2021; 31.
[272] Dirican M, Yan C, Zhu P, Zhang X. Composite solid electrolytes for all-solid-state lithium batteries. Mater Sci Eng R-Rep 2019;136:27–46.
[273] Larrabide A, Rey I, Lizundia E. Environmental Impact Assessment of Solid Polymer Electrolytes for Solid-State Lithium Batteries. Adv Energy Sustain Res 2022; 3:2200079.
[274] Mandade P, Weil M, Baumann M, Wei Z. Environmental life cycle assessment of emerging solid-state batteries: A review. Chem Eng J Adv 2023;13:100439.
[275] Azhari L, Bong S, Ma X, Wang Y. Recycling for all solid-state lithium-ion batteries. Matter 2020;3:1845–61.
[276] Ahuis M, Doose S, Vogt D, Michalowski P, Zellmer S, Kwade A. Recycling of solid-state batteries. Nat. Energy 2024;9:373–85.
[277] Sun H, Xie X, Huang Q, Wang Z, Chen K, Li X, et al. Fluorinated Poly-oxalate Electrolytes Stabilizing both Anode and Cathode Interfaces for All-Solid-State Li/NMC811 Batteries. Angew Chem 2021;133:18483–91.
[278] Kim JH, Kim JH, Kim JM, Lee YG, Lee SY. Superlattice crystals–mimic, flexible/functional ceramic membranes: Beyond polymeric battery separators. Adv Funct Mater 2015;5:1500954.
[279] Xia S, Wu X, Zhang Z, Cui Y, Liu W. Practical challenges and future perspectives of all-solid-state lithium-metal batteries. Chem 2019;5:753–85.
[280] Yuan L, Hao J, Kao C-C, Wu C, Liu H-K, Dou S-X, et al. Regulation methods for the Zn/electrolyte interphase and the effectiveness evaluation in aqueous Zn-ion batteries. Energy Environ Sci 2021;14:5669–89.
[281] Miao Y-E, Zhu G-N, Hou H, Xia Y-Y, Liu T. Electrospun polyimide nanofiber-based nonwoven separators for lithium-ion batteries. J Power Sources 2013;226: 82–6.
[282] Zhu Z, Tang Y, Lv Z, Wei J, Zhang Y, Wang R, et al. Fluoroethylene Carbonate Enabling a Robust LiF-rich Solid Electrolyte Interphase to Enhance the Stability of the MoS_2 Anode for Lithium-Ion Storage. Angew Chem 2018;130:3718–22.
[283] Michalak B, BzB B, Sommer H, Brezesinski T, Jr J. Electrochemical cross-talk leading to gas evolution and capacity fade in $LiNi_{0.5}Mn_{1.5}O_4$/graphite full-cells. J Phys Chem C 2017;121:211–6.
[284] Gong W, Gu J, Ruan S, Shen C. A high-strength electrospun PPESK fibrous membrane for lithium-ion battery separator. Polym Bull 2019;76:5451–62.
[285] Zhang SS. A review on the separators of liquid electrolyte Li-ion batteries. J Power Sources 2007;164:351–64.
[286] Arora P, Zhang Z. Battery separators. Chem Rev 2004;104:4419–62.
[287] Bandhauer TM, Garimella S, Fuller TF. A critical review of thermal issues in lithium-ion batteries. J Electrochem Soc 2011;158:R1.
[288] Wang Y, Wang S, Fang J, Ding L-X, Wang H. A nano-silica modified polyimide nanofiber separator with enhanced thermal and wetting properties for high safety lithium-ion batteries. J Membr Sci 2017;537:248–54.
[289] Wen J, Yu Y, Chen C. A Review on Lithium-Ion Batteries Safety Issues: Existing Problems and Possible Solutions. Mater Express 2012;2:197–212.
[290] Han C, Cao Y, Zhang S, Bai L, Yang M, Fang S, et al. Separator with Nitrogen–Phosphorus Flame-Retardant for $LiNi_xCo_yMn_{1-x-y}O_2$ Cathode-Based Lithium-ion Batteries. Small 2023;2207453.
[291] Ryou MH, Lee YM, Park JK, Choi JW. Mussel-inspired polydopamine-treated polyethylene separators for high-power Li-ion batteries. Adv Mater 2011;23: 3066–70.
[292] Feng X, Fang M, He X, Ouyang M, Lu L, Wang H, et al. Thermal runaway features of large format prismatic lithium ion battery using extended volume accelerating rate calorimetry. J Power Sources 2014;255:294–301.
[293] Zhao C, Sun Q, Luo J, Liang J, Liu Y, Zhang L, et al. 3D porous garnet/gel polymer hybrid electrolyte for safe solid-state Li–O_2 batteries with long lifetimes. Chem Mater 2020;32:10113–9.
[294] Li M, Zhang Z, Yin Y, Guo W, Bai Y, Zhang F, et al. Novel polyimide separator prepared with two porogens for safe lithium-ion batteries. ACS Appl Mater Interfaces 2019;12:3610–6.
[295] Hitz EM, Xie H, Lin Y, Connell JW, Rubloff GW, Lin C-F, et al. Ion-Conducting, Electron-Blocking Layer for High-Performance Solid Electrolytes. Small Struct 2021;2:2100014.
[296] Xia H, Lv Z, Zhang W, Wei J, Liu L, Cao S, et al. Hygroscopic Chemistry Enables Fire-Tolerant Supercapacitors with a Self-Healable “Solute-in-Air” lectrolyte. Adv Mater 2022;34:2109857.
[297] Kim DH, Lee Y-H, Song YB, Kwak H, Lee S-Y, Jung YS. Thin and flexible solid electrolyte membranes with ultrahigh thermal stability derived from solution-processable Li argyrodites for all-solid-state Li-ion batteries. ACS Energy Lett 2020;5:718–27.
[298] Fu K, Gong Y, Dai J, Gong A, Han X, Yao Y, et al. Flexible, solid-state, ion-conducting membrane with 3D garnet nanofiber networks for lithium batteries. PNAS 2016;113:7094–9.
[299] Song Y, Liu X, Ren D, Liang H, Wang L, Hu Q, et al. Simultaneously blocking chemical crosstalk and internal short circuit via gel-stretching derived nanoporous non-shrinkage separator for safe lithium-ion batteries. Adv Mater 2022;34:2106335.
[300] Fu J, Wang H, Du Z, Liu Y, Sun Q, Li H. A high-safety, flame-retardant cellulose-based separator with encapsulation structure for lithium-ion battery. SmartMat 2023;4:e1182.
[301] Liu Y, Li C, Li C, Xu L, Zhou S, Zhang Z, et al. Porous, robust, thermally stable, and flame retardant nanocellulose/polyimide separators for safe lithium-ion batteries. J Mater Chem A 2023;11:23360–9.

[302] Liu Y, Li C, Li C, Liang Z, Hu X, Liu H, et al. Highly thermally stable, highly electrolyte-wettable hydroxyapatite/cellulose nanofiber hybrid separators for lithium-ion batteries. ACS Appl Energ Mater 2023;6:3862–71.
[303] Chou L-Y, Ye Y, Lee HK, Huang W, Xu R, Gao X, et al. Electrolyte-resistant dual materials for the synergistic safety enhancement of lithium-ion batteries. Nano Lett 2021;21:2074–80.
[304] Yang C, Tong H, Luo C, Yuan S, Chen G, Yang Y. Boehmite particle coating modified microporous polyethylene membrane: A promising separator for lithium ion batteries. J Power Sources 2017;348:80–6.
[305] Zeng G, Zhao J, Feng C, Chen D, Meng Y, Boateng B, et al. Flame-retardant bilayer separator with multifaceted van der Waals interaction for lithium-ion batteries. ACS Appl Mater Interfaces 2019;11:26402–11.
[306] Huang B, Hua H, Peng L, Wang X, Shen X, Li R, et al. The functional separator for lithium-ion batteries based on phosphonate modified nano-scale silica ceramic particles. J Power Sources 2021;498:229908.
[307] Liu Z, Peng Y, Meng T, Yu L, Wang S, Hu X. Thermal-triggered fire-extinguishing separators by phase change materials for high-safety lithium-ion batteries. Energy Storage Mater 2022;47:445–52.
[308] Duan J, Yuan R, Huang H, Sun C, Lei J, Yuan X, et al. Geminal dicationic ionic liquid-based freestanding ion membrane for high-safety lithium batteries. ACS Appl Mater Interfaces 2021;13:16238–45.
[309] Stalin S, Choudhury S, Zhang K, Archer LA. Multifunctional cross-linked polymeric membranes for safe, high-performance lithium batteries. Chem Mater 2018; 30:2058–66.
[310] Deimede V, Elmasides C. Separators for lithium-ion batteries: a review on the production processes and recent developments. Energy Technol 2015;3:453–68.
[311] Boyden A, Soo VK, Doolan M. The environmental impacts of recycling portable lithium-ion batteries. Procedia CIRP 2016;48:188–93.
[312] Baum ZJ, Bird RE, Yu X, Ma J. Lithium-ion battery recycling— overview of techniques and trends. ACS Publications 2022.
[313] Kaya M. State-of-the-art lithium-ion battery recycling technologies. Circ Econ 2022;1:100015.
[314] Zhang R, Zheng Y, Duan J, Hu P, Huang Y. Batteries for electric vehicles: opportunities and challenges. Science 2017;358:10–3.
[315] Wang A, Tan R, Breakwell C, Wei X, Fan Z, Ye C, et al. Solution-processable redox-active polymers of intrinsic microporosity for electrochemical energy storage. J Am Chem Soc 2022;144:17198–208.
[316] Jiang J, Dahn JR. ARC studies of the thermal stability of three different cathode materials: $LiCoO_2$; $Li[Ni_{0.1}Co_{0.8}Mn_{0.1}]O_2$; and $LiFePO_4$, in $LiPF_6$ and LiBoB EC/DEC electrolytes. Electrochem Commun 2004;6:39–43.
[317] Andersson A. Lithium extraction/insertion in $LiFePO_4$: an X-ray diffraction and Mössbauer spectroscopy study. Solid State Ion 2000;130:41–52.
[318] Doughty DH, Roth EP. A General Discussion of Li Ion Battery Safety. Electrochem Soc Interface 2012;21:37.
[319] Yan W, Yang S, Huang Y, Yang Y, Guohui Y. A review on doping/coating of nickel-rich cathode materials for lithium-ion batteries. J Alloys Compd 2020;819.
[320] Yu Y, Wang J, Zhang P, Zhao J. A detailed thermal study of usual $LiNi_{0.5}Co_{0.2}Mn_{0.\ 3}O_2$, $LiMn_2O_4$ and $LiFePO_4$ cathode materials for lithium ion batteries. J Energy Storage 2017;12:37–44.
[321] Pang P, Wang Z, Tan X, Deng Y, Nan J, Xing Z, et al. $LiCoO_2$@$LiNi_{0.45}Al_{0.05}Mn_{0.5}O_2$ as high-voltage lithium-ion battery cathode materials with improved cycling performance and thermal stability. Electrochim Acta 2019;327:135018.
[322] Fu A, Zhang Z, Lin J, Zou Y, Qin C, Xu C, et al. Highly stable operation of $LiCoO_2$ at cut-off≥ 4.6 V enabled by synergistic structural and interfacial manipulation. Energy Storage Mater 2022;46:406–16.
[323] Noh H-J, Youn S, Yoon CS, Sun Y-K. Comparison of the structural and electrochemical properties of layered $Li[Ni_xCo_yMn_z]O_2$ (x = 1/3, 0.5, 0.6, 0.7, 0.8 and 0.85) cathode material for lithium-ion batteries. J Power Sources. 2013;233:121-30.
[324] Li Y, Liu X, Ren D, Hsu H, Xu G-L, Hou J, et al. Toward a high-voltage fast-charging pouch cell with TiO_2 cathode coating and enhanced battery safety. Nano Energy 2020;71:104643.
[325] Wu Y-S, Pham Q-T, Yang C-C, Chern C-S, Babulal LM, Seenivasan M, et al. Study of electrochemical performance and thermal property of $LiNi_{0.5}Co_{0.2}Mn_{0.3}O_2$ cathode materials coated with a novel oligomer additive for high-safety lithium-ion batteries. Chem. Eng J 2021;405:126727.
[326] Zhong Z, Chen L, Huang S, Shang W, Kong L, Sun M, et al. Single-crystal LiNi0. 5Co0. 2Mn0. 3O2: a high thermal and cycling stable cathodes for lithium-ion batteries. J Mater Sci. 2020;55:2913-22.
[327] You L, Tang J, Wu Q, Zhang C, Liu D, Huang T, et al. $LiFePO_4$-coated $LiNi_{0.6}Co_{0.2}Mn_{0.2}O_2$ for lithium-ion batteries with enhanced cycling performance at elevated temperatures and high voltages. RSC Adv 2020;10:37916–22.
[328] Sun H-H, Manthiram A. Impact of microcrack generation and surface degradation on a nickel-rich layered $Li[Ni_{0.9}Co_{0.\ 05}Mn_{0.05}]O_2$ cathode for lithium-ion batteries. Chem Mater 2017;29:8486–93.
[329] Qian G, Zhang Y, Li L, Zhang R, Xu J, Cheng Z, et al. Single-crystal nickel-rich layered-oxide battery cathode materials: synthesis, electrochemistry, and intra-granular fracture. Energy Storage Mater 2020;27:140–9.
[330] Sun Y-K, Chen Z, Noh H-J, Lee D-J, Jung H-G, Ren Y, et al. Nanostructured high-energy cathode materials for advanced lithium batteries. Nat Mater 2012;11: 942–7.
[331] El Moutchou S, Aziam H, Mansori M, Saadoune I. Thermal stability of Lithium-ion batteries: Case study of NMC811 and LFP cathode materials. Mater Today: Proc 2022;51:A1–7.
[332] Kim JH, Kim H, Choi W, Park M-S. Bifunctional surface coating of $LiNbO_3$ on high-Ni layered cathode materials for lithium-ion batteries. ACS Appl Mater Interfaces 2020;12:35098–104.
[333] Zhang R, Wang C, Zou P, Lin R, Ma L, Yin L, et al. Compositionally complex doping for zero-strain zero-cobalt layered cathodes. Nature 2022;610:67–73.
[334] Sun Y-K. High-capacity layered cathodes for next-generation electric vehicles. ACS Energy Lett 2019;4:1042–4.
[335] Zhou P, Meng H, Zhang Z, Chen C, Lu Y, Cao J, et al. Stable layered Ni-rich $LiNi_{0.9}Co_{0.07}Al_{0.03}O_2$ microspheres assembled with nanoparticles as high-performance cathode materials for lithium-ion batteries. J Mater Chem A 2017;5:2724–31.
[336] Li H, Zhou P, Liu F, Li H, Cheng F, Chen J. Stabilizing nickel-rich layered oxide cathodes by magnesium doping for rechargeable lithium-ion batteries. Chem Sci 2019;10:1374–9.
[337] Bian X, Fu Q, Pang Q, Gao Y, Wei Y, Zou B, et al. Multi-functional surface engineering for Li-excess layered cathode material targeting excellent electrochemical and thermal safety properties. ACS Appl Mater Interfaces 2016;8:3308–18.
[338] Wang Y, Gu H-T, Song J-H, Feng Z-H, Zhou X-B, Zhou Y-N, et al. Suppressing Mn reduction of Li-rich Mn-based cathodes by F-doping for advanced lithium-ion batteries. J Phys Chem C 2018;122:27836–42.
[339] Liu J, Lin X, Han T, Li X, Gu C, Li J. A novel litchi-like LiFePO4 sphere/reduced graphene oxide composite Li-ion battery cathode with high capacity, good rate-performance and low-temperature property. Appl Surf Sci 2018;459:233–41.
[340] Huang X, Zhang K, Liang F, Dai Y, Yao Y. Optimized solvothermal synthesis of $LiFePO_4$ cathode material for enhanced high-rate and low temperature electrochemical performances. Electrochim Acta 2017;258:1149–59.
[341] Liu J, Liang K, He J, Li J, Huang X, Zhang X, et al. Functionalized porous conductive carbon layer improves the low-temperature performance of $LiFePO_4$ cathode material for lithium-ion batteries. Carbon 2024;229:119483.
[342] Yu Y, Guo J, Xiang M, Su C, Liu X, Bai H, et al. Enhancing the durable performance of LiMn2O4 at high-rate and elevated temperature by nickel-magnesium dual doping. Sci Rep 2019;9:16864.
[343] Qiu T, Wang J, Lu Y, Yang W. Improved elevated temperature performance of commercial $LiMn_2O_4$ coated with $LiNi_{0.\ 5}Mn_{1.5}O_4$. Electrochim Acta 2014;147: 626–35.
[344] Zhou A, Xu J, Dai X, Yang B, Lu Y, Wang L, et al. Improved high-voltage and high-temperature electrochemical performances of $LiCoO_2$ cathode by electrode sputter-coating with Li_3PO_4. J Power Sources 2016;322:10–6.
[345] Li M, Bai F, Yao Q, Wang H, Li P. Double function-layers construction strategy promotes the cycling stability of $LiCoO_2$ under high temperature and high voltage. Electrochim Acta 2023;449:142197.

[346] Razmjoo Khollari MA, Azar MK, Esmaeili M, Malekpour N, Hosseini-Hosseinabad SM, Moakhar RS, et al. Electrochemical Performance and elevated temperature properties of the TiO_2-coated $Li[Ni_{0.8}Co_{0.1}Mn_{0.1}]O_2$ cathode material for high-safety Li-ion batteries. ACS Appl Energ Mater 2021;4:5304–15.
[347] Song L, Tang F, Xiao Z, Cao Z, Zhu H. Energy Storage and Thermostability of Li_3VO_4-Coated $LiNi_{0.8}Co_{0.1}Mn_{0.1}O_2$ as Cathode Materials for Lithium Ion Batteries. Front Chem 2018;6:546.
[348] Liu W, Oh P, Liu X, Myeong S, Cho W, Cho J. Countering voltage decay and capacity fading of lithium-rich cathode material at 60 C by hybrid surface protection layers. Adv Energy Mater 2015;5:1500274.
[349] Nam GW, Park N-Y, Park K-J, Yang J, Liu J, Yoon CS, et al. Capacity Fading of Ni-Rich NCA Cathodes: Effect of Microcracking Extent. ACS Energy Lett 2019;4:2995–3001.
[350] Bak SM, Hu E, Zhou Y, Yu X, Senanayake SD, Cho SJ, et al. Structural changes and thermal stability of charged $LiNi_xMn_yCo_zO_2$ cathode materials studied by combined in situ time-resolved XRD and mass spectroscopy. ACS Appl Mater Interfaces 2014;6:22594–601.
[351] Yoon W-S, Kim K-B, Kim M-G, Lee M-K, Shin H-J, Lee J-M. Oxygen Contribution on Li-Ion Intercalation-Deintercalation in $LiAl_yCo_{1-y}O_2$ Investigated by O K-Edge and Co L-Edge X-Ray Absorption Spectroscopy. J Electrochem Soc 2002;149.
[352] Liu W, Oh P, Liu X, Lee MJ, Cho W, Chae S, et al. Nickel-rich layered lithium transition-metal oxide for high-energy lithium-ion batteries. Angew Chem Int Ed 2015;54:4440–57.
[353] Zhang SS. Problems and their origins of Ni-rich layered oxide cathode materials. Energy Storage Mater 2020;24:247–54.
[354] Yoon CS, Ryu H-H, Park G-T, Kim J-H, Kim K-H, Sun Y-K. Extracting maximum capacity from Ni-rich $Li[Ni_{0.95}Co_{0.025}Mn_{0.025}]O_2$cathodes for high-energy-density lithium-ion batteries. J Mater Chem A 2018;6:4126–32.
[355] Ryu HH, Park GT, Yoon CS, Sun YK. Microstructural Degradation of Ni-Rich $Li[Ni_xCo_yMn_{1-x-y}]O_2$ Cathodes During Accelerated Calendar Aging. Small 2018;14:e1803179.
[356] Mu L, Lin R, Xu R, Han L, Xia S, Sokaras D, et al. Oxygen Release Induced Chemomechanical Breakdown of Layered Cathode Materials. Nano Lett 2018;18:3241–9.
[357] Sim SJ, Lee SH, Jin BS, Kim HS. Use of carbon coating on $LiNi_{0.8}Co_{0.1}Mn_{0.1}O_2$ cathode material for enhanced performances of lithium-ion batteries. Sci Rep 2020;10:11114.
[358] Chen Z, Qin Y, Amine K, Sun YK. Role of surface coating on cathode materials for lithium-ion batteries. J Mater Chem 2010;20.
[359] Yu R, Banis MN, Wang C, Wu B, Huang Y, Cao S, et al. Tailoring bulk Li-ion diffusion kinetics and surface lattice oxygen activity for high-performance lithium-rich manganese-based layered oxides. Energy Storage Mater 2021;37:509–20.
[360] Sallard S, Sheptyakov D, Villevieille C. Improved electrochemical performances of Li-rich nickel cobalt manganese oxide by partial substitution of Li^+ by Mg^{2+}. J Power Sources 2017;359:27–36.
[361] Li J, Cameron AR, Li H, Glazier S, Xiong D, Chatzidakis M, et al. Comparison of Single Crystal and Polycrystalline $LiNi_{0.5}Mn_{0.3}Co_{0.2}O_2$ Positive Electrode Materials for High Voltage Li-Ion Cells. J Electrochem Soc 2017;164:A1534–44.
[362] Liu H, Wolfman M, Karki K, Yu YS, Stach EA, Cabana J, et al. Intergranular Cracking as a Major Cause of Long-Term Capacity Fading of Layered Cathodes. Nano Lett 2017;17:3452–7.
[363] Ryu H-H, Park K-J, Yoon CS, Sun Y-K. Capacity Fading of Ni-Rich $Li[Ni_xCo_yMn_{1-x-y}]O_2$ ($0.6 \leq x \leq 0.95$) Cathodes for High-Energy-Density Lithium-Ion Batteries: Bulk or Surface Degradation? Chem Mater 2018;30:1155–63.
[364] Xu X, Huo H, Jian J, Wang L, Zhu H, Xu S, et al. Radially Oriented Single-Crystal Primary Nanosheets Enable Ultrahigh Rate and Cycling Properties of $LiNi_{0.8}Co_{0.1}Mn_{0.1}O_2$ Cathode Material for Lithium-ion Batteries. Adv Energy Mater 2019;9.
[365] Zhang W, Xiao L, Zheng J, Zhong Y, Shi B, Chen H, et al. Effect of Nb_2O_5 nanocoating on the thermal stability and electrochemical performance of $LiNi_{0.6}Co_{0.2}Mn_{0.2}O_2$ cathode materials for lithium ion batteries. J Alloys Compd 2021;880.
[366] Li Y, Liu X, Ren D, Hsu H, Xu G-L, Hou J, et al. Toward a high-voltage fast-charging pouch cell with TiO_2 cathode coating and enhanced battery safety. Nano Energy 2020;71.
[367] Wang L, Liu G, Ding X, Zhan C, Wang X. Simultaneous Coating and Doping of a Nickel-Rich Cathode by an Oxygen Ion Conductor for Enhanced Stability and Power of Lithium-Ion Batteries. ACS Appl Mater Interfaces 2019;11:33901–12.
[368] Wu Y-S, Pham Q-T, Yang C-C, Chern C-S, Musuvadhi Babulal L, Seenivasan M, et al. Study of electrochemical performance and thermal property of $LiNi_{0.5}Co_{0.2}Mn_{0.3}O_2$ cathode materials coated with a novel oligomer additive for high-safety lithium-ion batteries. Chem. Eng J 2021;405.
[369] Kang KS, Seong MJ, Oh SH, Yu JS, Yim T. Surface-Modified Ni-Rich Layered Oxide Cathode Via Thermal Treatment of Poly(Vinylidene Fluoride) for Lithium-ion Batteries. Bull Korean Chem Soc 2020;41:1107–13.
[370] Liang L, Sun X, Wu C, Hou L, Sun J, Zhang X, et al. Nasicon-Type Surface Functional Modification in Core-Shell $LiNi_{0.5}Mn_{0.3}Co_{0.2}O_2$@$NaTi_2(PO_4)_3$ Cathode Enhances Its High-Voltage Cycling Stability and Rate Capacity toward Li-Ion Batteries. ACS Appl Mater Interfaces 2018;10:5498–510.
[371] Guan P, Zhou L, Yu Z, Sun Y, Liu Y, Wu F, et al. Recent progress of surface coating on cathode materials for high-performance lithium-ion batteries. J Energy Chem 2020;43:220–35.
[372] Pang P, Wang Z, Tan X, Deng Y, Nan J, Xing Z, et al. $LiCoO_2$@$LiNi_{0.45}Al_{0.05}Mn_{0.5}O_2$ as high-voltage lithium-ion battery cathode materials with improved cycling performance and thermal stability. Electrochim Acta 2019;327.
[373] Zhang L, Xiao L, Zheng J, Wang H, Chen H, Zhu Y. Effect of Nb^{5+} Doping and $LiNbO_3$ Coating on the Structure and Surface of a $LiNi_{0.8}Mn_{0.2}O_2$ Cathode Material for Lithium-Ion Batteries. J Electrochem Soc 2021;168.
[374] Abbate M, Lala SM, Montoro LA, Ti- RJM. Al-, and Cu-Doping Induced Gap States in $LiFePO_4$. Electrochem Solid-State Lett 2005;8.
[375] Prosini PP, Zane D, Pasquali M. Improved electrochemical performance of a $LiFePO_4$-based composite cathode. Electrochim Acta 2001;46:3517–23.
[376] Wang D, Li H, Shi S, Huang X, Chen L. Improving the rate performance of $LiFePO_4$ by Fe-site doping. Electrochim Acta 2005;50:2955–8.
[377] Jin C, Zhang X, He W, Wang Y, Li H, Wang Z, et al. Effect of ion doping on the electrochemical performances of $LiFePO_4$–$Li_3V_2(PO_4)_3$ composite cathode materials. RSC Adv 2014;4:15332–9.
[378] Woo SW, Myung ST, Bang H, Kim DW, Sun YK. Improvement of electrochemical and thermal properties of $Li[Ni_{0.8}Co_{0.1}Mn_{0.1}]O_2$ positive electrode materials by multiple metal (Al, Mg) substitution. Electrochim Acta 2009;54:3851–6.
[379] Liang C, Kong F, Longo RC, Zhang C, Nie Y, Zheng Y, et al. Site-dependent multicomponent doping strategy for Ni-rich $LiNi_{1-2y}Co_yMn_yO_2$ ($y = 1/12$) cathode materials for Li-ion batteries. J Mater Chem A 2017;5:25303–13.
[380] Yin S, Deng W, Chen J, Gao X, Zou G, Hou H, et al. Fundamental and solutions of microcrack in Ni-rich layered oxide cathode materials of lithium-ion batteries. Nano Energy 2021;83.
[381] Kim JH, Kim H, Kim W-J, Kim Y-C, Jung JY, Rhee DY, et al. Incorporation of Titanium into Ni-Rich Layered Cathode Materials for Lithium-Ion Batteries. ACS Appl Energ Mater 2020;3:12204–11.
[382] Kong X, Zhang Y, Li J, Yang H, Dai P, Zeng J, et al. Single-crystal structure helps enhance the thermal performance of Ni-rich layered cathode materials for lithium-ion batteries. Chem. Eng J 2022;434.
[383] Zhong Z, Chen L, Huang S, Shang W, Kong L, Sun M, et al. Single-crystal $LiNi_{0.5}Co_{0.2}Mn_{0.3}O_2$: a high thermal and cycling stable cathodes for lithium-ion batteries. J Mater Sci 2019;55:2913–22.
[384] Jin H-Z, Han X-F, Radjenovic PM, Tian J-H, Li J-F. Facile and Effective Positive Temperature Coefficient (PTC) Layer for Safer Lithium-Ion Batteries. J Phys Chem C 2021;125:1761–6.
[385] Seaby T, Lin T-E, Hu Y-X, Yuan Q-H, Wang L-Z. An analysis of F-doping in Li-rich cathodes. Rare Met 2022;41:1771–96.
[386] You B, Wang Z, Shen F, Chang Y, Peng W, Li X, et al. Research Progress of Single-Crystal Nickel-Rich Cathode Materials for Lithium Ion Batteries. Small Methods 2021;5:e2100234.
[387] Sun HH, Ryu H-H, Kim U-H, Weeks JA, Heller A, Sun Y-K, et al. Beyond Doping and Coating: Prospective Strategies for Stable High-Capacity Layered Ni-Rich Cathodes. ACS Energy Lett 2020;5:1136–46.

[388] Baginska M, Blaiszik BJ, Rajh T, Sottos NR, White SR. Enhanced autonomic shutdown of Li-ion batteries by polydopamine coated polyethylene microspheres. J Power Sources 2014;269:735–9.
[389] Feng XM, Ai XP, Yang HX. A positive-temperature-coefficient electrode with thermal cut-off mechanism for use in rechargeable lithium batteries. Electrochem Commun 2004;6:1021–4.
[390] Wang FM, Alemu T, Yeh NH, Wang XC, Lin YW, Hsu CC, et al. Interface Interaction Behavior of Self-Terminated Oligomer Electrode Additives for a Ni-Rich Layer Cathode in Lithium-Ion Batteries: Voltage and Temperature Effects. ACS Appl Mater Interfaces 2019;11:39827–40.
[391] Murdock BE, Toghill KE, Tapia-Ruiz N. A perspective on the sustainability of cathode materials used in lithium-ion batteries. Adv Energy Mater 2021;11:2102028.
[392] Gutsch M, Leker J. Costs, carbon footprint, and environmental impacts of lithium-ion batteries–From cathode active material synthesis to cell manufacturing and recycling. Appl Energy 2024;353:122132.
[393] Wentker M, Greenwood M, Asaba MC, Leker J. A raw material criticality and environmental impact assessment of state-of-the-art and post-lithium-ion cathode technologies. J Energy Storage 2019;26:101022.
[394] Or T, Gourley SW, Kaliyappan K, Yu A, Chen Z. Recycling of mixed cathode lithium-ion batteries for electric vehicles: Current status and future outlook. Carbon Energy 2020;2:6–43.
[395] Raj T, Chandrasekhar K, Kumar AN, Sharma P, Pandey A, Jang M, et al. Recycling of cathode material from spent lithium-ion batteries: Challenges and future perspectives. J Hazard Mater 2022;429:128312.
[396] Ding G, Ding FL, Fan X, Gao X, Cao G, Ban J, et al. Research on green recycling of lithium-ion batteries cathode waste powder. Chem. Eng J 2024. 152837.
[397] Bae H, Kim Y. Technologies of lithium recycling from waste lithium ion batteries: a review. Mater Adv 2021;2:3234–50.
[398] Zhu P, Gastol D, Marshall J, Sommerville R, Goodship V, Kendrick E. A review of current collectors for lithium-ion batteries. J Power Sources 2021;485:229321.
[399] Hao H, Tan R, Ye C, Low CTJ. Carbon-coated current collectors in lithium-ion batteries and supercapacitors: Materials, manufacture and applications. Carbon Energy 2024. e604.
[400] Ma T, Xu G-L, Li Y, Wang L, He X, Zheng J, et al. Revisiting the corrosion of the aluminum current collector in lithium-ion batteries. J Phys Chem Lett 2017;8:1072–7.
[401] Killer M, Farrokhseresht M, Paterakis NG. Implementation of large-scale Li-ion battery energy storage systems within the EMEA region. Appl Energy 2020;260:114166.
[402] Du J, Liu Y, Mo X, Li Y, Li J, Wu X, et al. Impact of high-power charging on the durability and safety of lithium batteries used in long-range battery electric vehicles. Appl Energy 2019;255:113793.
[403] Deng W, Zhu W, Zhou X, Liu Z. Graphene nested porous carbon current collector for lithium metal anode with ultrahigh areal capacity. Energy Storage Mater 2018;15:266–73.
[404] Li S, Church BC. Electrochemical stability of aluminum current collector in aqueous rechargeable lithium-ion battery electrolytes. J Appl Electrochem 2017;47:839–53.
[405] Jiang X, Chen J, Yang Y, Lv Y, Ren Y, Li W, et al. Corrosion protection of copper current collector of lithium-ion batteries by doped polypyrrole coatings. Int J Electrochem Sci 2020;15:2667–76.
[406] Warner JT. The Handbook of Lithium-ion Battery Pack Design: Chemistry, Components, Types, and Terminology. Leiden: Elsevier; 2024.
[407] Li L, Yang J, Tan R, Shu W, Low CJ, Zhang Z, et al. Large-scale current collectors for regulating heat transfer and enhancing battery safety. Nat Chem Eng 2024;1:1–10.
[408] Dadbakhsh S, Mertens R, Hao L, Van Humbeeck J, Kruth JP. Selective laser melting to manufacture “in situ” metal matrix composites: a review. Adv Eng Mater 2019;21:1801244.
[409] Hosseini S, Karimzadeh F, Enayati M. Mechanochemical synthesis of Al_2O_3/Co nanocomposite by aluminothermic reaction. Adv Powder Technol 2012;23:334–7.
[410] Udhayabanu V, Singh N, Murty B. Mechanical activation of aluminothermic reduction of NiO by high energy ball milling. J Alloys Compd 2010;497:142–6.
[411] La P, Yang J, Cockayne DJ, Liu W, Xue Q, Li Y. Bulk nanocrystalline Fe_3Al-based material prepared by aluminothermic reaction. Adv Mater 2006;18:733–7.
[412] Li Y, Feng X, Ren D, Ouyang M, Lu L, Han X. Thermal runaway triggered by plated lithium on the anode after fast charging. ACS Appl Mater Interfaces 2019;11:46839–50.
[413] Wang Z, Yang H, Li Y, Wang G, Wang J. Thermal runaway and fire behaviors of large-scale lithium ion batteries with different heating methods. J Hazard Mater 2019;379:120730.
[414] Feng X, Ren D, He X, Ouyang M. Mitigating thermal runaway of lithium-ion batteries. Joule 2020;4:743–70.
[415] Dai W, Ma T, Yan Q, Gao J, Tan X, Lv L, et al. Metal-level thermally conductive yet soft graphene thermal interface materials. ACS Nano 2019;13:11561–71.
[416] Ye Y, Chou L-Y, Liu Y, Wang H, Lee HK, Huang W, et al. Ultralight and fire-extinguishing current collectors for high-energy and high-safety lithium-ion batteries. Nat Energy 2020;5:786–93.
[417] Liu Z, Dong Y, Qi X, Wang R, Zhu Z, Yan C, et al. Stretchable separator/current collector composite for superior battery safety. Energy Environ Sci 2022;15:5313–23.
[418] Li N, Zhao J, Long Z, Song R, Cui Y, Lin J, et al. Metalized Plastic Current Collectors Incorporated with Halloysite Nanotubes toward Highly Safe Lithium-ion Batteries. Adv Funct Mater 2024;2316582.
[419] Wen S, Li Z, Zou C, Zhong W, Wang C, Chen J, et al. Improved performances of lithium-ion batteries by conductive polymer modified copper current collector. New J Chem 2021;45:10541–8.
[420] Cao L, Li L, Xue Z, Yang W, Zou H, Chen S, et al. The aluminum current collector with honeycomb-like surface and thick Al_2O_3 film increased durability and enhanced safety for lithium-ion batteries. J Porous Mater 2020;27:1677–83.
[421] Wang M, Noelle DJ, Shi Y, Le AV, Qiao Y. Effect of notch depth of modified current collector on internal-short-circuit mitigation for lithium-ion battery. J Phys D: Appl Phys 2017;51:015502.
[422] Khatibi H, Hassan E, Frisone D, Amiriyan M, Farahati R, Farhad S. Recycling and Reusing Copper and Aluminum Current-Collectors from Spent Lithium-Ion Batteries. Energies 2022;15:9069.
[423] Natarajan S, Akshay M, Aravindan V. Recycling/reuse of current collectors from spent lithium-ion batteries: benefits and issues. Adv Sustain Syst 2022;6:2100432.
[424] Natarajan S, Bhattarai RM, Sudhakaran M, Mok YS, Kim SJ. Recycling of spent graphite and copper current collector for lithium-ion and sodium-ion batteries. J Power Sources 2023;577:233170.
[425] Chen W, Han X, Pan Y, Yuan Y, Kong X, Liu L, et al. Defects in Lithium-Ion Batteries: From Origins to Safety Risks. Green Energy Intell Transp 2024. 100235.
[426] Liu Y, Zhang R, Wang J, Wang Y. Current and future lithium-ion battery manufacturing. iScience 2021;24:102332.
[427] Chen F, Chen T, Wu Z, Kong X, Meng X, Han X, et al. Optimizing lithium-ion battery electrode manufacturing: Advances and prospects in process simulation. J Power Sources 2024;610:234717.
[428] Hawley WB, Li J. Electrode manufacturing for lithium-ion batteries—Analysis of current and next generation processing. J Energy Storage 2019;25:100862.
[429] Sun Y, Yuan Y, Lu L, Han X, Kong X, Wang H, et al. A comprehensive research on internal short circuits caused by copper particle contaminants on cathode in lithium-ion batteries. eTransportation 2022;13:100183.
[430] Jansen T, Kandula MW, Hartwig S, Hoffmann L, Haselrieder W, Dilger K. Influence of laser-generated cutting edges on the electrical performance of large lithium-ion pouch cells. Batteries 2019;5:73.
[431] Yao X-Y, Saxena S, Su L, Pecht MG. The explosive nature of tab burrs in Li-ion batteries. IEEE Access 2019;7:45978–82.
[432] Keppeler M, Tran H-Y, Braunwarth W. The Role of Pilot Lines in Bridging the Gap Between Fundamental Research and Industrial Production for Lithium-Ion Battery Cells Relevant to Sustainable Electromobility: A Review. Energy Technol 2021;9:2100132.

[433] Zwicker M, Moghadam M, Zhang W, Nielsen C. Automotive battery pack manufacturing–a review of battery to tab joining. Journal of Advanced Joining Processes 2020;2020:100017.
[434] Brand M, Gläser S, Geder J, Menacher S, Obpacher S, Jossen A, et al. Electrical safety of commercial Li-ion cells based on NMC and NCA technology compared to LFP technology. In: 2013 World Electric Vehicle Symposium and Exhibition (EVS27): IEEE; 2013. p. 1–9.
[435] Zhao N, Zhao D, Xu L-p, Chen L, Wen Y, Zhang XJJON. A multimode responsive aptasensor for adenosine detection. J Nanomaterials 2014;2014:360347.
[436] Yang N, Zhang X, Shang B, Li G. Unbalanced discharging and aging due to temperature differences among the cells in a lithium-ion battery pack with parallel combination. J Power Sources 2016;306:733–41.
[437] An SJ, Li J, Daniel C, Mohanty D, Nagpure S, Wood III DL. The state of understanding of the lithium-ion-battery graphite solid electrolyte interphase (SEI) and its relationship to formation cycling. Carbon 2016;105:52–76.
[438] Bhattacharya S, Alpas AT. Micromechanisms of solid electrolyte interphase formation on electrochemically cycled graphite electrodes in lithium-ion cells. Carbon 2012;50:5359–71.
[439] Knoche T, Surek F, Reinhart G. A process model for the electrolyte filling of lithium-ion batteries. Procedia CIRP 2016;41:405–10.
[440] Mao C, An SJ, Meyer III HM, Li J, Wood M, Ruther RE, et al. Balancing formation time and electrochemical performance of high energy lithium-ion batteries. J Power Sources 2018;402:107–15.
[441] Zhang Z, Yang J, Huang W, Wang H, Zhou W, Li Y, et al. Cathode-electrolyte interphase in lithium batteries revealed by cryogenic electron microscopy. Matter 2021;4:302–12.
[442] Sun G, Chen Y. Experimental study on the screening criteria of echelon use of returned power battery. Chin J Power Sources 2018;42:1818–21.
[443] Neupert S, Kowal J. Inhomogeneities in battery packs. World Electr Veh J 2018;9:20.
[444] Bruen T, Marco J. Modelling and experimental evaluation of parallel connected lithium ion cells for an electric vehicle battery system. J Power Sources 2016;310:91–101.
[445] Hu M, Wang J, Fu C, Qin D, Xie S. Study on cycle-life prediction model of lithium-ion battery for electric vehicles. Int J Electrochem Sci 2016;11:577–89.
[446] Xu S, Hou C, Yang S. A Li-ion battery management system for large-capacity energy storage. Energy Storage Sci Technol 2016;5:69.
[447] Schuster SF, Brand MJ, Berg P, Gleissenberger M, Jossen A. Lithium-ion cell-to-cell variation during battery electric vehicle operation. J Power Sources 2015;297:242–51.
[448] Jiang T, Sun J, Wang T, Tang Y, Chen S, Qiu S, et al. Sorting and grouping optimization method for second-use batteries considering aging mechanism. J Energy Storage 2021;44:103264.
[449] Li R, Zhang H, Li W, Zhao X, Zhou Y. Toward group applications: a critical review of the classification strategies of lithium-ion batteries. World Electr Veh J 2020;11:58.
[450] Yin H, Li Y, Kang Y, Zhang C. A two-stage sorting method combining static and dynamic characteristics for retired lithium-ion battery echelon utilization. J Energy Storage 2023;64:107178.
[451] Liu Y, Zhang C, Jiang J, Zhang L, Zhang W. Deduction of the transformation regulation on voltage curve for lithium-ion batteries and its application in parameters estimation. eTransportation 2022;12:100164.
[452] Changqing D, Dong L, Ci Z, Di G, YuHang W. Study on screening method of lithium ion power battery. Chin J Power Sources 2017;41:977–80.
[453] Ran A, Chen S, Zhang S, Liu S, Zhou Z, Nie P, et al. A gradient screening approach for retired lithium-ion batteries based on X-ray computed tomography images. RSC Adv 2020;10:19117–23.
[454] Felder MP, Götze J. State of charge classification for lithium-ion batteries using impedance based features. Adv Radio Sci 2017;15:93–7.
[455] Rahe C, Kelly ST, Rad MN, Sauer DU, Mayer J, Figgemeier E. Nanoscale X-ray imaging of ageing in automotive lithium ion battery cells. J Power Sources 2019;433:126631.
[456] Chen Y, Shu Y, Li X, Xiong C, Cao S, Wen X, et al. Research on detection algorithm of lithium battery surface defects based on embedded machine vision. J Intell Fuzzy Syst 2021;41:4327–35.
[457] Zeng Y, Yang Y, He Z, Gao M, Wang C, Hong M. Lead-acid battery automatic grouping system based on graph cuts. Electr Power Compon Syst 2016;44:450–8.
[458] Yun L, Sandoval J, Zhang J, Gao L, Garg A, Wang C-T. Lithium-ion battery packs formation with improved electrochemical performance for electric vehicles: experimental and clustering analysis. J Electrochem Energy Convers Storage 2019;16:021011.
[459] Chen H, Liu Y, Qu Z, Yang K, Zhang M, Hui D, et al. Experimental research on thermal runaway characterization and mechanism induced by the shell insulation failure for $LiFePO_4$ Lithium-ion battery. J Energy Storage 2024;84:110735.
[460] Lai X, Jin C, Yi W, Han X, Feng X, Zheng Y, et al. Mechanism, modeling, detection, and prevention of the internal short circuit in lithium-ion batteries: Recent advances and perspectives. Energy Storage Mater 2021;35:470–99.
[461] Sun X, Dong Y, Sun P, Zheng B. Effects of thermal insulation layer material on thermal runaway of energy storage lithium battery pack. J Energy Storage 2024;76:109812.
[462] Liu F, Wang J, Yang N, Wang F, Chen Y, Lu D, et al. Experimental study on the alleviation of thermal runaway propagation from an overcharged lithium-ion battery module using different thermal insulation layers. Energy 2022;257:124768.
[463] Yin B, Li Y, Wang S, Zheng Y. Corrosion resistance of calcium hexaaluminate insulating firebrick for synthesising ternary lithium-ion battery cathode materials. J Alloys Compd 2023;942:168953.
[464] Quan T, Xia Q, Wei X, Zhu Y. Recent Development of Thermal Insulating Materials for Li-Ion Batteries. Energies 2024;17:4412.
[465] Nambisan P, Manjunatha H, Ravadi P, Reddy HP, Bharath G, Kulkarni MA, et al. Characterization of commercial thermal barrier materials to prevent thermal runaway propagation in large format lithium-ion cells. J Energy Storage 2023;74:109414.
[466] Yu Y, Li Z, Wei Z, Chen S, Huang Z, Fang Z, et al. Enhancing battery module safety with insulation material: Hollow glass microspheres incorporating aerogel of varying particle sizes. Chem Eng J 2023;478:147400.
[467] Ouyang D, He Y, Weng J, Liu J, Chen M, Wang J. Influence of low temperature conditions on lithium-ion batteries and the application of an insulation material. RSC Adv 2019;9:9053–66.
[468] GmbH P. Insulating Coating on Battery Cells Instead of Foiling. IST Int Surf Technol 2024;17:34–6.
[469] Arnold JR, Voelker G, Shariaty A. UV coating processes to enhance Li ion battery performance and reduce costs. ECS Trans 2017;80:397.
[470] Yu H, Mu X, Zhu Y, Liao C, Han L, Wang J, et al. Sandwich structured ultra-strong-heat-shielding aerogel/copper composite insulation board for safe lithium-ion batteries modules. J Energy Chem 2023;76:438–47.
[471] Wang A, Juncheng J, Liu Y, Wu J, Ma Y, Li M, et al. Research progress of aerogel used in lithium-ion power batteries. J Loss Prev Process Ind 2024. 105433.
[472] Zou B, Zhang L, Xue X, Tan R, Jiang P, Ma B, et al. A review on the fault and defect diagnosis of lithium-ion battery for electric vehicles. Energies 2023;16:5507.
[473] Lu L, Han X, Li J, Hua J, Ouyang M. A review on the key issues for lithium-ion battery management in electric vehicles. J Power Sources 2013;226:272–88.
[474] Tian J, Xiong R, Shen W. A review on state of health estimation for lithium ion batteries in photovoltaic systems. eTransportation 2019;2.
[475] Li H, Qu Z, Xu T, Wang Y, Fan X, Jiang H, et al. SOC estimation based on the gas-liquid dynamics model using particle filter algorithm. Int J Energy Res 2022;46:22913–25.
[476] Zhou W, Zheng Y, Pan Z, Lu Q. Review on the battery model and SOC estimation method. Processes 2021;9:1685.
[477] Hannan MA, Lipu MSH, Hussain A, Mohamed A. A review of lithium-ion battery state of charge estimation and management system in electric vehicle applications: Challenges and recommendations. Renew Sust Energ Rev 2017;78:834–54.
[478] Wang S, Wang C, Takyi-Aninakwa P, Jin S, Fernandez C, Huang Q. An improved parameter identification and radial basis correction-differential support vector machine strategies for state-of-charge estimation of urban-transportation-electric-vehicle lithium-ion batteries. J Energy Storage 2024;80:110222.
[479] Wang S, Dang Q, Gao Z, Li B, Fernandez C, Blaabjerg F. An innovative square root-untraced Kalman filtering strategy with full-parameter online identification for state of power evaluation of lithium-ion batteries. J Energy Storage 2024;104:114555.

[480] Wang S, Zhang S, Wen S, Fernandez C. An accurate state-of-charge estimation of lithium-ion batteries based on improved particle swarm optimization-adaptive square root cubature kalman filter. J Power Sources 2024;624:235594.
[481] Truchot C, Dubarry M, Liaw BY. State-of-charge estimation and uncertainty for lithium-ion battery strings. Appl Energy 2014;119:218–27.
[482] Waag W, Sauer DU. Adaptive estimation of the electromotive force of the lithium-ion battery after current interruption for an accurate state-of-charge and capacity determination. Appl Energy 2013;111:416–27.
[483] Zhang Y, Song W, Lin S, Feng Z. A novel model of the initial state of charge estimation for $LiFePO_4$ batteries. J Power Sources 2014;248:1028–33.
[484] Wang H, Liu Y, Fu H, Li G. Estimation of State of Charge of Batteries for Electric Vehicles. Int J Control Autom 2013;6:185–94.
[485] Coleman M, Chi Kwan L, Chunbo Z, Hurley WG. State-of-Charge Determination From EMF Voltage Estimation: Using Impedance, Terminal Voltage, and Current for Lead-Acid and Lithium-Ion Batteries. IEEE Trans Ind Electron 2007;54:2550–7.
[486] He H, Zhang X, Xiong R, Xu Y, Guo H. Online model-based estimation of state-of-charge and open-circuit voltage of lithium-ion batteries in electric vehicles. Energy 2012;39:310–8.
[487] Jiang C, Taylor A, Duan C, Bai K. Extended Kalman Filter based battery state of charge (SOC) estimation for electric vehicles. 2013 IEEE Transportation Electrification Conference and Expo (ITEC). Detroit, MI, USA: IEEE; 2013. p. 1-5.
[488] Tian Y, Xia B, Sun W, Xu Z, Zheng W. A modified model based state of charge estimation of power lithium-ion batteries using unscented Kalman filter. J Power Sources 2014;270:619–26.
[489] Plett GL. Sigma-point Kalman filtering for battery management systems of LiPB-based HEV battery packs. J Power Sources 2006;161:1369–84.
[490] Zhang Y, Liu M, Chen H, Hou G. Source identification of polycyclic aromatic hydrocarbons in different ecological wetland components of the Qinkenpao Wetland in Northeast China. Ecotoxicol Environ Saf 2014;102:160–7.
[491] Affanni A, Bellini A, Concari C, Franceschini G, Lorenzani E, Tassoni C. EV battery state of charge: Neural network based estimation. IEEE International Electric Machines and Drives Conference. IEMDC'03. Madison, WI, USA: IEEE 2003;2003:684–8.
[492] Álvarez Antón JC, García Nieto PJ, Blanco Viejo C, Vilán Vilán JA. Support Vector Machines Used to Estimate the Battery State of Charge. IEEE Trans Power Electron 2013;28:5919–26.
[493] Zheng Y, Lu L, Han X, Li J, Ouyang M. $LiFePO_4$ battery pack capacity estimation for electric vehicles based on charging cell voltage curve transformation. J Power Sources 2013;226:33–41.
[494] Kim I-S. Nonlinear state of charge estimator for hybrid electric vehicle battery. IEEE Trans Power Electron 2008;23:2027–34.
[495] Xu J, Mi CC, Cao B, Deng J, Chen Z, Li SJITOVT. The state of charge estimation of lithium-ion batteries based on a proportional-integral observer. IEEE Trans Veh Technol 2013;63:1614–21.
[496] Xia B, Chen C, Tian Y, Sun W, Xu Z, Zheng W. A novel method for state of charge estimation of lithium-ion batteries using a nonlinear observer. J Power Sources 2014;270:359–66.
[497] Wang L, Wang L, Li Y. A novel state-of-charge estimation algorithm of EV battery based on bilinear interpolation. 2013 IEEE Vehicle Power and Propulsion Conference (VPPC). Beijing, China: IEEE; 2013. p. 1-4.
[498] Ranjbar AH, Banaei A, Khoobroo A, Fahimi BJITOSG. Online estimation of state of charge in Li-ion batteries using impulse response concept. IEEE Trans Smart Grid 2011;3:360–7.
[499] Hu C, Youn BD, Chung J. A multiscale framework with extended Kalman filter for lithium-ion battery SOC and capacity estimation. Appl Energy 2012;92:694–704.
[500] Berecibar M, Gandiaga I, Villarreal I, Omar N, Van Mierlo J, Van den Bossche P. Critical review of state of health estimation methods of Li-ion batteries for real applications. Renew Sust Energ Rev 2016;56:572–87.
[501] Piłatowicz G, Marongiu A, Drillkens J, Sinhuber P, Sauer DU. A critical overview of definitions and determination techniques of the internal resistance using lithium-ion, lead-acid, nickel metal-hydride batteries and electrochemical double-layer capacitors as examples. J Power Sources 2015;296:365–76.
[502] Zheng F, Jiang J, Sun B, Zhang W, Pecht M. Temperature dependent power capability estimation of lithium-ion batteries for hybrid electric vehicles. Energy 2016;113:64–75.
[503] Xiong R, Sun W, Yu Q, Sun F. Research progress, challenges and prospects of fault diagnosis on battery system of electric vehicles. Appl Energy 2020;279.
[504] Yu Q, Wang C, Li J, Xiong R, Pecht M. Challenges and outlook for lithium-ion battery fault diagnosis methods from the laboratory to real world applications. eTransportation 2023;17.
[505] Zhao R, Zhang S, Liu J, Gu J. A review of thermal performance improving methods of lithium ion battery: Electrode modification and thermal management system. J Power Sources 2015;299:557–77.
[506] Wu W, Wang S, Wu W, Chen K, Hong S, Lai Y. A critical review of battery thermal performance and liquid based battery thermal management. Energy Conv Manag 2019;182:262–81.
[507] Du S, Lai Y, Ai L, Ai L, Cheng Y, Tang Y, et al. An investigation of irreversible heat generation in lithium ion batteries based on a thermo-electrochemical coupling method. Appl Therm Eng 2017;121:501–10.
[508] Fleischhammer M, Waldmann T, Bisle G, Hogg B-I, Wohlfahrt-Mehrens M. Interaction of cyclic ageing at high-rate and low temperatures and safety in lithium-ion batteries. J Power Sources 2015;274:432–9.
[509] Yang L, Tai N, Fan C, Meng Y. Energy regulating and fluctuation stabilizing by air source heat pump and battery energy storage system in microgrid. Renew Energy 2016;95:202–12.
[510] Wang T, Tseng KJ, Zhao J. Development of efficient air-cooling strategies for lithium-ion battery module based on empirical heat source model. Appl Therm Eng 2015;90:521–9.
[511] Park Y, Jun S, Kim S, Lee D-H. Design optimization of a loop heat pipe to cool a lithium ion battery onboard a military aircraft. J Mech Sci Technol 2010;24:609–18.
[512] Rao Z, Wang S, Wu M, Lin Z, Li F. Experimental investigation on thermal management of electric vehicle battery with heat pipe. Energy Conv Manag 2013;65:92–7.
[513] Wang C-Y, Zhang G, Ge S, Xu T, Ji Y, Yang X-G, et al. Lithium-ion battery structure that self-heats at low temperatures. Nature 2016;529:515–8.
[514] Jiang J, Ruan H, Sun B, Wang L, Gao W, Zhang W. A low-temperature internal heating strategy without lifetime reduction for large-size automotive lithium-ion battery pack. Appl Energy 2018;230:257–66.
[515] Guo S, Xiong R, Wang K, Sun F. A novel echelon internal heating strategy of cold batteries for all-climate electric vehicles application. Appl Energy 2018;219:256–63.
[516] Chen K, Li Z, Chen Y, Long S, Hou J, Song M, et al. Design of Parallel Air-Cooled Battery Thermal Management System through Numerical Study. Energies 2017;10.
[517] Xie J, Xie Y, Yuan C. Numerical study of heat transfer enhancement using vortex generator for thermal management of lithium ion battery. Int J Heat Mass Transfer 2019;129:1184–93.
[518] Chen K, Wang S, Song M, Chen L. Structure optimization of parallel air-cooled battery thermal management system. Int J Heat Mass Transfer 2017;111:943–52.
[519] Wang W, Zhang X, Xin C, Rao Z. An experimental study on thermal management of lithium ion battery packs using an improved passive method. Appl Therm Eng 2018;134:163–70.
[520] Situ W, Zhang G, Li X, Yang X, Wei C, Rao M, et al. A thermal management system for rectangular $LiFePO_4$ battery module using novel double copper mesh-enhanced phase change material plates. Energy 2017;141:613–23.
[521] Babapoor A, Azizi M, Karimi G. Thermal management of a Li-ion battery using carbon fiber-PCM composites. Appl Therm Eng 2015;82:281–90.
[522] Zhao J, Lv P, Rao Z. Experimental study on the thermal management performance of phase change material coupled with heat pipe for cylindrical power battery pack. Exp Therm Fluid Sci 2017;82:182–8.

[523] Putra N, Ariantara B, Pamungkas RA. Experimental investigation on performance of lithium-ion battery thermal management system using flat plate loop heat pipe for electric vehicle application. Appl Therm Eng 2016;99:784–9.
[524] Wang Q, Rao Z, Huo Y, Wang S. Thermal performance of phase change material/oscillating heat pipe-based battery thermal management system. Int J Therm Sci 2016;102:9–16.
[525] Chen D, Jiang J, Kim G-H, Yang C, Pesaran A. Comparison of different cooling methods for lithium ion battery cells. Appl Therm Eng 2016;94:846–54.
[526] Rana S, Kumar R, Bharj RS. Lithium-ion Battery Thermal Management Techniques and Their Current Readiness Level. Energy Technol 2022;11.
[527] Wan J, Song J, Yang Z, Kirsch D, Jia C, Xu R, et al. Highly anisotropic conductors. Adv Mater 2017;29:1703331.
[528] Luo J, Zou D, Wang Y, Wang S. Huang L. Battery thermal management systems (BTMs) based on phase change material (PCM): A comprehensive review. Chem Eng J; 2022. p. 430.
[529] Shah K, McKee C, Chalise D, Jain A. Experimental and numerical investigation of core cooling of Li-ion cells using heat pipes. Energy 2016;113:852–60.
[530] Yang L, Zhou F, Sun L, Wang S. Thermal management of lithium-ion batteries with nanofluids and nano-phase change materials: a review. J Power Sources 2022;539.
[531] Evzelman M, Ur Rehman MM, Hathaway K, Zane R, Costinett D, Maksimovic D. Active Balancing System for Electric Vehicles With Incorporated Low-Voltage Bus. IEEE Trans Power Electron 2016;31:7887–95.
[532] Dong B, Han Y. A new architecture for battery charge equalization. 2011 IEEE Energy Conversion Congress and Exposition. Phoenix, AZ, USA: IEEE; 2011. p. 928-34.
[533] Tarascon JM, Armand M. Issues and challenges facing rechargeable lithium batteries. Nature 2001;414:359–67.
[534] Schludi C, Joos J. Lightweight and safe composite battery housings. Lightw Des Worldw 2019;12:44–7.
[535] Pistoia G, Liaw B. Behaviour of lithium-ion batteries in electric vehicles: battery health, performance, safety, and cost. Berlin: Springer; 2018.
[536] Liu B, Jia Y, Yuan C, Wang L, Gao X, Yin S, et al. Safety issues and mechanisms of lithium-ion battery cell upon mechanical abusive loading: A review. Energy Storage Mater 2020;24:85–112.
[537] Zhang X, Wierzbicki T. Characterization of plasticity and fracture of shell casing of lithium-ion cylindrical battery. J Power Sources 2015;280:47–56.
[538] Horiba T. Lithium-Ion Battery Systems Proc IEEE 2014;102:939–50.
[539] Coren F, Huemer-Kals S, Stelzer PS, Fischer P. Crashworthiness of C-SMC: A structural battery case for automotive application. FISITA Web Congress 2020. Czech Republic: Trauner Verlag; 2020.
[540] Jia Y, Uddin M, Li Y, Xu JJJOES. Thermal runaway propagation behavior within 18,650 lithium-ion battery packs: A modeling study. J Energy Storage 2020; 31:101668.
[541] Zhai H, Li H, Ping P, Huang Z, Wang Q. An experimental-based Domino prediction model of thermal runaway propagation in 18,650 lithium-ion battery modules. Int J Heat Mass Transfer 2021;181:122024.
[542] Mishra D, Shah K, Jain A. Investigation of the impact of flow of vented gas on propagation of thermal runaway in a Li-ion battery pack. J Electrochem Soc 2021;168:060555.
[543] Chen L, Pereira C, Pannala S, Munjurulimana D, Goossens H. Mitigation of cylindrical lithium ion battery thermal runaway propagation with a flame retardant polypropylene thermal barrier. J Energy Storage 2025;108:115042.
[544] Peng R, Kong D, Ping P, Gao W, Wang G, Gong S, et al. Experimental investigation of the influence of venting gases on thermal runaway propagation in lithium-ion batteries with enclosed packaging. eTransportation 2024;23:100388.
[545] Lei X, Xie F, Wang J, Zhang CJJOT, Engineering T. A review of lithium-ion battery state of health and remaining useful life estimation methods based on bibliometric analysis. J Traffic Transp Eng 2024;11:1420–46.
[546] Quan W, Liu J, Luo J, Dong H, Ren Z, Li G, et al. A comparative study on the thermal runaway process mechanism of a pouch cell based on Li-rich layered oxide cathodes with different activation degrees. RSC Adv 2024;14:35074–80.
[547] Li M, Hu Y, Lu C, Li B, Tian W, Zhang J, et al. Effect of hydrostatic pressure on electrochemical performance of soft package lithium-ion battery for autonomous underwater vehicles. J Energy Storage 2022;54:105325.
[548] Wierzbicki T, Sahraei E. Homogenized mechanical properties for the jellyroll of cylindrical Lithium-ion cells. J Power Sources 2013;241:467–76.
[549] Zhang G, Wei X, Tang X, Zhu J, Chen S, Dai H. Internal short circuit mechanisms, experimental approaches and detection methods of lithium-ion batteries for electric vehicles: A review. Renew Sustain Energy Rev 2021;141:110790.
[550] Costa CM, Lee Y-H, Kim J-H, Lee S-Y, Lanceros-Mendez S. Recent advances on separator membranes for lithium-ion battery applications: From porous membranes to solid electrolytes. Energy Storage Mater 2019;22:346–75.
[551] Santhanagopalan S, Smith K, Neubauer J, Kim G-H, Pesaran A, Keyser M. Design and analysis of large lithium-ion battery systems. Artech House 2014.
[552] Fichtner M, Edström K, Ayerbe E, Berecibar M, Bhowmik A, Castelli IE, et al. Rechargeable batteries of the future—the state of the art from a BATTERY 2030+ perspective. Adv Energy Mater 2022;12:2102904.
[553] Franco AA, Rucci A, Brandell D, Frayret C, Gaberscek M, Jankowski P, et al. Boosting rechargeable batteries R&D by multiscale modeling: myth or reality? Chem Rev 2019;119:4569–627.
[554] Du J, Lin Y, Yang W, Lian C, Liu H. Application of simulation in thermal safety design of lithium-ion batteries. Energy Storage Sci Technol 2022;11:866.
[555] Zhang H, Ren D, Ming H, Zhang W, Cao G, Liu J, et al. Digital twin enables rational design of ultrahigh-power lithium-ion batteries. Adv Energy Mater 2023;13: 2202660.
[556] Amiri MN, Håkansson A, Burheim OS, Lamb JJ. Lithium-ion battery digitalization: Combining physics-based models and machine learning. Renew Sustain Energy Rev 2024;200:114577.
[557] Borah M, Wang Q, Moura S, Sauer DU, Li W. Synergizing physics and machine learning for advanced battery management. Commun Eng 2024;3:134.
[558] Tu H, Moura S, Wang Y, Fang H. Integrating physics-based modeling with machine learning for lithium-ion batteries. Appl Energy 2023;329:120289.
[559] Wang Y, Han X, Guo D, Lu L, Chen Y, Ouyang M. Physics-informed recurrent neural network with fractional-order gradients for state-of-charge estimation of lithium-ion battery. IEEE J Radio Freq Identif 2022;6:968–71.
[560] Lin W-J, Chen K-C. Evolution of parameters in the Doyle-Fuller-Newman model of cycling lithium ion batteries by multi-objective optimization. Appl Energy 2022;314:118925.
[561] Innocenti A, Moisés IÁ, Gohy J-F, Passerini S. A modified Doyle-Fuller-Newman model enables the macroscale physical simulation of dual-ion batteries. J Power Sources 2023;580:233429.
[562] Mevawalla A, Panchal S, Tran M-K, Fowler M, Fraser R. One dimensional fast computational partial differential model for heat transfer in lithium-ion batteries. J Energy Storage 2021;37:102471.
[563] Mevawalla A, Panchal S, Tran M-K, Fowler M, Fraser R. Mathematical heat transfer modeling and experimental validation of lithium-ion battery considering: tab and surface temperature, separator, electrolyte resistance, anode-cathode irreversible and reversible heat. Batteries 2020;6:61.
[564] Dong T, Wang Y, Cao W, Zhang W, Jiang F. Analysis of lithium-ion battery thermal models inaccuracy caused by physical properties uncertainty. Appl Therm Eng 2021;198:117513.
[565] Mukhopadhyay A, Sheldon BW. Deformation and stress in electrode materials for Li-ion batteries. Prog Mater Sci 2014;63:58–116.
[566] Renganathan S, Sikha G, Santhanagopalan S, White RE. Theoretical analysis of stresses in a lithium ion cell. J Electrochem Soc 2009;157:A155.
[567] Huang L, Liu L, Lu L, Feng X, Han X, Li W, et al. A review of the internal short circuit mechanism in lithium-ion batteries: Inducement, detection and prevention. Int J Energy Res 2021;45:15797–831.
[568] Deng J, Bae C, Marcicki J, Masias A, Miller T. Safety modelling and testing of lithium-ion batteries in electrified vehicles. Nat Energy 2018;3:261–6.
[569] Peng R, Kong D, Ping P, Wang G, Gao X, Lv H, et al. Thermal runaway modeling of lithium-ion batteries at different scales: Recent advances and perspectives. Energy Storage Mater 2024. 103417.
[570] Li S, Liu Q, Zhou J, Pan T, Gao L, Zhang W, et al. Hierarchical Co3O4 nanofiber–carbon sheet skeleton with superior Na/Li-philic property enabling highly stable alkali metal batteries. Adv Funct Mater 2019;29:1808847.

[571] Wu S, Bai Y, Luan W, Wang Y, Li W, Wang L, et al. Thermal runaway model of high-nickel large format lithium-ion battery under thermal abuse conditions. IOP Conference Series: Earth and Environmental Science: IOP Publishing. 2021.
[572] Xie Y, He X, Li W, Zhang Y, Dan D, Lee K, et al. A novel electro-thermal coupled model of lithium-ion pouch battery covering heat generation distribution and tab thermal behaviours. Int J Energy Res 2020;44:11725–41.
[573] Valentin O, Thivel P-X, Kareemulla T, Cadiou F, Bultel Y. Modeling of thermo-mechanical stresses in Li-ion battery. J Energy Storage 2017;13:184–92.
[574] Gao T, Lu W. Machine learning toward advanced energy storage devices and systems. Iscience 2021;24.
[575] Chen X, Liu X, Shen X, Zhang Q. Applying machine learning to rechargeable batteries: from the microscale to the macroscale. Angew Chem 2021;133:24558–70.
[576] Tian X, Zhou S, Hao H, Ruan H, Gaddam RR, Dutta RC, et al. Machine learning and density functional theory for catalyst and process design in hydrogen production. Chain 2024;1:150–66.
[577] Feng Z, Eiubovi I, Shao Y, Fan Z, Tan R. Review of digital twin technology applications in hydrogen energy. Chain 2024;1:54–74.
[578] Feng Z, Luo Y, Li D, Pan J, Tan R, Chen Y. Integrating Digital Twins and Machine Learning for Advanced Control in Green Hydrogen Production. Chain 2025;2:1–14.
[579] Zhang L, Shen Z, Sajadi SM, Prabuwono AS, Mahmoud MZ, Cheraghian G, et al. The machine learning in lithium-ion batteries: A review. Eng Anal Bound Elem 2022;141:1–16.
[580] Wei Z, He Q, Zhao Y. Machine learning for battery research. J Power Sources 2022;549:232125.
[581] Kim SW, Oh K-Y, Lee S. Novel informed deep learning-based prognostics framework for on-board health monitoring of lithium-ion batteries. Appl Energy 2022;315:119011.
[582] Salucci CB, Bakdi A, Glad IK, Vanem E, De Bin R. A novel semi-supervised learning approach for State of Health monitoring of maritime lithium-ion batteries. J Power Sources 2023;556:232429.
[583] Bian X, Liu L, Yan J. A model for state-of-health estimation of lithium ion batteries based on charging profiles. Energy 2019;177:57–65.
[584] Das K, Kumar R, Krishna A. Analyzing electric vehicle battery health performance using supervised machine learning. Renew Sustain Energy Rev 2024;189:113967.
[585] Zhang X, Tang B, Zhou Z. Unsupervised machine learning accelerates solid electrolyte discovery. Green Energy Environ 2021;6:3–4.
[586] Yu Q, Yang Y, Tang A, Wu Z, Xu Y, Shen W, et al. Unsupervised learning for lithium-ion batteries fault diagnosis and thermal runaway early warning in real-world electric vehicles. J Energy Storage 2025;109:115194.
[587] Gu X, Shang Y, Kang Y, Li J, Mao Z, Zhang C. An early minor-fault diagnosis method for lithium-ion battery packs based on unsupervised learning. IEEE-CAA J Autom Sin 2023;10:810–2.
[588] Namdari A, Samani MA, Durrani TS. Lithium-ion battery prognostics through reinforcement learning based on entropy measures. Algorithms 2022;15:393.
[589] Tavakol-Moghaddam Y, Boroushaki M, Astaneh M. Reinforcement learning for battery energy management: a new balancing approach for Li-ion battery packs. Res Eng 2024;23:102532.
[590] Lv C, Zhou X, Zhong L, Yan C, Srinivasan M, Seh ZW, et al. Machine learning: an advanced platform for materials development and state prediction in lithium-ion batteries. Adv Mater 2022;34:2101474.
[591] Zhao J, Feng X, Pang Q, Fowler M, Lian Y, Ouyang M, et al. Battery safety: Machine learning-based prognostics. Progr Energy Combust Sci 2024;102:101142.
[592] Duquesnoy M, Liu C, Dominguez DZ, Kumar V, Ayerbe E, Franco AA. Machine learning-assisted multi-objective optimization of battery manufacturing from synthetic data generated by physics-based simulations. Energy Storage Mater 2023;56:50–61.
[593] Liu K, Wang Y, Lai X. Data Science-based battery manufacturing management. Data Science-Based Full-Lifespan Management of Lithium-Ion Battery: Manufacturing. Operation and Reutilization: Springer 2022:49–90.
[594] Liu X, Zhang L, Yu H, Wang J, Li J, Yang K, et al. Bridging multiscale characterization technologies and digital modeling to evaluate lithium battery full lifecycle. Adv Energy Mater 2022;12:2200889.
[595] Pang H, Wu L, Liu J, Liu X, Liu K. Physics-informed neural network approach for heat generation rate estimation of lithium-ion battery under various driving conditions. J Energy Chem 2023;78:1–12.
[596] Meng H, Hu M, Kong Z, Niu Y, Liang J, Nie Z, et al. Risk analysis of lithium-ion battery accidents based on physics-informed data-driven Bayesian networks. Reliab Eng Syst Saf 2024;251:110294.
[597] Wen P, Ye Z-S, Li Y, Chen S, Xie P, Zhao S. Physics-informed neural networks for prognostics and health management of lithium-ion batteries. IEEE Trans Intell Veh 2023;9:2276–89.
[598] Wang F, Zhai Z, Zhao Z, Di Y, Chen X. Physics-informed neural network for lithium-ion battery degradation stable modeling and prognosis. Nat Commun 2024;15:4332.
[599] Cao R, Zhang Z, Shi R, Lu J, Zheng Y, Sun Y, et al. Model-constrained deep learning for online fault diagnosis in Li-ion batteries over stochastic conditions. Nat Commun 2025;16:1651.
[600] Han X, Wang Z, Wei Z. A novel approach for health management online-monitoring of lithium-ion batteries based on model-data fusion. Appl Energy 2021;302:117511.
[601] Xie M, Su C, Bu X, Yang C, Chen B. A Fault Prediction Method for Lithium-ion Batteries by Fusing Internal and External Features with Stacked Integration Models. J Electrochem Soc 2025;172:030522.
[602] Krewer U, Röder F, Harinath E, Braatz RD, Bedürftig B, Findeisen R. Dynamic models of Li-ion batteries for diagnosis and operation: a review and perspective. J Electrochem Soc 2018;165:A3656.
[603] Bansal P, Li Y. Multiphysics-Informed Machine Learning for Mechanical-Induced Degradation of Silicon Anode. ASME International Mechanical Engineering Congress and Exposition. Am Soc Mech Eng 2023. p. V011T12A08.
[604] Shen L, Wang Z, Xu S, Law HM, Zhou Y, Ciucci F. Harnessing database-supported high-throughput screening for the design of stable interlayers in halide-based all-solid-state batteries. Nat Commun 2025;16:3687.
[605] Weddle PJ, Kim S, Chen B-R, Yi Z, Gasper P, Colclasure AM, et al. Battery state-of-health diagnostics during fast cycling using physics-informed deep-learning. J Power Sources 2023;585:233582.
[606] Najera-Flores DA, Hu Z, Chadha M, Todd MD. A Physics-Constrained Bayesian neural network for battery remaining useful life prediction. Appl Math Model 2023;122:42–59.